ASTROPHYSICAL GYROKINETICS: KINETIC AND FLUID TURBULENT CASCADES IN MAGNETIZED WEAKLY COLLISIONAL PLASMAS

A. A. SCHEKOCHIHIN,[1,2] S. C. COWLEY,[2,3] W. DORLAND,[4] G. W. HAMMETT,[5] G. G. HOWES,[6] E. QUATAERT,[7] AND T. TATSUNO[4]

ABSTRACT

This paper presents a theoretical framework for understanding plasma turbulence in astrophysical plasmas. It is motivated by observations of electromagnetic and density fluctuations in the solar wind, interstellar medium and galaxy clusters, as well as by models of particle heating in accretion disks. All of these plasmas and many others have turbulent motions at weakly collisional and collisionless scales. The paper focuses on turbulence in a strong mean magnetic field. The key assumptions are that the turbulent fluctuations are small compared to the mean field, spatially anisotropic with respect to it and that their frequency is low compared to the ion cyclotron frequency. The turbulence is assumed to be forced at some system-specific outer scale. The energy injected at this scale has to be dissipated into heat, which ultimately cannot be accomplished without collisions. A *kinetic cascade* develops that brings the energy to collisional scales both in space and velocity. The nature of the kinetic cascade in various scale ranges depends on the physics of plasma fluctuations that exist there. There are four special scales that separate physically distinct regimes: the electron and ion gyroscales, the mean free path and the electron diffusion scale. In each of the scale ranges separated by these scales, the fully kinetic problem is systematically reduced to a more physically transparent and computationally tractable system of equations, which are derived in a rigorous way. In the *"inertial range"* above the ion gyroscale, the kinetic cascade separates into two parts: a cascade of Alfvénic fluctuations and a passive cascade of density and magnetic-field-strength fluctuations. The former are governed by the Reduced Magnetohydrodynamic (RMHD) equations at both the collisional and collisionless scales; the latter obey a linear kinetic equation along the (moving) field lines associated with the Alfvénic component (in the collisional limit, these compressive fluctuations become the slow and entropy modes of the conventional MHD). In the *"dissipation range"* below ion gyroscale, there are again two cascades: the kinetic-Alfvén-wave (KAW) cascade governed by two fluid-like Electron Reduced Magnetohydrodynamic (ERMHD) equations and a passive cascade of ion entropy fluctuations both in space and velocity. The latter cascade brings the energy of the inertial-range fluctuations that was Landau-damped at the ion gyroscale to collisional scales in the phase space and leads to ion heating. The KAW energy is similarly damped at the electron gyroscale and converted into electron heat. Kolmogorov-style scaling relations are derived for all of these cascades. The relationship between the theoretical models proposed in this paper and astrophysical applications and observations is discussed in detail.

Subject headings: magnetic fields—methods: analytical—MHD—plasmas—turbulence

1. INTRODUCTION

As observations of velocity, density and magnetic fields in astrophysical plasmas probe ever smaller scales, turbulence—i.e., broadband disordered fluctuations usually characterized by power-law energy spectra—emerges as a fundamental and ubiquitous feature.

One of the earliest examples of observed turbulence in space was the detection of a Kolmogorov $k^{-5/3}$ spectrum of magnetic fluctuations in the solar wind over a frequency range of about three decades (first reported by Matthaeus & Goldstein 1982; Bavassano et al. 1982 and confirmed to a high degree of accuracy by a multitude of subse-quent observations, e.g., Marsch & Tu 1990a; Horbury et al. 1996; Leamon et al. 1998; Bale et al. 2005; see Fig. 1). Another famous example in which the Kolmogorov power law appears to hold is the electron density spectrum in the interstellar medium (ISM)—in this case it emerges from observations by various methods in several scale intervals and, when these are pieced together, the power law famously extends over as many as 12 decades of scales (Armstrong et al. 1981, 1995; Lazio et al. 2004), a record that has earned it the name of "the Great Power Law in the Sky." Numerous other measurements in space and astrophysical plasmas, from the magnetosphere to galaxy clusters, result in Kolmogorov (or consistent with Kolmogorov) spectra but also show steeper power laws at very small (microphysical) scales (these observations are discussed in more detail in § 8).

Power-law spectra spanning broad bands of scales are symptomatic of the fundamental role of turbulence as a mechanism of transferring energy from the *outer scale(s)* (henceforth denoted L), where the energy is injected to the *inner scale(s)*, where it is dissipated. As these scales tend to be widely separated in astrophysical systems, one way for the system to bridge this scale gap is to fill it with fluctuations; the power-law spectra then arise due to scale invariance at the intermediate scales. Besides being one of the more easily mea-

Electronic address: a.schekochihin1@physics.ox.ac.uk

[1] Rudolf Peierls Centre for Theoretical Physics, University of Oxford, Oxford OX1 3NP, UK.
[2] Plasma Physics, Blackett Laboratory, Imperial College, London SW7 2AZ, UK.
[3] Euratom/UKAEA Fusion Association, Culham Science Centre, Abington OX14 3DB, UK.
[4] Department of Physics, University of Maryland, College Park, MD 20742-3511.
[5] Princeton Plasma Physics Laboratory, Princeton, NJ 08543-0451.
[6] Department of Physics and Astronomy, University of Iowa, Iowa City, IA 52242-1479.
[7] Department of Astronomy, University of California, Berkeley, CA 94720-3411.

surable characteristics of the multi-scale nature of turbulence, power-law (and, particularly, Kolmogorov) spectra evoke a number of fundamental physical ideas that lie at the heart of the turbulence theory: universality of small-scale physics, energy cascade, locality of interactions, etc. In this paper, we shall revisit and generalize these ideas for the problem of *kinetic* plasma turbulence,[8] so it is perhaps useful to remind the reader how they emerge in a standard argument that leads to the $k^{-5/3}$ spectrum (Kolmogorov 1941; Obukhov 1941).

1.1. *Kolmogorov Turbulence*

Suppose the average energy per unit time per unit volume that the system dissipates is ε. This energy has to be transferred from some (large) outer scale L at which it is injected to some (small) inner scale(s) at which the dissipation occurs (see § 1.5). It is assumed that in the range of scales intermediate between the outer and the inner (the *inertial range*), the statistical properties of the turbulence are universal (independent of the macrophysics of injection or of the microphysics of dissipation), spatially homogeneous and isotropic and the energy transfer is local in scale space. The flux of kinetic energy through any inertial-range scale λ is independent of λ:

$$\frac{u_\lambda^2}{\tau_\lambda} \sim \varepsilon = \text{const}, \qquad (1)$$

where the (constant) density of the medium is absorbed into ε, u_λ is the typical velocity fluctuation associated with the scale λ, and τ_λ is the cascade time.[9] Since interactions are assumed local, τ_λ must be expressed in terms of quantities associated with scale λ. It is then dimensionally inevitable that $\tau_\lambda \sim \lambda/u_\lambda$ (the nonlinear interaction time, or turnover time), so we get

$$u_\lambda \sim (\varepsilon\lambda)^{1/3}. \qquad (2)$$

This corresponds to a $k^{-5/3}$ spectrum of kinetic energy.

1.2. *MHD Turbulence and Critical Balance*

That astronomical data appear to point to a ubiquitous nature of what, in its origin, is a dimensional result for the turbulence in a neutral fluid, might appear surprising. Indeed, the astrophysical plasmas in question are highly conducting and support magnetic fields whose energy is at least comparable to the kinetic energy of the motions. Let us consider a situation where the plasma is threaded by a uniform dynamically strong magnetic field B_0 (the *mean*, or *guide, field*; see § 1.3 for a brief discussion of the validity of this assumption). In the presence of such a field, there is no dimensionally unique way of determining the cascade time τ_λ because besides the nonlinear interaction time λ/u_λ, there is a second characteristic time associated with the fluctuation of size λ, namely the Alfvén time $l_{\|\lambda}/v_A$, where v_A is the Alfvén speed and $l_{\|\lambda}$ is the typical scale of the fluctuation along the magnetic field.

The first theories of magnetohydrodynamic (MHD) turbulence (Iroshnikov 1963; Kraichnan 1965; Dobrowolny et al. 1980) calculated τ_λ by assuming an isotropic cascade ($l_{\|\lambda} \sim \lambda$) of weakly interacting Alfvén-wave packets ($\tau_\lambda \gg l_{\|\lambda}/v_A$)

---

[8] An outline of a Kolmogorov-style approach to kinetic turbulence was given in a recent paper by Schekochihin et al. (2008b). It can be read as a conceptual introduction to the present paper, which is much more detailed and covers a much broader set of topics.

[9] This is the version of Kolmogorov's theory due to Obukhov 1941.
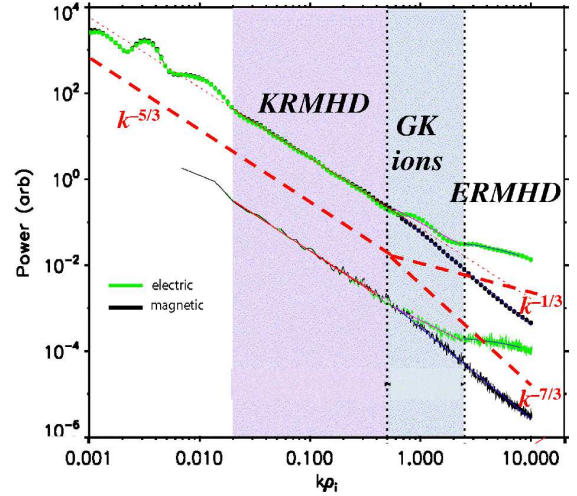

FIG. 1.— Spectra of electric and magnetic fluctuations in the solar wind at 1 AU (see Table 1 for the solar-wind parameters corresponding to this plot). This figure is adapted with permission from Fig. 3 of Bale et al. (2005) (copyright 2005 by the American Physical Society). We have added the reference slopes for Alfvén-wave and kinetic-Alfvén-wave turbulence in bold dashed (red) lines and labeled "KRMHD," "GK ions," and "ERMHD" the wavenumber intervals where these analytical descriptions are valid (see § 3, § 5 and § 7).

and obtained a $k^{-3/2}$ spectrum. The failure of the observed spectra to conform to this law (see references above) and especially the observational (see references at the end of this subsection) and experimental (Robinson & Rusbridge 1971; Zweben et al. 1979) evidence of anisotropy of MHD fluctuations led to the isotropy assumption being discarded (Montgomery & Turner 1981).

The modern form of MHD turbulence theory is commonly associated with the names of Goldreich & Sridhar (1995, 1997, henceforth, GS). It can be summarized as follows. Assume that (a) all electromagnetic perturbations are strongly anisotropic, so that their characteristic scales along the mean field are much larger than those across it, $l_{\|\lambda} \gg \lambda$, or, in terms of wavenumbers, $k_\| \ll k_\perp$; (b) the interactions between the Alfvén-wave packets are strong and the turbulence at sufficiently small scales always arranges itself in such a way that the Alfvén timescale and the perpendicular nonlinear interaction timescale are comparable to each other, i.e.,

$$\omega \sim k_\| v_A \sim k_\perp u_\perp, \qquad (3)$$

where ω is the typical frequency of the fluctuations and $u_\perp$ is the velocity fluctuation perpendicular to the mean field. Taken scale by scale, this assumption, known as the *critical balance*, removes the dimensional ambiguity of the MHD turbulence theory. Thus, the cascade time is $\tau_\lambda \sim l_{\|\lambda}/v_A \sim \lambda/u_\lambda$, whence

$$u_\lambda \sim (\varepsilon l_{\|\lambda}/v_A)^{1/2} \sim (\varepsilon\lambda)^{1/3}, \qquad (4)$$

$$l_{\|\lambda} \sim l_0^{1/3}\lambda^{2/3}, \qquad (5)$$

where $l_0 = v_A^3/\varepsilon$. The scaling relation (4) is equivalent to a $k_\perp^{-5/3}$ spectrum of kinetic energy, while Eq. (5) quantifies the anisotropy by establishing the relationship between the perpendicular and parallel scales. Note that Eq. (4) implies that in terms of the parallel wavenumbers, the kinetic-energy spectrum is $\sim k_\|^{-2}$.

The above considerations apply to Alfvénic fluctuations,

i.e., *perpendicular* velocities and magnetic-field perturbations from the mean given (at each scale) by $\delta B_\perp \sim u_\perp \sqrt{4\pi\rho_0}$, where ρ_0 is the mean mass density of the plasma (see Fig. 1 and discussion in § 8.1.1). Other low-frequency MHD modes—slow waves and the entropy mode—turn out to be passively advected by the Alfvénic component of the turbulence (this follows from the anisotropy; see Lithwick & Goldreich 2001, and §§ 2.4-2.6, § 5.5, and § 6.3 for further discussion of the compressive fluctuations).

As we have mentioned above, the anisotropy was, in fact, incorporated into MHD turbulence theory already by Montgomery & Turner (1981). However, these authors' view differed from the GS theory in that they thought of MHD turbulence as essentially two dimensional, described by a Kolmogorov-like cascade (Fyfe et al. 1977), with an admixture of Alfvén waves having some spectrum in $k_\parallel$ unrelated to the perpendicular structure of the turbulence (note that Higdon 1984, while adopting a similar view, anticipated the scaling relation (5), but did not seem to consider it to be anything more than the confirmation of an essentially 2D nature of the turbulence). In what we are referring to here as GS turbulence, the 2D and Alfvénic fluctuations are not separate components of the turbulence. The turbulence is three dimensional, with correlations parallel and perpendicular to the (local) mean field related at each scale by the critical balance assumption.

Indeed, intuitively, we cannot have $k_\parallel v_A \ll k_\perp u_\perp$: the turbulence cannot be any more 2D than allowed by the critical balance because fluctuations in any two planes perpendicular to the mean field can only remain correlated if an Alfvén wave can propagate between them in less than their perpendicular decorrelation time. In the opposite limit, weakly interacting Alfén waves with fixed $k_\parallel$ and $\omega = k_\parallel v_A \gg k_\perp u_\perp$ can be shown to give rise to an energy cascade towards smaller perpendicular scales where the turbulence becomes strong and Eq. (3) is satisfied (Goldreich & Sridhar 1997; Galtier et al. 2000; Yousef et al. 2009). Thus, there is a natural tendency towards critical balance in a system containing nonlinearly interacting Alfvén waves. We will see in what follows that critical balance may, in fact, be taken as a general physical principle relating parallel scales (associated with linear propagation) and perpendicular scales (associated with nonlinear interaction) in anisotropic plasma turbulence (see § 7.5, § 7.9.4, § 7.10.3).

We emphasize that, the anisotropy of astrophysical plasma turbulence is an observed phenomenon. It is seen most clearly in the spacecraft measurements of the turbulent fluctuations in the solar wind (Belcher & Davis 1971; Matthaeus et al. 1990; Bieber et al. 1996; Dasso et al. 2005; Bigazzi et al. 2006; Sorriso-Valvo et al. 2006; Horbury et al. 2005, 2008; Osman & Horbury 2007; Hamilton et al. 2008) and in the magnetosheath Sahraoui et al. (2006); Alexandrova et al. (2008b). In a recent key development, solar-wind data analysis by Horbury et al. (2008) approaches quantitative corroboration of the critical balance conjecture by confirming the scaling of the spectrum with the parallel wavenumber $\sim k_\parallel^{-2}$ that follows from the first scaling relation in Eq. (4). Anisotropy is also observed indirectly in the ISM (Wilkinson et al. 1994; Trotter et al. 1998; Rickett et al. 2002; Dennett-Thorpe & de Bruyn 2003), including recently in molecular clouds (Heyer et al. 2008), and, with unambiguous consistency, in numerical simulations of MHD turbulence (Shebalin et al. 1983; Oughton et al. 1994; Cho & Vishniac

2000; Maron & Goldreich 2001; Cho et al. 2002; Müller et al. 2003).[10]

1.3. *MHD Turbulence with and without a Mean Field*

In the discussion above, treating MHD turbulence as turbulence of Alfvénic fluctuations depended on assuming the presence of a mean (guide) field B_0 that is strong compared to the magnetic fluctuations, $\delta B/B_0 \sim u/v_A \ll 1$. We will also need this assumption in the formal developments to follow (see § 2.1, § 3.1). Is it legitimate to expect that such a spatially regular field will be generically present? Kraichnan (1965) argued that in a generic situation in which all magnetic fields are produced by the turbulence itself via the dynamo effect, one could assume that the strongest field will be at the outer scale and that this field will play the role of an (approximately) uniform guide field for the Alfvén waves in the inertial range. Formally, this amounts to assuming that in the inertial range,

$$\frac{\delta B}{B_0} \ll 1, \quad k_\parallel L \ll 1. \qquad (6)$$

It is, however, by no means obvious that this should be true. When a strong mean field is imposed by some external mechanism, the turbulent motions cannot bend it significantly, so only small perturbations are possible and $\delta B \ll B_0$. In contrast, without a strong imposed field, the energy density of the magnetic fluctuations is at most comparable to the kinetic-energy density of the plasma motions, which are then sufficiently energetic to randomly tangle the field, so $\delta B \gg B_0$.

In the weak-mean-field case, the dynamically strong stochastic magnetic field is a result of saturation of the *small-scale, or fluctuation, dynamo*—amplification of magnetic field due to random stretching by the turbulent motions (see review by Schekochihin & Cowley 2007). The definitive theory of this saturated state remains to be discovered. Both physical arguments and numerical evidence (Schekochihin et al. 2004; Yousef et al. 2007) suggest that the magnetic field in this case is organized in folded flux sheets (or ribbons). The length of these folds is comparable to the outer scale, while the scale of the field-direction reversals transverse to the fold is determined by the dissipation physics: in MHD with isotropic viscosity and resistivity, it is the resistive scale.[11] Although Alfvén waves prop-

---

[10] The numerical evidence is much less clear on the scaling of the spectrum. The fact that the spectrum is closer to $k_\perp^{-3/2}$ than to $k_\perp^{-5/3}$ in numerical simulations (Maron & Goldreich 2001; Müller et al. 2003; Mason et al. 2007; Perez & Boldyrev 2008, 2009; Beresnyak & Lazarian 2008b) prompted Boldyrev (2006) to propose a scaling argument that allows an anisotropic Alfvénic turbulence with a $k_\perp^{-3/2}$ spectrum. His argument is based on the conjecture that the fluctuating velocity and magnetic fields tend to partially align at small scales, an idea that has had considerable numerical support (Maron & Goldreich 2001; Beresnyak & Lazarian 2006, 2008b; Mason et al. 2006; Matthaeus et al. 2008a). The alignment weakens nonlinear interactions and alters the scalings. Another modification of the GS theory leading to an anisotropic $k_\perp^{-3/2}$ spectrum was proposed by Gogoberidze (2007), who assumed that MHD turbulence with a strong mean field is dominated by non-local interactions with the outer scale. However, in both arguments, the basic assumption that the turbulence is strong is retained. This is the main assumption that we make in this paper: the critical balance conjecture (3) is used below not as a scaling prescription but in a weaker sense of an ordering assumption, i.e., we simply take the wave propagation terms in the equations to be comparable to the nonlinear terms. It is not hard to show that the results derived in what follows remain valid whether or not the alignment is present. We note that observationally, only in the solar wind does one measure the spectra with sufficient accuracy to state that they are consistent with $k_\perp^{-5/3}$ but *not* with $k_\perp^{-3/2}$ (see § 8.1.1).

[11] In weakly collisional astrophysical plasmas, such a description is not

agating along the folds may exist (Schekochihin et al. 2004; Schekochihin & Cowley 2007), the presence of the small-scale direction reversals means that there is no scale-by-scale equipartition between the velocity and magnetic fields: while the magnetic energy is small-scale dominated due to the direction reversals,[12] the kinetic energy should be contained primarily at the outer scale, with some scaling law in the inertial range.

Thus, at the current level of understanding we have to assume that there are two asymptotic regimes of MHD turbulence: anisotropic Alfvénic turbulence with $\delta B \ll B_0$ and isotropic MHD turbulence with small-scale field reversals and $\delta B \gg B_0$. In this paper, we shall only discuss the first regime. The origin of the mean field may be external (as, e.g., in the solar wind, where it is the field of the Sun) or due to some form of *mean-field dynamo* (rather than small-scale dynamo), as usually expected for galaxies (see, e.g., Shukurov 2007).

Note finally that the condition $\delta B \ll B_0$ need not be satisfied at the outer scale and in fact is not satisfied in most space or astrophysical plasmas, where more commonly $\delta B \sim B_0$ at the outer scale. This, however, is sufficient for the Kraichnan hypothesis to hold and for an Alfénic cascade to be set up, so at small scales (in the inertial range and beyond), the assumptions (6) are satisfied.

1.4. *Kinetic Turbulence*

The GS theory of MHD turbulence (§ 1.2) allows us to make sense of the magnetized turbulence observed in cosmic plasmas exhibiting the same statistical scaling as turbulence in a neutral fluid (although the underlying dynamics are very different in these two cases!). However, there is an aspect of the observed astrophysical turbulence that undermines the applicability of any type of fluid description: in most cases, the inertial range where the Kolmogorov scaling holds extends to scales far below the mean free path deep into the collisionless regime. For example, in the case of the solar wind, the mean free path is close to 1 AU, so all scales are collisionless—an extreme case, which also happens to be the best studied, thanks to the possibility of in situ measurements (see § 8).

The proper way of treating such plasmas is using kinetic theory, not fluid equations. The basis for the application of the MHD fluid description to them has been the following well known result from the linear theory of plasma waves: while the fast, slow and entropy modes are damped at the mean-free-path scale both by collisional viscosity (Braginskii 1965, see § 6.1.2) and by collisionless wave–particle interactions (Barnes 1966, see § 6.2.2), the Alfvén waves are only damped at the ion gyroscale. It has, therefore, been assumed that the MHD description, inasmuch as it concerns the Alfvén-wave cascade, can be extended to the ion gyroscale, with the understanding that this cascade is decoupled from the damped cascades of the rest of the MHD modes. This approach and its application to the turbulence in the ISM are best explained by Lithwick & Goldreich (2001).

While the fluid description may be sufficient to understand the Alfvénic fluctuations in the inertial range, it is cer-

tainly inadequate for everything else: the compressive fluctuations in the inertial range and turbulence in the dissipation range (below the ion gyroscale), where power-law spectra are also detected (e.g., Denskat et al. 1983; Leamon et al. 1998; Czaykowska et al. 2001; Smith et al. 2006; Sahraoui et al. 2006; Alexandrova et al. 2008a,b, see also Fig. 1). The fundamental challenge that a comprehensive theory of astrophysical plasma turbulence must meet is to give the full account of how the turbulent fluctuation energy injected at the outer scale is cascaded to small scales and deposited into particle heat. We shall see (§ 3.4 and § 3.5) that the familiar concept of an energy cascade can be generalized in the kinetic framework as the *kinetic cascade* of a single quantity that we call the *generalized energy* (see also Schekochihin et al. 2008b, and references therein). The small scales developed in the process are small scales both in the position and velocity space. The fundamental reason for this is the low collisionality of the plasma: since heating cannot ultimately be accomplished without collisions, large gradients in phase space are necessary for the collisions to be effective.

The idea of a generalized energy cascade in phase space as the engine of kinetic plasma turbulence is the central concept of this paper. In order to understand the physics of the kinetic cascade in various scale ranges, we derive in what follows a hierarchy of simplified, yet rigorous, reduced kinetic, fluid and hybrid descriptions. While the full kinetic theory of turbulence is very difficult to handle either analytically or numerically, the models we derive are much more tractable. For all, the regimes of applicability (scale/parameter ranges, underlying assumptions) are clearly stated. In each of these regimes, the kinetic cascade splits into several channels of energy transfer, some of them familiar (e.g., the Alfvénic cascade, § 5.3 and § 5.4), others conceptually new (e.g., the kinetic cascade of collisionless compressive fluctuations, § 6.2, or the entropy cascade, §§ 7.9-7.12).

So as to introduce this theoretical framework in a way that is both analytically systematic and physically intelligible, let us first consider the characteristic scales that are relevant to the problem of astrophysical turbulence (§ 1.5). The models we derive are previewed in § 1.6, at the end of which the plan of further developments is given.

1.5. *Scales in the Problem*
1.5.1. *Outer Scale*

It is a generic feature of turbulent systems that energy is injected via some large-scale mechanism: "large scale" here means some scale (or a range of scales) comparable to the size of the system, depending on its global properties, and much larger than the microphysical scales at which energy is dissipated and converted into heat (§ 1.5.2). Examples of large-scale stirring of turbulent fluctuations include the solar activity in the corona (launching Alfvén waves to produce turbulence in the solar wind); supernova explosions in the ISM (e.g., Norman & Ferrara 1996; Ferrière 2001); the magnetorotational instability in accretion disks (Balbus & Hawley 1998); merger events, galaxy wakes and active galactic nuclei in galaxy clusters (e.g., Subramanian et al. 2006; Enßlin & Vogt 2006; Chandran 2005a). Since in this paper we are concerned with the local properties of astrophysical plasmas, let us simply assume that energy injection occurs at some characteristic *outer scale L*. All further considerations will apply to scales that are much smaller than L and we will assume that the particular character of the energy injection

---

applicable: the field reversal scale is most probably determined by more complicated and as yet poorly understood kinetic plasma effects; below this scale, an Alfvénic turbulence of the kind discussed in this paper may exist (Schekochihin & Cowley 2006).

[12] See Haugen et al. (2004) for an alternative view. Note also that the numerical evidence cited above pertains to *forced* simulations. In *decaying* MHD turbulence simulations, the magnetic energy does indeed appear to be at the outer scale (Biskamp & Müller 2000), so one might expect an Alfvénic cascade deep in the inertial range.
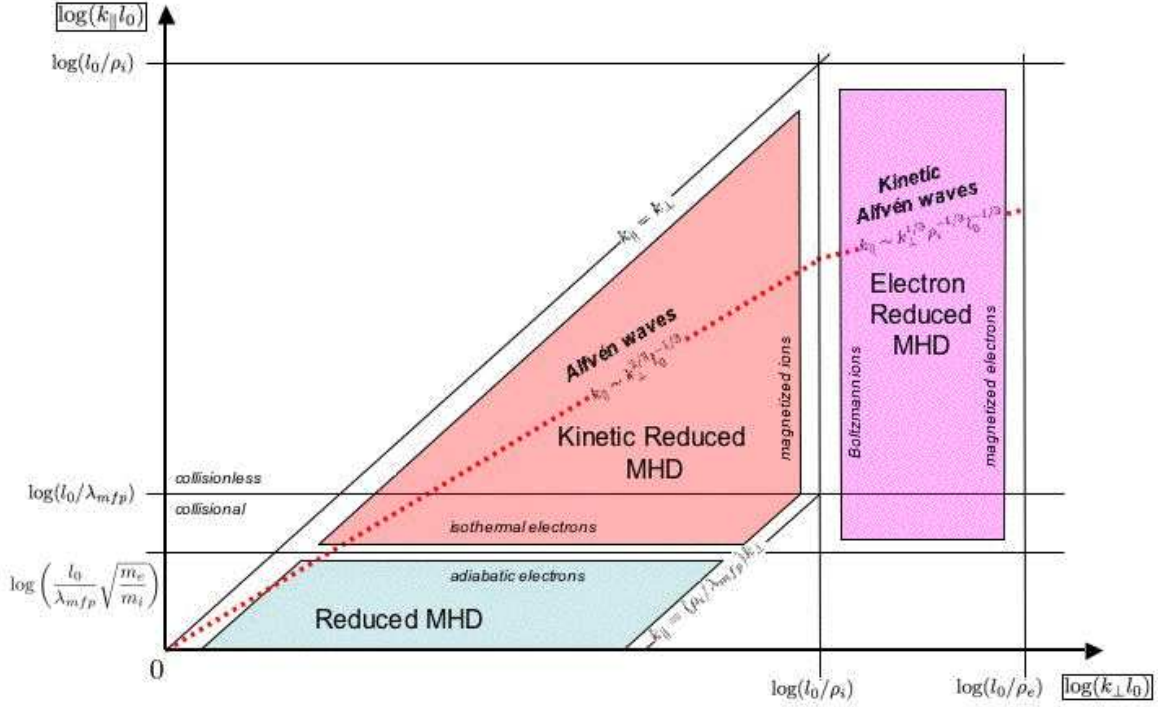
FIG. 2.— Partition of the wavenumber space by characteristic scales. The wavenumbers are normalized by $l_0 \sim v_A^3/\varepsilon$, where ε is the total power input (see § 1.2). Dotted line shows the path an Alfvén-wave cascade starting at the outer scale $L \sim l_0$ takes through the wavenumber space. We also show the regions of validity of the three tertiary approximations. They all require $k_\parallel \ll k_\perp$ (anisotropic fluctuations) and $k_\parallel \rho_i \ll 1$ (i.e., $k_\parallel v_{\mathrm{th}i} \ll \Omega_i$, low-frequency limit). Reduced MHD (RMHD, § 2) is valid when $k_\perp \rho_i \ll k_\parallel \lambda_{\mathrm{mfp}i} \ll (m_e/m_i)^{1/2}$ (strongly magnetized collisional limit, adiabatic electrons). The regions of validity of Kinetic Reduced MHD (KRMHD, § 5) and Electron Reduced MHD (ERMHD, § 7) lie within that of the isothermal electron/gyrokinetic ion approximation (Fig. 4) with the additional requirement that $k_\perp \rho_i \ll \min(1, k_\parallel \lambda_{\mathrm{mfp}i})$ (strongly magnetized ions) for KRMHD or $k_\perp \rho_i \gg 1$ (unmagnetized ions) for ERMHD. The collisional limit of KRMHD (§ 6.1 and Appendix D), $(m_e/m_i)^{1/2} \ll k_\parallel \lambda_{\mathrm{mfp}i} \ll 1$, is similar to RMHD, except electrons are isothermal. The dotted line is the scaling of $k_\parallel$ vs $k_\perp$ from critical balance in both the Alfvén-wave [§ 1.2, Eq. (5)] and kinetic-Alfvén-wave [§ 7.5, Eq. (241)] regimes.

does not matter at these small scales.

In most astrophysical situations, one cannot assume that equilibrium quantities such as density, temperature, mean velocity and mean magnetic field are uniform at the outer scale. However, at scales much smaller than L, the gradients of the small-scale fluctuating fields are much larger than the outer-scale gradients (although the fluctuation amplitudes are much smaller; for the mean magnetic field, this assumption is discussed in some detail in § 1.3), so we may neglect the equilibrium gradients and consider the turbulence to be homogeneous. Specifically, this is a good assumption if $k_\parallel L \gg 1$ [Eq. (6)], i.e., not only the perpendicular scales but also the much larger parallel ones are still shorter than the outer scale. Note that we cannot generally assume that the outer-scale energy injection is anisotropic, so the anisotropy is also the property of small scales only.

1.5.2. Microscales

There are four microphysical scales that mark the transitions between distinct physical regimes:

Electron diffusion scale. — At $k_\parallel \lambda_{\mathrm{mfp}i}(m_i/m_e)^{1/2} \gg 1$, the electron response is isothermal (§ 4.4, Appendix A.4). At $k_\parallel \lambda_{\mathrm{mfp}i}(m_i/m_e)^{1/2} \ll 1$, it is adiabatic (§ 4.8.4, Appendix A.3).

Mean free path. — At $k_\parallel \lambda_{\mathrm{mfp}i} \gg 1$, the plasma is collisionless. In this regime, wave–particle interactions can damp compressive fluctuations via Barnes damping (§ 6.2.2), so kinetic de-

scription becomes essential. At $k_\parallel \lambda_{\mathrm{mfp}i} \ll 1$, the plasma is collisional and fluid-like (§ 6.1, Appendices A and D).

Ion gyroscale. — At $k_\perp \rho_i \ll 1$, ions (as well as the electrons) are magnetized and the magnetic field is frozen into the ion flow (the $\mathbf{E} \times \mathbf{B}$ velocity field). At $k_\perp \rho_i \sim 1$, ions can exchange energy with electromagnetic fluctuations via wave–particle interactions (and ion heating eventually occurs via a kinetic ion-entropy cascade, see §§ 7.9-7.10). At $k_\perp \rho_i \gg 1$, the ions are unmagnetized and have a Boltzmann response (§ 7.2). Note that the ion inertial scale $d_i = \rho_i/\sqrt{\beta_i}$ is comparable to the ion gyroscale unless the plasma beta $\beta_i = 8\pi n_i T_i/B^2$ is very different from unity. In the theories developed below, d_i does not play a special role except in the limit of $T_i \ll T_e$, which is not common in astrophysical plasmas (see further discussion in § 7.1 and Appendix E).

Electron gyroscale. — At $k_\perp \rho_e \ll 1$, electrons are magnetized and the magnetic field is frozen into the electron flow (§ 4, § 7, Appendix C). At $k_\perp \rho_e \sim 1$, the electrons absorb the energy of the electromagnetic fluctuations via wave–particle interactions (leading to electron heating via a kinetic electron-entropy cascade, see § 7.12).

Typical values of these scales and of several other key parameters are given in Table 1. In Fig. 2, we show how the wavenumber space, $(k_\perp, k_\parallel)$, is divided by these scales into several domains, where the physics is different. Further partitioning of the wavenumber space results from comparing $k_\perp \rho_i$ and $k_\parallel \lambda_{\mathrm{mfp}i}$ ($k_\perp \rho_i \ll k_\parallel \lambda_{\mathrm{mfp}i}$ is the limit of strong magnetiza-

TABLE 1
REPRESENTATIVE PARAMETERS FOR ASTROPHYSICAL PLASMAS.

Parameter	Solar wind at 1 AU[a]	Warm ionized ISM[b]	Accretion flow near Sgr A*[c]	Galaxy clusters (cores)[d]
$n_e = n_i$, cm^{-3}	30	0.5	10^6	6×10^{-2}
T_e, K	$\sim T_i$[e]	8000	10^{11}	3×10^7
T_i, K	5×10^5	8000	$\sim 10^{12}$[f]	?[e]
B, G	10^{-4}	10^{-6}	30	7×10^{-6}
β_i	5	14	4	130
$v_{\mathrm{th}i}$, km/s	90	10	10^5	700
v_A, km/s	40	3	7×10^4	60
U, km/s[f]	~ 10	~ 10	$\sim 10^4$	$\sim 10^2$
L, km[f]	$\sim 10^5$	$\sim 10^{15}$	$\sim 10^8$	$\sim 10^{17}$
$(m_i/m_e)^{1/2}\lambda_{\mathrm{mfp}i}$, km	10^{10}	2×10^8	4×10^{10}	4×10^{16}
$\lambda_{\mathrm{mfp}i}$, km[g]	3×10^8	6×10^6	10^9	10^{15}
ρ_i, km	90	1000	0.4	10^4
ρ_e, km	2	30	0.003	200

[a] Values for slow wind (mean flow speed $V_{\mathrm{sw}} = 350$ km/s in this case) measured by Cluster spacecraft and taken from Bale et al. (2005), except the value of T_e, which they do not report, but which is expected to be of the same order as T_i (Newbury et al. 1998). Note that the data interval studied by Bale et al. (2005) is slightly atypical, with β_i higher than usual in the solar wind (the full range of β_i variation in the solar wind is roughly between 0.1 and 10; see Howes et al. 2008a for another, perhaps more typical, fiducial set of slow-wind parameters and Appendix A of the review by Bruno & Carbone 2005 for slow- and fast-wind parameters measured by Helios 2). However, we use their parameter values as our representative example because the spectra they report show with particular clarity both the electric and magnetic fluctuations in both the inertial and dissipation ranges (see Fig. 1). See further discussion in § 8.1 and § 8.2.
[b] Typical values (see, e.g., Norman & Ferrara 1996; Ferrière 2001). See discussion in § 8.4.
[c] Values based on observational constraints for the radio-emitting plasma around the Galactic Center (Sgr A*) as interpreted by Loeb & Waxman (2007) (see also Quataert 2003). See discussion in § 8.5.
[d] Values for the core region of the Hydra A cluster taken from Enßlin & Vogt (2006); see Schekochihin & Cowley 2006 for a consistent set of numbers for the hot plasmas outside the cores. See discussion in § 8.6.
[e] We assume $T_i \sim T_e$ for these estimates.
[f] Rough order-of-magnitude estimate.
[g] Defined $\lambda_{\mathrm{mfp}i} = v_{\mathrm{th}i}/\nu_{ii}$, where ν_{ii} is given by Eq. (52).

tion, see Appendix A.2) and, most importantly, from comparing parallel and perpendicular wavenumbers. As we explained above, observational and numerical evidence tells us that Alfvénic turbulence is anisotropic, $k_\parallel \ll k_\perp$. In Fig. 2, we sketch the path the turbulent cascade is expected to take in the wavenumber space (we use the scalings of $k_\parallel$ with $k_\perp$ that follow from the GS argument for the Alfvén waves and an analogous argument for the kinetic Alfvén waves, reviewed in § 1.2 and § 7.5, respectively).

1.6. Kinetic and Fluid Models

What is the correct analytical description of the turbulent plasma fluctuations along the (presumed) path of the cascade? As we promised above, it is going to be possible to simplify the full kinetic theory substantially. These simplifications can be obtained in the form of a hierarchy of approximations and as these emerge, specific physical mechanisms that control the turbulent cascade in various physical regimes become more transparent.

Gyrokinetics (§ 3). — The starting point for these developments and the primary approximation in the hierarchy is *gyrokinetics*, a low-frequency kinetic theory resulting from averaging over the cyclotron motion of the particles. Gyrokinetics is appropriate for the study of subsonic plasma turbulence in virtually all astrophysically relevant parameter ranges (Howes et al. 2006). For fluctuations at frequencies lower than the ion cyclotron frequency, $\omega \ll \Omega_i$, gyrokinetics can be systematically derived by making use of the following two assumptions, which also underpin the GS theory (§ 1.2): (a) anisotropy of the turbulence, so $\epsilon \sim k_\parallel/k_\perp$ is used as the small parameter, and (b) strong interactions, i.e., the fluctuation amplitudes are assumed to be such that wave propagation and nonlinear interaction occur on comparable timescales: from Eq. (3), $u_\perp/v_A \sim \epsilon$. The first of these assumptions implies that fluctuations at Alfvénic frequencies satisfy $\omega \sim k_\parallel v_A \ll \Omega_i$ even when their perpendicular scale is such $k_\perp \rho_i \sim 1$. This makes gyrokinetics an ideal tool both for analytical theory and for numerical studies of astrophysical plasma turbulence; the numerical approaches are also made attractive by the long experience of gyrokinetic simulations accumulated in the fusion research and by the existence of publicly available gyrokinetic codes (Kotschenreuther et al. 1995; Jenko et al. 2000; Candy & Waltz 2003; Chen & Parker 2003). A concise review of gyrokinetics is provided in § 3 (see Howes et al. 2006 for a detailed derivation). The reader is urged to pay particular attention to § 3.4 and § 3.5, where the concept of the *kinetic cascade* of *generalized energy* is introduced and the particle heating in gyrokinetics is discussed (Appendix F introduces additional conservation laws that arise in 2D and sometimes also in 3D). This establishes the conceptual framework in which most of the subsequent physical arguments are presented. The region of validity of gyrokinetics is illustrated in Fig. 3: it covers virtually the entire path of the turbulent cascade, except the largest (outer) scales, where one cannot assume anisotropy. Note that the two-fluid theory, which is the starting point for the MHD theory (see Appendix A), is not a good description at collisionless scales. It is important to mention, however, that the formulation of gyrokinetics that we adopt, while appropriate for treating fluctuations at collisionless scales, does nevertheless require a certain (weak) degree of collisionality (see discussion in § 3.1.3 and an extended treatment of collisions in gyrokinetics in Appendix B).

Isothermal Electron Fluid (§ 4). — While gyrokinetics constitutes a significant simplification, it is still a fully kinetic description. Further progress towards simpler models is achieved by showing that, for parallel scales smaller than the electron diffusion scale, $k_\parallel \lambda_{\mathrm{mfp}i} \gg (m_e/m_i)^{1/2}$, and perpendicular scales larger than the electron gyroscale, $k_\perp \rho_e \ll 1$, the electrons are a magnetized isothermal fluid while ions must be treated (gyro)kinetically. This is the secondary approximation in our hierarchy, derived in § 4 via an asymptotic expansion in $(m_e/m_i)^{1/2}$ (see also Appendix C.1). The plasma is described by the ion gyrokinetic equation and two fluid-like equations that contain electron dynamics—these are summarized in § 4.9. The region of validity of this approximation is illustrated in Fig. 4: it does not capture the dissipative effects around the electron diffusion scale or the electron heating, but it remains uniformly valid as the cascade passes from collisional to collisionless scales and also as it crosses the ion gyroscale.

In order to elucidate the nature of the turbulence above and below the ion gyroscale, we derive two tertiary approximations, one of which is valid for $k_\perp \rho_i \ll 1$ (§ 5 and § 6) and the other for $k_\perp \rho_i \gg 1$ (§ 7; see also Appendix C, which gives a non-rigorous, non-gyrokinetic, but perhaps more intuitive, derivation of the results of § 4 and § 7.2).

Kinetic Reduced MHD (§ 5 and § 6). — On scales above the ion gyroscale, known as the *"inertial range"* we demonstrate that the decoupling of the Alfvén-wave cascade and its indifference to both collisional and collisionless damping are explicit and analytically provable properties. We show rigorously that the Alfvén-wave cascade is governed by a closed set of two fluid-like equations for the stream and flux functions—the Reduced Magnetohydrodynamics (RMHD)—independently of the collisionality (§ 5.3 and § 5.4; the derivation of RMHD from MHD and its properties are presented in § 2). The cascade proceeds via interaction of oppositely propagating wave packets and is decoupled from the density and magnetic-field-strength fluctuations (the "compressive" modes; in the collisional limit, these are the entropy and slow modes; see § 6.1 and Appendix D). The latter are passively mixed by the Alfvén waves, but, unlike in the fluid (collisional) limit, this passive cascade is governed by a (simplified) kinetic equation for the ions (§ 5.5). Together with RMHD, it forms a hybrid fluid-kinetic description of magnetized turbulence in a weakly collisional plasma, which we call *Kinetic Reduced MHD (KRMHD)*. The KRMHD equations are summarized in § 5.7. Their collisional and collisionless limits are explored in § 6.1 and § 6.2, respectively. Whereas the Alfvén waves are undamped in this approximation, the compressive fluctuations are subject to damping both in the collisional (Braginskii 1965 viscous damping, § 6.1.2) and collisionless (Barnes 1966 damping, § 6.2.2) limits. In the collisionless limit, the compressive component of the turbulence is a simple example of an essentially kinetic turbulence, including such features as conservation of generalized energy despite collisionless damping and (parallel) phase mixing, possibly leading to ion heating (§§ 6.2.3-6.2.5). How strongly the compressive fluctuations are damped depends on the parallel scale of these fluctuations. Since the ion kinetic equation turns out to be linear along the moving field lines associated with the Alfvén waves, the compressive fluctuations do not, in the absence of finite-gyroradius effects, develop small parallel scales and their cascade may be only weakly damped above the ion gyroscale—this is discussed in § 6.3.

Electron Reduced MHD (§ 7). — At the ion gyroscale, the Alfvénic and the compressive cascades are no longer decoupled and their energy is partially damped via collisionless wave–particle interactions (§ 7.1). This part of the energy is channeled into ion heat. The rest of it is converted into a cascade of kinetic Alfvén waves (KAW). This cascade extends through what is known as the *"dissipation range"* to the electron gyroscale, where its turn comes to be damped via wave–particle interaction and transferred into electron heat. The KAW turbulence is again anisotropic with $k_\parallel \ll k_\perp$. It is governed by a pair of fluid-like equations, also derived from gyrokinetics. We call them *Electron Reduced MHD (ERMHD)*. In the high-beta limit, they coincide with the reduced (anisotropic) form of the previously known Electron MHD (Kingsep et al. 1990). The ERMHD equations are derived in § 7.2 (see also Appendix C.2) and the KAW cas-

cade is considered in §§ 7.3-7.5. The fate of the inertial-range energy collisionlessly damped at the ion gyroscale is investigated in §§ 7.9-7.11; an analogous consideration for the KAW energy damped at the electron gyroscale is presented in § 7.12. In these sections, we introduce the notion of the *entropy cascade*—a nonlinear phase-mixing process whereby the collisionless damping occurring at the ion and electron gyroscales is made irreversible and particles are heated. This part of the cascade is purely kinetic and its salient feature is the particle distribution functions developing small scales in the gyrokinetic phase space. Note that besides deriving rigorous sets of equations for the dissipation-range turbulence, § 7 also presents a number of Kolmogorov-style scaling predictions—both for the KAW cascade (§ 7.5) and for the entropy cascade (§ 7.9.2, § 7.10.2, § 7.10.4, § 7.12).

Hall Reduced MHD (Appendix E). — The reduced (anisotropic) form of the popular Hall MHD system can be derived as a special limit of gyrokinetics ($k_\perp \rho_i \ll 1$, $T_i \ll T_e$, $\beta_i \ll 1$). The resulting *Hall Reduced MHD (HRMHD)* equations are a convenient model for some purposes because they simultaneously capture the cold-ion, low-beta limits of both the KRMHD and ERMHD systems. However, they are usually not strictly applicable in space and astrophysical plasmas of interest, where ions are rarely cold and β_i is not particularly low. The HRMHD equations are derived in § E.1, the kinetic cascade of generalized energy in the Hall limit is discussed in § E.2, and the circumstances under which the ion inertial and ion sound scales become important in theories of plasma turbulence are summarized in § E.4. Theories of the dissipation-range turbulence based on Hall MHD are briefly discussed in § 8.2.6.

The regions of validity of the tertiary approximations—KRMHD and ERMHD—are illustrated in Fig. 2. In this figure, we also show the region of validity of the RMHD system derived from the standard compressible MHD equations by assuming anisotropy of the turbulence and strong interactions. This derivation is the fluid analog of the derivation of gyrokinetics. We present it in § 2, before embarking on the gyrokinetics-based path outlined above, in order to make a connection with the conventional MHD treatment and to demonstrate with particular simplicity how the assumption of anisotropy leads to a reduced fluid system in which the decoupling of the cascades of the Alfvén waves and of the compressive modes is manifest (Appendix A extends this derivation to Braginskii 1965 two-fluid equations in the limit of strong magnetization; it also works out rigorously the transition from the fluid limit to the KRMHD equations).

The main formal developments of this paper are contained in §§ 3-7. The outline given above is meant to help the reader navigate these sections. In § 8, we discuss at some length how our results apply to various astrophysical plasmas with weak collisionality: the solar wind and the magnetosheath, the ISM, accretion disks, and galaxy clusters (§ 8.1 and § 8.2 can also be read as an overall summary of the paper in light of the evidence available from space-plasma measurements). Finally, in § 9, we provide a brief epilogue and make a few remarks about future directions of inquiry.

2. REDUCED MHD AND THE DECOUPLING OF TURBULENT CASCADES

Consider the equations of compressible MHD

$$\frac{d\rho}{dt} = -\rho \nabla \cdot \mathbf{u}, \tag{7}$$

$$\rho \frac{d\mathbf{u}}{dt} = -\nabla \left(p + \frac{B^2}{8\pi} \right) + \frac{\mathbf{B} \cdot \nabla \mathbf{B}}{4\pi}, \tag{8}$$

$$\frac{ds}{dt} = 0, \quad s = \frac{p}{\rho^\gamma}, \quad \gamma = \frac{5}{3}, \tag{9}$$

$$\frac{d\mathbf{B}}{dt} = \mathbf{B} \cdot \nabla \mathbf{u} - \mathbf{B} \nabla \cdot \mathbf{u}, \tag{10}$$

where ρ is the mass density, $\mathbf{u}$ velocity, p pressure, $\mathbf{B}$ magnetic field, s the entropy density, and $d/dt = \partial/\partial t + \mathbf{u} \cdot \nabla$ (the conditions under which these equations are valid are discussed in Appendix A). Consider a uniform static equilibrium with a straight mean field in the z direction, so

$$\rho = \rho_0 + \delta\rho, \quad p = p_0 + \delta p, \quad \mathbf{B} = B_0 \hat{\mathbf{z}} + \delta\mathbf{B}, \tag{11}$$

where ρ_0, p_0, and B_0 are constants. In what follows, the subscripts $\parallel$ and $\perp$ will be used to denote the projections of fields, variables and gradients on the mean-field direction $\hat{\mathbf{z}}$ and onto the plane (x, y) perpendicular to this direction, respectively.

2.1. RMHD Ordering

As we explained in the Introduction, observational and numerical evidence makes it safe to assume that the turbulence in such a system will be anisotropic with $k_\parallel \ll k_\perp$ (at scales smaller than the outer scale, $k_\parallel L \gg 1$; see § 1.3 and § 1.5.1). Let us, therefore, introduce a small parameter $\epsilon \sim k_\parallel/k_\perp$ and carry out a systematic expansion of Eqs. (7-10) in ϵ. In this expansion, the fluctuations are treated as small, but not arbitrarily so: in order to estimate their size, we shall adopt the critical-balance conjecture (3), which is now treated *not* as a detailed scaling prescription but as an ordering assumption. This allows us to introduce the following ordering:

$$\frac{\delta\rho}{\rho_0} \sim \frac{u_\perp}{v_A} \sim \frac{u_\parallel}{v_A} \sim \frac{\delta p}{p_0} \sim \frac{\delta B_\perp}{B_0} \sim \frac{\delta B_\parallel}{B_0} \sim \frac{k_\parallel}{k_\perp} \sim \epsilon, \tag{12}$$

where $v_A = B_0/\sqrt{4\pi\rho_0}$ is the Alfvén speed. Note that this means that we order the Mach number

$$M \sim \frac{u}{c_s} \sim \frac{\epsilon}{\sqrt{\beta_i}}, \tag{13}$$

where $c_s = (\gamma p_0/\rho_0)^{1/2}$ is the speed of sound and

$$\beta = \frac{8\pi p_0}{B_0^2} = \frac{2}{\gamma} \frac{c_s^2}{v_A^2} \tag{14}$$

is the plasma beta, which is ordered to be order unity in the ϵ expansion (subsidiary limits of high and low β can be taken after the ϵ expansion is done; see § 2.4).

In Eq. (12), we made two auxiliary ordering assumptions: that the velocity and magnetic-field fluctuations have the character of Alfvén and slow waves ($\delta B_\perp/B_0 \sim u_\perp/v_A$, $\delta B_\parallel/B_0 \sim u_\parallel/v_A$) and that the relative amplitudes of the Alfvén-wave-polarized fluctuations ($\delta B_\perp/B_0$, $u_\perp/v_A$), slow-wave-polarized fluctuations ($\delta B_\parallel/B_0$, $u_\parallel/v_A$) and density/pressure/entropy fluctuations ($\delta\rho/\rho_0$, $\delta p/p_0$) are all the same order. Strictly speaking, whether this is the case depends on the energy sources that drive the turbulence: as we shall see, if no slow waves (or entropy fluctuations) are launched, none will be present. However, in astrophysical contexts, the

outer-scale energy input may be assumed random and, therefore, comparable power is injected into all types of fluctuations.

We further assume that the characteristic frequency of the fluctuations is $\omega \sim k_\parallel v_A$ [Eq. (3)], meaning that the fast waves, for which $\omega \simeq k_\perp(v_A^2 + c_s^2)^{1/2}$, are ordered out. This restriction must be justified empirically. Observations of the solar-wind turbulence confirm that it is primarily Alfvénic (see, e.g., Bale et al. 2005) and that its compressive component is substantially pressure-balanced (Roberts 1990; Burlaga et al. 1990; Marsch & Tu 1993; Bavassano et al. 2004, see Eq. (22) below). A weak-turbulence calculation of compressible MHD turbulence in low-beta plasmas (Chandran 2005b) suggests that only a small amount of energy is transferred from the fast waves to Alfvén waves with large $k_\parallel$. A similar conclusion emerges from numerical simulations (Cho & Lazarian 2002, 2003). As the fast waves are also expected to be subject to strong collisionless damping and/or to strong dissipation after they steepen into shocks, we eliminate them from our consideration of the problem and concentrate on low-frequency turbulence.

2.2. Alfvén Waves

We start by observing that the Alfvén-wave-polarized fluctuations are two-dimensionally solenoidal: since, from Eq. (7),

$$\nabla \cdot \mathbf{u} = -\frac{d}{dt} \frac{\delta\rho}{\rho_0} = O(\epsilon^2) \tag{15}$$

and $\nabla \cdot \delta\mathbf{B} = 0$ exactly, separating the $O(\epsilon)$ part of these divergences gives $\nabla_\perp \cdot \mathbf{u}_\perp = 0$ and $\nabla_\perp \cdot \delta\mathbf{B}_\perp = 0$. To lowest order in the ϵ expansion, we may, therefore, express $\mathbf{u}_\perp$ and $\delta\mathbf{B}_\perp$ in terms of scalar stream (flux) functions:

$$\mathbf{u}_\perp = \hat{\mathbf{z}} \times \nabla_\perp \Phi, \qquad \frac{\delta\mathbf{B}_\perp}{\sqrt{4\pi\rho_0}} = \hat{\mathbf{z}} \times \nabla_\perp \Psi. \tag{16}$$

Evolution equations for Φ and Ψ are obtained by substituting the expressions (16) into the perpendicular parts of the induction equation (10) and the momentum equation (8)—of the latter the curl is taken to annihilate the pressure term. Keeping only the terms of the lowest order, $O(\epsilon^2)$, we get

$$\frac{\partial\Psi}{\partial t} + \{\Phi, \Psi\} = v_A \frac{\partial\Phi}{\partial z}, \tag{17}$$

$$\frac{\partial}{\partial t} \nabla_\perp^2 \Phi + \{\Phi, \nabla_\perp^2 \Phi\} = v_A \frac{\partial}{\partial z} \nabla_\perp^2 \Psi + \{\Psi, \nabla_\perp^2 \Psi\}, \tag{18}$$

where $\{\Phi, \Psi\} = \hat{\mathbf{z}} \cdot (\nabla_\perp \Phi \times \nabla_\perp \Psi)$ and we have taken into account that, to lowest order,

$$\frac{d}{dt} = \frac{\partial}{\partial t} + \mathbf{u}_\perp \cdot \nabla_\perp = \frac{\partial}{\partial t} + \{\Phi, \cdots\}, \tag{19}$$

$$\hat{\mathbf{b}} \cdot \nabla = \frac{\partial}{\partial z} + \frac{\delta\mathbf{B}_\perp}{B_0} \cdot \nabla_\perp = \frac{\partial}{\partial z} + \frac{1}{v_A} \{\Psi, \cdots\}. \tag{20}$$

Here $\hat{\mathbf{b}} = \mathbf{B}/B_0$ is the unit vector along the perturbed field line.

Equations (17-18) are known as the Reduced Magnetohydrodynamics (RMHD). The first derivations of these equations (in the context of fusion plasmas) are due to Kadomtsev & Pogutse (1974) and to Strauss (1976). These were followed by many systematic derivations and generalizations employing various versions and refinements of the basic expansion, taking into account the non-Alfvénic

modes (which we will do in § 2.4), and including the effects of spatial gradients of equilibrium fields (e.g., Strauss 1977; Montgomery 1982; Hazeltine 1983; Zank & Matthaeus 1992; Kinney & McWilliams 1997; Bhattacharjee et al. 1998; Kruger et al. 1998). A comparative review of these expansion schemes and their (often close) relationship to ours is outside the scope of this paper. One important point we wish to emphasize is that we do not assume the plasma beta [defined in Eq. (14)] to be either large or small.

Equations (17) and (18) form a closed set, meaning that the Alfvén-wave cascade decouples from the slow waves and density fluctuations. It is to the turbulence described by Eqs. (17-18) that the GS theory outlined in § 1.2 applies.[13] In § 5.3, we will show that Eqs. (17) and (18) correctly describe inertial-range Alfvénic fluctuations even in a collisionless plasma, where the full MHD description [Eqs. (7-10)] is not valid.

2.3. *Elsasser Fields*

The MHD equations (7-10) in the incompressible limit ($\rho = $ const) acquire a symmetric form if written in terms of the Elsasser fields $\mathbf{z}^{\pm} = \mathbf{u} \pm \delta\mathbf{B}/\sqrt{4\pi\rho}$ (Elsasser 1950). Let us demonstrate how this symmetry manifests itself in the reduced equations derived above.

We introduce *Elsasser potentials* $\zeta^{\pm} = \Phi \pm \Psi$, so that $\mathbf{z}_{\perp}^{\pm} = \hat{\mathbf{z}} \times \nabla_{\perp}\zeta^{\pm}$. For these potentials, Eqs. (17-18) become

$$\frac{\partial}{\partial t}\nabla_{\perp}^2\zeta^{\pm} \mp v_A\frac{\partial}{\partial z}\nabla_{\perp}^2\zeta^{\pm} = -\frac{1}{2}\left(\{\zeta^+, \nabla_{\perp}^2\zeta^-\} + \{\zeta^-, \nabla_{\perp}^2\zeta^+\} \mp \nabla_{\perp}^2\{\zeta^+, \zeta^-\}\right).$$ (21)

These equations show that the RMHD has a simple set of exact solutions: if $\zeta^- = 0$ or $\zeta^+ = 0$, the nonlinear term vanishes and the other, non-zero, Elsasser potential is simply a fluctuation of arbitrary shape and magnitude propagating along the mean field at the Alfvén speed v_A: $\zeta^{\pm} = f^{\pm}(x, y, z \mp v_At)$. These solutions are finite-amplitude Alfvén-wave packets of arbitrary shape. Only counterpropagating such solutions can interact and thereby give rise to the Alfvén-wave cascade (Kraichnan 1965). Note that these interactions are conservative in the sense that the "+" and "−" waves scatter off each other without exchanging energy.

Note that the individual conservation of the "+" and "−" waves' energies means that the energy fluxes associated with these waves need not be equal, so instead of a single Kolmogorov flux ε assumed in the scaling arguments

reviewed in § 1.2, we could have $\varepsilon^+ \neq \varepsilon^-$. The GS theory can be generalized to this case of *imbalanced* Alfvénic cascades (Lithwick et al. 2007; Beresnyak & Lazarian 2008a; Chandran 2008), but here we will focus on the balanced turbulence, $\varepsilon^+ \sim \varepsilon^-$. If one considers the turbulence forced in a physical way (i.e., without forcing the magnetic field, which would break the flux conservation), the resulting cascade would always be balanced. In the real world, imbalanced Alfvénic fluxes are measured in the fast solar wind, where the influence of initial conditions in the solar atmosphere is more pronounced, while the slow-wind turbulence is approximately balanced (Marsch & Tu 1990a; see also reviews by Tu & Marsch 1995; Bruno & Carbone 2005 and references therein).

2.4. *Slow Waves and the Entropy Mode*

In order to derive evolution equations for the remaining MHD modes, let us first revisit the perpendicular part of the momentum equation and use Eq. (12) to order terms in it. In the lowest order, $O(\epsilon)$, we get the pressure balance

$$\nabla_{\perp}\left(\delta p + \frac{B_0\delta B_{\parallel}}{4\pi}\right) = 0 \quad \Rightarrow \quad \frac{\delta p}{p_0} = -\gamma\frac{v_A^2}{c_s^2}\frac{\delta B_{\parallel}}{B_0}.$$ (22)

Using Eq. (22) and the entropy equation (9), we get

$$\frac{d\delta s}{dt} = 0, \quad \frac{\delta s}{s_0} = \frac{\delta p}{p_0} - \gamma\frac{\delta\rho}{\rho_0} = -\gamma\left(\frac{\delta\rho}{\rho_0} + \frac{v_A^2}{c_s^2}\frac{\delta B_{\parallel}}{B_0}\right),$$ (23)

where $s_0 = p_0/\rho_0^{\gamma}$. Now, substituting Eq. (15) for $\nabla \cdot \mathbf{u}$ in the parallel component of the induction equation (10), we get

$$\frac{d}{dt}\left(\frac{\delta B_{\parallel}}{B_0} - \frac{\delta\rho}{\rho_0}\right) - \hat{\mathbf{b}}\cdot\nabla u_{\parallel} = 0.$$ (24)

Combining Eqs. (23) and (24), we obtain

$$\frac{d}{dt}\frac{\delta\rho}{\rho_0} = -\frac{1}{1 + c_s^2/v_A^2}\hat{\mathbf{b}}\cdot\nabla u_{\parallel},$$ (25)

$$\frac{d}{dt}\frac{\delta B_{\parallel}}{B_0} = \frac{1}{1 + v_A^2/c_s^2}\hat{\mathbf{b}}\cdot\nabla u_{\parallel}.$$ (26)

Finally, we take the parallel component of the momentum equation (8) and notice that, due to the pressure balance (22) and to the smallness of the parallel gradients, the pressure term is $O(\epsilon^3)$, while the inertial and tension terms are $O(\epsilon^2)$. Therefore,

$$\frac{du_{\parallel}}{dt} = v_A^2\hat{\mathbf{b}}\cdot\nabla\frac{\delta B_{\parallel}}{B_0}.$$ (27)

Equations (26-27) describe the slow-wave-polarized fluctuations, while Eq. (23) describes the zero-frequency entropy mode, which is decoupled from the slow waves.[14] The nonlinearity in Eqs. (26-27) enters via the derivatives defined in

---

[13] The Alfvén-wave turbulence in the RMHD system has been studied by many authors. Some of the relevant numerical investigations are due to Kinney & McWilliams (1998), Dmitruk et al. (2003), Oughton et al. (2004), Rappazzo et al. (2007, 2008), Perez & Boldyrev (2008, 2009). Analytical theory has mostly been confined to the weak-turbulence paradigm (Ng & Bhattacharjee 1996, 1997; Bhattacharjee & Ng 2001; Galtier et al. 2002; Lithwick & Goldreich 2003; Galtier & Chandran 2006; Nazarenko 2008). We note that adopting the critical balance [Eq. (3)] as an ordering assumption for the expansion in $k_{\parallel}/k_{\perp}$ does not preclude one from subsequently attempting a weak-turbulence approach: the latter should simply be treated as a subsidiary expansion. Indeed, implementing the anisotropy assumption on the level of MHD equations rather than simultaneously with the weak-turbulence closure (Galtier et al. 2000) significantly reduces the amount of algebra. One should, however, bear in mind that the weak-turbulence approximation always breaks down at some sufficiently small scale—namely, when $k_{\perp} \sim (v_A/U)^2 k_{\parallel}^2 L$, where L is the outer scale of the turbulence, U velocity at the outer scale, and $k_{\parallel}$ the parallel wavenumber of the Alfvén waves (see Goldreich & Sridhar 1997 or the review by Schekochihin & Cowley 2007). Below this scale, interactions cannot be assumed weak.

[14] For other expansion schemes leading to reduced sets of equations for these "compressive" fluctuations see references in § 2.2. Note that the nature of the density fluctuations described above is distinct from the so called "pseudosound" density fluctuations that arise in the "nearly incompressible" MHD theories (Montgomery et al. 1987; Matthaeus & Brown 1988; Matthaeus et al. 1991; Zank & Matthaeus 1993). The "pseudosound" is essentially the density response caused by the nonlinear pressure fluctuations calculated from the incompressibility constraint. The resulting density fluctuations are second order in Mach number and, therefore, order ϵ^2 in our expansion [see Eq. (13)]. The passive density fluctuations derived in this section are order ϵ and, therefore, supersede the "pseudosound" (see review by Tu & Marsch 1995 for a discussion of the relevant solar-wind evidence).

Eqs. (19-20) and is due solely to interactions with Alfvén waves. Thus, both the slow-wave and the entropy-mode cascades occur via passive scattering/mixing by Alfvén waves, in the course of which there is no energy exchange between the cascades.

Note that in the high-beta limit, $c_s \gg v_A$ [see Eq. (14)], the entropy mode is dominated by density fluctuations [Eq. (23), $c_s \gg v_A$], which also decouple from the slow-wave cascade [Eq. (25), $c_s \gg v_A$]. and are passively mixed by the Alfvén-wave turbulence:

$$\frac{d\delta\rho}{dt} = 0. \tag{28}$$

The high-beta limit is equivalent to the incompressible approximation for the slow waves.

In § 5.5, we will derive a kinetic description for the inertial-range compressive fluctuations (density and magnetic-field strength), which is more generally valid in weakly collisional plasmas and which reduces to Eqs. (26-27) in the collisional limit (see Appendix D). While these fluctuations will in general satisfy a kinetic equation, they will remain passive with respect to the Alfvén waves.

2.5. *Elsasser Fields for the Slow Waves*

The original Elsasser (1950) symmetry was derived for incompressible MHD equations. However, for the "compressive" slow-wave fluctuations, we may introduce generalized Elsasser fields:

$$z_\parallel^\pm = u_\parallel \pm \frac{\delta B_\parallel}{\sqrt{4\pi\rho_0}} \left(1 + \frac{v_A^2}{c_s^2}\right)^{1/2}. \tag{29}$$

Straightforwardly, the evolution equation for these fields is

$$\frac{\partial z_\parallel^\pm}{\partial t} \mp \frac{v_A}{\sqrt{1 + v_A^2/c_s^2}} \frac{\partial z_\parallel^\pm}{\partial z} =$$
$$-\frac{1}{2}\left(1 \mp \frac{1}{\sqrt{1 + v_A^2/c_s^2}}\right)\left\{\zeta^+, z_\parallel^\pm\right\}$$
$$-\frac{1}{2}\left(1 \pm \frac{1}{\sqrt{1 + v_A^2/c_s^2}}\right)\left\{\zeta^-, z_\parallel^\pm\right\}. \tag{30}$$

In the high-beta limit ($v_A \ll c_s$), the generalized Elsasser fields (29) become the parallel components of the conventional incompressible Elsasser fields. We see that only in this limit do the slow waves interact exclusively with the counterpropagating Alfvén waves, and so only in this limit does setting $\zeta^- = 0$ or $\zeta^+ = 0$ gives rise to finite-amplitude slow-wave-packet solutions $z_\parallel^\pm = f^\pm(x, y, z \mp v_A t)$ analogous to the finite-amplitude Alfvén-wave packets discussed in § 2.3.[15] For general β, the phase speed of the slow waves is smaller than that of the Alfvén waves and, therefore, Alfvén waves can "catch up" and interact with the slow waves that travel in the same direction. All of these interactions are of scattering type and involve no exchange of energy.

2.6. *Scalings for Passive Fluctuations*

[15] Obviously, setting *both* $\zeta^\pm = 0$ does always enable these finite-amplitude slow-wave solutions. More non-trivially, such finite-amplitude solutions exist in the Lagrangian frame associated with the Alfvén waves—this is discussed in detail in § 6.3.

The scaling of the passively mixed scalar fields introduced above is slaved to the scaling of the Alfvénic fluctuations. Consider for example the entropy mode [Eq. (23)]. As in Kolmogorov–Obukhov theory (see § 1.1), one assumes a local-in-scale-space cascade of scalar variance and a constant flux ε_s of this variance. Then, analogously to Eq. (1),

$$\frac{v_{\text{th}i}^2}{s_0^2} \frac{\delta s_\lambda^2}{\tau_\lambda} \sim \varepsilon_s. \tag{31}$$

Since the cascade time is $\tau_\lambda^{-1} \sim \mathbf{u}_\perp \cdot \nabla_\perp \sim v_A/l_{\parallel\lambda} \sim \varepsilon/u_{\perp\lambda}^2$,

$$\frac{\delta s_\lambda}{s_0} \sim \left(\frac{\varepsilon_s}{\varepsilon}\right)^{1/2} \frac{u_{\perp\lambda}}{v_{\text{th}i}}, \tag{32}$$

so the scalar fluctuations have the same scaling as the turbulence that mixes them (Obukhov 1949; Corrsin 1951). In GS turbulence, the scalar-variance spectrum should, therefore, be $k_\perp^{-5/3}$ (Lithwick & Goldreich 2001). The same argument applies to all passive fields.

It is the (presumably) passive electron-density spectrum that provides the main evidence of the $k^{-5/3}$ scaling in the interstellar turbulence (Armstrong et al. 1981, 1995; Lazio et al. 2004, see further discussion in § 8.4.1). The explanation of this spectrum in terms of passive mixing of the entropy mode, originally proposed by Higdon (1984), was developed on the basis of the GS theory by Lithwick & Goldreich (2001). The turbulent cascade of the compressive fluctuations and the relevant solar-wind data is discussed further in § 6.3. In particular, it will emerge that the anisotropy of these fluctuations remains a non-trivial issue: is there an analog of the scaling relation (5)? The scaling argument outlined above does not invoke any assumptions about the relationship between the parallel and perpendicular scales of the compressive fluctuations (other than the assumption that they are anisotropic). Lithwick & Goldreich (2001) argue that the parallel scales of the Alfvénic fluctuations will imprint themselves on the passively advected compressive ones, so Eq. (5) holds for the latter as well. In § 6.3, we examine this conclusion in view of the solar-wind evidence and of the fact that the equations for the compressive modes become linear in the Lagrangian frame associated with the Alfvénic turbulence.

2.7. *Five RMHD Cascades*

Thus, the anisotropy and critical balance (3) taken as ordering assumptions lead to a neat decomposition of the MHD turbulent cascade into a decoupled Alfvén-wave cascade and cascades of slow waves and entropy fluctuations passively scattered/mixed by the Alfvén waves. More precisely, Eqs. (23), (21) and (30) imply that, for arbitrary β, there are five conserved quantities:[16]

$$W_{\text{AW}}^\pm = \frac{1}{2}\int d^3\mathbf{r}\, \rho_0 |\nabla_\perp \zeta^\pm|^2 \qquad \text{(Alfven waves),} \tag{33}$$

$$W_{\text{sw}}^\pm = \frac{1}{2}\int d^3\mathbf{r}\, \rho_0 |z_\parallel^\pm|^2 \qquad \text{(slow waves),} \tag{34}$$

$$W_s = \frac{1}{2}\int d^3\mathbf{r}\, \frac{\delta s^2}{s_0^2} \qquad \text{(entropy fluctuations).} \tag{35}$$

[16] Note that magnetic helicity of the perturbed field is not an invariant of RMHD, except in two dimensions (see Appendix F.4). In 2D, there is also conservation of the mean square flux, $\int d^3\mathbf{r} |\Psi|^2$ (see Appendix F.2).

W_{AW}^+ and W_{AW}^- are always cascaded by interaction with each other, W_s is passively mixed by W_{AW}^+ and W_{AW}^-, $W_{sw}^\pm$ are passively scattered by $W_{AW}^\mp$ and, unless $\beta \gg 1$, also by $W_{AW}^\pm$.

This is an example of splitting of the overall energy cascade into several channels (recovered as a particular case of the more general kinetic cascade in Appendix D.2)—a concept that will repeatedly arise in the kinetic treatment to follow.

The decoupling of the slow- and Alfvén-wave cascades in MHD turbulence was studied in some detail and confirmed in direct numerical simulations by Maron & Goldreich (2001, for $\beta \gg 1$) and by Cho & Lazarian (2002, 2003, for a range of values of β). The derivation given in § 2.2 and § 2.4 (cf. Lithwick & Goldreich 2001) provides a straightforward theoretical basis for these results, assuming anisotropy of the turbulence (which was also confirmed in these numerical studies).

It turns out that the decoupling of the Alfvén-wave cascade that we demonstrated above for the anisotropic MHD turbulence is a uniformly valid property of plasma turbulence at both collisional and collisionless scales and that this cascade is correctly described by the RMHD equations (17-18) all the way down to the ion gyroscale, while the fluctuations of density and magnetic-field strength do not satisfy simple fluid evolution equations anymore and require solving the kinetic equation. In order to prove this, we adopt a kinetic description and apply to it the same ordering (§ 2.1) as we used to reduce the MHD equations. The kinetic theory that emerges as a result is called gyrokinetics.

3. GYROKINETICS

The gyrokinetic formalism was first worked out for linear waves by Rutherford & Frieman (1968) and by Taylor & Hastie (1968) (see also Catto 1978; Antonsen & Lane 1980; Catto et al. 1981) and subsequently extended to the nonlinear regime by Frieman & Chen (1982). Rigorous derivations of the gyrokinetic equation based on the Hamiltonian formalism were developed by Dubin et al. (1983, electrostatic) and Hahm et al. (1988, electromagnetic). This approach is reviewed in Brizard & Hahm (2007). A more pedestrian, but perhaps also more transparent exposition of the gyrokinetics in a straight mean field can be found in Howes et al. (2006), who also provide a detailed explanation of the gyrokinetic ordering in the context of astrophysical plasma turbulence and a treatment of the linear waves and damping rates. Here we review only the main points so as to allow the reader to understand the present paper without referring elsewhere.

In general, a plasma is completely described by the distribution function $f_s(t, \mathbf{r}, \mathbf{v})$—the probability density for a particle of species s ($= i, e$) to be found at the spatial position $\mathbf{r}$ moving with velocity $\mathbf{v}$. This function obeys the kinetic Vlasov–Landau (or Boltzmann) equation

$$\frac{\partial f_s}{\partial t} + \mathbf{v} \cdot \nabla f_s + \frac{q_s}{m_s}\left(\mathbf{E} + \frac{\mathbf{v} \times \mathbf{B}}{c}\right) \cdot \frac{\partial f_s}{\partial \mathbf{v}} = \left(\frac{\partial f_s}{\partial t}\right)_c, \quad (36)$$

where q_s and m_s are the particle's charge and mass, c is the speed of light, and the right-hand side is the collision term (quadratic in f). The electric and magnetic fields are

$$\mathbf{E} = -\nabla \varphi - \frac{1}{c}\frac{\partial \mathbf{A}}{\partial t}, \quad \mathbf{B} = \nabla \times \mathbf{A}. \quad (37)$$

The first equality is Faraday's law uncurled, the second the magnetic-field solenoidality condition; we shall use the Coulomb gauge, $\nabla \cdot \mathbf{A} = 0$. The fields satisfy the Poisson and the Ampère–Maxwell equations with the charge and current densities determined by $f_s(t, \mathbf{r}, \mathbf{v})$:

$$\nabla \cdot \mathbf{E} = 4\pi \sum_s q_s n_s = 4\pi \sum_s q_s \int d^3\mathbf{v}\, f_s, \quad (38)$$

$$\nabla \times \mathbf{B} - \frac{1}{c}\frac{\partial \mathbf{E}}{\partial t} = \frac{4\pi}{c}\mathbf{j} = \frac{4\pi}{c}\sum_s q_s \int d^3\mathbf{v}\, \mathbf{v} f_s. \quad (39)$$

3.1. Gyrokinetic Ordering and Dimensionless Parameters

As in § 2 we set up a static equilibrium with a uniform mean field, $\mathbf{B}_0 = B_0\hat{\mathbf{z}}$, $\mathbf{E}_0 = 0$, assume that the perturbations will be anisotropic with $k_\parallel \ll k_\perp$ (at scales smaller than the outer scale, $k_\parallel L \gg 1$; see § 1.3 and § 1.5.1), and construct an expansion of the kinetic theory around this equilibrium with respect to the small parameter $\epsilon \sim k_\parallel/k_\perp$. We adopt the ordering expressed by Eqs. (3) and (12), i.e., we assume the perturbations to be strongly interacting Alfvén waves plus electron density and magnetic-field-strength fluctuations.

Besides ϵ, several other dimensionless parameters are present, all of which are formally considered to be of order unity in the gyrokinetic expansion: the electron–ion mass ratio m_e/m_i, the charge ratio

$$Z = q_i/|q_e| = q_i/e \quad (40)$$

(for hydrogen, this is 1, which applies to most astrophysical plasmas of interest to us), the temperature ratio[17]

$$\tau = T_i/T_e, \quad (41)$$

and the plasma (ion) beta

$$\beta_i = \frac{v_{thi}^2}{v_A^2} = \frac{8\pi n_i T_i}{B_0^2} = \beta\left(1 + \frac{Z}{\tau}\right)^{-1}, \quad (42)$$

where $v_{thi} = (2T_i/m_i)^{1/2}$ is the ion thermal speed and the total β was defined in Eq. (14) based on the total pressure $p = n_i T_i + n_e T_e$. We shall occasionally also use the electron beta

$$\beta_e = \frac{8\pi n_e T_e}{B_0^2} = \frac{Z}{\tau}\beta_i. \quad (43)$$

The total beta is $\beta = \beta_i + \beta_e$.

3.1.1. Wavenumbers and Frequencies

As we want our theory to be uniformly valid at all (perpendicular) scales above, at or below the ion gyroscale, we order

$$k_\perp \rho_i \sim 1, \quad (44)$$

where $\rho_i = v_{thi}/\Omega_i$ is the ion gyroradius, $\Omega_i = q_i B_0/cm_i$ the ion cyclotron frequency. Note that

$$\rho_e = \frac{Z}{\sqrt{\tau}}\sqrt{\frac{m_e}{m_i}}\,\rho_i. \quad (45)$$

---

[17] It can be shown that equilibrium temperatures change on the timescale $\sim (\epsilon^2\omega)^{-1}$ (Howes et al. 2006). On the other hand, from standard theory of collisional transport (e.g., Helander & Sigmar 2002), the ion and electron temperatures equalize on the timescale $\sim \nu_{ie}^{-1} \sim (m_i/m_e)^{1/2}\nu_{ii}^{-1}$ [see Eq. (51)]. Therefore, τ can depart from unity by an amount of order $\epsilon^2(\omega/\nu_{ii})(m_i/m_e)^{1/2}$. In our ordering scheme [Eq. (49)], this is $O(\epsilon^2)$ and, therefore, we should simply set $\tau = 1 + O(\epsilon^2)$. However, we shall carry the parameter τ because other ordering schemes are possible that permit arbitrary values of τ. These are appropriate to plasmas with very weak collisions. For example, in the solar wind, τ appears to be order unity but not exactly 1 (Newbury et al. 1998), while in accretion flows near the black hole, some models predict $\tau \gg 1$ (see § 8.5).
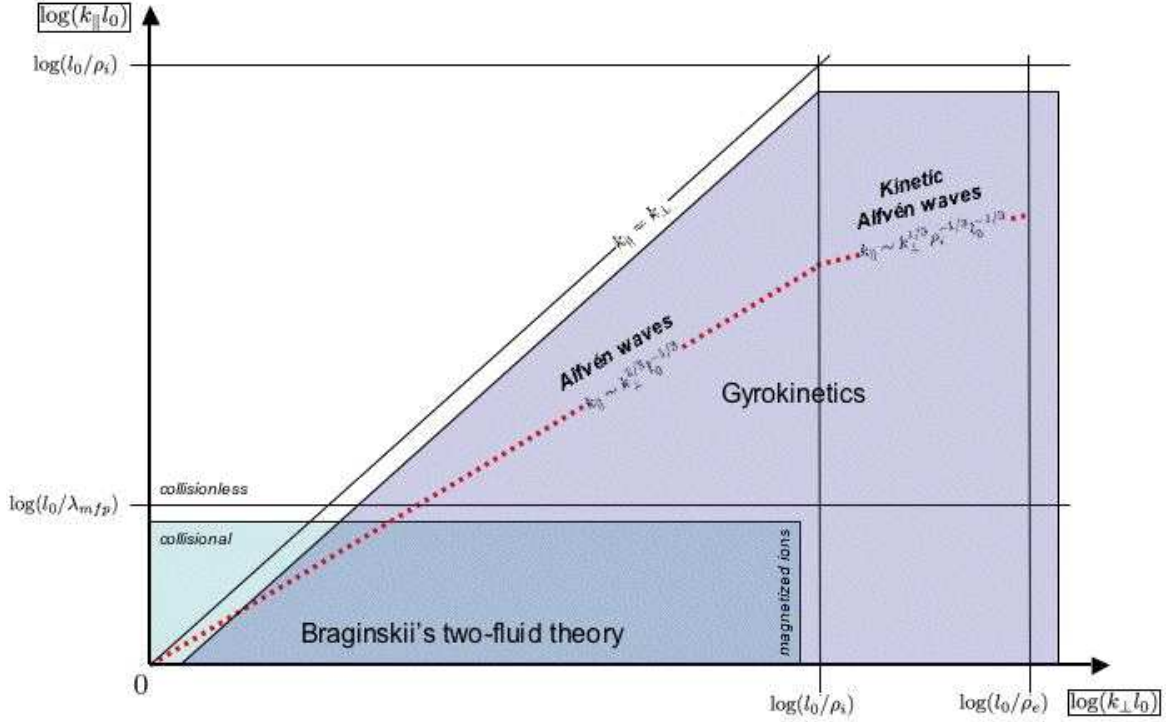
FIG. 3.— Regions of validity in the wavenumber space of two primary approximations—the two-fluid (Appendix A.1) and gyrokinetic (§ 3). The gyrokinetic theory holds when $k_\parallel \ll k_\perp$ and $\omega \ll \Omega_i$ [when $k_\parallel \ll k_\perp < \rho_i^{-1}$, the second requirement is automatically satisfied for Alfvén, slow and entropy modes; see Eq. (46)]. The two-fluid equations hold when $k_\parallel \lambda_{\text{mfp}i} \ll 1$ (collisional limit) and $k_\perp \rho_i \ll 1$ (magnetized plasma). Note that the gyrokinetic theory holds for all but the very largest (outer) scales, where anisotropy cannot be assumed.

Assuming Alfvénic frequencies implies

$$\frac{\omega}{\Omega_i} \sim \frac{k_\parallel v_A}{\Omega_i} \sim \frac{k_\perp \rho_i}{\sqrt{\beta_i}} \epsilon. \qquad (46)$$

Thus, gyrokinetics is a low-frequency limit that averages over the timescales associated with the particle gyration. Because we have assumed that the fluctuations are anisotropic and have (by order of magnitude) Alfvénic frequencies, we see from Eq. (46) that their frequency remains far below Ω_i at all scales, including the ion and even electron gyroscale—the gyrokinetics remains valid at all of these scales and the cyclotron-frequency effects are negligible (cf. Quataert & Gruzinov 1999).

3.1.2. Fluctuations

Equation (3) allows us to order the fluctuations of the scalar potential: on the one hand, we have from Eq. (3) $u_\perp \sim \epsilon v_A$; on the other hand, the plasma mass flow velocity is (to the lowest order) the $\mathbf{E} \times \mathbf{B}$ drift velocity of the ions, $u_\perp \sim cE_\perp/B_0 \sim ck_\perp \varphi/B_0$, so

$$\frac{e\varphi}{T_e} \sim \frac{\tau}{Z} \frac{1}{k_\perp \rho_i \sqrt{\beta_i}} \epsilon. \qquad (47)$$

All other fluctuations (magnetic, density, parallel velocity) are ordered according to Eq. (12).

Note that the ordering of the flow velocity dictated by Eq. (3) means that we are considering the limit of small Mach numbers:

$$M \sim \frac{u}{v_{\text{thi}}} \sim \frac{\epsilon}{\sqrt{\beta_i}}. \qquad (48)$$

This means that the gyrokinetic description in the form used

below does not extend to large sonic flows that can be present in many astrophysical systems. It is, in principle, possible to extend the gyrokinetics to systems with sonic flows (e.g., in the toroidal geometry; see Artun & Tang 1994; Sugama & Horton 1997). However, we do not follow this route because such flows belong to the same class of non-universal outer-scale features as background density and temperature gradients, system-specific geometry etc.—these can all be ignored at small scales, where the turbulence should be approximately homogeneous and subsonic (as long as $k_\parallel L \gg 1$, see discussion in § 1.5.1).

3.1.3. Collisions

Finally, we want our theory to be valid both in the collisional and the collisionless regimes, so we do not assume ω to be either smaller or larger than the (ion) collision frequency ν_{ii}:

$$\frac{\omega}{\nu_{ii}} \sim \frac{k_\parallel \lambda_{\text{mfp}i}}{\sqrt{\beta_i}} \sim 1, \qquad (49)$$

where $\lambda_{\text{mfp}i} = v_{\text{thi}}/\nu_{ii}$ is the ion mean free path (this ordering can actually be inferred from equating the gyrokinetic entropy production terms to the collisional entropy production; see extended discussion in Howes et al. 2006). Note that the ordering (49) holds on the understanding that we have ordered $k_\perp \rho_i \sim 1$ [Eq. (44)] because the fluctuation frequency can depend on $k_\perp \rho_i$ in the dissipation range (see § 7.3).

Other collision rates are related to ν_{ii} via a set of standard formulae (see, e.g., Helander & Sigmar 2002), which will be useful in what follows:

$$\nu_{ei} = Z\nu_{ee} = \frac{\tau^{3/2}}{Z^2} \sqrt{\frac{m_i}{m_e}} \nu_{ii}, \qquad (50)$$

$$\nu_{ie} = \frac{8}{3\sqrt{\pi}} \frac{\tau^{3/2}}{Z} \sqrt{\frac{m_e}{m_i}} \nu_{ii}, \tag{51}$$

$$\nu_{ii} = \frac{\sqrt{2}\pi Z^4 e^4 n_i \ln \Lambda}{m_i^{1/2} T_i^{3/2}}, \tag{52}$$

where $\ln \Lambda$ is the Coulomb logarithm and the numerical factor in the definition of ν_{ie} has been inserted for future notational convenience (see Appendix A). We always define

$$\lambda_{\mathrm{mfp}i} = \frac{v_{\mathrm{th}i}}{\nu_{ii}}, \quad \lambda_{\mathrm{mfp}e} = \frac{v_{\mathrm{th}e}}{\nu_{ei}} = \left(\frac{Z}{\tau}\right)^2 \lambda_{\mathrm{mfp}i}. \tag{53}$$

The ordering of the collision frequency expressed by Eq. (49) means that collisions, while not dominant as in the fluid description (Appendix A), are still retained in the version of the gyrokinetic theory adopted by us. Their presence is required in order for us to be able to assume that the equilibrium distribution is Maxwellian [Eq. (54) below] and for the heating and entropy production to be treated correctly (§ 3.4 and § 3.5). However, our ordering of collisions and of the fluctuation amplitudes (§ 3.1.2) imposes certain limitations: thus, we cannot treat the class of nonlinear phenomena involving particle trapping by parallel-varying fluctuations, non-Maxwellian tails of particle distributions, plasma instabilities arising from the equilibrium pressure anisotropies (mirror, firehose) and their possible nonlinear evolution to large amplitudes (see discussion in § 8.3).

The region of validity of the gyrokinetic approximation in the wavenumber space is illustrated in Fig. 3—it embraces all of the scales that are expected to be traversed by the anisotropic energy cascade (except the scales close to the outer scale).

As we explained above, m_e/m_i, β_i, $k_\perp \rho_i$ and $k_\parallel \lambda_{\mathrm{mfp}i}$ (or ω/ν_{ii}) are assigned order unity in the gyrokinetic expansion. Subsidiary expansions in small m_e/m_i (§ 4) and in small or large values of the other three parameters (§§ 5-7) can be carried out at a later stage as long as their values are not so large or small as to interfere with the primary expansion in ϵ. These expansions will yield simpler models of turbulence with more restricted domains of validity than gyrokinetics.

3.2. Gyrokinetic Equation

Given the gyrokinetic ordering introduced above, the expansion of the distribution function up to first order in ϵ can be written as

$$f_s(t,\mathbf{r},\mathbf{v}) = F_{0s}(v) - \frac{q_s \varphi(t,\mathbf{r})}{T_{0s}} F_{0s}(v) + h_s(t,\mathbf{R}_s,v_\perp,v_\parallel). \tag{54}$$

To zeroth order, it is a Maxwellian:[18]

$$F_{0s}(v) = \frac{n_{0s}}{(\pi v_{\mathrm{th}s}^2)^{3/2}} \exp\left(-\frac{v^2}{v_{\mathrm{th}s}^2}\right), \quad v_{\mathrm{th}s} = \sqrt{\frac{2T_{0s}}{m_s}}, \tag{55}$$

with uniform density n_{0s} and temperature T_{0s} and no mean flow. As will be explained in more detail in § 3.5, F_{0s} has a slow time dependence via the equilibrium temperature, $T_{0s} = T_{0s}(\epsilon^2 t)$. This reflects the slow heating of the plasma as the turbulent energy is dissipated. However, T_{0s} can be treated as a constant with respect to the time dependence of the first-order

[18] The use of isotropic equilibrium is a significant idealization—this is discussed in more detail in § 8.3.

distribution function (the timescale of the turbulent fluctuations). The first-order part of the distribution function is composed of the Boltzmann response [second term in Eq. (54), ordered in Eq. (47)] and the *gyrocenter distribution function* h_s. The spatial dependence of the latter is expressed not by the particle position $\mathbf{r}$ but by the position $\mathbf{R}_s$ of the particle gyrocenter (or guiding center)—the center of the ring orbit that the particle follows in a strong guide field:

$$\mathbf{R}_s = \mathbf{r} + \frac{\mathbf{v}_\perp \times \hat{\mathbf{z}}}{\Omega_s}. \tag{56}$$

Thus, some of the velocity dependence of the distribution function is subsumed in the $\mathbf{R}_s$ dependence of h_s. Explicitly, h_s depends only on two velocity-space variables: it is customary in the gyrokinetic literature for these to be chosen as the particle energy $\varepsilon_s = m_s v^2/2$ and its first adiabatic invariant $\mu_s = m_s v_\perp^2/2B_0$ (both conserved quantities to two lowest orders in the gyrokinetic expansion). However, in a straight uniform guide field $B_0\hat{\mathbf{z}}$, the pair $(v_\perp, v_\parallel)$ is a simpler choice, which will mostly be used in what follows (we shall sometimes find an alternative pair, v and $\xi = v_\parallel/v$, useful, especially where collisions are concerned). It must be constantly kept in mind that derivatives of h_s with respect to the velocity-space variables are taken at constant $\mathbf{R}_s$, *not* at constant $\mathbf{r}$.

The function h_s satisfies *the gyrokinetic equation:*

$$\frac{\partial h_s}{\partial t} + v_\parallel \frac{\partial h_s}{\partial z} + \frac{c}{B_0}\left\{\langle\chi\rangle_{\mathbf{R}_s}, h_s\right\} = \frac{q_s F_{0s}}{T_{0s}} \frac{\partial \langle\chi\rangle_{\mathbf{R}_s}}{\partial t} + \left(\frac{\partial h_s}{\partial t}\right)_{\mathrm{c}}, \tag{57}$$

where

$$\chi(t,\mathbf{r},\mathbf{v}) = \varphi - \frac{v_\parallel A_\parallel}{c} - \frac{\mathbf{v}_\perp \cdot \mathbf{A}_\perp}{c}, \tag{58}$$

the Poisson brackets are defined in the usual way:

$$\left\{\langle\chi\rangle_{\mathbf{R}_s}, h_s\right\} = \hat{\mathbf{z}} \cdot \left(\frac{\partial \langle\chi\rangle_{\mathbf{R}_s}}{\partial \mathbf{R}_s} \times \frac{\partial h_s}{\partial \mathbf{R}_s}\right), \tag{59}$$

and the ring average notation is introduced:

$$\langle \chi(t,\mathbf{r},\mathbf{v})\rangle_{\mathbf{R}_s} = \frac{1}{2\pi} \int_0^{2\pi} d\vartheta \, \chi\left(t, \mathbf{R}_s - \frac{\mathbf{v}_\perp \times \hat{\mathbf{z}}}{\Omega_s}, \mathbf{v}\right), \tag{60}$$

where ϑ is the angle in the velocity space taken in the plane perpendicular to the guide field $B_0\hat{\mathbf{z}}$. Note that, while χ is a function of $\mathbf{r}$, its ring average is a function of $\mathbf{R}_s$. Note also that the ring averages depend on the species index, as does the gyrocenter variable $\mathbf{R}_s$. Equation (57) is derived by transforming the first-order kinetic equation to the gyrocenter variable (56) and ring averaging the result (see Howes et al. 2006, or the references given at the beginning of § 3). The ring-averaged collision integral $(\partial h_s/\partial t)_{\mathrm{c}}$ is discussed in Appendix B.

3.3. Field Equations

To Eq. (57), we must append the equations that determine the electromagnetic field, namely, the potentials $\varphi(t,\mathbf{r})$ and $\mathbf{A}(t,\mathbf{r})$ that enter the expression for χ [Eq. (58)]. In the non-relativistic limit ($v_{\mathrm{th}i} \ll c$), these are the plasma quasi-neutrality constraint [which follows from the Poisson equation (38) to lowest order in $v_{\mathrm{th}i}/c$]:

$$0 = \sum_s q_s \delta n_s = \sum_s q_s \left[-\frac{q_s \varphi}{T_{0s}} n_{0s} + \int d^3 \mathbf{v} \langle h_s\rangle_{\mathbf{r}}\right] \tag{61}$$

and the parallel and perpendicular parts of Ampère's law [Eq. (39) to lowest order in ϵ and in v_{thi}/c]:

$$\nabla_\perp^2 A_\| = -\frac{4\pi}{c} j_\| = -\frac{4\pi}{c} \sum_s q_s \int d^3\mathbf{v}\, v_\| \langle h_s \rangle_\mathbf{r}, \qquad (62)$$

$$\nabla_\perp^2 \delta B_\| = -\frac{4\pi}{c} \hat{\mathbf{z}} \cdot (\nabla_\perp \times \mathbf{j}_\perp)$$

$$= -\frac{4\pi}{c} \hat{\mathbf{z}} \cdot \left[\nabla_\perp \times \sum_s q_s \int d^3\mathbf{v} \langle \mathbf{v}_\perp h_s \rangle_\mathbf{r} \right], \quad (63)$$

where we have used $\delta B_\| = \hat{\mathbf{z}} \cdot (\nabla_\perp \times \mathbf{A}_\perp)$ and dropped the displacement current. Since field variables φ, $A_\|$ and $\delta B_\|$ are functions of the spatial variable $\mathbf{r}$, not of the gyrocenter variable $\mathbf{R}_s$, we had to determine the contribution from the gyrocenter distribution function h_s to the charge distribution at fixed $\mathbf{r}$ by performing a gyroaveraging operation dual to the ring average defined in Eq. (60):

$$\langle h_s(t, \mathbf{R}_s, v_\perp, v_\|) \rangle_\mathbf{r} = \frac{1}{2\pi} \int_0^{2\pi} d\vartheta\, h_s\left(t, \mathbf{r} + \frac{\mathbf{v}_\perp \times \hat{\mathbf{z}}}{\Omega_s}, v_\perp, v_\| \right). \tag{64}$$

In other words, the velocity-space integrals in Eqs. (61-63) are performed over h_s at constant $\mathbf{r}$, rather than constant $\mathbf{R}_s$. If we Fourier transform h_s in $\mathbf{R}_s$, the gyroaveraging operation takes a simple mathematical form:

$$\langle h_s \rangle_\mathbf{r} = \sum_\mathbf{k} \langle e^{i\mathbf{k}\cdot\mathbf{R}_s} \rangle_\mathbf{r} h_{s\mathbf{k}}(t, v_\perp, v_\|)$$

$$= \sum_\mathbf{k} e^{i\mathbf{k}\cdot\mathbf{r}} \left\langle \exp\left(i\mathbf{k} \cdot \frac{\mathbf{v}_\perp \times \hat{\mathbf{z}}}{\Omega_s} \right) \right\rangle_\mathbf{r} h_{s\mathbf{k}}(t, v_\perp, v_\|)$$

$$= \sum_\mathbf{k} e^{i\mathbf{k}\cdot\mathbf{r}} J_0(a_s) h_{s\mathbf{k}}(t, v_\perp, v_\|), \tag{65}$$

where $a_s = k_\perp v_\perp / \Omega_s$ and J_0 is a Bessel function that arose from the angle integral in the velocity space. In Eq. (63), an analogous calculation taking into account the angular dependence of $\mathbf{v}_\perp$ leads to

$$\delta B_\| = -\frac{4\pi}{B_0} \sum_\mathbf{k} e^{i\mathbf{k}\cdot\mathbf{r}} \sum_s \int d^3\mathbf{v}\, m_s v_\perp^2 \frac{J_1(a_s)}{a_s} h_{s\mathbf{k}}(t, v_\perp, v_\|). \tag{66}$$

Note that Eq. (63) [and, therefore, Eq. (66)] is the gyrokinetic equivalent of the perpendicular pressure balance that appeared in § 2 [Eq. (22)]:

$$\nabla_\perp^2 \frac{B_0 \delta B_\|}{4\pi} = \nabla_\perp \cdot \sum_s \frac{q_s B_0}{c} \int d^3\mathbf{v} \langle \hat{\mathbf{z}} \times \mathbf{v}_\perp h_s \rangle_\mathbf{r}$$

$$= \nabla_\perp \cdot \sum_s \Omega_s m_s \int d^3\mathbf{v} \frac{\partial \mathbf{v}_\perp}{\partial \vartheta} h_s\left(t, \mathbf{r} + \frac{\mathbf{v}_\perp \times \hat{\mathbf{z}}}{\Omega_s}, v_\perp, v_\| \right)$$

$$= -\nabla_\perp \nabla_\perp : \sum_s \int d^3\mathbf{v}\, m_s \langle \mathbf{v}_\perp \mathbf{v}_\perp h_s \rangle_\mathbf{r} = -\nabla_\perp \nabla_\perp : \delta \mathbf{P}_\perp, (67)$$

where we have integrated by parts with respect to the gyroangle ϑ and used $\partial \mathbf{v}_\perp / \partial\vartheta = \hat{\mathbf{z}} \times \mathbf{v}_\perp$, $\partial^2 \mathbf{v}_\perp / \partial\vartheta^2 = -\mathbf{v}_\perp$ (cf. the Appendix of Roach et al. 2005).

Once the fields are determined, they have to be substituted into χ [Eq. (58)] and the result ring averaged [Eq. (60)]. Again, we emphasize that φ, $A_\|$ and $\delta B_\|$ are functions of $\mathbf{r}$, while $\langle \chi \rangle_{\mathbf{R}_s}$ is a function of $\mathbf{R}_s$. The transformation is accomplished via a calculation analogous to the one that led to

Eqs. (65) and (66):

$$\langle \chi \rangle_{\mathbf{R}_s} = \sum_\mathbf{k} e^{i\mathbf{k}\cdot\mathbf{R}_s} \langle \chi \rangle_{\mathbf{R}_s,\mathbf{k}}, \tag{68}$$

$$\langle \chi \rangle_{\mathbf{R}_s,\mathbf{k}} = J_0(a_s)\left(\varphi_\mathbf{k} - \frac{v_\| A_{\|\mathbf{k}}}{c} \right) + \frac{T_{0s}}{q_s} \frac{2v_\perp^2}{v_{ths}^2} \frac{J_1(a_s)}{a_s} \frac{\delta B_{\|\mathbf{k}}}{B_0}. \tag{69}$$

The last equation establishes a correspondence between the Fourier transforms of the fields with respect to $\mathbf{r}$ and the Fourier transform of $\langle \chi \rangle_{\mathbf{R}_s}$ with respect to $\mathbf{R}_s$.

3.4. Generalized Energy and the Kinetic Cascade

As promised in § 1.4, the central unifying concept of this paper is now introduced.

If we multiply the gyrokinetic equation (57) by $T_{0s} h_s / F_{0s}$ and integrate over the velocities and gyrocenters, we find that the nonlinear term conserves the variance of h_s and

$$\frac{d}{dt} \int d^3\mathbf{v} \int d^3\mathbf{R}_s \frac{T_{0s} h_s^2}{2F_{0s}} = \int d^3\mathbf{v} \int d^3\mathbf{R}_s\, q_s \frac{\partial \langle \chi \rangle_{\mathbf{R}_s}}{\partial t} h_s$$

$$+ \int d^3\mathbf{v} \int d^3\mathbf{R}_s \frac{T_{0s} h_s}{F_{0s}} \left(\frac{\partial h_s}{\partial t} \right)_c. \tag{70}$$

Let us now sum this equation over all species. The first term on the right-hand side is

$$\sum_s q_s \int d^3\mathbf{v} \int d^3\mathbf{R}_s \frac{\partial \langle \chi \rangle_{\mathbf{R}_s}}{\partial t} h_s$$

$$= \int d^3\mathbf{r} \sum_s q_s \int d^3\mathbf{v} \left\langle \frac{\partial \chi}{\partial t} h_s \right\rangle_\mathbf{r}$$

$$= \int d^3\mathbf{r} \left[\frac{\partial \varphi}{\partial t} \sum_s q_s \int d^3\mathbf{v} \langle h_s \rangle_\mathbf{r} - \frac{1}{c} \frac{\partial \mathbf{A}}{\partial t} \cdot \sum_s q_s \int d^3\mathbf{v} \langle \mathbf{v} h_s \rangle_\mathbf{r} \right]$$

$$= \frac{d}{dt} \int d^3\mathbf{r} \sum_s \frac{q_s^2 \varphi^2 n_{0s}}{2T_{0s}} + \int d^3\mathbf{r}\, \mathbf{E} \cdot \mathbf{j}, \tag{71}$$

where we have used Eq. (61) and Ampère's law [Eqs. (62-63)] to express the integrals of h_s. The second term on the right-hand side is the total work done on plasma per unit time. Using Faraday's law [Eq. (37)] and Ampère's law [Eq. (39)], it can be written as

$$\int d^3\mathbf{r}\, \mathbf{E} \cdot \mathbf{j} = -\frac{d}{dt} \int d^3\mathbf{r} \frac{|\delta \mathbf{B}|^2}{8\pi} + P_{ext}, \tag{72}$$

where $P_{ext} \equiv -\int d^3\mathbf{r}\, \mathbf{E} \cdot \mathbf{j}_{ext}$ is the total power injected into the system by the external energy sources (outer-scale stirring; in terms of the Kolmogorov energy flux ε used in the scaling arguments in § 1.2, $P_{ext} = V m_i n_{0i} \varepsilon$, where V is the system volume). Combining Eqs. (70-72), we find (Howes et al. 2006)

$$\frac{dW}{dt} \equiv \frac{d}{dt} \int d^3\mathbf{r} \left[\sum_s \left(\int d^3\mathbf{v} \frac{T_{0s} \langle h_s^2 \rangle_\mathbf{r}}{2F_{0s}} - \frac{q_s^2 \varphi^2 n_{0s}}{2T_{0s}} \right) + \frac{|\delta \mathbf{B}|^2}{8\pi} \right]$$

$$= P_{ext} + \sum_s \int d^3\mathbf{v} \int d^3\mathbf{R}_s \frac{T_{0s} h_s}{F_{0s}} \left(\frac{\partial h_s}{\partial t} \right)_c. \tag{73}$$

W is a positive definite quantity—this becomes explicit if we use Eq. (61) to express it in terms of the total perturbed distribution function $\delta f_s = -q_s \varphi F_{0s}/T_{0s} + h_s$ [see Eq. (54)]:

$$W = \int d^3\mathbf{r} \left(\sum_s \int d^3\mathbf{v} \frac{T_{0s} \delta f_s^2}{2F_{0s}} + \frac{|\delta \mathbf{B}|^2}{8\pi} \right). \tag{74}$$

We will refer to W as the *generalized energy*. We use this term to emphasize the role of W as the cascaded quantity in gyrokinetic turbulence (see below). This quantity is, in fact, the gyrokinetic version of a collisionless kinetic invariant variously referred to as the *generalized grand canonical potential* (see Hallatschek 2004, who points out the fundamental role of this quantity in plasma turbulence simulations) or *free energy* (e.g., Fowler 1968; Scott 2007). The non-magnetic part of W is related to the perturbed entropy of the system (Krommes & Hu 1994; Sugama et al. 1996; Howes et al. 2006; Schekochihin et al. 2008b, see discussion in § 3.5).[19]

Equation (73) is a conservation law of the generalized energy: P_{ext} is the source and the second term on the right-hand side, which is negative definite, represents collisional dissipation. This suggests that we might think of kinetic plasma turbulence in terms of the generalized energy W injected by the outer-scale stirring and dissipated by collisions. In order for the dissipation to be important, the collisional term in Eq. (73) has to become comparable to P_{ext}. This can happen in two ways:

1. At collisional scales ($k_\| \lambda_{\text{mfp}i} \sim 1$) due to deviations of the perturbed distribution function from a local perturbed Maxwellian (see § 6.1 and Appendix D);

2. At collisionless scales ($k_\| \lambda_{\text{mfp}i} \gg 1$) due the development of small scales in the velocity space—large gradients in $v_\|$ (see § 6.2.4) or $v_\perp$ (which is accompanied by the development of small perpendicular scales in the position space; see § 7.9.1).

Thus, the dissipation is only important at particular (small) scales, which are generally well separated from the outer scale. The generalized energy is transferred from the outer scale to the dissipation scales via a nonlinear cascade. We shall call it *the kinetic cascade*. It is analogous to the energy cascade in fluid or MHD turbulence, but a conceptually new feature is present: the small scales at which dissipation happens are small scales both in the velocity and position space. Whereas the large gradients in $v_\|$ are produced by the *linear* parallel phase mixing, whose role in the kinetic dissipation processes has been appreciated for some time (Landau 1946; Hammett et al. 1991; Krommes & Hu 1994; Krommes 1999; Watanabe & Sugama 2004, see § 6.2.4), the emergence of large gradients in $v_\perp$ is due to an essentially *nonlinear* phase mixing mechanism (§ 7.9.1). At spatial scales smaller than the ion gyroradius, this nonlinear perpendicular phase mixing turns out to be a faster and, therefore, presumably the dominant way of generating small-scale structure in the velocity space. It was anticipated in the development of gyrofluid moment hierarchies by Dorland & Hammett (1993). Here we treat it for the first time as a phase-space turbulent cascade: this is done in § 7.9 and § 7.10 (see also Schekochihin et al. 2008b).

In the sections that follow, we shall derive particular forms of W for various limiting cases of the gyrokinetic theory (§ 4.7, § 5.6, § 6.2.5, § 7.8, Appendices D.2 and E.2). We shall see that the kinetic cascade of W is, indeed, a direct generalization of the more familiar fluid cascades (such as

the RMHD cascades discussed in § 2) and that W contains the energy invariants of the fluid models in the appropriate limits. In these limits, the cascade of the generalized energy will split into several decoupled cascades, as it did in the case of RMHD (§ 2.7). Whenever one of the physically important scales (§ 1.5.2) is crossed and a change of physical regime occurs, these cascades are mixed back together into the overall kinetic cascade of W, which can then be split in a different way as it emerges on the "opposite side" of the transition region in the scale space. The conversion of the Alfvénic cascade into the KAW cascade and the entropy cascade at $k_\perp \rho_i \sim 1$ is the most interesting example of such a transition, discussed in § 7.

The generalized energy appears to be the only quadratic invariant of gyrokinetics in three dimensions; in two dimensions, many other invariants appear (see Appendix F).

3.5. *Heating and Entropy*

In a stationary state, all of the the turbulent power injected by the external stirring is dissipated and thus transferred into heat. Mathematically, this is expressed as a slow increase in the temperature of the Maxwellian equilibrium. In gyrokinetics, the heating timescale is ordered as $\sim (\epsilon^2 \omega)^{-1}$.

Even though the dissipation of turbulent fluctuations may be occurring "collisionlessly" at scales such that $k_\| \lambda_{\text{mfp}i} \gg 1$ (e.g., via wave–particle interaction at the ion gyroscale; § 7.1), the resulting heating must ultimately be effected with the help of collisions. This is because heating is an irreversible process and it is a small amount of collisions that make "collisionless" damping irreversible. In other words, slow heating of the Maxwellian equilibrium is equivalent to entropy production and Boltzmann's H-theorem rigorously requires collisions to make this possible. Indeed, the total entropy of species s is

$$S_s = -\int d^3\mathbf{r} \int d^3\mathbf{v}\, f_s \ln f_s$$

$$= -\int d^3\mathbf{r} \int d^3\mathbf{v} \left(F_{0s} \ln F_{0s} + \frac{\delta f_s^2}{2 F_{0s}} \right) + O(\epsilon^3), \quad (75)$$

where we took $\int d^3\mathbf{r}\, \delta f_s = 0$. It is then not hard to show that

$$\frac{3}{2} V n_{0s} \frac{1}{T_{0s}} \frac{dT_{0s}}{dt} = \overline{\frac{dS_s}{dt}} = -\overline{\int d^3\mathbf{v} \int d^3\mathbf{R}_s \frac{T_{0s} h_s}{F_{0s}} \left(\frac{\partial h_s}{\partial t} \right)_c}, \quad (76)$$

where the overlines mean averaging over times longer than the characteristic time of the turbulent fluctuations $\sim \omega^{-1}$ but shorter than the typical heating time $\sim (\epsilon^2 \omega)^{-1}$ (see Howes et al. 2006; Schekochihin et al. 2008b for a detailed derivation of this and related results on heating in gyrokinetics; see also earlier discussions of the entropy production in gyrokinetics by Krommes & Hu 1994; Krommes 1999; Sugama et al. 1996). We have omitted the term describing the interspecies collisional temperature equalization. Note that both sides of Eq. (76) are order $\epsilon^2 \omega$.

If we now time average Eq. (73) in a similar fashion, the left-hand side vanishes because it is a time derivative of a quantity fluctuating on the timescale $\sim \omega^{-1}$ and we confirm that the right-hand side of Eq. (76) is simply equal to the average power $\overline{P_{\text{ext}}}$ injected by external stirring. The import of Eq. (76) is that it tells us that heating can only be effected by collisions, while Eq. (73) implies that the injected power gets to the collisional scales in velocity and position space by means of a kinetic cascade of generalized energy.

---

[19] Note also that a quadratic form involving both the perturbed distribution function and the electromagnetic field appears, in a more general form than Eq. (74), in the formulation of the energy principle for the Kinetic MHD approximation (Kruskal & Oberman 1958; Kulsrud 1962, 1964). Regarding the relationship between Kinetic MHD and gyrokinetics, see footnote 23.

The first term in the expression for the generalized energy (74) is $-\sum_s T_{0s}\delta S_s$, where δS_s is the perturbed entropy [see Eq. (75)]. The second term in Eq. (74) is magnetic energy. Collisionless damping of electromagnetic fluctuations can be thought of as a redistribution of the generalized energy, transferring the electromagnetic energy into entropy fluctuations, while the total W is conserved (a simple example of how that happens for collisionless compressive fluctuations in the inertial range is worked out in § 6.2.3).

The contribution to the perturbed entropy from the gyrocenter distribution is the integral of $-h_s^2/2F_{0s}$, whose evolution equation (70) can be viewed as the gyrokinetic version of the H-theorem. The first term on the right-hand side of this equation represents the wave–particle interaction (collisionless damping). Under time average, it is related to the work done on plasma [Eq. (71)] and hence to the average externally injected power $\overline{P_{\rm ext}}$ via time-averaged Eq. (72).[20] In a stationary state, this is balanced by the second term in the right-hand side of Eq. (70), which is the collisional-heating, or entropy-production, term that also appears in Eq. (76). Thus, the generalized energy channeled by collisionless damping into entropy fluctuations is eventually converted into heat by collisions. The sub-gyroscale entropy cascade, which brings the perturbed distribution function h_s to collisional scales, will be discussed further in § 7.9 and § 7.10 (see also Schekochihin et al. 2008b).

This concludes a short primer on gyrokinetics necessary (and sufficient) for adequate understanding of what is to follow. Formally, all further analytical derivations in this paper are simply subsidiary expansions of the gyrokinetics in the parameters we listed in § 3.1: in § 4, we expand in $(m_e/m_i)^{1/2}$, in § 5 in $k_\perp\rho_i$ (followed by further subsidiary expansions in large and small $k_\parallel\lambda_{\rm mfpi}$ in § 6), and in § 7 in $1/k_\perp\rho_i$.

4. ISOTHERMAL ELECTRON FLUID

In this section, we carry out an expansion of the electron gyrokinetic equation in powers of $(m_e/m_i)^{1/2} \simeq 0.02$ (for hydrogen plasma). In virtually all cases of interest, this expansion can be done while still considering $\sqrt{\beta_i}$, $k_\perp\rho_i$, and $k_\parallel\lambda_{\rm mfpi}$ to be order unity.[21] Note that the assumption $k_\perp\rho_i \sim 1$ together with Eq. (45) mean that

$$k_\perp\rho_e \sim k_\perp\rho_i(m_e/m_i)^{1/2} \ll 1, \qquad (77)$$

i.e., the expansion in $(m_e/m_i)^{1/2}$ means also that we are considering scales larger than the electron gyroradius. The idea of such an expansion of the electron kinetic equation has been utilized many times in plasma physics literature. The mass-ratio expansion of the gyrokinetic equation in a form very similar to what is presented below is found in Snyder & Hammett (2001).

[20] Note that Eq. (72) is valid not only in the integral form but also individually for each wavenumber: indeed, using the Fourier-transformed Faraday and Ampère's laws, we have $\mathbf{E_k} \cdot \mathbf{j_k^*} + \mathbf{E_k^*} \cdot \mathbf{j_k} = \mathbf{E_k} \cdot \mathbf{j_{ext,k}^*} + \mathbf{E_k^*} \cdot \mathbf{j_{ext,k}} - (1/4\pi)\partial|\delta\mathbf{B_k}|^2/\partial t$. In a stationary state, time averaging eliminates the time derivative of the magnetic-fluctuation energy, so $\overline{\mathbf{E_k} \cdot \mathbf{j_k^*} + \mathbf{E_k^*} \cdot \mathbf{j_k}} = 0$ at all $\mathbf{k}$ except those corresponding to the outer scale, where the external energy injection occurs. This means that below the outer scale, the work done on one species balances the work done on the other. The wave–particle interaction term in the gyrokinetic equation is responsible for this energy exchange.

[21] One notable exception is the LAPD device at UCLA, where $\beta \sim 10^{-4} - 10^{-3}$ (due mostly to the electron pressure because the ions are cold, $\tau \sim 0.1$, so $\beta_i \sim \beta_e/10$; see, e.g., Morales et al. 1999; Carter et al. 2006). This interferes with the mass-ratio expansion.

The primary import of this section will be technical: we shall dispense with the electron gyrokinetic equation and thus prepare the necessary ground for further approximations. The main results are summarized in § 4.9. A reader who is only interested in following qualitatively the major steps in the derivation may skip to this summary.

4.1. Ordering the Terms in the Kinetic Equation

In view of Eq. (77), $a_e \ll 1$, so we can expand the Bessel functions arising from averaging over the electron ring motion:

$$J_0(a_e) = 1 - \frac{1}{4}a_e^2 + \cdots, \qquad \frac{J_1(a_e)}{a_e} = \frac{1}{2}\left(1 - \frac{1}{8}a_e^2 + \cdots\right). \quad (78)$$

Keeping only the lowest-order terms of the above expansions in Eq. (69) for $\langle\chi\rangle_{\mathbf{R}_e}$, then substituting this $\langle\chi\rangle_{\mathbf{R}_e}$ and $q_e = -e$ in the electron gyrokinetic equation, we get the following kinetic equation for the electrons, accurate up to and including the first order in $(m_e/m_i)^{1/2}$ (or in $k_\perp\rho_e$):

$$\underbrace{\frac{\partial h_e}{\partial t}}_{①} + \underbrace{v_\parallel\frac{\partial h_e}{\partial z}}_{⓪} + \frac{c}{B_0}\left\{\underbrace{\varphi}_{①} \underbrace{-\frac{v_\parallel A_\parallel}{c}}_{⓪} \underbrace{-\frac{T_{0e}}{e}\frac{v_\perp^2}{v_{\rm the}^2}\frac{\delta B_\parallel}{B_0}}_{①}, h_e\right\}$$

$$= \underbrace{-\frac{eF_{0e}}{T_{0e}}\frac{\partial}{\partial t}\left(\underbrace{\varphi}_{①} \underbrace{-\frac{v_\parallel A_\parallel}{c}}_{⓪} \underbrace{-\frac{T_{0e}}{e}\frac{v_\perp^2}{v_{\rm the}^2}\frac{\delta B_\parallel}{B_0}}_{①}\right)}_{} + \underbrace{\left(\frac{\partial h_e}{\partial t}\right)_c}_{⓪}. \quad (79)$$

Note that φ, $A_\parallel$, $\delta B_\parallel$ in Eq. (79) are taken at $\mathbf{r} = \mathbf{R}_e$. We have indicated the lowest order to which each of the terms enters if compared with $v_\parallel\partial h_e/\partial z$. In order to obtain these estimates, we have assumed that the physical ordering introduced in § 3.1 holds with respect to the subsidiary expansion in $(m_e/m_i)^{1/2}$ as well as for the primary gyrokinetic expansion in ϵ, so we can use Eqs. (3) and (12) to order terms with respect to $(m_e/m_i)^{1/2}$. We have also made use of Eqs. (45), (47), and of the following three relations:

$$\frac{k_\parallel v_\parallel}{\omega} \sim \frac{v_{\rm the}}{v_A} \sim \sqrt{\frac{\beta_i}{\tau}}\sqrt{\frac{m_i}{m_e}}, \qquad (80)$$

$$\frac{(v_\parallel/c)A_\parallel}{\varphi} \sim \frac{v_{\rm the}\delta B_\perp}{ck_\perp\varphi} \sim \frac{1}{k_\perp\rho_e}\frac{T_{0e}}{e\varphi}\frac{\delta B_\perp}{B_0} \sim \sqrt{\frac{\beta_i}{\tau}}\sqrt{\frac{m_i}{m_e}}, (81)$$

$$\frac{T_{0e}}{e\varphi}\frac{v_\perp^2}{v_{\rm the}^2}\frac{\delta B_\parallel}{B_0} \sim \frac{Z}{\tau}k_\perp\rho_i\sqrt{\beta_i}. \qquad (82)$$

The collision term is estimated to be zeroth order because [see Eqs. (49), (50)]

$$\frac{\nu_{ei}}{\omega} \sim \frac{\tau^{3/2}\sqrt{\beta_i}}{Z^2}\sqrt{\frac{m_i}{m_e}}\frac{1}{k_\parallel\lambda_{\rm mfpi}}. \qquad (83)$$

The consequences of other possible orderings of the collision terms are discussed in § 4.8. We remind the reader that all dimensionless parameters except $k_\parallel/k_\perp \sim \epsilon$ and $(m_e/m_i)^{1/2}$ are held to be order unity.

We now let $h_e = h_e^{(0)} + h_e^{(1)} + \dots$ and carry out the expansion to two lowest orders in $(m_e/m_i)^{1/2}$.

4.2. Zeroth Order

To zeroth order, the electron kinetic equation is

$$v_\| \hat{\mathbf{b}} \cdot \nabla h_e^{(0)} = v_\| \frac{eF_{0e}}{cT_{0e}} \frac{\partial A_\|}{\partial t} + \left(\frac{\partial h_e^{(0)}}{\partial t} \right)_c, \qquad (84)$$

where we have assembled the terms in the left-hand side to take the form of the derivative of the distribution function along the perturbed magnetic field:

$$\hat{\mathbf{b}} \cdot \nabla = \frac{\partial}{\partial z} + \frac{\delta \mathbf{B}_\perp}{B_0} \cdot \nabla = \frac{\partial}{\partial z} - \frac{1}{B_0} \{ A_\|, \cdots \}. \qquad (85)$$

We now multiply Eq. (84) by $h_e^{(0)}/F_{0e}$ and integrate over $\mathbf{v}$ and $\mathbf{r}$ (since we are only retaining lowest-order terms, the distinction between $\mathbf{r}$ and $\mathbf{R}_e$ does not matter here). Since $\nabla \cdot \mathbf{B} = 0$, the left-hand side vanishes (assuming that all perturbations are either periodic or vanish at the boundaries) and we get

$$\int d^3\mathbf{r} \int d^3\mathbf{v} \frac{h_e^{(0)}}{F_{0e}} \left(\frac{\partial h_e^{(0)}}{\partial t} \right)_c = -\frac{en_{0e}}{cT_{0e}} \int d^3\mathbf{r} \frac{\partial A_\|}{\partial t} u_{\|e}^{(0)} = 0. \qquad (86)$$

The right-hand side of this equation is zero because the electron flow velocity is zero in the zeroth order, $u_{\|e}^{(0)} = (1/n_{0e}) \int d^3\mathbf{v} v_\| h_e^{(0)} = 0$. This is a consequence of the parallel Ampére's law [Eq. (62)], which can be written as follows

$$u_{\|e} = \frac{c}{4\pi en_{0e}} \nabla_\perp^2 A_\| + u_{\|i}, \qquad (87)$$

where

$$u_{\|i} = \sum_{\mathbf{k}} e^{i\mathbf{k}\cdot\mathbf{r}} \frac{1}{n_{0i}} \int d^3\mathbf{v} v_\| J_0(a_i) h_{i\mathbf{k}}. \qquad (88)$$

The three terms in Eq. (87) can be estimated as follows

$$\frac{u_{\|e}^{(0)}}{v_A} \sim \frac{\epsilon v_{\text{the}}}{v_A} \sim \sqrt{\frac{\beta_i}{\tau}} \sqrt{\frac{m_i}{m_e}} \epsilon, \qquad (89)$$

$$\frac{u_{\|i}}{v_A} \sim \epsilon, \qquad (90)$$

$$\frac{c\nabla_\perp^2 A_\|}{4\pi en_{0e}v_A} \sim \frac{k_\perp \rho_i}{Z\sqrt{\beta_i}} \epsilon, \qquad (91)$$

where we have used the fundamental ordering (12) of the slow waves ($u_{\|i} \sim \epsilon v_A$) and Alfvén waves ($\delta B_\perp \sim \epsilon B_0$). Thus, the two terms in the right-hand side of Eq. (87) are one order of $(m_e/m_i)^{1/2}$ smaller than $u_{\|e}^{(0)}$, which means that to zeroth order, the parallel Ampère's law is $u_{\|e}^{(0)} = 0$.

The collision operator in Eq. (86) contains electron–electron and electron–ion collisions. To lowest order in $(m_e/m_i)^{1/2}$, the electron–ion collision operator is simply the pitch-angle scattering operator [see Eq. (B20) in Appendix B and recall that $u_{\|i}$ is first order]. Therefore, we may then rewrite Eq. (86) as follows

$$\int d^3\mathbf{r} \int d^3\mathbf{v} \frac{h_e^{(0)}}{F_{0e}} C_{ee}[h_e^{(0)}]$$

$$- \int d^3\mathbf{r} \int d^3\mathbf{v} \frac{\nu_D^{ei}(v)}{F_{0e}} \frac{1-\xi^2}{2} \left(\frac{\partial h_e^{(0)}}{\partial \xi} \right)^2 = 0. \qquad (92)$$

Both terms in this expression are negative definite and must, therefore, vanish individually. This implies that $h_e^{(0)}$ must be a perturbed Maxwellian distribution with zero mean velocity (this follows from the proof of Boltzmann's H theorem;

see, e.g., Longmire 1963), i.e., the full electron distribution function to zeroth order in the mass-ratio expansion is [see Eq. (54)]:

$$f_e = F_{0e} + \frac{e\varphi}{T_{0e}} + h_e^{(0)} = \frac{n_e}{(2\pi T_e/m_e)^{3/2}} \exp \left(-\frac{m_e v^2}{2T_e} \right), \qquad (93)$$

where $n_e = n_{0e} + \delta n_e$, $T_e = T_{0e} + \delta T_e$. Expanding around the unperturbed Maxwellian F_{0e}, we get

$$h_e^{(0)} = \left[\frac{\delta n_e}{n_{0e}} - \frac{e\varphi}{T_{0e}} + \left(\frac{v^2}{v_{\text{the}}^2} - \frac{3}{2} \right) \frac{\delta T_e}{T_{0e}} \right] F_{0e}, \qquad (94)$$

where the fields are taken at $\mathbf{r} = \mathbf{R}_e$. Now substitute this solution back into Eq. (84). The collision term vanishes and the remaining equation must be satisfied at all values of v. This gives

$$\frac{1}{c} \frac{\partial A_\|}{\partial t} + \hat{\mathbf{b}} \cdot \nabla \varphi = \hat{\mathbf{b}} \cdot \nabla \frac{T_{0e}}{e} \frac{\delta n_e}{n_{0e}}, \qquad (95)$$

$$\hat{\mathbf{b}} \cdot \nabla \frac{\delta T_e}{T_{0e}} = 0. \qquad (96)$$

The collision term is neglected in Eq. (95) because, for $h_e^{(0)}$ given by Eq. (94), it vanishes to zeroth order.

4.3. *Flux Conservation*

Equation (95) implies that the magnetic flux is conserved and magnetic-field lines cannot be broken to lowest order in the mass-ratio expansion. Indeed, we may follow Cowley (1985) and argue that the left-hand side of Eq. (95) is minus the projection of the electric field on the total magnetic field [see Eq. (37)], so we have

$$\mathbf{E} \cdot \hat{\mathbf{b}} = -\hat{\mathbf{b}} \cdot \nabla \left(\frac{T_{0e}}{e} \frac{\delta n_e}{n_{0e}} \right); \qquad (97)$$

hence the total electric field is

$$\mathbf{E} = (\hat{\mathbf{I}} - \hat{\mathbf{b}}\hat{\mathbf{b}}) \cdot \left(\mathbf{E} + \nabla \frac{T_{0e}}{e} \frac{\delta n_e}{n_{0e}} \right) - \nabla \frac{T_{0e}}{e} \frac{\delta n_e}{n_{0e}} \qquad (98)$$

and Faraday's law becomes

$$\frac{\partial \mathbf{B}}{\partial t} = -c\nabla \times \mathbf{E} = \nabla \times (\mathbf{u}_{\text{eff}} \times \mathbf{B}), \qquad (99)$$

$$\mathbf{u}_{\text{eff}} = \frac{c}{B^2} \left(\mathbf{E} + \nabla \frac{T_{0e}}{e} \frac{\delta n_e}{n_{0e}} \right) \times \mathbf{B}, \qquad (100)$$

i.e., the magnetic field lines are frozen into the velocity field $\mathbf{u}_{\text{eff}}$. In Appendix C.1, we show that this effective velocity is the part of the electron flow velocity $\mathbf{u}_e$ perpendicular to the total magnetic field $\mathbf{B}$ [see Eq. (C6)].

The flux conservation is broken in the higher orders of the mass-ratio expansion. In the first order, Ohmic resistivity formally enters in Eq. (95) (unless collisions are even weaker than assumed so far; if they are downgraded one order as is done in §4.8.3, resistivity enters in the second order). In the second order, the electron inertia and the finiteness of the electron gyroradius also lead to unfreezing of the flux. This can be seen formally by keeping second-order terms in Eq. (79), multiplying it by $v_\|$ and integrating over velocities. The relative importance of these flux unfreezing mechanisms is evaluated in §7.7.

4.4. *Isothermal Electrons*

Equation (96) mandates that the perturbed electron temperature must remain constant along the perturbed field lines. Strictly speaking, this does not preclude δT_e varying across the field lines. However, we shall now assume $\delta T_e = \text{const}$ (has no spatial variation), which is justified, e.g., if the field lines are stochastic. Assuming that no spatially uniform perturbations exist, we may set $\delta T_e = 0$. Equation (94) then reduces to

$$h_e^{(0)} = \left(\frac{\delta n_e}{n_{0e}} - \frac{e\varphi}{T_{0e}} \right) F_{0e}(v), \qquad (101)$$

or, using Eq. (54),

$$\delta f_e = \frac{\delta n_e}{n_{0e}} F_{0e}(v). \qquad (102)$$

Hence follows the equation of state for isothermal electrons:

$$\delta p_e = T_{0e}\delta n_e. \qquad (103)$$

4.5. *First Order*

We now integrate Eq. (79) over the velocity space and retain the lowest (first) order terms only. Using Eq. (101), we get

$$\frac{\partial}{\partial t} \left(\frac{\delta n_e}{n_{0e}} - \frac{\delta B_\parallel}{B_0} \right) + \frac{c}{B_0} \left\{ \varphi, \frac{\delta n_e}{n_{0e}} - \frac{\delta B_\parallel}{B_0} \right\}$$

$$+ \frac{\partial u_{\parallel e}}{\partial z} - \frac{1}{B_0} \left\{ A_\parallel, u_{\parallel e} \right\} + \frac{cT_{0e}}{eB_0} \left\{ \frac{\delta n_e}{n_{0e}}, \frac{\delta B_\parallel}{B_0} \right\} = 0, \quad (104)$$

where the parallel electron velocity is first order:

$$u_{\parallel e} = u_{\parallel e}^{(1)} = \frac{1}{n_{0e}} \int d^3\mathbf{v}\, v_\parallel h_e^{(1)}. \qquad (105)$$

The velocity-space integral of the collision term does not enter because it is subdominant by at least one factor of $(m_e/m_i)^{1/2}$: indeed, as shown in Appendix B.1, the velocity integration leads to an extra factor of $k_\perp^2 \rho_e^2$, so that

$$\frac{1}{n_{0e}} \int d^3\mathbf{v} \left(\frac{\partial h_e}{\partial t} \right)_c \sim \nu_{ei} k_\perp^2 \rho_e^2 \frac{\delta n_e}{n_{0e}}$$

$$\sim \sqrt{\tau \frac{m_e}{m_i}} k_\perp^2 \rho_i^2 \nu_{ii} \frac{\delta n_e}{n_{0e}}, \qquad (106)$$

where we have used Eqs. (45) and (50). The collision term is subdominant because of the ordering of the ion collision frequency given by Eq. (49).

4.6. *Field Equations*

Using Eq. (101) and $q_i = Ze$, $n_{0e} = Zn_{0i}$, $T_{0e} = T_{0i}/\tau$, we derive from the quasi-neutrality equation (61) [see also Eq. (65)]

$$\frac{\delta n_e}{n_{0e}} = \frac{\delta n_i}{n_{0i}} = -\frac{Ze\varphi}{T_{0i}} + \sum_\mathbf{k} e^{i\mathbf{k}\cdot\mathbf{r}} \frac{1}{n_{0i}} \int d^3\mathbf{v} J_0(a_i) h_{i\mathbf{k}}, \quad (107)$$

and, from the perpendicular part of Ampère's law [Eq. (66), using also Eq. (107)],

$$\frac{\delta B_\parallel}{B_0} = \frac{\beta_i}{2} \left\{ \left(1 + \frac{Z}{\tau} \right) \frac{Ze\varphi}{T_{0i}} - \sum_\mathbf{k} e^{i\mathbf{k}\cdot\mathbf{r}} \right.$$

$$\left. \times \frac{1}{n_{0i}} \int d^3\mathbf{v} \left[\frac{Z}{\tau} J_0(a_i) + \frac{2v_\perp^2}{v_{\text{thi}}^2} \frac{J_1(a_i)}{a_i} \right] h_{i\mathbf{k}} \right\}. \quad (108)$$

The parallel electron velocity, $u_{\parallel e}$, is determined from the parallel part of Ampère's law, Eq. (87).

The ion distribution function h_i that enters these equations has to be determined by solving the ion gyrokinetic equation: Eq. (57) with $s = i$.

4.7. *Generalized Energy*

The generalized energy (§ 3.4) for the case of isothermal electrons is calculated by substituting Eq. (102) into Eq. (74):

$$W = \int d^3\mathbf{r} \left(\int d^3\mathbf{v} \frac{T_{0i}\delta f_i^2}{2F_{0i}} + \frac{n_{0e}T_{0e}}{2} \frac{\delta n_e^2}{n_{0e}^2} + \frac{|\delta \mathbf{B}|^2}{8\pi} \right), \quad (109)$$

where $\delta f_i = h_i - \left(Ze\varphi/T_{0i} \right) F_{0i}$ [see Eq. (54)].

4.8. *Validity of the Mass-Ratio Expansion*

Let us examine the range of spatial scales in which the equations derived above are valid. In carrying out the expansion in $(m_e/m_i)^{1/2}$, we ordered $k_\perp \rho_i \sim 1$ [Eq. (77)] and $k_\parallel \lambda_{\text{mfp}i} \sim 1$ [Eq. (83)]. Formally, this means that the perpendicular and parallel wavelengths of the perturbations must not be so small or so large as to interfere with the mass ratio expansion. We now discuss the four conditions that this requirement leads to and whether any of them can be violated without destroying the validity of the equations derived above.

4.8.1. $k_\perp \rho_i \ll (m_i/m_e)^{1/2}$.

This is equivalent to demanding that $k_\perp \rho_e \ll 1$, a condition that was, indeed, essential for the expansion to hold [Eq. (78)]. This is not a serious limitation because electrons can be considered well magnetized at virtually all scales of interest for astrophysical applications. However, we do forfeit the detailed information about some important electron physics at $k_\perp \rho_e \sim 1$: for example such effects as wave damping at the electron gyroscale and the electron heating (although the total amount of the electron heating can be deduced by subtracting the ion heating from the total energy input). The breaking of the flux conservation (resistivity) is also an effect that requires incorporation of the finite electron gyroscale physics.

4.8.2. $k_\perp \rho_i \gg (m_e/m_i)^{1/2}$.

If this condition is broken, the small-$k_\perp \rho_i$ expansion, carried out in § 5, must, formally speaking, precede the mass-ratio expansion. However, it turns out that the small-$k_\perp \rho_i$ expansion commutes with the mass-ratio expansion (Schekochihin et al. 2007, see also footnote 23), so we may use the equations derived in §§ 4.2-4.6 when $k_\perp \rho_i \lesssim (m_e/m_i)^{1/2}$.

4.8.3. $k_\parallel \lambda_{\text{mfp}i} \ll (m_i/m_e)^{1/2}$.

Let us consider what happens if this condition is broken and $k_\parallel \lambda_{\text{mfp}i} \gtrsim (m_i/m_e)^{1/2}$. In this case, the collisions become even weaker and the expansion procedure must be modified. Namely, the collision term picks up one extra order of $(m_e/m_i)^{1/2}$, so it is first order in Eq. (79). To zeroth order, the electron kinetic equation no longer contains collisions: instead of Eq. (84), we have

$$v_\parallel \hat{\mathbf{b}} \cdot \nabla h_e^{(0)} = v_\parallel \frac{eF_{0e}}{cT_{0e}} \frac{\partial A_\parallel}{\partial t}. \qquad (110)$$

We may seek the solution of this equation in the form $h_e^{(0)} = H(t, \mathbf{R}_e) F_{0e} + h_{e,\text{hom}}^{(0)}$, where $H(t, \mathbf{R}_e)$ is an unknown function to
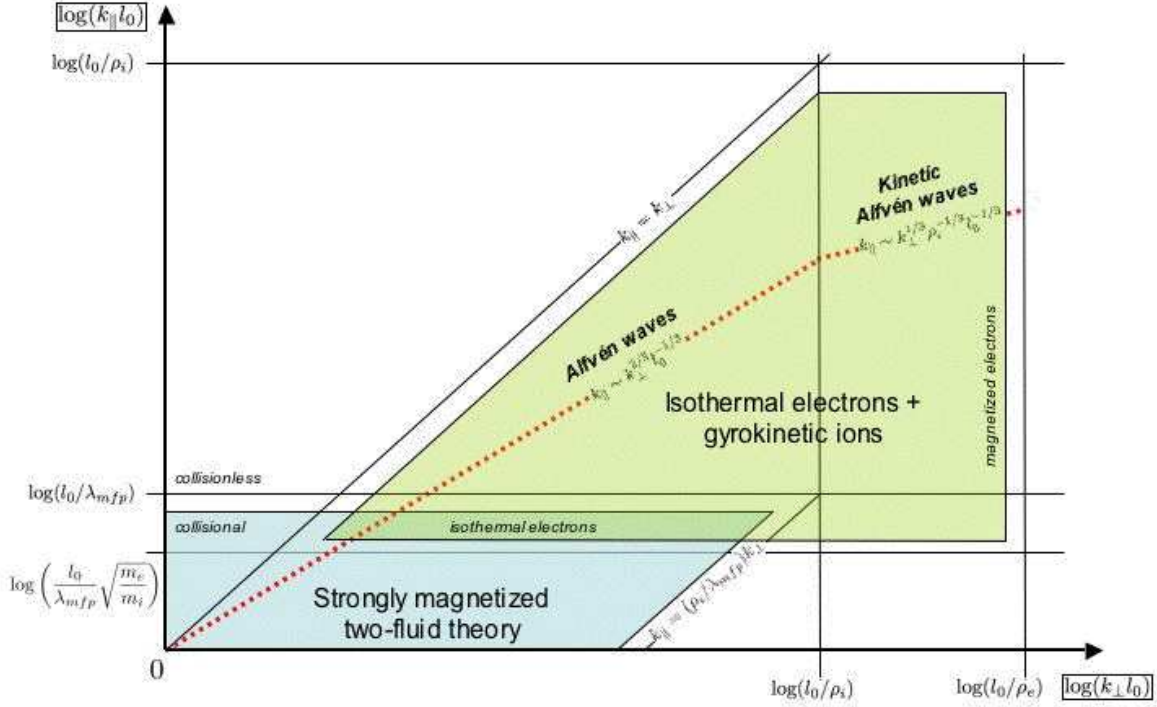
FIG. 4.— Region of validity in the wavenumber space of the secondary approximation—isothermal electrons and gyrokinetic ions (§ 4). It is the region of validity of the gyrokinetic approximation (Fig. 3) further circumscribed by two conditions: $k_\parallel \lambda_{\mathrm{mfp}i} \gg (m_e/m_i)^{1/2}$ (isothermal electrons) and $k_\perp \rho_e \ll 1$ (magnetized electrons). The region of validity of the strongly magnetized two-fluid theory (Appendix A.2) is also shown. It is the same as for the full two-fluid theory plus the additional constraint $k_\perp \rho_i \ll k_\parallel \lambda_{\mathrm{mfp}i}$. The region of validity of MHD (or one-fluid theory) is the subset of this with $k_\parallel \lambda_{\mathrm{mfp}i} \ll (m_e/m_i)^{1/2}$ (adiabatic electrons).

be determined and $h_{e,\mathrm{hom}}^{(0)}$ is the homogeneous solution satisfying

$$\hat{\mathbf{b}} \cdot \nabla h_{e,\mathrm{hom}}^{(0)} = 0, \tag{111}$$

i.e., $h_{e,\mathrm{hom}}^{(0)}$ must be constant along the perturbed magnetic field. This is a generalization of Eq. (96). Again assuming stochastic field lines, we conclude that $h_{e,\mathrm{hom}}^{(0)}$ is independent of space. If we rule out spatially uniform perturbations, we may set $h_{e,\mathrm{hom}}^{(0)} = 0$. The unknown function $H(t, \mathbf{R}_e)$ is readily expressed in terms of δn_e and φ:

$$\frac{\delta n_e}{n_{0e}} = \frac{e\varphi}{T_{0e}} + \frac{1}{n_{0e}} \int d^3 \mathbf{v} h_e^{(0)} \quad \Rightarrow \quad H = \frac{\delta n_e}{n_{0e}} - \frac{e\varphi}{T_{0e}}, \tag{112}$$

so $h_e^{(0)}$ is again given by Eq. (101), so the equations derived in §§ 4.2-4.6 are unaltered. Thus, the mass-ratio expansion remains valid at $k_\parallel \lambda_{\mathrm{mfp}i} \gtrsim (m_i/m_e)^{1/2}$.

4.8.4. $k_\parallel \lambda_{\mathrm{mfp}i} \gg (m_e/m_i)^{1/2}$.

If the parallel wavelength of the fluctuations is so long that this is violated, $k_\parallel \lambda_{\mathrm{mfp}i} \lesssim (m_e/m_i)^{1/2}$, the collision term in Eq. (79) is minus first order. This is the lowest-order term in the equation. Setting it to zero obliges $h_e^{(0)}$ to be a perturbed Maxwellian again given by Eq. (94). Instead of Eq. (84), the zeroth-order kinetic equation is

$$v_\parallel \hat{\mathbf{b}} \cdot \nabla h_e^{(0)} = v_\parallel \frac{eF_{0e}}{cT_{0e}} \frac{\partial A_\parallel}{\partial t} + \left(\frac{\partial h_e^{(1)}}{\partial t} \right)_c. \tag{113}$$

Now the collision term in this order contains $h_e^{(1)}$, which can be determined from Eq. (113) by inverting the colli-

sion operator. This sets up a perturbation theory that in due course leads to the Reduced MHD version of the general MHD equations—this is what was considered in § 2. Equation (96) no longer needs to hold, so the electrons are not isothermal. In this true one-fluid limit, both electrons and ions are adiabatic with equal temperatures [see Eq. (115) below]. The collisional transport terms in this limit (parallel and perpendicular resistivity, viscosity, heat fluxes, etc.) were calculated [starting not from gyrokinetics but from the general Vlasov–Landau equation (36)] in exhaustive detail by Braginskii (1965). His results and the way RMHD emerges from them are reviewed in Appendix A.

In physical terms, the electrons can no longer be isothermal if the parallel electron diffusion time becomes longer than the characteristic time of the fluctuations (the Alfvén time):

$$\frac{1}{v_{\mathrm{th}e}\lambda_{\mathrm{mfp}i}k_\parallel^2} \gtrsim \frac{1}{k_\parallel v_A} \quad \Leftrightarrow \quad k_\parallel \lambda_{\mathrm{mfp}i} \lesssim \frac{1}{\sqrt{\beta_i}} \sqrt{\frac{m_e}{m_i}}. \tag{114}$$

Furthermore, under a similar condition, electron and ion temperatures must equalize: this happens if the ion–electron collision time is shorter than the Alfvén time,

$$\frac{1}{\nu_{ie}} \lesssim \frac{1}{k_\parallel v_A} \quad \Leftrightarrow \quad k_\parallel \lambda_{\mathrm{mfp}i} \lesssim \sqrt{\beta_i} \sqrt{\frac{m_e}{m_i}} \tag{115}$$

(see Lithwick & Goldreich 2001 for a discussion of these conditions in application to the ISM).

4.9. *Summary*

The original gyrokinetic description introduced in § 3 was a system of two kinetic equations [Eq. (57)] that evolved the electron and ion distribution functions h_e, h_i and three field

equations [Eqs. (61-63)] that related φ, $A_\parallel$ and $\delta B_\parallel$ to h_e and h_i. In this section, we have taken advantage of the smallness of the electron mass to treat the electrons as an isothermal magnetized fluid, while ions remained fully gyrokinetic.

In mathematical terms, we solved the electron kinetic equation and replaced the gyrokinetics with a simpler closed system of equations that evolve 6 unknown functions: φ, $A_\parallel$, $\delta B_\parallel$, δn_e, $u_{\parallel e}$ and h_i. These satisfy two fluid-like evolution equations (95) and (104), three integral relations (107), (108), and (87) which involve h_i, and the kinetic equation (57) for h_i. The system is simpler because the full electron distribution function has been replaced by two scalar fields δn_e and $u_{\parallel e}$. We now summarize this new system of equations: denoting $a_i = k_\perp v_\perp / \Omega_i$, we have

$$\frac{1}{c}\frac{\partial A_\parallel}{\partial t} + \hat{\mathbf{b}}\cdot\nabla\varphi = \hat{\mathbf{b}}\cdot\nabla\frac{T_{0e}}{e}\frac{\delta n_e}{n_{0e}}, \qquad (116)$$

$$\frac{d}{dt}\left(\frac{\delta n_e}{n_{0e}} - \frac{\delta B_\parallel}{B_0}\right) + \hat{\mathbf{b}}\cdot\nabla u_{\parallel e} = -\frac{cT_{0e}}{eB_0}\left\{\frac{\delta n_e}{n_{0e}}, \frac{\delta B_\parallel}{B_0}\right\}, (117)$$

$$\frac{\delta n_e}{n_{0e}} = -\frac{Ze\varphi}{T_{0i}} + \sum_{\mathbf{k}} e^{i\mathbf{k}\cdot\mathbf{r}}\frac{1}{n_{0i}}\int d^3\mathbf{v}\, J_0(a_i)h_{i\mathbf{k}}, \qquad (118)$$

$$u_{\parallel e} = \frac{c}{4\pi e n_{0e}}\nabla_\perp^2 A_\parallel + \sum_{\mathbf{k}} e^{i\mathbf{k}\cdot\mathbf{r}}\frac{1}{n_{0i}}\int d^3\mathbf{v}\, v_\parallel J_0(a_i)h_{i\mathbf{k}}, (119)$$

$$\frac{\delta B_\parallel}{B_0} = \frac{\beta_i}{2}\left\{\left(1+\frac{Z}{\tau}\right)\frac{Ze\varphi}{T_{0i}} - \sum_{\mathbf{k}} e^{i\mathbf{k}\cdot\mathbf{r}}\right.$$
$$\left. \times \frac{1}{n_{0i}}\int d^3\mathbf{v}\left[\frac{Z}{\tau}J_0(a_i) + \frac{2v_\perp^2}{v_{\mathrm{th}i}^2}\frac{J_1(a_i)}{a_i}\right]h_{i\mathbf{k}}\right\}, \qquad (120)$$

and Eq. (57) for $s = i$ and ion–ion collisions only:

$$\frac{\partial h_i}{\partial t} + v_\parallel\frac{\partial h_i}{\partial z} + \frac{c}{B_0}\{\langle\chi\rangle_{\mathbf{R}_i}, h_i\} = \frac{Ze}{T_{0i}}\frac{\partial\langle\chi\rangle_{\mathbf{R}_i}}{\partial t}F_{0i} + \langle C_{ii}[h_i]\rangle_{\mathbf{R}_i}, \qquad (121)$$

where $\langle C_{ii}[\dots]\rangle_{\mathbf{R}_i}$ is the gyrokinetic ion–ion collision operator (see Appendix B) and the ion–electron collisions have been neglected to lowest order in $(m_e/m_i)^{1/2}$ [see Eq. (51)]. Note that Eqs. (116-117) have been written in a compact form, where

$$\frac{d}{dt} = \frac{\partial}{\partial t} + \mathbf{u}_E\cdot\nabla = \frac{\partial}{\partial t} + \frac{c}{B_0}\{\varphi, \cdots\} \qquad (122)$$

is the convective derivative with respect to the $\mathbf{E}\times\mathbf{B}$ drift velocity, $\mathbf{u}_E = -c\nabla_\perp\varphi\times\hat{\mathbf{z}}/B_0$, and

$$\hat{\mathbf{b}}\cdot\nabla = \frac{\partial}{\partial z} + \frac{\delta\mathbf{B}_\perp}{B_0}\cdot\nabla = \frac{\partial}{\partial z} - \frac{1}{B_0}\{A_\parallel, \cdots\} \qquad (123)$$

is the gradient along the total magnetic field (mean field plus perturbation).

The generalized energy conserved by Eqs. (116-121) is given by Eq. (109).

It is worth observing that the left-hand side of Eq. (116) is simply minus the component of the electric field along the total magnetic field [see Eq. (37)]. This was used in §4.3 to prove that the magnetic flux described by Eq. (116) is exactly conserved (see §7.7 for a discussion of scales at which this conservation is broken). Equation (116) is the projection of the generalized Ohm's law onto the total magnetic field—the

right-hand side of this equation is the so-called thermoelectric term. This is discussed in more detail in Appendix C.1, where we also show that Eq. (117) is the parallel part of Faraday's law and give a qualitative non-gyrokinetic derivation of Eqs. (116-117).

We will refer to Eqs. (116-121) as *the equations of isothermal electron fluid.* They are valid in a broad range of scales: the only constraints are that $k_\parallel \ll k_\perp$ (gyrokinetic ordering, §3.1), $k_\perp\rho_e \ll 1$ (electrons are magnetized, §4.8.1) and $k_\parallel\lambda_{\mathrm{mfp}i} \gg (m_e/m_i)^{1/2}$ (electrons are isothermal, §4.8.4). The region of validity of Eqs. (116-121) in the wavenumber space is illustrated in Fig. 4. A particular advantage of this hybrid fluid-kinetic system is that it is uniformly valid across the transition from magnetized to unmagnetized ions (i.e., from $k_\perp\rho_i \ll 1$ to $k_\perp\rho_i \gg 1$).

5. TURBULENCE IN THE INERTIAL RANGE: KINETIC RMHD

Our goal in this section is to derive a reduced set of equations that describe the magnetized plasma in the limit of small $k_\perp\rho_i$. Before we proceed with an expansion in $k_\perp\rho_i$, we need to make a formal technical step, the usefulness of which will become clear shortly. A reader with no patience for this or any of the subsequent technical developments may skip to the summary at the end of this section (§5.7).

5.1. *A Technical Step*

Let us formally split the ion gyrocenter distribution function into two parts:

$$h_i = \frac{Ze}{T_{0i}}\left\langle\varphi - \frac{\mathbf{v}_\perp\cdot\mathbf{A}_\perp}{c}\right\rangle_{\mathbf{R}_i}F_{0i} + g$$
$$= \sum_{\mathbf{k}} e^{i\mathbf{k}\cdot\mathbf{R}_i}\left[J_0(a_i)\frac{Ze\varphi_{\mathbf{k}}}{T_{0i}} + \frac{2v_\perp^2}{v_{\mathrm{th}i}^2}\frac{J_1(a_i)}{a_i}\frac{\delta B_{\parallel\mathbf{k}}}{B_0}\right]F_{0i} + g. (124)$$

Then g satisfies the following equation, obtained by substituting Eq. (124) and the expression for $\partial A_\parallel/\partial t$ that follows from Eq. (116) into the ion gyrokinetic equation (121):

$$\underbrace{\frac{\partial g}{\partial t} + v_\parallel\frac{\partial g}{\partial z} + \frac{c}{B_0}\{\langle\chi\rangle_{\mathbf{R}_i}, g\} - \langle C_{ii}[g]\rangle_{\mathbf{R}_i}}_{\textcircled{0}} =$$

$$-\frac{Ze}{T_{0i}}v_\parallel\underbrace{\left\langle\frac{1}{B_0}\{A_\parallel, \varphi - \langle\varphi\rangle_{\mathbf{R}_i}\}\right\rangle}_{\textcircled{1}}$$

$$+\underbrace{\hat{\mathbf{b}}\cdot\nabla\left(\frac{T_{0e}}{e}\frac{\delta n_e}{n_{0e}} - \left\langle\frac{\mathbf{v}_\perp\cdot\mathbf{A}_\perp}{c}\right\rangle_{\mathbf{R}_i}\right)}_{\textcircled{0}}\bigg\rangle_{\mathbf{R}_i} F_{0i}$$

$$+\frac{Ze}{T_{0i}}\left\langle C_{ii}\left[\left\langle\underbrace{\varphi}_{\textcircled{1}} - \underbrace{\frac{\mathbf{v}_\perp\cdot\mathbf{A}_\perp}{c}}_{\textcircled{0}}\right\rangle_{\mathbf{R}_i}F_{0i}\right]\right\rangle_{\mathbf{R}_i}. \qquad (125)$$

In the above equation, we have used compact notation in writing out the nonlinear terms: e.g., $\langle\{A_\parallel, \varphi - \langle\varphi\rangle_{\mathbf{R}_i}\}\rangle_{\mathbf{R}_i} = \langle\{A_\parallel(\mathbf{r}), \varphi(\mathbf{r})\}\rangle_{\mathbf{R}_i} - \{\langle A_\parallel\rangle_{\mathbf{R}_i}, \langle\varphi\rangle_{\mathbf{R}_i}\}$, where the first Poisson bracket involves derivatives with respect to $\mathbf{r}$ and the second with respect to $\mathbf{R}_i$.

The field equations (118-120) rewritten in terms of g are

$$\underbrace{\frac{\delta n_{\mathbf{k}e}}{n_{0e}}}_{\textcircled{0}} - \underbrace{\Gamma_1(\alpha_i)\frac{\delta B_{\|\mathbf{k}}}{B_0}}_{\textcircled{0}} + \underbrace{\left[1 - \Gamma_0(\alpha_i)\right]\frac{Ze\varphi_{\mathbf{k}}}{T_{0i}}}_{\textcircled{1}}$$

$$= \underbrace{\frac{1}{n_{0i}}\int d^3\mathbf{v}\, J_0(a_i) g_{\mathbf{k}}}_{\textcircled{0}}, \qquad (126)$$

$$\underbrace{u_{\|\mathbf{k}e}}_{\textcircled{0}} + \underbrace{\frac{c}{4\pi e n_{0e}}k_\perp^2 A_{\|\mathbf{k}}}_{\textcircled{1}} = \underbrace{\frac{1}{n_{0i}}\int d^3\mathbf{v}\, v_\| J_0(a_i) g_{\mathbf{k}}}_{\textcircled{0}} = u_{\|\mathbf{k}i}, \quad (127)$$

$$\underbrace{\frac{Z}{\tau}\frac{\delta n_{\mathbf{k}e}}{n_{0e}}}_{\textcircled{0}} + \underbrace{\left[\Gamma_2(\alpha_i) + \frac{2}{\beta_i}\right]\frac{\delta B_{\|\mathbf{k}}}{B_0}}_{\textcircled{0}} - \underbrace{\left[1 - \Gamma_1(\alpha_i)\right]\frac{Ze\varphi_{\mathbf{k}}}{T_{0i}}}_{\textcircled{1}}$$

$$= \underbrace{-\frac{1}{n_{0i}}\int d^3\mathbf{v}\, \frac{2v_\perp^2}{v_{\text{th}i}^2}\frac{J_1(a_i)}{a_i} g_{\mathbf{k}}}_{\textcircled{0}}, \quad (128)$$

where $a_i = k_\perp v_\perp/\Omega_i$, $\alpha_i = k_\perp^2\rho_i^2/2$ and we have defined

$$\Gamma_0(\alpha_i) = \frac{1}{n_{0i}}\int d^3\mathbf{v}\, [J_0(a_i)]^2 F_{0i}$$
$$= I_0(\alpha_i)e^{-\alpha_i} = 1 - \alpha_i + \cdots, \qquad (129)$$

$$\Gamma_1(\alpha_i) = \frac{1}{n_{0i}}\int d^3\mathbf{v}\, \frac{2v_\perp^2}{v_{\text{th}i}^2}J_0(a_i)\frac{J_1(a_i)}{a_i}F_{0i} = -\Gamma_0'(\alpha_i)$$

$$= [I_0(\alpha_i) - I_1(\alpha_i)]e^{-\alpha_i} = 1 - \frac{3}{2}\alpha_i + \cdots, \qquad (130)$$

$$\Gamma_2(\alpha_i) = \frac{1}{n_{0i}}\int d^3\mathbf{v}\, \left[\frac{2v_\perp^2}{v_{\text{th}i}^2}\frac{J_1(a_i)}{a_i}\right]^2 F_{0i} = 2\Gamma_1(\alpha_i). \quad (131)$$

Underneath each term in Eqs. (125-128), we have indicated the lowest order in $k_\perp\rho_i$ to which this term enters.

5.2. *Subsidiary Ordering in $k_\perp\rho_i$*

In order to carry out a subsidiary expansion in small $k_\perp\rho_i$, we must order all terms in Eqs. (95-104) and (125-128) with respect to $k_\perp\rho_i$. Let us again assume, like we did when expanding the electron equation (§ 4), that the ordering introduced for the gyrokinetics in § 3.1 holds also for the subsidiary expansion in $k_\perp\rho_i$. First note that, in view of Eq. (47), we must regard $Ze\varphi/T_{0i}$ to be minus first order:

$$\frac{Ze\varphi}{T_{0i}} \sim \frac{\epsilon}{k_\perp\rho_i\sqrt{\beta_i}}. \qquad (132)$$

Also, as $\delta B_\perp/B_0 \sim \epsilon$ [Eq. (12)],

$$\frac{(v_\|/c)A_\|}{\varphi} \sim \frac{v_{\text{th}i}\delta B_\perp}{ck_\perp\varphi} \sim \frac{1}{k_\perp\rho_i}\frac{T_{0i}}{Ze\varphi}\frac{\delta B_\perp}{B_0} \sim \sqrt{\beta_i}, \quad (133)$$

so φ and $(v_\|/c)A_\|$ are same order.

Since $u_\| = u_{\|i}$ (electrons do not contribute to the mass flow), assuming that slow waves and Alfvén waves have comparable

energies implies $u_{\|i} \sim u_\perp$. As $u_{\|i}$ is determined by the second equality in Eq. (127), we can order g [using Eq. (12)]:

$$\frac{g}{F_{0i}} \sim \frac{u_\|}{v_{\text{th}i}} \sim \frac{u_\perp}{v_{\text{th}i}} \sim \frac{\epsilon}{\sqrt{\beta_i}}, \qquad (134)$$

so g is zeroth order in $k_\perp\rho_i$. Similarly, $\delta n_e/n_{0e} \sim \delta B_\|/B_0 \sim \epsilon$ are zeroth order in $k_\perp\rho_i$—this follows directly from Eq. (12).

Together with Eq. (3), the above considerations allow us to order all terms in our equations. The ordering of the collision term involving φ is explained in Appendix B.2.

5.3. *Alfvén Waves: Kinetic Derivation of RMHD*

We shall now show that the RMHD equations (17-18) hold in this approximation. There is a simple correspondence between the stream and flux functions defined in Eq. (16) and the electromagnetic potentials φ and $A_\|$:

$$\Phi = \frac{c}{B_0}\varphi, \quad \Psi = -\frac{A_\|}{\sqrt{4\pi m_i n_{0i}}}. \qquad (135)$$

The first of these definitions says that the perpendicular flow velocity $\mathbf{u}_\perp$ is the $\mathbf{E}\times\mathbf{B}$ drift velocity; the second definition is the standard MHD relation between the magnetic flux function and the parallel component of the vector potential.

5.3.1. *Derivation of Eq. (17)*

Deriving Eq. (17) is straightforward: in Eq. (95), we retain only the lowest—minus first—order terms (those that contain φ and $A_\|$). The result is

$$\frac{\partial A_\|}{\partial t} + c\frac{\partial\varphi}{\partial z} - \frac{c}{B_0}\left\{A_\|,\varphi\right\} = 0. \qquad (136)$$

Using Eq. (135) and the definition of the Alfvén speed, $v_A = B_0/\sqrt{4\pi m_i n_{0i}}$, we get Eq. (17). By the argument of § 4.3, Eq. (136) expresses the fact that that magnetic-field lines are frozen into the $\mathbf{E}\times\mathbf{B}$ velocity field, which is the mean flow velocity associated with the Alfvén waves (see § 5.4).

5.3.2. *Derivation of Eq. (18)*

As we are about to see, in order to derive Eq. (18), we have to separate the first-order part of the $k_\perp\rho_i$ expansion. The easiest way to achieve this, is to integrate Eq. (125) over the velocity space (keeping $\mathbf{r}$ constant) and expand the resulting equation in small $k_\perp\rho_i$. Using Eqs. (126) and (127) to express the velocity-space integrals of g, we get

$$\underbrace{\frac{\partial}{\partial t}\left[1 - \Gamma_0(\alpha_i)\right]\frac{Ze\varphi_{\mathbf{k}}}{T_{0i}}}_{\textcircled{1}} + \underbrace{\frac{\partial}{\partial t}\left[\frac{\delta n_{\mathbf{k}e}}{n_{0e}} - \Gamma_1(\alpha_i)\frac{\delta B_{\|\mathbf{k}}}{B_0}\right]}_{\textcircled{0}}$$

$$+ \frac{\partial}{\partial z}\left(\underbrace{u_{\|\mathbf{k}e}}_{\textcircled{0}} + \underbrace{\frac{c}{4\pi e n_{0e}}k_\perp^2 A_{\|\mathbf{k}}}_{\textcircled{1}}\right)$$

$$+ \underbrace{\frac{c}{B_0}\frac{1}{n_{0i}}\int d^3\mathbf{v}\, J_0(a_i)\{\langle\chi\rangle_{\mathbf{R}_i}, g\}_{\mathbf{k}}}_{\textcircled{0}}$$

$$= \frac{1}{n_{0i}}\int d^3\mathbf{v}\, J_0(a_i)\left\langle C_{ii}\left[\frac{Ze}{T_{0i}}\left\langle\underbrace{\varphi}_{\textcircled{3}} - \underbrace{\frac{\mathbf{v}_\perp\cdot\mathbf{A}_\perp}{c}}_{\textcircled{2}}\right\rangle_{\mathbf{R}_i}\right.\right. F_{0i}$$

$$+ \left. g \underbrace{\Big] \Big\rangle}_{\textcircled{2}} \right|_{\mathbf{R}_i,\mathbf{k}}. \qquad (137)$$

Underneath each term, the lowest order in $k_\perp \rho_i$ to which it enters is shown. We see that terms containing φ are all first order, so it is up to this order that we shall retain terms. The collision term integrated over the velocity space picks up two extra orders of $k_\perp \rho_i$ (see Appendix B.1), so it is second order and can, therefore, be dropped. As a consequence of quasi-neutrality, the zeroth-order part of the above equation exactly coincides with Eq. (104), i.e, $\delta n_i/n_{0i} = \delta n_e/n_{0e}$ satisfy the same equation. Indeed, neglecting second-order terms (but not first-order ones!), the nonlinear term in Eq. (137) (the last term on the left-hand side) is

$$\frac{c}{B_0}\left\{\varphi, \frac{1}{n_{0i}}\int d^3\mathbf{v}\, g\right\} - \frac{1}{B_0}\left\{A_\parallel, \frac{1}{n_{0i}}\int d^3\mathbf{v}\, v_\parallel g\right\}$$
$$+ \frac{cT_{0i}}{ZeB_0}\left\{\frac{\delta B_\parallel}{B_0}, \frac{1}{n_{0i}}\int d^3\mathbf{v}\, \frac{v_\perp^2}{v_{\mathrm{th}i}^2}g\right\}, \quad (138)$$

and, using Eqs. (126-128) to express velocity-space integrals of g in the above expression, we find that the zeroth-order part of the nonlinearity is the same as the nonlinearity in Eq. (104), while the first-order part is

$$-\frac{c}{B_0}\left\{\varphi, \frac{1}{2}\rho_i^2\nabla_\perp^2\frac{Ze\varphi}{T_{0i}}\right\} + \frac{1}{B_0}\left\{A_\parallel, \frac{c}{4\pi e n_{0e}}\nabla_\perp^2 A_\parallel\right\}, \quad (139)$$

where we have used the expansion (129) of $\Gamma_0(\alpha_i)$ and converted it back into x space.

Thus, if we subtract Eq. (104) from Eq. (137), the remainder is first order and reads

$$\frac{\partial}{\partial t}\frac{1}{2}\rho_i^2\nabla_\perp^2\frac{Ze\varphi}{T_{0i}} + \frac{c}{B_0}\left\{\varphi, \frac{1}{2}\rho_i^2\nabla_\perp^2\frac{Ze\varphi}{T_{0i}}\right\}$$
$$+ \frac{\partial}{\partial z}\frac{c}{4\pi e n_{0e}}\nabla_\perp^2 A_\parallel - \frac{1}{B_0}\left\{A_\parallel, \frac{c}{4\pi e n_{0e}}\nabla_\perp^2 A_\parallel\right\} = 0. \,(140)$$

Multiplying Eq. (140) by $2T_{0i}/Ze\rho_i^2$ and using Eq. (135), we get the second RMHD equation (18).

We have established that the Alfvén-wave component of the turbulence is decoupled and fully described by the RMHD equations (17) and (18). This result is the same as that in § 2.2 but now we have proven that collisions do not affect the Alfvén waves and that a fluid-like description only requires $k_\perp \rho_i \ll 1$ to be valid.

5.4. Why Alfvén Waves Ignore Collisions

Let us write explicitly the distribution function of the ion gyrocenters [Eq. (124)] to two lowest orders in $k_\perp \rho_i$:

$$h_i = \frac{Ze}{T_{0i}}\langle\varphi\rangle_{\mathbf{R}_i} F_{0i} + \frac{v_\perp^2}{v_{\mathrm{th}i}^2}\frac{\delta B_\parallel}{B_0}F_{0i} + g + \cdots, \qquad (141)$$

where, up to corrections of order $k_\perp^2 \rho_i^2$, the ring-averaged scalar potential is $\langle\varphi\rangle_{\mathbf{R}_i} = \varphi(\mathbf{R}_i)$, the scalar potential taken at the position of the ion gyrocenter. Note that in Eq. (141), the first term is minus first order in $k_\perp \rho_i$ [see Eq. (132)], the second and third terms are zeroth order [Eq. (134)], and all terms of first and higher orders are omitted. In order to compute the full ion distribution function given by Eq. (54), we have to

convert h_i to the $\mathbf{r}$ space. Keeping terms up to zeroth order, we get

$$\frac{Ze}{T_{0i}}\langle\varphi\rangle_{\mathbf{R}_i} \simeq \frac{Ze}{T_{0i}}\varphi(\mathbf{R}_i) = \frac{Ze}{T_{0i}}\left[\varphi(\mathbf{r}) + \frac{\mathbf{v}_\perp\times\hat{\mathbf{z}}}{\Omega_i}\cdot\nabla\varphi(\mathbf{r}) + \cdots\right]$$
$$= \frac{Ze}{T_{0i}}\varphi(\mathbf{r}) + \frac{2\mathbf{v}_\perp\cdot\mathbf{u}_E}{v_{\mathrm{th}i}^2} + \ldots, \qquad (142)$$

where $\mathbf{u}_E = -c\nabla\varphi(\mathbf{r})\times\hat{\mathbf{z}}/B_0$, the $\mathbf{E}\times\mathbf{B}$ drift velocity. Substituting Eq. (142) into Eq. (141) and then Eq. (141) into Eq. (54), we find

$$f_i = F_{0i} + \frac{2\mathbf{v}_\perp\cdot\mathbf{u}_E}{v_{\mathrm{th}i}^2}F_{0i} + \frac{v_\perp^2}{v_{\mathrm{th}i}^2}\frac{\delta B_\parallel}{B_0}F_{0i} + g + \cdots. \qquad (143)$$

The first two terms can be combined into a Maxwellian with mean perpendicular flow velocity $\mathbf{u}_\perp = \mathbf{u}_E$. These are the terms responsible for the Alfvén waves. The remaining terms, which we shall denote $\delta\tilde{f}_i$, are the perturbation of the Maxwellian in the moving frame of the Alfvén waves—they describe the passive (compressive) component of the turbulence (see § 5.5). Thus, the ion distribution function is

$$f_i = \frac{n_{0i}}{(\pi v_{\mathrm{th}i}^2)^{3/2}}\exp\left[-\frac{(\mathbf{v}_\perp - \mathbf{u}_E)^2 + v_\parallel^2}{v_{\mathrm{th}i}}\right] + \delta\tilde{f}_i. \qquad (144)$$

This sheds some light on the indifference of Alfvén waves to collisions: Alfvénic perturbations do not change the Maxwellian character of the ion distribution. Unlike in a neutral fluid or gas, where viscosity arises when particles transport the local mean momentum a distance $\sim \lambda_{\mathrm{mfp}i}$, the particles in a magnetized plasma instantaneously take on the local $\mathbf{E}\times\mathbf{B}$ velocity (they take a cyclotron period to adjust, so, roughly speaking, ρ_i plays the role of the mean free path). Thus, there is no memory of the mean perpendicular motion and, therefore, no perpendicular momentum transport.

Some readers may find it illuminating to notice that Eq. (140) can be interpreted as stating simply $\nabla\cdot\mathbf{j} = 0$: the first two terms represent the divergence of the polarization current, which is perpendicular to the magnetic field;[22] the last two terms are $\hat{\mathbf{b}}\cdot\nabla j_\parallel$. No contribution to the current arises from the collisional term in Eq. (137) as ion–ion collisions cause no particle transport to lowest order in $k_\perp \rho_i$.

5.5. Compressive Fluctuations

The equations that describe the density (δn_e) and magnetic-field-strength ($\delta B_\parallel$) fluctuations follow immediately from Eqs. (125-128) if only zeroth-order terms are kept. In these equations, terms that involve φ and $A_\parallel$ also contain factors $\sim k_\perp^2 \rho_i^2$ and are, therefore, first-order [with the exception of the nonlinearity on the left-hand side of Eq. (125)]. The fact that $\langle C_{ii}[\langle\varphi\rangle_{\mathbf{R}_i}F_{0i}]\rangle_{\mathbf{R}_i}$ in Eq. (125) is first order is proved in Appendix B.2. Dropping these terms along with all other contributions of order higher than zeroth and making use of Eq. (69)

---

[22] The polarization-drift velocity is formally higher order than $\mathbf{u}_E$ in the gyrokinetic expansion. However, since $\mathbf{u}_E$ does not produce any current, the lowest-order contribution to the perpendicular current comes from the polarization drift. The higher-order contributions to the gyrocenter distribution function did not need to be calculated explicitly because the information about the polarization charge is effectively carried by the quasi-neutrality condition (61). We do not belabor this point because, in our approach, the notion of polarization charge is only ever brought in for interpretative purposes, but is not needed to carry out calculations. For further qualitative discussion of the role of the polarization charge and polarization drift in gyrokinetics, we refer the reader to Krommes 2006 and references therein.

to write out $\langle\chi\rangle_{\mathbf{R}_i}$, we find that Eq. (125) takes the form

$$\frac{dg}{dt} + v_{\parallel}\hat{\mathbf{b}}\cdot\nabla\left[g + \left(\frac{Z}{\tau}\frac{\delta n_e}{n_{0e}} + \frac{v_{\perp}^2}{v_{\text{th}i}^2}\frac{\delta B_{\parallel}}{B_0}\right)F_{0i}\right]$$
$$= \left\langle C_{ii}\left[g + \frac{v_{\perp}^2}{v_{\text{th}i}^2}\frac{\delta B_{\parallel}}{B_0}F_{0i}\right]\right\rangle_{\mathbf{R}_i}, \qquad (145)$$

where we have used definitions (122-123) of the convective time derivative d/dt and the total gradient along the magnetic field $\hat{\mathbf{b}}\cdot\nabla$ to write our equation in a compact form. Note that, in view of the correspondence between Φ, Ψ and φ, $A_{\parallel}$ [Eq. (135)], these nonlinear derivatives are the same as those defined in Eqs. (19-20). The collision term in the right-hand side of the above equation is the zeroth-order limit of the gyrokinetic ion–ion collision operator: a useful model form of it is given in Appendix B.3 [Eq. (B18)].

To zeroth order, Eqs. (126-128) are

$$\frac{\delta n_e}{n_{0e}} - \frac{\delta B_{\parallel}}{B_0} = \frac{1}{n_{0i}}\int d^3\mathbf{v}\,g, \qquad (146)$$

$$u_{\parallel} = \frac{1}{n_{0i}}\int d^3\mathbf{v}\,v_{\parallel}g, \qquad (147)$$

$$\frac{Z}{\tau}\frac{\delta n_e}{n_{0e}} + 2\left(1 + \frac{1}{\beta_i}\right)\frac{\delta B_{\parallel}}{B_0} = -\frac{1}{n_{0i}}\int d^3\mathbf{v}\,\frac{v_{\perp}^2}{v_{\text{th}i}^2}g. \qquad (148)$$

Note that $u_{\parallel}$ is not an independent quantity—it can be computed from the ion distribution but is not needed for the determination of the latter.

Equations (145-148) evolve the ion distribution function g, the "slow-wave quantities" $u_{\parallel}$, $\delta B_{\parallel}$, and the density fluctuations δn_e. The nonlinearities in Eq. (145), contained in d/dt and $\hat{\mathbf{b}}\cdot\nabla$, involve the Alfvén-wave quantities Φ and Ψ (or, equivalently, φ and $A_{\parallel}$) determined separately and independently by the RMHD equations (17-18). The situation is qualitatively similar to that in MHD (§ 2.4), except now a kinetic description is necessary—Eqs. (145-148) replace Eqs. (25-27)—and the nonlinear scattering/mixing of the slow waves and the entropy mode by the Alfvén waves takes the form of passive advection of the distribution function g. The density and magnetic-field-strength fluctuations are velocity-space moments of g.

Another way to understand the passive nature of the compressive component of the turbulence discussed above is to think of it as the perturbation of a local Maxwellian equilibrium associated with the Alfvén waves. Indeed, in § 5.4, we split the full ion distribution function [Eq. (144)] into such a local Maxwellian and its perturbation

$$\delta\tilde{f}_i = g + \frac{v_{\perp}^2}{v_{\text{th}i}^2}\frac{\delta B_{\parallel}}{B_0}F_{0i}. \qquad (149)$$

It is this perturbation that contains all the information about the compressive component; the second term in the above expression enforces to lowest order the conservation of the first adiabatic invariant $\mu_i = m_i v_{\perp}^2/2B$. In terms of the function (149), Eqs. (145-148) take a somewhat more compact form (cf. Schekochihin et al. 2007):

$$\frac{d}{dt}\left(\delta\tilde{f}_i - \frac{v_{\perp}^2}{v_{\text{th}i}^2}\frac{\delta B_{\parallel}}{B_0}F_{0i}\right) + v_{\parallel}\hat{\mathbf{b}}\cdot\nabla\left(\delta\tilde{f}_i + \frac{Z}{\tau}\frac{\delta n_e}{n_{0e}}F_{0i}\right)$$
$$= \left\langle C_{ii}\left[\delta\tilde{f}_i\right]\right\rangle_{\mathbf{R}_i}, \quad (150)$$
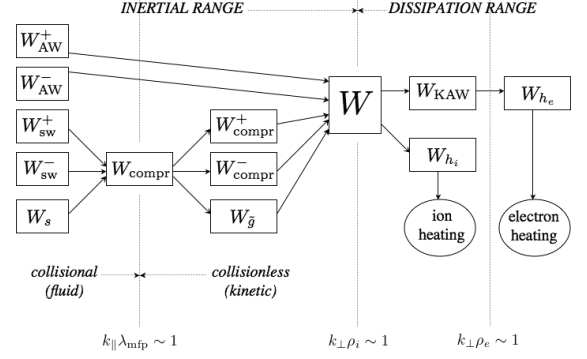

FIG. 5.— Channels of the kinetic cascade of generalized energy (§ 3.4) from large to small scales: see § 2.7 and Appendix D.2 (inertial range, collisional regime), § 5.6 and § 6.2.5 (inertial range, collisionless regime), § 7.8 and § 7.12 (dissipation range). Note that some ion heating probably also results from the collisional and collisionless damping of the compressive fluctuations in the inertial range (see § 6.1.2 and § 6.2.4).

$$\frac{\delta n_e}{n_{0e}} = \frac{1}{n_{0i}}\int d^3\mathbf{v}\,\delta\tilde{f}_i, \qquad (151)$$

$$\frac{\delta B_{\parallel}}{B_0} = -\frac{\beta_i}{2}\frac{1}{n_{0i}}\int d^3\mathbf{v}\left(\frac{Z}{\tau} + \frac{v_{\perp}^2}{v_{\text{th}i}^2}\right)\delta\tilde{f}_i. \qquad (152)$$

5.6. Generalized Energy: Three KRMHD Cascades

The generalized energy (§ 3.4) in the limit $k_{\perp}\rho_i \ll 1$ is calculated by substituting into Eq. (109) the perturbed ion distribution function $\delta f_i = 2\mathbf{v}_{\perp}\cdot\mathbf{u}_E F_{0i}/v_{\text{th}i}^2 + \delta\tilde{f}_i$ [see Eqs. (143) and (149)]. After performing velocity integration, we get

$$W = \int d^3\mathbf{r}\left[\frac{m_i n_{0i}u_E^2}{2} + \frac{\delta B_{\perp}^2}{8\pi}\right.$$
$$\left. + \frac{n_{0i}T_{0i}}{2}\left(\frac{Z}{\tau}\frac{\delta n_e^2}{n_{0e}^2} + \frac{2}{\beta_i}\frac{\delta B_{\parallel}^2}{B_0^2} + \frac{1}{n_{0i}}\int d^3\mathbf{v}\,\frac{\delta\tilde{f}_i^2}{F_{0i}}\right)\right]$$
$$= W_{\text{AW}} + W_{\text{compr}}. \qquad (153)$$

We see that the kinetic energy of the Alfvénic fluctuations has emerged from the ion-entropy part of the generalized energy. The first two terms in Eq. (153) are the total (kinetic plus magnetic) energy of the Alfvén waves, denoted W_{AW}. As we learned from § 5.3, it cascades independently of the rest of the generalized energy, W_{compr}, which contains the compressive component of the turbulence (§ 5.5) and is the invariant conserved by Eqs. (150-152).

In terms of the potentials used in our discussion of RMHD in § 2, we have

$$W_{\text{AW}} = \int d^3\mathbf{r}\,\frac{m_i n_{0i}}{2}\left(|\nabla_{\perp}\Phi|^2 + |\nabla_{\perp}\Psi|^2\right)$$
$$= \int d^3\mathbf{r}\,\frac{m_i n_{0i}}{2}\left(|\nabla_{\perp}\zeta^+|^2 + |\nabla_{\perp}\zeta^-|^2\right)$$
$$= W_{\text{AW}}^+ + W_{\text{AW}}^- \qquad (154)$$

where W_{AW}^+ and W_{AW}^- are the energies of the "+" and "−" waves [Eq. (33)], which, as we know from § 2.3, cascade by scattering off each other but without exchanging energy.

Thus, the kinetic cascade in the limit $k_{\perp}\rho_i \ll 1$ is split, independently of the collisionality, into three cascades: of W_{AW}^+,

W_{AW}^- and W_{compr}. The compressive cascade is, in fact, split into three independent cascades—the splitting is different in the collisional limit (Appendix D.2) and in the collisionless one (§ 6.2.5). Figure 5 schematically summarizes both the splitting of the kinetic cascade that we have worked out so far and the upcoming developments.

5.7. *Summary*

In § 4, gyrokinetics was reduced to a hybrid fluid-kinetic system by means of an expansion in the electron mass, which was valid for $k_\perp \rho_e \ll 1$. In this section, we have further restricted the scale range by taking $k_\perp \rho_i \ll 1$ and as a result have been able to achieve a further reduction in the complexity of the kinetic theory describing the turbulent cascades. The reduced theory derived here evolves 5 unknown functions: Φ, Ψ, $\delta B_\parallel$, δn_e and g. The stream and flux functions, Φ and Ψ are related to the fluid quantities (perpendicular velocity and magnetic field perturbations) via Eq. (16) and to the electromagnetic potentials φ, $A_\parallel$ via Eq. (135). They satisfy a closed system of equations, Eqs. (17-18), which describe the decoupled cascade of Alfvén waves. These are the same equations that arise from the MHD approximations, but we have now proven that their validity does not depend on the assumption of high collisionality (the fluid limit) and extends to scales well below the mean free path, but above the ion gyroscale. The physical reasons for this are explained in § 5.4. The density and magnetic-field-strength fluctuations (the "compressive" fluctuations, or the slow waves and the entropy mode in the MHD limit) now require a kinetic description in terms of the ion distribution function g [or $\delta \tilde{f}_i$, Eq. (149)], evolved by the kinetic equation (145) [or Eq. (150)]. The kinetic equation contains δn_e and $\delta B_\parallel$, which are, in turn calculated in terms of the velocity-space integrals of g via Eqs. (146) and (148) [or Eqs. (151) and (152)]. The nonlinear evolution (turbulent cascade) of g, $\delta B_\parallel$ and δn_e is due solely to passive advection of g by the Alfvén-wave turbulence.

Let us summarize the new set of equations:

$$\frac{\partial \Psi}{\partial t} = v_A \hat{\mathbf{b}} \cdot \nabla \Phi, \tag{155}$$

$$\frac{d}{dt} \nabla_\perp^2 \Phi = v_A \hat{\mathbf{b}} \cdot \nabla \nabla_\perp^2 \Psi, \tag{156}$$

$$\frac{dg}{dt} + v_\parallel \hat{\mathbf{b}} \cdot \nabla \left[g + \left(\frac{Z}{\tau} \frac{\delta n_e}{n_{0e}} + \frac{v_\perp^2}{v_{\mathrm{th}i}^2} \frac{\delta B_\parallel}{B_0} \right) F_{0i} \right]$$
$$= \left\langle C_{ii} \left[g + \frac{v_\perp^2}{v_{\mathrm{th}i}^2} \frac{\delta B_\parallel}{B_0} F_{0i} \right] \right\rangle_{\mathbf{R}_i}, \tag{157}$$

$$\frac{\delta n_e}{n_{0e}} = - \left[\frac{Z}{\tau} + 2 \left(1 + \frac{1}{\beta_i} \right) \right]^{-1} \frac{1}{n_{0i}} \int d^3 \mathbf{v} \left[\frac{v_\perp^2}{v_{\mathrm{th}i}^2} - 2 \left(1 + \frac{1}{\beta_i} \right) \right] g, \tag{158}$$

$$\frac{\delta B_\parallel}{B_0} = - \left[\frac{Z}{\tau} + 2 \left(1 + \frac{1}{\beta_i} \right) \right]^{-1} \frac{1}{n_{0i}} \int d^3 \mathbf{v} \left(\frac{v_\perp^2}{v_{\mathrm{th}i}^2} + \frac{Z}{\tau} \right) g, \tag{159}$$

where

$$\frac{d}{dt} = \frac{\partial}{\partial t} + \{\Phi, \cdots\}, \quad \hat{\mathbf{b}} \cdot \nabla = \frac{\partial}{\partial z} + \frac{1}{v_A} \{\Psi, \cdots\}. \tag{160}$$

An explicit form of the collision term in the right-hand side of Eq. (157) is provided in Appendix B.3 [Eq. (B18)].

The generalized energy conserved by Eqs. (155-159) is given by Eq. (153). The kinetic cascade is split, the Alfvénic

cascade proceeding independently of the compressive one (see Fig. 5).

The decoupling of the Alfvénic cascade is manifested by Eqs. (155-156) forming a closed subset. As already noted in § 4.9, Eq. (155) is the component of Ohm's law along the total magnetic field, $\mathbf{B} \cdot \mathbf{E} = 0$. Equation (156) can be interpreted as the evolution equation for the vorticity of the perpendicular plasma flow velocity, which is the $\mathbf{E} \times \mathbf{B}$ drift velocity.

We shall refer to the system of equations (155-159) as *Kinetic Reduced Magnetohydrodynamics (KRMHD).*[23] It is a hybrid fluid-kinetic description of low-frequency turbulence in strongly magnetized weakly collisional plasma that is uniformly valid at all scales satisfying $k_\perp \rho_i \ll \min(1, k_\parallel \lambda_{\mathrm{mfp}i})$ (ions are strongly magnetized)[24] and $k_\parallel \lambda_{\mathrm{mfp}i} \gg (m_e/m_i)^{1/2}$ (electrons are isothermal), as illustrated in Fig. 2. Therefore, it smoothly connects the collisional and collisionless regimes and is the appropriate theory for the study of the turbulent cascades in the inertial range. The KRMHD equations generalize rather straightforwardly to plasmas that are so collisionless that one cannot assume a Maxwellian equilibrium distribution function (Chen et al. 2009)—a situation that is relevant in some of the solar-wind measurements (see further discussion in § 8.3).

KRMHD describe what happens to the turbulent cascade at or below the ion gyroscale—we shall move on to these scales in § 7, but first we would like to discuss the turbulent cascades of density and magnetic-field-strength fluctuations and their damping by collisional and collisionless mechanisms.

6. COMPRESSIVE FLUCTUATIONS IN THE INERTIAL RANGE

Here we first derive the nonlinear equations that govern the evolution of the compressive (density and magnetic-field-strength) fluctuations in the collisional ($k_\parallel \lambda_{\mathrm{mfp}i} \ll 1$, § 6.1 and Appendix D) and collisionless ($k_\parallel \lambda_{\mathrm{mfp}i} \gg 1$, § 6.2) limits, discuss the linear damping that these fluctuations undergo in the two limits and work out the form the generalized energy takes for compressive fluctuations (which is particularly interesting in the collisionless limit, §§ 6.2.3-6.2.5). As in previous sections, an impatient reader may skip to § 6.3 where the results of the previous two subsections are summarized and the implications for the structure of the turbulent cascades of the density and field-strength fluctuations are discussed.

6.1. *Collisional Regime*
6.1.1. *Equations*

In the collisional regime, $k_\parallel \lambda_{\mathrm{mfp}i} \ll 1$, the fluid limit is recovered by expanding Eqs. (155-159) in small $k_\parallel \lambda_{\mathrm{mfp}i}$. The calculation that is necessary to achieve this is done in Appendix D (see also Appendix A.4). The result is a closed set

---

[23] The term is introduced by analogy with a popular fluid-kinetic system known as Kinetic MHD, or KMHD (see Kulsrud 1964, 1983). KMHD is derived for magnetized plasmas ($\rho_i \ll \lambda_{\mathrm{mfp}i}$) under the assumption that $k\rho_s \ll 1$ and $\omega \ll \Omega_s$ but without assuming either strong anisotropy ($k_\parallel \ll k_\perp$) or small fluctuations ($|\delta \mathbf{B}| \ll B_0$). The KRMHD equations (155-159) can be recovered from KMHD by applying to it the GK-RMHD ordering [Eq. (12) and § 3.1] and an expansion in $(m_e/m_i)^{1/2}$ (Schekochihin et al. 2007). This means that the $k_\perp \rho_i$ expansion (§ 5), which for KMHD is the primary expansion, commutes with the gyrokinetic expansion (§ 3) and the $(m_e/m_i)^{1/2}$ expansion (§ 4), both of which preceded it in this paper.

[24] The condition $k_\perp \rho_i \ll k_\parallel \lambda_{\mathrm{mfp}i}$ must be satisfied because in our estimates of the collision terms (Appendix B.2) we took $k_\perp \rho_i \ll 1$ while assuming that $k_\parallel \lambda_{\mathrm{mfp}i} \sim 1$.

of three fluid equations that evolve $\delta B_\parallel$, δn_e and $u_\parallel$:

$$\frac{d}{dt}\frac{\delta B_\parallel}{B_0} = \hat{\mathbf{b}} \cdot \nabla u_\parallel + \frac{d}{dt}\frac{\delta n_e}{n_{0e}}, \tag{161}$$

$$\frac{du_\parallel}{dt} = v_A^2 \hat{\mathbf{b}} \cdot \nabla \frac{\delta B_\parallel}{B_0} + \nu_{\parallel i}\hat{\mathbf{b}} \cdot \nabla \left(\hat{\mathbf{b}} \cdot \nabla u_\parallel\right), \tag{162}$$

$$\frac{d}{dt}\frac{\delta T_i}{T_{0i}} = \frac{2}{3}\frac{d}{dt}\frac{\delta n_e}{n_{0e}} + \kappa_{\parallel i}\hat{\mathbf{b}} \cdot \nabla \left(\hat{\mathbf{b}} \cdot \nabla \frac{\delta T_i}{T_{0i}}\right), \tag{163}$$

where

$$\left(1 + \frac{Z}{\tau}\right)\frac{\delta n_e}{n_{0e}} = -\frac{\delta T_i}{T_{0i}} - \frac{2}{\beta_i}\left(\frac{\delta B_\parallel}{B_0} + \frac{1}{3v_A^2}\nu_{\parallel i}\hat{\mathbf{b}} \cdot \nabla u_\parallel\right), \tag{164}$$

and $\nu_{\parallel i}$ and $\kappa_{\parallel i}$ are the coefficients of parallel ion viscosity and thermal diffusivity, respectively. The viscous and thermal diffusion are anisotropic because plasma is magnetized, $\lambda_{\mathrm{mfp}i} \gg \rho_i$ (Braginskii 1965). The method of calculation of $\nu_{\parallel i}$ and $\kappa_{\parallel i}$ is explained in Appendix D.3. Here we shall ignore numerical prefactors of order unity and give order-of-magnitude values for these coefficients:

$$\nu_{\parallel i} \sim \kappa_{\parallel i} \sim \frac{v_{\mathrm{th}i}^2}{\nu_{ii}} \sim v_{\mathrm{th}i}\lambda_{\mathrm{mfp}i}. \tag{165}$$

If we set $\nu_{\parallel i} = \kappa_{\parallel i} = 0$, Eqs. (161-164) are the same as the RMHD equations of § 2 with the sound speed defined as

$$c_s = v_A\sqrt{\frac{\beta_i}{2}\left(\frac{Z}{\tau} + \frac{5}{3}\right)} = \sqrt{\frac{ZT_{0e}}{m_i} + \frac{5}{3}\frac{T_{0i}}{m_i}}. \tag{166}$$

This is the natural definition of c_s for the case of adiabatic ions, whose specific heat ratio is $\gamma_i = 5/3$, and isothermal electrons, whose specific heat ratio is $\gamma_e = 1$ [because $\delta p_e = T_{0e}\delta n_e$; see Eq. (103)]. Note that Eq. (164) is equivalent to the pressure balance [Eq. (22) of § 2] with $p = n_i T_i + n_e T_e$ and $\delta p_e = T_{0e}\delta n_e$.

As in § 2, the fluctuations described by Eqs. (161-164) separate into the zero-frequency entropy mode and the left- and right-propagating slow waves with

$$\omega = \pm\frac{k_\parallel v_A}{\sqrt{1 + v_A^2/c_s^2}} \tag{167}$$

[see Eq. (30)]. All three are cascaded independently of each other via nonlinear interaction with the Alfvén waves. In Appendix D.2, we show that the generalized energy W_{compr} for this system, given in § 5.6, splits into the three familiar invariants W_{sw}^+, W_{sw}^-, and W_s, defined by Eqs. (34-35) (see Fig. 5).

6.1.2. *Dissipation*

The diffusion terms add dissipation to the equations. Because diffusion occurs along the field lines of the total magnetic field (mean field plus perturbation), the diffusive terms are nonlinear and the dissipation process also involves interaction with the Alfvén waves. We can estimate the characteristic parallel scale at which the diffusion terms become important by balancing the nonlinear cascade time and the typical diffusion time:

$$k_\parallel v_A \sim v_{\mathrm{th}i}\lambda_{\mathrm{mfp}i}k_\parallel^2 \quad \Leftrightarrow \quad k_\parallel\lambda_{\mathrm{mfp}i} \sim 1/\sqrt{\beta_i}, \tag{168}$$

where we have used Eq. (165).

Technically speaking, the cutoff given by Eq. (168) always lies in the range of $k_\parallel$ that is outside the region of validity

of the small-$k_\parallel\lambda_{\mathrm{mfp}i}$ expansion adopted in the derivation of Eqs. (161-163). In fact, in the low-beta limit, the collisional cutoff falls manifestly in the collisionless scale range, i.e., the collisional (fluid) approximation breaks down before the slow-wave and entropy cascades are damped and one must use the collisionless (kinetic) limit to calculate the damping (see § 6.2.2). The situation is different in the high-beta limit: in this case, the expansion in small $k_\parallel\lambda_{\mathrm{mfp}i}$ can be reformulated as an expansion in small $1/\sqrt{\beta_i}$ and the cutoff falls within the range of validity of the fluid approximation. Equations (161-163) in this limit are

$$\frac{d}{dt}\frac{\delta B_\parallel}{B_0} = \hat{\mathbf{b}} \cdot \nabla u_\parallel, \tag{169}$$

$$\frac{du_\parallel}{dt} = v_A^2 \hat{\mathbf{b}} \cdot \nabla \frac{\delta B_\parallel}{B_0} + \nu_{\parallel i}\hat{\mathbf{b}} \cdot \nabla \left(\hat{\mathbf{b}} \cdot \nabla u_\parallel\right), \tag{170}$$

$$\frac{d}{dt}\frac{\delta n_e}{n_{0e}} = \frac{1 + Z/\tau}{5/3 + Z/\tau}\kappa_{\parallel i}\hat{\mathbf{b}} \cdot \nabla \left(\hat{\mathbf{b}} \cdot \nabla \frac{\delta n_e}{n_{0e}}\right). \tag{171}$$

As in § 2 [Eq. (28)], the density fluctuations [Eq. (171)] have decoupled from the slow waves [Eqs. (169-170)]. The former are damped by thermal diffusion, the latter by viscosity. The corresponding linear dispersion relations are

$$\omega = -i\frac{1 + Z/\tau}{5/3 + Z/\tau}\kappa_{\parallel i}k_\parallel^2, \tag{172}$$

$$\omega = \pm k_\parallel v_A\sqrt{1 - \left(\frac{\nu_{\parallel i}k_\parallel}{2v_A}\right)^2} - i\frac{\nu_{\parallel i}k_\parallel^2}{2}. \tag{173}$$

Equation (172) describes strong diffusive damping of the density fluctuations. The slow-wave dispersion relation (173) has two distinct regimes:

1. When $k_\parallel < 2v_A/\nu_{\parallel i}$, it describes viscously damped slow waves. In particular, in the limit $k_\parallel\lambda_{\mathrm{mfp}i} \ll 1/\sqrt{\beta_i}$, we have

$$\omega \simeq \pm k_\parallel v_A - i\frac{\nu_{\parallel i}k_\parallel^2}{2}. \tag{174}$$

2. For $k_\parallel > 2v_A/\nu_{\parallel i}$, both solutions become purely imaginary, so the slow waves are converted into aperiodic decaying fluctuations. The stronger-damped (diffusive) branch has $\omega \simeq -i\nu_{\parallel i}k_\parallel^2$, the weaker-damped one has

$$\omega \simeq -i\frac{v_A^2}{\nu_{\parallel i}} \sim -\frac{i}{\beta_i}\frac{v_{\mathrm{th}i}}{\lambda_{\mathrm{mfp}i}} \sim -\frac{i}{\sqrt{\beta_i}}\frac{v_A}{\lambda_{\mathrm{mfp}i}}. \tag{175}$$

This damping effect is called viscous relaxation. It is valid until $k_\parallel\lambda_{\mathrm{mfp}i} \sim 1$, where it is replaced by the collisionless damping discussed in § 6.2.2 [see Eq. (190)].

The viscous and thermal-diffusive dissipation mechanisms described above lead, in the limits where they are efficient, to ion heating via the standard fluid (collisional) route, involving the development of small parallel scales in the position space, but not in velocity space (see § 3.4 and § 3.5).

6.2. *Collisionless Regime*

6.2.1. *Equations*

In the collisionless regime, $k_\parallel\lambda_{\mathrm{mfp}i} \gg 1$, the collision integral in the right-hand side of the kinetic equation (157) can be

neglected. The $v_\perp$ dependence can then be integrated out of Eq. (157). Indeed, let us introduce the following two auxiliary functions:

$$G_n(v_\parallel) = -\left[\frac{Z}{\tau} + 2\left(1 + \frac{1}{\beta_i}\right)\right]^{-1}$$
$$\times \frac{2\pi}{n_{0i}} \int_0^\infty dv_\perp \, v_\perp \left[\frac{v_\perp^2}{v_{thi}^2} - 2\left(1 + \frac{1}{\beta_i}\right)\right] g, \quad (176)$$

$$G_B(v_\parallel) = -\left[\frac{Z}{\tau} + 2\left(1 + \frac{1}{\beta_i}\right)\right]^{-1}$$
$$\times \frac{2\pi}{n_{0i}} \int_0^\infty dv_\perp \, v_\perp \left(\frac{v_\perp^2}{v_{thi}^2} + \frac{Z}{\tau}\right) g. \quad (177)$$

In terms of these functions,

$$\frac{\delta n_e}{n_{0e}} = \int dv_\parallel \, G_n, \quad \frac{\delta B_\parallel}{B_0} = \int dv_\parallel \, G_B \quad (178)$$

and Eq. (157) reduces to the following two coupled one-dimensional kinetic equations

$$\frac{dG_n}{dt} + v_\parallel \hat{\mathbf{b}} \cdot \nabla G_n = -\left[\frac{Z}{\tau} + 2\left(1 + \frac{1}{\beta_i}\right)\right]^{-1} v_\parallel F_M(v_\parallel)$$
$$\times \hat{\mathbf{b}} \cdot \nabla \left[\frac{Z}{\tau}\left(1 + \frac{2}{\beta_i}\right)\frac{\delta n_e}{n_{0e}} + \frac{2}{\beta_i}\frac{\delta B_\parallel}{B_0}\right], \quad (179)$$

$$\frac{dG_B}{dt} + v_\parallel \hat{\mathbf{b}} \cdot \nabla G_B = \left[\frac{Z}{\tau} + 2\left(1 + \frac{1}{\beta_i}\right)\right]^{-1} v_\parallel F_M(v_\parallel)$$
$$\times \hat{\mathbf{b}} \cdot \nabla \left[\frac{Z}{\tau}\left(1 + \frac{Z}{\tau}\right)\frac{\delta n_e}{n_{0e}} + \left(2 + \frac{Z}{\tau}\right)\frac{\delta B_\parallel}{B_0}\right], \quad (180)$$

where $F_M(v_\parallel) = (1/\sqrt{\pi} v_{thi}) \exp(-v_\parallel^2/v_{thi}^2)$ is a one-dimensional Maxwellian. This system can be diagonalized, so it splits into two decoupled equations

$$\frac{dG^\pm}{dt} + v_\parallel \hat{\mathbf{b}} \cdot \nabla G^\pm = \frac{v_\parallel F_M(v_\parallel)}{\Lambda^\pm} \hat{\mathbf{b}} \cdot \nabla \int_{-\infty}^{+\infty} dv_\parallel' \, G^\pm(v_\parallel'), \quad (181)$$

where

$$\Lambda^\pm = -\frac{\tau}{Z} + \frac{1}{\beta_i} \pm \sqrt{\left(1 + \frac{\tau}{Z}\right)^2 + \frac{1}{\beta_i^2}} \quad (182)$$

and we have introduced a new pair of functions

$$G^+ = G_B + \frac{1}{\sigma}\left(1 + \frac{Z}{\tau}\right)G_n, \quad G^- = G_n + \frac{1}{\sigma}\frac{\tau}{Z}\frac{2}{\beta_i}G_B, \quad (183)$$

where

$$\sigma = 1 + \frac{\tau}{Z} + \frac{1}{\beta_i} + \sqrt{\left(1 + \frac{\tau}{Z}\right)^2 + \frac{1}{\beta_i^2}}. \quad (184)$$

Equation (181) describes two decoupled kinetic cascades, which we will discuss in greater detail in §§ 6.2.3-6.2.5.

6.2.2. *Collisionless Damping*

Fluctuations described by Eq. (181) are subject to collisionless damping. Indeed, let us linearize Eq. (181), Fourier transform in time and space, divide through by $-i(\omega - k_\parallel v_\parallel)$, and integrate over $v_\parallel$. This gives the following dispersion relation (the "−" branch is for G^-, the "+" branch for G^+)

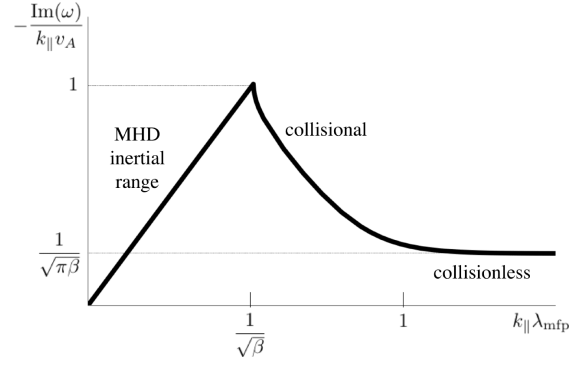$$\zeta_i Z(\zeta_i) = \Lambda^\pm - 1, \quad (185)$$

FIG. 6.— Schematic log-log plot (artist's impression) of the ratio of the damping rate of magnetic-field-strength fluctuations to the Alfvén frequency $k_\parallel v_A$ in the high-beta limit [see Eqs. (173) and (190)]. In Barnes et al. (2009), this plot is reproduced via a direct numerical solution of the linearized ion gyrokinetic equation with collisions.

where $\zeta_i = \omega/|k_\parallel|v_{thi} = \omega/|k_\parallel|v_A\sqrt{\beta_i}$ and we have used the plasma dispersion function (Fried & Conte 1961)

$$Z(\zeta_i) = \frac{1}{\sqrt{\pi}} \int_{-\infty}^\infty dx \frac{e^{-x^2}}{x - \zeta_i} \quad (186)$$

(the integration is along the Landau contour). This function is not to be confused with the ion charge parameter $Z = q_i/e$.

Formally, Eq. (185) has an infinite number of solutions. When $\beta_i \sim 1$, they are all strongly damped with damping rates $\text{Im}(\omega) \sim |k_\parallel|v_{thi} \sim |k_\parallel|v_A$, so the damping time is comparable to the characteristic timescale on which the Alfvén waves cause these fluctuations to cascade to smaller scales.

It is interesting to consider the high- and low-beta limits.

High-Beta Limit. — When $\beta_i \gg 1$, we have in Eq. (185)

$$\Lambda^- - 1 \simeq -2\left(1 + \frac{\tau}{Z}\right), \qquad G^- \simeq G_n, \quad (187)$$

$$\Lambda^+ - 1 \simeq \frac{1}{\beta_i}, \qquad G^+ \simeq G_B + \frac{1}{2}\frac{Z}{\tau}G_n. \quad (188)$$

The "−" branch corresponds to the density fluctuations. The solution of Eq. (185) has $\text{Im}(\zeta_i) \sim 1$, so these fluctuations are strongly damped:

$$\omega \sim -i|k_\parallel|v_A\sqrt{\beta_i}. \quad (189)$$

The damping rate is much greater than the Alfvénic rate $k_\parallel v_A$ of the nonlinear cascade. In contrast, for the "+" branch, the damping rate is small: it can be obtained by expanding $Z(\zeta_i) = i\sqrt{\pi} + O(\zeta_i)$, which gives[25]

$$\omega = -i\frac{|k_\parallel|v_{thi}}{\sqrt{\pi}\beta_i} = -i\frac{|k_\parallel|v_A}{\sqrt{\pi\beta_i}}. \quad (190)$$

Since G_n is strongly damped, Eq. (188) implies $G^+ \simeq G_B$, i.e., the fluctuations that are damped at the rate (190) are predominantly of the magnetic-field strength. The damping rate is a

[25] This is the gyrokinetic limit ($k_\parallel/k_\perp \ll 1$) of the more general damping effect known in astrophysics as the Barnes (1966) damping and in plasma physics as transit-time damping. We remind the reader that our approach was to carry out the gyrokinetic expansion (in small $k_\parallel/k_\perp$) first, and then take the high-beta limit as a subsidiary expansion. A more standard approach in the linear theory of plasma waves is to take the limit of high β_i while treating $k_\parallel/k_\perp$ as an arbitrary quantity. A detailed calculation of the damping rates done in this way can be found in Foote & Kulsrud (1979).

constant (independent of $k_\parallel$) small fraction $\sim 1/\sqrt{\beta_i}$ of the Alfvénic cascade rate.

In Fig. 6, we give a schematic plot of the damping rate of the magnetic-field-strength fluctuations (slow waves) connecting the fluid and kinetic limits for $\beta_i \gg 1$.

Low-Beta Limit. — When $\beta_i \ll 1$, we have

$$\Lambda^- - 1 \simeq -\left(1 + \frac{\tau}{Z}\right), \qquad G^- \simeq G_n + \frac{\tau}{Z} G_B, \qquad (191)$$

$$\Lambda^+ - 1 \simeq \frac{2}{\beta_i}, \qquad\qquad G^+ \simeq G_B. \qquad (192)$$

For the "−" branch, we again have $\text{Im}(\zeta_i) \sim 1$, so

$$\omega \sim -i|k_\parallel|v_A\sqrt{\beta_i}, \qquad (193)$$

which now is much smaller than the Alfvénic cascade rate $k_\parallel v_A$. For the "+" branch (predominantly the field-strength fluctuations), we seek a solution with $\zeta = -i\tilde{\zeta}_i$ and $\tilde{\zeta}_i \gg 1$. Then Eq. (185) becomes $\zeta_i Z(\zeta_i) \simeq 2\sqrt{\pi}\,\tilde{\zeta}_i \exp(\tilde{\zeta}_i) = 2/\beta_i$. Up to logarithmically small corrections, this gives $\tilde{\zeta}_i \simeq \sqrt{|\ln \beta_i|}$, whence

$$\omega \sim -i|k_\parallel|v_A\sqrt{\beta_i|\ln \beta_i|}. \qquad (194)$$

While this damping rate is slightly greater than that of the "−" branch, it is still much smaller than the Alfvénic cascade rate.

6.2.3. *Collisionless Invariants*

Equation (181) obeys a conservation law, which is very easy to derive. Multiplying Eq. (181) by $G^\pm/F_M$ and integrating over space and velocities and performing integration by parts in the right-hand side, we get

$$\frac{d}{dt} \int d^3\mathbf{r} \int dv_\parallel \frac{(G^\pm)^2}{2F_M}$$
$$= -\frac{1}{\Lambda^\pm} \int d^3\mathbf{r} \left(\int dv_\parallel G^\pm\right) \hat{\mathbf{b}} \cdot \nabla \int dv_\parallel v_\parallel G^\pm. \quad (195)$$

On the other hand, integrating Eq. (181) over $v_\parallel$ gives

$$\frac{d}{dt} \int dv_\parallel G^\pm = -\hat{\mathbf{b}} \cdot \nabla \int dv_\parallel v_\parallel G^\pm. \qquad (196)$$

Using this to express the right-hand side of Eq. (195) as a full time derivative, we find

$$\frac{dW_{\text{compr}}^\pm}{dt} = 0, \qquad (197)$$

where the two invariants are

$$W_{\text{compr}}^\pm = \int d^3\mathbf{r} \frac{n_{0i}T_{0i}}{2} \left[\int dv_\parallel \frac{(G^\pm)^2}{F_M} - \frac{1}{\Lambda^\pm} \left(\int dv_\parallel G^\pm\right)^2 \right]. \qquad (198)$$

It is useful (and always possible) to split

$$G^\pm = F_M \int dv_\parallel G^\pm + \tilde{G}^\pm, \qquad (199)$$

where $\int dv_\parallel \tilde{G}^\pm = 0$ by construction. Then

$$W_{\text{compr}}^\pm = \int d^3\mathbf{r} \frac{n_{0i}T_{0i}}{2} \left[\int dv_\parallel \frac{(\tilde{G}^\pm)^2}{F_M} \right.$$
$$\left. + \left(1 - \frac{1}{\Lambda^\pm}\right) \left(\int dv_\parallel G^\pm\right)^2 \right]. \qquad (200)$$

Written in this form, the two invariants $W_{\text{compr}}^\pm$ are manifestly positive definite quantities because $\Lambda^+ > 1$ and $\Lambda^- < 0$. The invariants regulate the two decoupled kinetic cascades of compressive fluctuations in the collisionless regime. The collisionless damping derived in § 6.2.2 leads to exponential decay of the density and field-strength fluctuations, or, equivalently, of $\int dv_\parallel G^\pm$, while conserving $W_{\text{compr}}^\pm$. This means that the damping is merely a redistribution of the conserved quantity $W_{\text{compr}}^\pm$: the first term in Eq. (200) grows to compensate for the decay of the second.

6.2.4. *Linear Parallel Phase Mixing*

In dynamical terms, how does the kinetic system Eq. (181) arrange for the integral of the distribution function $G^\pm(v_\parallel)$ to decay while allowing its norm to grow? This is a very well known phenomenon of (linear) phase mixing (Landau 1946; Hammett et al. 1991; Krommes & Hu 1994; Krommes 1999; Watanabe & Sugama 2004). To put it in simple terms, the solution of the linearized Eq. (181) consists of the inhomogeneous part, which contains the collisionless damping and the homogeneous part (solution of the left-hand side = 0) given by $G^\pm \propto e^{-ik_\parallel v_\parallel t}$, the so-called ballistic response (this is also the nonlinear solution if t and $k_\parallel$ are interpreted as Lagrangian variables in the frame of the Alfvén waves; see § 6.3). As time goes on, this part of the solution becomes increasingly oscillatory in $v_\parallel$, so its velocity integral tends to zero, while its amplitude does not decay. It is such ballistic contributions that make up the $\tilde{G}^\pm$ term in Eq. (200).

As the velocity gradient of $\tilde{G}^\pm$ increases with time, $\partial \tilde{G}^\pm/\partial v_\parallel \sim k_\parallel t G^\pm$, at some point it can become sufficiently large to activate the collision integral [the right-hand side of Eq. (157)], which has so far been neglected. This way the collisionless damping of compressive fluctuations can be turned into ion heating—a simple example of a more general principle of how electromagnetic fluctuation energy is transferred into heat via the entropy part of the generalized energy (§ 3.5). Indeed, we will prove in § 6.2.5 that the invariants $W_{\text{compr}}^\pm$ are constituent parts of the overall generalized energy functional for the compressive fluctuations, so their cascade to small scales in phase space is part of the overall kinetic cascade introduced in § 3.4.

It is not entirely clear how efficient is the parallel-phase-mixing route to ion heating and, therefore, whether the collisionlessly damped energy of compressive fluctuations ends up in the ion heat or rather reaches the ion gyroscale and couples back to the Alfvénic component of the turbulence (§ 7.1). The answer to this question will depend on whether compressive fluctuations can develop large $k_\parallel$—a non-trivial issue further discussed in § 6.3.

6.2.5. *Generalized Energy: Three Collisionless Cascades*

We will now show how the generalized energy for compressive fluctuations in the collisionless regime incorporates the two invariants derived in § 6.2.3.

Rewriting the compressive part of the KRMHD generalized energy [Eq. (153)] in terms of the function g [see Eq. (149)], we get

$$W_{\text{compr}} = \frac{n_{0i}T_{0i}}{2} \int d^3\mathbf{r} \left\{ \frac{1}{n_{0i}} \int d^3\mathbf{v} \frac{g^2}{F_{0i}} \right.$$
$$\left. + \frac{Z}{\tau} \left(\frac{\delta n_e}{n_{0e}} - \frac{\delta B_\parallel}{B_0}\right)^2 - \left[\frac{Z}{\tau} + 2\left(1 + \frac{1}{\beta_i}\right)\right] \frac{\delta B_\parallel^2}{B_0^2} \right\}. \qquad (201)$$

Using Eqs. (178) and (183), we can express δn_e and $\delta B_\parallel$ in terms of $\int dv_\parallel G^\pm$ as follows

$$\frac{\delta n_e}{n_{0e}} = \frac{1}{\kappa}\left(\sigma\int dv_\parallel G^- - \frac{\tau}{Z}\frac{2}{\beta_i}\int dv_\parallel G^+\right), \qquad (202)$$

$$\frac{\delta B_\parallel}{B_0} = \frac{1}{\kappa}\left[\sigma\int dv_\parallel G^+ - \left(1+\frac{Z}{\tau}\right)\int dv_\parallel G^-\right], \quad (203)$$

where σ was defined in Eq. (184) and

$$\kappa = \sqrt{\left(1+\frac{\tau}{Z}\right)^2 + \frac{1}{\beta_i^2}}. \qquad (204)$$

In order to express g in terms of $G^\pm$, we have to reconstruct the $v_\perp$ dependence of g, which we integrated out at the beginning of § 6.2.1.

Let us represent the distribution function as follows

$$g = \frac{n_{0i}}{\pi v_{\text{th}i}^2}e^{-x}\hat{g}(x,v_\parallel), \quad \hat{g}(x,v_\parallel) = \sum_{l=0}^\infty L_l(x)G_l(v_\parallel), \ (205)$$

where $x = v_\perp^2/v_{\text{th}i}^2$ and we have expanded $\hat{g}$ in Laguerre polynomials $L_l(x) = (e^x/l!)(d^l/dx^l)x^le^{-x}$. Since Laguerre polynomials are orthogonal, the first term in Eq. (201) splits into a sum of "energies" associated with the expansion coefficients:

$$\frac{1}{n_{0i}}\int d^3\mathbf{v}\frac{g^2}{F_{0i}} = \sum_{l=0}^\infty \int dv_\parallel \frac{G_l^2}{F_M}. \qquad (206)$$

The expansion coefficients are determined via the Laguerre transform:

$$G_l(v_\parallel) = \int_0^\infty dx\, e^{-x}L_l(x)\hat{g}(x,v_\parallel). \qquad (207)$$

As $L_0 = 1$ and $L_1 = 1-x$, it is easy to see that δn_e and $\delta B_\parallel$ can be expressed as linear combinations of $\int dv_\parallel G_0$ and $\int dv_\parallel G_1$ [see Eqs. (176-178)]. Using Eqs. (176), (177), and (183), we can show that

$$G_0 = -\frac{1}{\kappa}\left[\left(\sigma-\frac{2}{\beta_i}\right)\Lambda^+G^+ + \frac{Z}{\tau}\left(\sigma-1-\frac{\tau}{Z}\right)\Lambda^-G^-\right], \ (208)$$

$$G_1 = \frac{1}{\kappa}\left[\sigma\Lambda^+G^+ - \left(1+\frac{Z}{\tau}\right)\Lambda^-G^-\right], \qquad (209)$$

where $G^\pm$ satisfy Eq. (181). As follows from Eq. (157) (neglecting the collision integral), all higher-order expansion coefficients satisfy a simple homogeneous equation:

$$\frac{dG_l}{dt} + v_\parallel\hat{\mathbf{b}}\cdot\nabla G_l = 0, \quad l > 1. \qquad (210)$$

Thus, the distribution function can be explicitly written in terms of $G^\pm$:

$$g = \left[G_0(v_\parallel) + \left(1-\frac{v_\perp^2}{v_{\text{th}i}^2}\right)G_1(v_\parallel)\right]\frac{n_{0i}}{\pi v_{\text{th}i}^2}e^{-v_\perp^2/v_{\text{th}i}^2} + \tilde{g}, \ (211)$$

where G_0 and G_1 are given by Eqs. (208-209) and $\tilde{g}$ comprises the rest of the Laguerre expansion (all G_l with $l > 1$), i.e., it is the homogeneous solution of Eq. (157) that does not contribute to either density or magnetic-field strength:

$$\frac{d\tilde{g}}{dt} + v_\parallel\hat{\mathbf{b}}\cdot\nabla\tilde{g} = 0, \quad \int d^3\mathbf{v}\,\tilde{g} = 0, \quad \int d^3\mathbf{v}\frac{v_\perp^2}{v_{\text{th}i}^2}\tilde{g} = 0. \ (212)$$

Now substituting Eqs. (208) and (209) into Eq. (206) and then substituting the result and Eqs. (202-203) into Eq. (201), we find after some straightforward manipulations

$$W_{\text{compr}} = \int d^3\mathbf{r}\int d^3\mathbf{v}\frac{T_{0i}\tilde{g}^2}{2F_{0i}}$$
$$+ 4\left[1+\frac{1}{\kappa}\left(1+\frac{\tau}{Z}\right)\right](\Lambda^+)^2W_{\text{compr}}^+$$
$$+ 2\frac{Z^2}{\tau^2}\left(1+\frac{1}{\kappa}\frac{1}{\beta_i}\right)(\Lambda^-)^2W_{\text{compr}}^-, \qquad (213)$$

where κ is defined by Eq. (204) and $W_{\text{compr}}^\pm$ are the two independent invariants that we derived in § 6.2.3. Thus, the generalized energy for compressive fluctuations splits into three independently cascading parts: $W_{\text{compr}}^\pm$ associated with the density and magnetic-field-strength fluctuations and a purely kinetic part given by the first term in Eq. (213) (see Fig. 5). The dynamical evolution of this purely kinetic component is described by Eq. (212)—it is a passively mixed, undamped ballistic-type mode.

All three cascade channels lead to small perpendicular spatial scales via passive mixing by the Alfvénic turbulence and also to small scales in $v_\parallel$ via the parallel phase mixing process discussed in § 6.2.4 (note that $\tilde{g}$ is subject to this process as well).

6.3. *Parallel and Perpendicular Cascades*

Let us return to the kinetic equation (157) and transform it to the Lagrangian frame associated with the velocity field $\mathbf{u}_\perp = \hat{\mathbf{z}}\times\nabla_\perp\Phi$ of the Alfvén waves: $(t,\mathbf{r}) \to (t,\mathbf{r}_0)$, where

$$\mathbf{r}(t,\mathbf{r}_0) = \mathbf{r}_0 + \int_0^t dt'\,\mathbf{u}_\perp(t',\mathbf{r}(t',\mathbf{r}_0)). \qquad (214)$$

In this frame, the convective derivative d/dt defined in Eq. (160) turns into $\partial/\partial t$, while the parallel spatial gradient $\hat{\mathbf{b}}\cdot\nabla$ can be calculated by employing the Cauchy solution for the perturbed magnetic field $\delta\mathbf{B}_\perp = \hat{\mathbf{z}}\times\nabla_\perp\Psi$:

$$\hat{\mathbf{b}}(t,\mathbf{r}) = \hat{\mathbf{z}} + \frac{\delta\mathbf{B}_\perp(t,\mathbf{r})}{B_0} = \hat{\mathbf{b}}(0,\mathbf{r}_0)\cdot\nabla_0\mathbf{r}, \qquad (215)$$

where $\mathbf{r}$ is given by Eq. (214) and $\nabla_0 = \partial/\partial\mathbf{r}_0$. Then

$$\hat{\mathbf{b}}\cdot\nabla = \hat{\mathbf{b}}(0,\mathbf{r}_0)\cdot\left(\nabla_0\mathbf{r}\right)\cdot\nabla = \hat{\mathbf{b}}(0,\mathbf{r}_0)\cdot\nabla_0 = \frac{\partial}{\partial s_0}, \ (216)$$

where s_0 is the arc length along the perturbed magnetic field taken at $t = 0$ [if $\delta\mathbf{B}_\perp(0,\mathbf{r}_0) = 0$, $s_0 = z_0$]. Thus, in the Lagrangian frame associated with the Alfvénic component of the turbulence, Eq. (157) is linear. This means that, if the effect of finite ion gyroradius is neglected, the KRMHD system does not give rise to a cascade of density and magnetic-field-strength fluctuations to smaller scales along the moving (perturbed) field lines, i.e., $\hat{\mathbf{b}}\cdot\nabla\delta n_e$ and $\hat{\mathbf{b}}\cdot\nabla\delta B_\parallel$ do not increase. In contrast, there is a perpendicular cascade (cascade in $k_\perp$): the perpendicular wandering of field lines due to the Alfvénic turbulence causes passive mixing of δn_e and $\delta B_\parallel$ in the direction transverse to the magnetic field (see § 2.6 for a quick recapitulation of the standard scaling argument on the passive cascade that leads to a $k_\perp^{-5/3}$ in the perpendicular di-
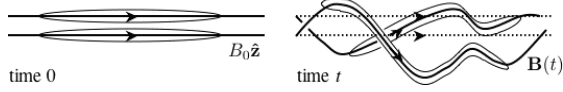
FIG. 7.— Lagrangian mixing of passive fields: fluctuations develop small scales across, but not along the exact field lines.

rection). Figure 7 illustrates this situation.[26]

We emphasize that this lack of nonlinear refinement of the scale of δn_e and $\delta B_\parallel$ along the moving field lines is a particular property of the compressive component of the turbulence, not shared by the Alfvén waves. Indeed, unlike Eq. (157), the RMHD equations (155-156), do not reduce to a linear form under the Lagrangian transformation (214), so the Alfvén waves should develop small scales both across and along the perturbed magnetic field.

Whether the density and magnetic-field-strength fluctuations develop small scales along the magnetic field has direct physical and observational consequences. Damping of these fluctuations, both in the collisional and collisionless regimes, discussed in §6.1.2 and §6.2.2, respectively, depends precisely on their scale along the perturbed field: indeed, the linear results derived there are exact in the Lagrangian frame (214). To summarize these results, the damping rate of δn_e and $\delta B_\parallel$ at $\beta_i \sim 1$ is

$$\gamma \sim v_{\mathrm{th}i}\lambda_{\mathrm{mfp}i}k_{\parallel 0}^2, \qquad k_{\parallel 0}\lambda_{\mathrm{mfp}i} \ll 1, \qquad (217)$$

$$\gamma \sim v_{\mathrm{th}i}k_{\parallel 0}, \qquad k_{\parallel 0}\lambda_{\mathrm{mfp}i} \gg 1, \qquad (218)$$

where $k_{\parallel 0} \sim \hat{\mathbf{b}}\cdot\nabla$ is the wavenumber along the perturbed field (i.e., if there is no parallel cascade, the wavenumber of the large-scale stirring).

Whether this damping cuts off the cascades of δn_e and $\delta B_\parallel$ depends on the relative magnitudes of the damping rate γ for a given $k_\perp$ and the characteristic rate at which the Alfvén waves cause δn_e and $\delta B_\parallel$ to cascade to higher $k_\perp$. This rate is $\omega_A \sim k_{\parallel A}v_A$, where $k_{\parallel A}$ is the parallel wave number of the Alfvén waves that have the same $k_\perp$. Since the Alfvén waves do have a parallel cascade, assuming scale-by-scale critical balance (3) leads to [Eq. (5)]

$$k_{\parallel A} \sim k_\perp^{2/3}l_0^{-1/3}. \qquad (219)$$

If, in contrast to the Alfvén waves, δn_e and $\delta B_\parallel$ have no parallel cascade, $k_{\parallel 0}$ does not grow with $k_\perp$, so, for large enough $k_\perp$, $k_{\parallel 0} \ll k_{\parallel A}$ and $\gamma \ll \omega_A$. This means that, despite the damping, the density and field-strength fluctuations should have perpendicular cascades extending to the ion gyroscale.

The validity of the argument at the beginning of this section that ruled out the parallel cascade of δn_e and $\delta B_\parallel$ is not quite as obvious as it might appear. Lithwick & Goldreich (2001) argued that the dissipation of δn_e and $\delta B_\parallel$ at the ion gyroscale would cause these fluctuations to become uncorrelated at the same parallel scales as the Alfvénic fluctuations by which they are mixed, i.e., $k_{\parallel 0} \sim k_{\parallel A}$. The damping rate then becomes comparable to the cascade rate, cutting off the cascades of density and field-strength fluctuations at $k_\parallel\lambda_{\mathrm{mfp}i} \sim 1$. The corresponding perpendicular cutoff wavenumber is [see

[26] Note that effectively, there is also a cascade in $k_\parallel$ if the latter is measured along the unperturbed field—more precisely, a cascade in k_z. This is due to the perpendicular deformation of the perturbed magnetic field by the Alfvén-wave turbulence: since $\nabla_\perp$ grows while $\hat{\mathbf{b}}\cdot\nabla$ remains the same, we have from Eq. (123) $\partial/\partial z \simeq -(\delta\mathbf{B}_\perp/B_0)\cdot\nabla_\perp$.

Eq. (219)]

$$k_\perp \sim l_0^{1/2}\lambda_{\mathrm{mfp}i}^{-3/2}. \qquad (220)$$

Asymptotically speaking, in a weakly collisional plasma, this cutoff is far above the ion gyroscale, $k_\perp\rho_i \ll 1$. However, the relatively small value of $\lambda_{\mathrm{mfp}i}$ in the warm ISM, which was the main focus of Lithwick & Goldreich 2001, meant that the numerical value of the perpendicular cutoff scale given by Eq. (220) was, in fact, quite close both to the ion gyroscale (see Table 1) and to the observational estimates for the inner scale of the electron-density fluctuations in the ISM (Spangler & Gwinn 1990; Armstrong et al. 1995). Thus, it was not possible to tell whether Eq. (220), rather than $k_\perp \sim \rho_i^{-1}$, represented the correct prediction.

The situation is rather different in the nearly collisionless case of the solar wind, where the cutoff given by Eq. (220) would mean that very little density or field-strength fluctuations should be detected above the ion gyroscale. Observations do not support such a conclusion: the density fluctuations appear to follow a $k^{-5/3}$ law at all scales larger than a few times ρ_i (Lovelace et al. 1970; Woo & Armstrong 1979; Celnikier et al. 1983, 1987; Coles & Harmon 1989; Marsch & Tu 1990b; Coles et al. 1991), consistently with the expected behavior of an undamped passive scalar field (see §2.6). An extended range of $k^{-5/3}$ scaling above the ion gyroscale is also observed for the fluctuations of the magnetic-field strength (Marsch & Tu 1990b; Bershadskii & Sreenivasan 2004; Hnat et al. 2005; Alexandrova et al. 2008a).

These observational facts suggest that the cutoff formula (220) does not apply. This does not, however, conclusively vitiate the Lithwick & Goldreich (2001) theory. Heuristically, their argument is plausible, although it is, perhaps, useful to note that in order for the effect of the perpendicular dissipation terms, not present in the KRMHD equations (157-159), to be felt, the density and field-strength fluctuations should reach the ion gyroscale in the first place. Quantitatively, the failure of the compressive fluctuations in the solar wind to be damped could still be consistent with the Lithwick & Goldreich (2001) theory because of the relative weakness of the collisionless damping, especially at low beta (§6.2.2)—the explanation they themselves favor. The way to check observationally whether this explanation suffices would be to make a comparative study of the compressive fluctuations for solar-wind data with different values of β_i. If the strength of the damping is the decisive factor, one should always see cascades of both δn_e and $\delta B_\parallel$ at low β_i, no cascades at $\beta_i \sim 1$, and a cascade of $\delta B_\parallel$ but not δn_e at high β_i (in this limit, the damping of the density fluctuations is strong, of the field-strength weak; see §6.2.2). If, on the other hand, the parallel cascade of the compressive fluctuations is intrinsically inefficient, very little β_i dependence is expected and a perpendicular cascade should be seen in all cases.

Obviously, an even more direct observational (or numerical) test would be the detection or non-detection of near-perfect alignment of the density and field-strength structures with the moving field lines (*not* with the mean magnetic field—see footnote 26), but it is not clear how to measure this reliably. It is interesting, in this context, that in near-the-Sun measurements, the density fluctuations are reported to have the form of highly anisotropic filaments aligned with the magnetic field (Armstrong et al. 1990; Grall et al. 1997; Woo & Habbal 1997). Another intriguing piece of observa-

tional evidence is the discovery that the local structure of the magnetic-field-strength and density fluctuations at 1 AU is, in a certain sense, correlated with the solar cycle (Kiyani et al. 2007; Hnat et al. 2007; Wicks et al. 2009)—this suggests a dependence on initial conditions that is absent in the Alfvénic fluctuations and that presumably should also disappear in the compressive fluctuations if the latter are fully mixed both in the perpendicular and parallel directions.

7. TURBULENCE IN THE DISSIPATION RANGE: ELECTRON RMHD AND THE ENTROPY CASCADE

7.1. *Transition at the Ion Gyroscale*

The validity of the theory discussed in § 5 and § 6 breaks down when $k_\perp \rho_i \sim 1$. As the ion gyroscale is approached, the Alfvén waves are no longer decoupled from the rest of the plasma dynamics. All modes now contain perturbations of density and magnetic-field strength and can be collisionlessly damped. Because of the low-frequency nature of the Alfvén-wave cascade, $\omega \ll \Omega_i$ even at $k_\perp \rho_i \sim 1$ [Eq. (46)], so the ion cyclotron resonance ($\omega - k_\parallel v_\parallel = \pm \Omega_i$) is not important, while the Landau one ($\omega = k_\parallel v_\parallel$) is. The linear theory of this collisionless damping in the gyrokinetic approximation is worked out in detail in Howes et al. (2006) (see also Gary & Borovsky 2008). Figure 8 shows the solutions of their dispersion relation that illustrate how the Alfvén wave becomes a dispersive *kinetic Alfvén wave (KAW)* (see § 7.3) and collisionless damping becomes important as the ion gyroscale is reached.

We stress that this transition occurs at the ion gyroscale, not at the ion inertial scale $d_i = \rho_i/\sqrt{\beta_i}$ (except in the limit of cold ions, $\tau = T_{0i}/T_{0e} \ll 1$; see Appendix E). This statement is true even when β_i is not order unity, as illustrated in Fig. 8: for the three cases plotted there, $k_\perp d_i = 1$ corresponds to $k_\perp \rho_i = 0.1$, 1 and 10 for $\beta_i = 0.01$, 1 and 100, respectively, but there is no trace of the ion inertial scale in the solutions of the linear dispersion relation. Nonlinearly, in the limit $\beta_i \ll 1$, we may consider the scales $k_\perp d_i \sim 1$ and expand the gyrokinetics in $k_\perp \rho_i = k_\perp d_i \sqrt{\beta_i} \ll 1$ in a way similar to how it was done in § 5 and obtain precisely the same results: Alfvénic fluctuations described by the RMHD equations and compressive fluctuations passively advected by them and satisfying the reduced kinetic equation derived in § 5.5. Thus, even though $d_i \gg \rho_i$ at low beta, there is no change in the nature of the turbulent cascade until $k_\perp \rho_i \sim 1$ is reached.

The nonlinear theory of what happens at $k_\perp \rho_i \sim 1$ is very poorly understood. It is, however, possible to make progress by examining what kind of fluctuations emerge on the other side of the transition, at $k_\perp \rho_i \gg 1$. As we will demonstrate below, it turns out that another turbulent cascade—this time of KAW—is possible in this so-called *dissipation range*. It can transfer the energy of KAW-like fluctuations down to the electron gyroscale, where electron Landau damping becomes important (see Howes et al. 2006). Some observational evidence of KAW is, indeed, available in the solar wind and the magnetosphere (Bale et al. 2005; Grison et al. 2005, see further discussion in § 8.2.4). Below we derive the equations that describe KAW-like fluctuations in the scale range $k_\perp \rho_i \gg 1$, $k_\perp \rho_e \ll 1$ (§ 7.2) and work out a Kolmogorov-style scaling theory for this cascade (§ 7.5).

Because of the presence of the collisionless damping at the ion gyroscale, only a certain fraction of the turbulent power arriving there from the inertial range is converted into the KAW cascade, while the rest is Landau-damped. The damping leads to the heating of the ions, but the process of deposit-

ing the collisionlessly damped fluctuation energy into the ion heat is non-trivial because, as we explained in § 3.5, collisions do need to play a role in order for true heating to occur. As we explained in § 3.5 and will see specifically for the dissipation range in § 7.8, the electromagnetic-fluctuation energy does not disappear as a result of the Landau damping but is converted into ion entropy fluctuations, while the generalized energy is conserved. Collisions are then accessed and ion heating achieved via a purely kinetic phenomenon: the ion entropy cascade in phase space (nonlinear phase mixing), for which a theory is developed in § 7.9 and § 7.10. A similar process of conversion of the KAW energy into electron entropy fluctuations and then electron heat is treated in § 7.12.

Figure 5 illustrates the routes energy takes from the ion gyroscale towards heating. Crucially, it is at $k_\perp \rho_i \sim 1$ that it is decided how much energy would eventually go into the ions and how much into electrons.[27] How this distribution of energy depends on plasma parameters (β_i and T_{0i}/T_{0e}) is an open theoretical question[28] of considerable astrophysical interest: e.g., the efficiency of ion heating is a key unknown in the theory of advection-dominated accretion flows (Quataert & Gruzinov 1999, see discussion in § 8.5) and of the solar corona (e.g., Cranmer & van Ballegooijen 2003); we will also see in § 7.11 that it may determine the form of the observed dissipation-range spectra in space plasmas.

A short summary of this section is given in § 7.14.

7.2. *Equations of Electron Reduced MHD*

The derivation is straightforward: when $a_i \sim k_\perp \rho_i \gg 1$, all Bessel functions in Eqs. (118-120) are small, so the integrals of the ion distribution function vanish and Eqs. (118-120) become

$$\frac{\delta n_e}{n_{0e}} = -\frac{Ze\varphi}{T_{0i}} = -\frac{2}{\sqrt{\beta_i}}\frac{\Phi}{\rho_i v_A},\tag{221}$$

$$u_{\parallel e} = \frac{c}{4\pi e n_{0e}}\nabla_\perp^2 A_\parallel = -\frac{\rho_i \nabla_\perp^2 \Psi}{\sqrt{\beta_i}}, \qquad u_{\parallel i} = 0,\tag{222}$$

$$\frac{\delta B_\parallel}{B_0} = \frac{\beta_i}{2}\left(1 + \frac{Z}{\tau}\right)\frac{Ze\varphi}{T_{0i}} = \sqrt{\beta_i}\left(1 + \frac{Z}{\tau}\right)\frac{\Phi}{\rho_i v_A},\tag{223}$$

where we used the definitions (135) of the stream and flux functions Φ and Ψ.

These equations are a reflection of the fact that, for $k_\perp \rho_i \gg 1$, the ion response is effectively purely Boltzmann, with the gyrokinetic part h_i contributing nothing to the fields or flows [see Eq. (54) with h_i omitted; h_i does, however, play an important role in the energy balance and ion heating, as explained in §§ 7.8-7.10 below]. The Boltzmann response for ion density is expressed by Eq. (221). Equation (222) states that the parallel ion flow velocity can be neglected. Finally, Eq. (223) expresses the pressure balance for Boltzmann (and, therefore, isothermal) electrons [Eq. (103)] and ions: if we write

$$\frac{B_0 \delta B_\parallel}{4\pi} = -\delta p_i - \delta p_e = -T_{0i}\delta n_i - T_{0e}\delta n_e,\tag{224}$$

---

[27] Some of the energy of compressive fluctuations may go into ion heat via collisional (§ 6.1.2) or collisionless (§ 6.2.2) damping of these fluctuations in the inertial range. Whether this is a significant ion heating mechanism depends on the efficiency of the parallel cascade (see § 6.2.4 and § 6.3).

[28] How much energy is converted into ion entropy fluctuations in the process of a *nonlinear* turbulent cascade is not necessarily directly related to the strength of the *linear* collisionless damping.
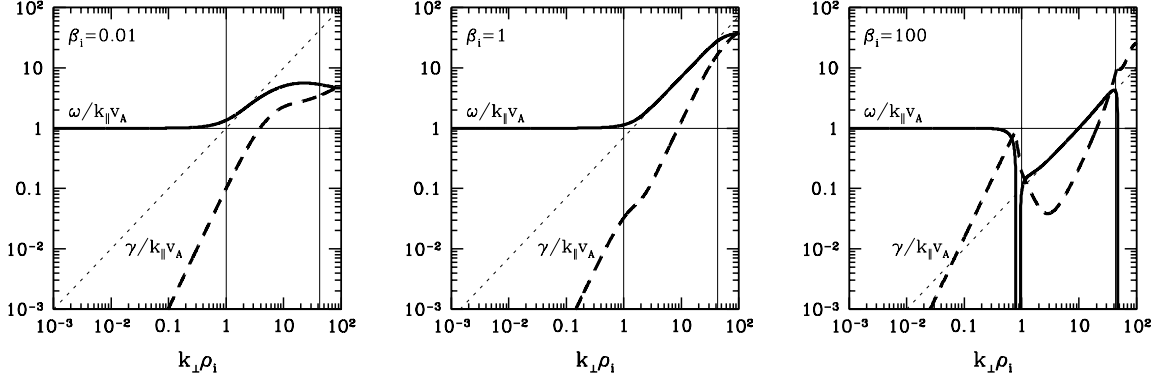
FIG. 8.— Numerical solutions of the linear gyrokinetic dispersion relation (for a detailed treatment of the linear theory, see Howes et al. 2006) showing the transition from the Alfvén wave to KAW between the inertial range ($k_\perp \rho_i \ll 1$) and the dissipation range ($k_\perp \rho_i \gtrsim 1$). We show three cases: low beta ($\beta_i = 0.01$), $\beta_i = 1$, and high beta ($\beta_i = 100$). In all three cases, $\tau = 1$ and $Z = 1$. Bold solid lines show the real frequency ω, bold dashed lines the damping rate γ, both normalized by $k_\parallel v_A$ (in gyrokinetics, $\omega/k_\parallel v_A$ and $\gamma/k_\parallel v_A$ are functions of $k_\perp$ only). Dotted lines show the asymptotic KAW solution (230). Horizontal solid line shows the Alfvén wave $\omega = k_\parallel v_A$. Vertical solid lines show $k_\perp \rho_i = 1$ and $k_\perp \rho_e = 1$. Note that the damping can be considered strong if the characteristic decay time is comparable or shorter than the wave period, i.e., $\gamma/\omega \gtrsim 1/2\pi$. Thus, in these plots, the damping at $k_\perp \rho_i \sim 1$ is relatively weak for $\beta_i = 1$, relatively strong for low beta and very strong for high beta.

it follows that

$$\frac{\delta B_\parallel}{B_0} = -\frac{\beta_i}{2}\left(1+\frac{Z}{\tau}\right)\frac{\delta n_e}{n_{0e}}, \tag{225}$$

which, combined with Eq. (221), gives Eq. (223). We remind the reader that the perpendicular Ampère's law, from which Eq. (223) was derived [Eq. (66) via Eq. (120)] is, in gyrokinetics, indeed equivalent to the statement of perpendicular pressure balance (see § 3.3).

Substituting Eqs. (221-223) into Eqs. (116-117), we obtain the following closed system of equations

$$\frac{\partial \Psi}{\partial t} = v_A\left(1+\frac{Z}{\tau}\right)\hat{\mathbf{b}}\cdot\nabla\Phi, \tag{226}$$

$$\frac{\partial \Phi}{\partial t} = -\frac{v_A}{2+\beta_i\left(1+Z/\tau\right)}\hat{\mathbf{b}}\cdot\nabla\left(\rho_i^2\nabla_\perp^2\Psi\right). \tag{227}$$

Note that, using Eq. (223), Eqs. (226) and (227) can be recast as two coupled evolution equations for the perpendicular and parallel components of the perturbed magnetic field, respectively [Eqs. (C10) in Appendix C.2].

We shall refer to Eqs. (226-227) as *Electron Reduced MHD (ERMHD)*. They are related to the Electron Magnetohydrodynamics (EMHD)—a fluid-like approximation that evolves the magnetic field only and arises if one assumes that the magnetic field is frozen into the electron flow velocity $\mathbf{u}_e$, while the ions are immobile, $\mathbf{u}_i = 0$ (Kingsep et al. 1990):

$$\frac{\partial \mathbf{B}}{\partial t} = -\frac{c}{4\pi e n_{0e}}\nabla\times\left[(\nabla\times\mathbf{B})\times\mathbf{B}\right]. \tag{228}$$

As explained in Appendix C.2, the result of applying the RMHD/gyrokinetic ordering (§ 2.1 and § 3.1) to Eq. (228), where $\mathbf{B} = B_0\hat{\mathbf{z}} + \delta\mathbf{B}$ and

$$\frac{\delta\mathbf{B}}{B_0} = \frac{1}{v_A}\hat{\mathbf{z}}\times\nabla_\perp\Psi + \hat{\mathbf{z}}\frac{\delta B_\parallel}{B_0}, \tag{229}$$

coincides with our Eqs. (226-227) in the effectively incompressible limits of $\beta_i \gg 1$ or $\beta_e = \beta_i Z/\tau \gg 1$. When betas are arbitrary, density fluctuations cannot be neglected compared to the magnetic-field-strength fluctuations [Eq. (225)] and give rise to perpendicular ion flows with $\nabla\cdot\mathbf{u}_i \neq 0$. Thus, our

ERMHD system constitutes the appropriate generalization of EMHD for low-frequency anisotropic fluctuations without the assumption of incompressibility.

A (more tenuous) relationship also exists between our ERMHD system and the so-called Hall MHD, which, like EMHD, is based on the magnetic field being frozen into the electron flow, but includes the ion motion via the standard MHD momentum equation [Eq. (8)]. Strictly speaking, Hall MHD can only be used in the limit of cold ions, $\tau = T_{0i}/T_{0e} \ll 1$ (see, e.g., Ito et al. 2004; Hirose et al. 2004, and Appendix E), in which case it can be shown to reduce to Eqs. (226-227) in the appropriate small-scale limit (Appendix E). Although $\tau \ll 1$ is not a natural assumption for most space and astrophysical plasmas, Hall MHD has, due to its simplicity, been a popular theoretical paradigm in the studies of space and astrophysical plasma turbulence (see § 8.2.6). We have therefore devoted Appendix E to showing how this approximation fits into the theoretical framework proposed here: namely, we derive the anisotropic low-frequency version of the Hall MHD approximation from gyrokinetics under the assumption $\tau \ll 1$ and discuss the role of the ion inertial and ion sound scales, which acquire physical significance in this limit. However, outside this Appendix, we assume $\tau \sim 1$ everywhere and shall not use Hall MHD.

The validity of the ERMHD equations as a model for plasma dynamics in the dissipation range is further discussed in § 7.6.

7.3. *Kinetic Alfvén Waves*

The linear modes supported by ERMHD are kinetic Alfvén waves (KAW) with frequencies

$$\omega_{\mathbf{k}} = \pm\sqrt{\frac{1+Z/\tau}{2+\beta_i\left(1+Z/\tau\right)}}\,k_\perp\rho_i k_\parallel v_A. \tag{230}$$

This dispersion relation is illustrated in Fig. 8: note that the transition from Alfvén waves to dispersive KAW always occurs at $k_\perp \rho_i \sim 1$, even when $\beta_i \ll 1$ or $\beta_i \gg 1$. In the latter case, there is a sharp frequency jump at the transition (accompanied by very strong ion Landau damping).

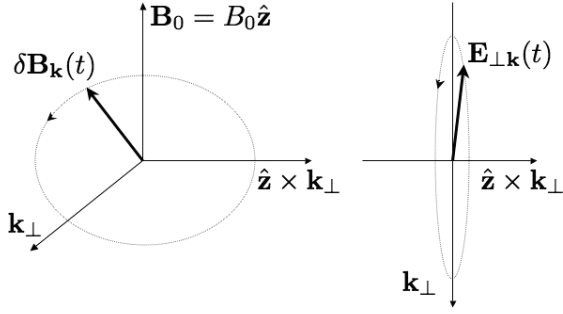The eigenfunctions corresponding to the two waves with

FIG. 9.— Polarization of the kinetic Alfvén wave, see Eqs. (232) and (233).

frequencies (230) are

$$\Theta_{\mathbf{k}}^{\pm} = \sqrt{\left(1+\frac{Z}{\tau}\right)\left[2+\beta_i\left(1+\frac{Z}{\tau}\right)\right]}\,\frac{\Phi_{\mathbf{k}}}{\rho_i} \mp k_\perp \Psi_{\mathbf{k}}. \quad (231)$$

Using Eqs. (229) and (223), the perturbed magnetic-field vector can be expressed as follows

$$\frac{\delta\mathbf{B}_{\mathbf{k}}}{B_0} = -i\hat{\mathbf{z}}\times\frac{\mathbf{k}_\perp}{k_\perp}\frac{\Theta_{\mathbf{k}}^+ - \Theta_{\mathbf{k}}^-}{2v_A} + \hat{\mathbf{z}}\sqrt{\frac{1+Z/\tau}{2+\beta_i\left(1+Z/\tau\right)}}\,\frac{\Theta_{\mathbf{k}}^+ + \Theta_{\mathbf{k}}^-}{2v_A},$$
$$(232)$$

so, for a single "+" or "−" wave (corresponding to $\Theta_{\mathbf{k}}^- = 0$ or $\Theta_{\mathbf{k}}^+ = 0$, respectively), $\delta\mathbf{B}_{\mathbf{k}}$ rotates in the plane perpendicular to the wave vector $\mathbf{k}_\perp$ clockwise with respect to the latter, while the wave propagates parallel or antiparallel to the guide field (Fig. 9).

The waves are elliptically right-hand polarized. Indeed, using Eq. (223), the perpendicular electric field is:

$$\mathbf{E}_{\perp\mathbf{k}} = -i\mathbf{k}_\perp\varphi + \frac{i\omega_{\mathbf{k}}}{c}\mathbf{A}_{\perp\mathbf{k}}$$
$$= \left[-i\mathbf{k}_\perp + \hat{\mathbf{z}}\times\mathbf{k}_\perp\frac{\omega_{\mathbf{k}}}{\Omega_i}\frac{\beta_i}{k_\perp^2\rho_i^2}\left(1+\frac{Z}{\tau}\right)\right]\varphi \quad (233)$$

(cf. Gary 1986; Hollweg 1999). The second term is small in the gyrokinetic expansion, so this is a very elongated ellipse (Fig. 9).

7.4. Finite-Amplitude Kinetic Alfvén Waves

As we are about to argue for a critically balanced KAW turbulence in a fashion analogous to the GS theory for the Alfvén waves (§ 1.2), it is a natural question to ask how similar the nonlinear properties of a putative KAW cascade will be to an Alfvén-wave cascade. As in the case of Alfvén waves, there are two counterpropagating linear modes [Eqs. (230) and (231)], and it turns out that certain superpositions of these modes (KAW packets) are also exact *nonlinear* solutions of Eqs. (226-227). Let us show that this is the case.

We might look for the nonlinear solutions of Eqs. (226-227) by requiring that the nonlinear terms vanish. Since $\hat{\mathbf{b}}\cdot\nabla = \partial/\partial z + (1/v_A)\{\Psi,\cdots\}$, this gives

$$\{\Psi,\Phi\} = 0 \quad \Rightarrow \quad \Psi = c_1\Phi, \quad (234)$$
$$\{\Psi,\rho_i^2\nabla_\perp^2\Psi\} = 0 \quad \Rightarrow \quad \rho_i^2\nabla_\perp^2\Psi = c_2\Psi, \quad (235)$$

where c_1 and c_2 are constants. Whether such solutions are possible is determined by substituting Eqs. (234) and (235) into Eqs. (226) and (227) and demanding that the two result-

ing *linear* equations be consistent with each other (both equations now just evolve Ψ). This is achieved if[29]

$$c_1^2 = -\frac{1}{c_2}\left(1+\frac{Z}{\tau}\right)\left[2+\beta_i\left(1+\frac{Z}{\tau}\right)\right], \quad (236)$$

so real solutions exist if $c_2 < 0$. In particular, wave packets consisting of KAW given by one of the linear eigenmodes (231) with an arbitrary shape in z but confined to a single shell $|\mathbf{k}_\perp| = k_\perp = $ const, satisfy Eqs. (234-236) with $c_2 = -k_\perp^2\rho_i^2$. This outcome is, in fact, only mildly non-trivial: in gyrokinetics, the Poisson bracket nonlinearity [Eq. (59)] vanishes for any monochromatic (in $\mathbf{k}_\perp$) mode because the Poisson bracket of two modes with wavenumbers $\mathbf{k}_\perp$ and $\mathbf{k}_\perp'$ is $\propto \hat{\mathbf{z}}\cdot(\mathbf{k}_\perp\times\mathbf{k}_\perp')$. Therefore, any monochromatic solution of the linearized equations is also an exact nonlinear solution. As we have shown above, a superposition of monochromatic KAW that have a fixed $k_\perp$, or, somewhat more generally, satisfy Eq. (235) with a fixed c_2, is still an exact solution.

Note that a similar procedure applied to the RMHD equations (17-18) returns the Elsasser solutions: perturbations of arbitrary shape that satisfy $\Phi = \pm\Psi$. The physical difference between these finite-amplitude Alfven-wave packets and the finite-amplitude KAW packets discussed above is that nonlinear interactions can occur not just between counterpropagating KAW but also between copropagating ones—a natural conclusion because KAW are dispersive (their group velocity along the guide field is $\propto v_A k_\perp\rho_i$), so copropagating waves with different $k_\perp$ can "catch up" with each other and interact.[30]

7.5. Scalings for KAW Turbulence

A scaling theory for the turbulence described by Eqs. (221-227) can be constructed along the same lines as the GS theory for the Alfvén-wave turbulence (§ 1.2). Namely, we shall assume that the turbulence below the ion gyroscale consists of KAW-like fluctuations with $k_\parallel \ll k_\perp$ (Quataert & Gruzinov 1999) and that the interactions between them are critically balanced (Cho & Lazarian 2004), i.e., that the propagation time and nonlinear interaction time are comparable at every scale. We stress that none of these assumptions are, strictly speaking, inevitable[31] (and, in fact, neither were they inevitable in the case of Alfvén waves). Since we have derived Eqs. (226-227) from gyrokinetics, the anisotropy of the fluctuations described by these equations is hard-wired, but it is not guaranteed that the actual physical cascade below the ion gyroscale is indeed anisotropic, although analysis of solar-wind measurements does seem to indicate that

---

[29] Formally speaking, c_1 and c_2 can depend on t and z. If this is allowed, we still recover Eq. (236), but in addition to it, we get the evolution equation $c_1\partial c_1/\partial t = v_A(1+Z/\tau)\partial c_1/\partial z$. This allows $c_1 = $ const, but there are, of course, other solutions. We shall not consider them here.

[30] The calculation above is analogous to the calculation by Mahajan & Krishan (2005) for incompressible Hall MHD (i.e., essentially, the high-β_e limit of the equations discussed in Appendix E), but the result is more general in the sense that it holds at arbitrary ion and electron betas. The Mahajan–Krishan solution in the EMHD limit amounts to noticing that Eq. (228) becomes linear for force-free (Beltrami) magnetic perturbations, $\nabla\times\delta\mathbf{B} = \lambda\delta\mathbf{B}$. Substituting Eq. (229) into this equation and using Eq. (223), we see that the force-free equation is equivalent to Eqs. (234-236) if $c_2 = -\lambda^2$ and the incompressible limit ($\beta_i \gg 1$ or $\beta_e = \beta_i Z/\tau \gg 1$) is taken.

[31] In fact, the EMHD turbulence was thought to be weak by several authors, who predicted a k^{-2} spectrum of magnetic energy assuming isotropy (Goldreich & Reisenegger 1992) or $k_\perp^{-5/2}$ for the anisotropic case (Voitenko 1998; Galtier & Bhattacharjee 2003; Galtier 2006).

at least a significant fraction of it is (see Leamon et al. 1998; Hamilton et al. 2008). Numerical simulations based on Eq. (228) (Biskamp et al. 1996, 1999; Ghosh et al. 1996; Ng et al. 2003; Cho & Lazarian 2004; Shaikh & Zank 2005) have revealed that the spectrum of magnetic fluctuations scales as $k_\perp^{-7/3}$, the outcome consistent with the assumptions stated above. Let us outline the argument that leads to this scaling.

First assume that the fluctuations are KAW-like and that Θ^+ and Θ^- [Eq. (231)] have similar scaling. This implies

$$\Psi_\lambda \sim \sqrt{1 + \beta_i} \frac{\lambda}{\rho_i} \Phi_\lambda \qquad (237)$$

(for the purposes of scaling arguments and order-of-magnitude estimates, we set $Z/\tau = 1$, but keep the β_i dependence so low- and high-beta limits could be recovered if necessary). The fact that fixed-$k_\perp$ KAW packets, which satisfy Eq. (237) with $\lambda = 1/k_\perp$, are exact nonlinear solutions of the ERMHD equations (§ 7.4) lends some credence to this assumption.

Assuming scale-space locality of interactions implies a constant-flux KAW cascade: analogously to Eq. (1),

$$\frac{(\Psi_\lambda/\lambda)^2}{\tau_{\mathrm{KAW}\lambda}} \sim \frac{(1+\beta_i)(\Phi_\lambda/\rho_i)^2}{\tau_{\mathrm{KAW}\lambda}} \sim \varepsilon_{\mathrm{KAW}} = \mathrm{const}, \quad (238)$$

where $\tau_{\mathrm{KAW}\lambda}$ is the cascade time and $\varepsilon_{\mathrm{KAW}}$ is the KAW energy flux proportional to the fraction of the total flux ε (or the total turbulent power $\overline{P_{\mathrm{ext}}}$; see § 3.4) that was converted into the KAW cascade at the ion gyroscale.

Using Eqs. (226-227) and Eq. (237), it is not hard to see that the characteristic nonlinear decorrelation time is λ^2/Φ_λ. If the turbulence is strong, then this time is comparable to the inverse KAW frequency [Eq. (230)] scale by scale and we may assume the cascade time is comparable to either:

$$\tau_{\mathrm{KAW}\lambda} \sim \frac{\lambda^2}{\Phi_\lambda} \sim \frac{1}{\sqrt{1+\beta_i}} \frac{\rho_i}{\lambda} \frac{v_A}{l_{\|\lambda}}. \qquad (239)$$

In other words, this says that $\partial/\partial z \sim (\delta \mathbf{B}_\perp/B_0) \cdot \nabla_\perp$ and so $\delta B_{\perp\lambda}/B_0 \sim \lambda/l_{\|\lambda}$ (note that the last relation confirms that our scaling arguments do not violate the gyrokinetic ordering; see § 2.1 and § 3.1). Equation (239) is the critical-balance assumption for KAW. As in the case of the Alfvén waves (§ 1.2), we might argue physically that the critical balance is set up because the parallel correlation length $l_{\|\lambda}$ is determined by the condition that a wave can propagate the distance $l_{\|\lambda}$ in one nonlinear decorrelation time corresponding to the perpendicular correlation length λ.

Combining Eqs. (238) and (239), we get the desired scaling relations for the KAW turbulence:

$$\Phi_\lambda \sim \left(\frac{\varepsilon_{\mathrm{KAW}}}{\varepsilon}\right)^{1/3} \frac{v_A}{(1+\beta_i)^{1/3}} l_0^{-1/3} \rho_i^{2/3} \lambda^{2/3}, \qquad (240)$$

$$l_{\|\lambda} \sim \left(\frac{\varepsilon}{\varepsilon_{\mathrm{KAW}}}\right)^{1/3} \frac{l_0^{1/3} \rho_i^{1/3} \lambda^{1/3}}{(1+\beta_i)^{1/6}}, \qquad (241)$$

where $l_0 = v_A^3/\varepsilon$, as in § 1.2. The first of these scaling relations is equivalent to a $k_\perp^{-7/3}$ spectrum of magnetic energy, the second quantifies the anisotropy (which is stronger than for the GS turbulence). Both scalings were confirmed in the numerical simulations of Cho & Lazarian (2004)—it is their detection of the scaling (241) that makes a particularly strong case

that KAW turbulence is not weak and that the critical balance hypothesis applies.

For KAW-like fluctuations, the density [Eq. (221)] and magnetic field [Eqs. (223) and (231)] have the same spectrum as the scalar potential, i.e., $k_\perp^{-7/3}$, while the electric field $E \sim k_\perp \varphi$ has a $k_\perp^{-1/3}$ spectrum. The solar-wind fluctuation spectra reported by Bale et al. (2005) indeed are consistent with a transition to KAW turbulence around the ion gyroscale: $k^{-5/3}$ magnetic and electric-field power spectra at $k\rho_i \ll 1$ are replaced, for $k\rho_i \gtrsim 1$, with what appears to be consistent with a $k^{-7/3}$ scaling for the magnetic-field spectrum and a $k^{-1/3}$ for the electric one (see Fig. 1). A similar result is recovered in fully gyrokinetic simulations with $\beta_i = 1$, $\tau = 1$ (Howes et al. 2008b). However, not all solar-wind observations are quite as straightforwardly supportive of the notion of the KAW cascade and much steeper magnetic-fluctuation spectra have also been reported (e.g., Denskat et al. 1983; Leamon et al. 1998; Smith et al. 2006). Possible reasons for this will emerge in § 7.6 and § 7.11 and the solar-wind data are further discussed in § 8.2.4 and § 8.2.5.

7.6. *Validity of the Electron RMHD and the Effect of Electron Landau Damping*

The ERMHD equations derived in § 7 are valid provided $k_\perp \rho_i \gg 1$ and also provided it is sufficient to use the leading order in the mass-ratio expansion (isothermal electrons; see § 4). In particular, this means that the electron Landau damping is neglected. Asymptotically speaking, this is a rigorous limit, but one must be cautious in applying it to real plasmas. Since the width of the scale range where $k_\perp \rho_i \gg 1$ and $k_\perp \rho_e \ll 1$ is only $\sim (m_i/m_e)^{1/2} \simeq 43$, for some values of the plasma parameters (T_{0i}/T_{0e} and β_i) there may not be a very broad interval of scales where the electron Landau damping is truly negligible. Consider, for example, the low-beta limit, $\beta_i \ll 1$. In this limit, the KAW frequency is $\omega \sim k_\perp \rho_i k_\| v_A$ [Eq. (230)]. The electron Landau damping becomes important when $\omega \sim k_\| v_{\mathrm{th}e}$, or $k_\perp \rho_e \sim \sqrt{\beta_i} \ll 1$, so the ERMHD approximation breaks down and, consequently, the KAW cascade, if any, should be interrupted well before the electron gyroscale is reached. Figure 8 shows the solution of the full gyrokinetic dispersion relation (Howes et al. 2006) for small, unity and large β_i. One can judge for which scales and how well (or how badly) the ERMHD approximation holds from the precision with which the exact frequency follows the asymptotic solution Eq. (230) and from the relative strength of the damping compared to the real frequency of the waves.

Non-negligible electron Landau damping may affect turbulence spectra because one can no longer assume a constant flux of KAW energy as we did in § 7.5. To evaluate the consequences of this effect, Howes et al. (2008a) constructed a simple model of spectral energy transfer and concluded that Landau damping leads to steepening of the KAW spectra—one of several possible reasons for steep dissipation-range spectra observed in space plasmas (see also § 7.11).

7.7. *Unfreezing of Flux*

As ERMHD is a limit of the isothermal-electron-fluid system (§ 4), the magnetic-field lines remain unbroken (see § 4.3). Within the orderings employed above (small mass ratio, $\nu_{ii} \sim \omega$, $\beta_i \sim 1$, $\tau \sim 1$), the flux unfreezes only in the vicinity of the electron gyroscale. It is interesting to evaluate somewhat more precisely the scale at which this happens as a function of plasma parameters.

Physically, there are three kinds of mechanisms by which the flux conservation is broken: electron inertia, the effects of finite electron gyroradius, and Ohmic resistivity. Let us take the $v_\parallel$ moment of the electron gyrokinetic equation [Eq. (57), $s = e$, integration at constant $\mathbf{r}$] and use Eq. (222) to evaluate the inertial term in the resulting parallel electron momentum equation:

$$\frac{cm_e}{e} \frac{\partial u_{\parallel e}}{\partial t} = \frac{\partial}{\partial t} d_e^2 \nabla_\perp^2 A_\parallel, \qquad (242)$$

where $d_e = \rho_e/\sqrt{\beta_e}$ is the electron inertial scale and $\beta_e = Z\beta_i/\tau$. Comparing this with the $\partial A_\parallel/\partial t$ term in the right-hand side of the electron momentum equation, we see that the electron inertia becomes important when $k_\perp \rho_e \sim \sqrt{\beta_e}$. The finite-gyroradius effects enter when $k_\perp \rho_e \sim 1$. Thus, at low β_e, the electron inertia becomes important above the electron gyroscale, whereas at high β_e, the finite-gyroradius effects enter first. Finally, the Ohmic resistivity comes from the collision term (see Appendix B.4):

$$\frac{cm_e}{e} \frac{1}{n_{0e}} \int d^3\mathbf{v}\, v_\parallel \left(\frac{\partial h_e}{\partial t} \right)_c \sim \frac{cm_e}{e} \nu_{ei} u_{\parallel e} \sim \nu_{ei} k_\perp^2 d_e^2 A_\parallel. \quad (243)$$

Thus, resistivity starts to act when $k_\perp d_e \sim (\omega/\nu_{ei})^{1/2}$. Using the KAW frequency [Eq. (230)] to estimate ω and assuming that τ is not small, we get

$$k_\perp \rho_e \sim k_\parallel \lambda_{\mathrm{mfp}i} \sqrt{\frac{\beta_i}{1+\beta_i} \frac{Z^2}{\tau^2}}. \qquad (244)$$

Thus, the resistive scale can only be larger the electron gyroscale if the plasma is collisional ($k_\parallel \lambda_{\mathrm{mfp}i} \ll 1$) and/or electrons are much colder than ions ($\tau \gg 1$) and/or $\beta_i \ll 1$. Note if only the last of these conditions is satisfied, the electron inertia still becomes important at larger scales than resistivity.

7.8. *Generalized Energy: KAW and Entropy Cascades*

The generalized energy (§ 3.4) in the limit $k_\perp \rho_i \gg 1$ is calculated by substituting Eqs. (221) and (223) into Eq. (109):

$$W = \int d^3\mathbf{r} \left\{ \int d^3\mathbf{v}\, \frac{T_{0i}\langle h_i^2 \rangle_\mathbf{r}}{2F_{0i}} + \frac{\delta B_\perp^2}{8\pi} \right.$$
$$\left. + \frac{n_{0i}T_{0i}}{2} \left(1 + \frac{Z}{\tau}\right) \left[1 + \frac{\beta_i}{2}\left(1 + \frac{Z}{\tau}\right)\right] \left(\frac{Ze\varphi}{T_{0i}}\right)^2 \right\}$$
$$= W_{h_i} + W_{\mathrm{KAW}}. \qquad (245)$$

Here the first term, W_{h_i}, is the total variance of h_i, which is proportional to minus the entropy of the ion gyrocenter distribution (see § 3.5) and whose cascade to collisional scales will be discussed in § 7.9 and § 7.10. The remaining two terms are the independently cascaded KAW energy:

$$W_{\mathrm{KAW}} = \int d^3\mathbf{r}\, \frac{m_i n_{0i}}{2} \left\{ |\nabla_\perp \Psi|^2 \right.$$
$$\left. + \left(1 + \frac{Z}{\tau}\right)\left[1 + \frac{\beta_i}{2}\left(1 + \frac{Z}{\tau}\right)\right] \frac{\Phi^2}{\rho_i^2} \right\}$$
$$= \int d^3\mathbf{r}\, \frac{m_i n_{0i}}{2} \left(|\Theta^+|^2 + |\Theta^-|^2 \right). \qquad (246)$$

Although we can write W_{KAW} as the sum of the energies of the "+" and "−" linear KAW eigenmodes [Eq. (231)], which

are also exact nonlinear solutions (§ 7.4), the two do not cascade independently and can exchange energy. Note that the ERMHD equations also conserve $\int d^3\mathbf{r}\, \Psi\Phi$, which is readily interpreted as the helicity of the perturbed magnetic field (see Appendix F.3). However, it does not affect the KAW cascade discussed in § 7.5 because it can be argued to have a tendency to cascade inversely (Appendix F.6).

Comparing the way the generalized energy is split above and below the ion gyroscale (see § 5.6 for the $k_\perp \rho_i \ll 1$ limit), we interpret what happens at the $k_\perp \rho_i \sim 1$ transition as a redistribution of the power that arrived from large scales between a cascade of KAW and a cascade of the (minus) gyrocenter entropy in the phase space (see Fig. 5). The latter cascade is the way in which the energy diverted from the electromagnetic fluctuations by the collisionless damping (wave–particle interaction) can be transferred to the collisional scales and deposited into heat (§ 7.1). The concept of entropy cascade as the key agent in the heating of the plasma was introduced in § 3.5, where we promised a more detailed discussion later on. We now proceed to this discussion.

7.9. *Entropy Cascade*

The ion-gyrocenter distribution function h_i satisfies the ion gyrokinetic equation (121), where ion–electron collisions are neglected under the mass-ratio expansion. At $k_\perp \rho_i \gg 1$, the dominant contribution to $\langle \chi \rangle_{\mathbf{R}_i}$ comes from the electromagnetic fluctuations associated with KAW turbulence. Since the KAW cascade is decoupled from the entropy cascade, h_i is a passive tracer of the ring-averaged KAW turbulence in phase space. Expanding the Bessel functions in the expression for $\langle \chi \rangle_{\mathbf{R}_i,\mathbf{k}}$ [$a_i \gg 1$ in Eq. (69) with $s = i$] and making use of Eqs. (222-223) and of the KAW scaling $\Psi \sim \Phi/k_\perp \rho_i$ [Eq. (231)], it is not hard to show that

$$\frac{Ze}{T_{0i}} \langle \chi \rangle_{\mathbf{R}_i,\mathbf{k}} \simeq \frac{Ze}{T_{0i}} \langle \varphi \rangle_{\mathbf{R}_i,\mathbf{k}} = \frac{2}{\sqrt{\beta_i}} \frac{J_0(a_i)\Phi_\mathbf{k}}{\rho_i v_A}, \qquad (247)$$

where

$$J_0(a_i) \simeq \sqrt{\frac{2}{\pi a_i}} \cos\left(a_i - \frac{\pi}{4}\right), \quad a_i = k_\perp \rho_i \frac{v_\perp}{v_{\mathrm{th}i}}, \quad (248)$$

so h_i satisfies [Eq. (121)]

$$\frac{\partial h_i}{\partial t} + v_\parallel \frac{\partial h_i}{\partial z} + \{\langle \Phi \rangle_{\mathbf{R}_i}, h_i\} = \frac{2}{\sqrt{\beta_i}\, \rho_i v_A} \frac{\partial \langle \Phi \rangle_{\mathbf{R}_i}}{\partial t} F_{0i} + \langle C_{ii}[h_i] \rangle_{\mathbf{R}_i} \qquad (249)$$

with the conservation law [Eq. (70), $s = i$]

$$\frac{1}{T_{0i}} \frac{dW_{h_i}}{dt} \equiv \frac{d}{dt} \int d^3\mathbf{v} \int d^3\mathbf{R}_i \frac{h_i^2}{2F_{0i}}$$
$$= \frac{2}{\sqrt{\beta_i}\, \rho_i v_A} \int d^3\mathbf{v} \int d^3\mathbf{R}_i \frac{\partial \langle \Phi \rangle_{\mathbf{R}_i}}{\partial t} h_i$$
$$+ \int d^3\mathbf{v} \int d^3\mathbf{R}_i \frac{h_i \langle C_{ii}[h_i] \rangle_{\mathbf{R}_i}}{F_{0i}}. \qquad (250)$$

7.9.1. *Nonlinear Perpendicular Phase Mixing*

The wave–particle interaction term (the first term on the right hand sides of these two equations) will shortly be seen to be subdominant at $k_\perp \rho_i \gg 1$. It represents the source of the invariant W_{h_i} due to the collisionless damping at the ion gyroscale of some fraction of the energy arriving from the inertial range. In a stationary turbulent state, we should have
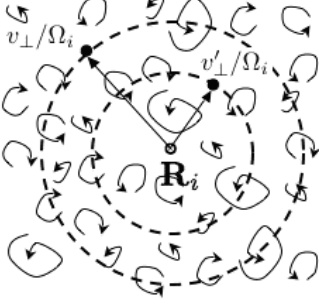
FIG. 10.— Nonlinear perpendicular phase-mixing mechanism: the gyrocenter distribution function at $\mathbf{R}_i$ of particles with velocities $v_\perp$ and $v'_\perp$ is mixed by turbulent fluctuations of the potential Φ ($\mathbf{E} \times \mathbf{B}$ flows) averaged over particle orbits separated by a distance greater than the correlation length of Φ.

$\overline{dW_{h_i}/dt} = 0$ and this source should be balanced on average by the (negative definite) collisional dissipation term (= heating; see § 3.5). This balance can only be achieved if h_i develops small scales in the velocity space and carries the generalized energy, or, in this case, entropy, to scales in the phase space at which collisions are important. A quick way to see this is by recalling that the collision operator has two velocity derivatives and can only balance the terms on the left-hand side of Eq. (249) if

$$\nu_{ii} v_{\mathrm{th}i}^2 \left(\frac{\partial}{\partial \mathbf{v}}\right)^2 \sim \omega \quad \Rightarrow \quad \frac{\delta v}{v_{\mathrm{th}i}} \sim \left(\frac{\nu_{ii}}{\omega}\right)^{1/2}, \quad (251)$$

where ω is the characteristic frequency of the fluctuations of h_i. If $\nu_{ii} \ll \omega$, $\delta v/v_{\mathrm{th}i} \ll 1$. This is certainly true for $k_\perp \rho_i \sim 1$: taking $\omega \sim k_\| v_A$ and using $k_\| \lambda_{\mathrm{mfp}i} \gg 1$ (which is the appropriate limit at and below the ion gyroscale for most of the plasmas of interest; cf. footnote 24), we have $\nu_{ii}/\omega \sim \sqrt{\beta_i}/k_\| \lambda_{\mathrm{mfp}i} \ll 1$.

The condition (251) means that the collision rate can be arbitrarily small—this will always be compensated by the sufficiently fine velocity-space structure of the distribution function to produce a finite amount of entropy production (heating) independent of ν_{ii} in the limit $\nu_{ii} \to +0$. The situation bears some resemblance to the emergence of small spatial scales in neutral-fluid turbulence with arbitrarily small but non-zero viscosity (Kolmogorov 1941). The analogy is not perfect, however, because the ion gyrokinetic equation (249) does not contain a nonlinear interaction term that would explicitly cause a cascade in the velocity space. Instead, the (ring-averaged) KAW turbulence mixes h_i in the gyrocenter space via the nonlinear term in Eq. (249), so h_i will have small-scale structure in $\mathbf{R}_i$ on characteristic scales much smaller than ρ_i. Let us assume that the dominant nonlinear effect is a local interaction of the small-scale fluctuations of h_i with the similarly small-scale component of $\langle\Phi\rangle_{\mathbf{R}_i}$. Since ring averaging is involved and $k_\perp \rho_i$ is large, the values of $\langle\Phi\rangle_{\mathbf{R}_i}$ corresponding to two velocities $\mathbf{v}$ and $\mathbf{v}'$ will come from spatially decorrelated electromagnetic fluctuations if $k_\perp v_\perp/\Omega_i$ and $k_\perp v'_\perp/\Omega_i$ [the argument of the Bessel function in Eq. (247)] differ by order unity, i.e., for

$$\frac{\delta v_\perp}{v_{\mathrm{th}i}} = \frac{|v_\perp - v'_\perp|}{v_{\mathrm{th}i}} \sim \frac{1}{k_\perp \rho_i} \quad (252)$$

(see Fig. 10). This relation gives a correspondence between the decorrelation scales of h_i in the position and velocity

space. Combining Eqs. (252) and (251), we see that there is a collisional cutoff scale determined by $k_\perp \rho_i \sim (\omega/\nu_{ii})^{1/2} \gg 1$.[32] The cutoff scale is much smaller than the ion gyroscale. In the range between these scales, collisional dissipation is small. The ion entropy fluctuations are transferred across this scale range by means of a cascade, for which we will construct a scaling theory in § 7.9.2 (and, for the case without the background KAW turbulence, in § 7.10).

It is important to emphasize that no matter how small the collisional cutoff scale is, all of the generalized energy channeled into the entropy cascade at the ion gyroscale eventually reaches it and is converted into heat. Note that the rate at which this happens is in general amplitude-dependent because the process is nonlinear, although we will argue in § 7.9.4 (see also § 7.10.3) that the nonlinear cascade time and the parallel linear propagation (particle streaming) time are related by a critical-balance-like condition (we will also argue there that the linear parallel phase mixing, which can generate small scales in $v_\|$, is a less efficient process than the nonlinear perpendicular one discussed above).

It is interesting to note the connection between the entropy cascade and certain aspects of the gyrofluid closure formalism developed by Dorland & Hammett (1993). In their theory, the emergence of small scales in $v_\perp$ manifested itself as the growth of high-order $v_\perp$ moments of the gyrocenter distribution function. They correctly identified this effect as a consequence of the nonlinear perpendicular phase mixing of the gyrocenter distribution function caused by a perpendicular-velocity-space spread in the ring-averaged $\mathbf{E} \times \mathbf{B}$ velocities (given by $\langle\mathbf{u}_E\rangle_{\mathbf{R}_i} = \hat{\mathbf{z}} \times \nabla\langle\Phi\rangle_{\mathbf{R}_i}$ in our notation) arising at and below the ion gyroscale.

7.9.2. *Scalings*

Since entropy is a conserved quantity, we will follow the well trodden Kolmogorov path, assume locality of interactions in scale space and constant entropy flux, and conclude, analogously to Eq. (1),

$$\frac{v_{\mathrm{th}i}^8}{n_{0i}^2} \frac{h_{i\lambda}^2}{} \sim \varepsilon_h = \mathrm{const}, \quad (253)$$

where ε_h is the entropy flux proportional to the fraction of the total turbulent power ε (or $\overline{P_{\mathrm{ext}}}$; see § 3.4) that was diverted into the entropy cascade at the ion gyroscale, and is the cascade time that we now need to find.

By the critical-balance assumption, the decorrelation time of the electromagnetic fluctuations in KAW turbulence is comparable at each scale to the KAW period at that scale and to the nonlinear interaction time [Eq. (239)]:

$$\tau_{\mathrm{KAW}\lambda} \sim \frac{\lambda^2}{\Phi_\lambda} \sim \left(\frac{\varepsilon}{\varepsilon_{\mathrm{KAW}}}\right)^{1/3} (1+\beta_i)^{1/3} \frac{l_0^{1/3} \rho_i^{-2/3} \lambda^{4/3}}{v_A}. \quad (254)$$

The characteristic time associated with the nonlinear term in Eq. (249) is longer than $\tau_{\mathrm{KAW}\lambda}$ by a factor of $(\rho_i/\lambda)^{1/2}$ due to the ring averaging, which reduces the strength of the nonlinear interaction. This weakness of the nonlinearity makes it possible to develop a systematic analytical theory of the entropy

[32] Another source of small-scale spatial smoothing comes from the perpendicular gyrocenter-diffusion terms $\sim -\nu_{ii}(v/v_{\mathrm{th}i})^2 k_\perp^2 \rho_i^2 h_{i\mathbf{k}}$ that arise in the ring-averaged collision operators, e.g., the second term in the model operator (B13). These terms again enforce a cutoff wavenumber such that $k_\perp \rho_i \sim (\omega/\nu_{ii})^{1/2} \gg 1$.

cascade (Schekochihin & Cowley 2009). It is also possible to estimate the cascade time via a more qualitative argument analogous to that first devised by Kraichnan (1965) for the weak turbulence of Alfvén waves: during each KAW correlation time $\tau_{\text{KAW}\lambda}$, the nonlinearity changes the amplitude of h_i by only a small amount:

$$\Delta h_{i\lambda} \sim (\lambda/\rho_i)^{1/2} h_{i\lambda} \ll h_{i\lambda}; \qquad (255)$$

these changes accumulate with time as a random walk, so after time t, the cumulative change in amplitude is $\Delta h_{i\lambda}(t/\tau_{\text{KAW}\lambda})^{1/2}$; finally, the cascade time $t = $ is the time after which the cumulative change in amplitude is comparable to the amplitude itself, which gives, using Eq. (254),

$$\sim \frac{\rho_i}{\lambda} \tau_{\text{KAW}\lambda} \sim \left(\frac{\varepsilon}{\varepsilon_{\text{KAW}}}\right)^{1/3} (1+\beta_i)^{1/3} \frac{l_0^{1/3} \rho_i^{1/3} \lambda^{1/3}}{v_A}. \quad (256)$$

Substituting this into Eq. (253), we get

$$h_{i\lambda} \sim \frac{n_{0i}}{v_{\text{th}i}^3} \left(\frac{\varepsilon_h}{\varepsilon}\right)^{1/2} \left(\frac{\varepsilon}{\varepsilon_{\text{KAW}}}\right)^{1/6} \frac{(1+\beta_i)^{1/6}}{\sqrt{\beta_i}} l_0^{-1/3} \rho_i^{1/6} \lambda^{1/6},$$
$$(257)$$

which corresponds to a $k_\perp^{-4/3}$ spectrum of entropy.

In the argument presented above, we assumed that the scaling of h_i was determined by the nonlinear mixing of h_i by the ring-averaged KAW fluctuations rather than by the wave–particle interaction term on the right-hand side of Eq. (249). We can now confirm the validity of this assumption. The change in amplitude of h_i in one KAW correlation time $\tau_{\text{KAW}\lambda}$ due to the wave–particle interaction term is

$$\Delta h_{i\lambda} \sim \frac{n_{0i}}{v_{\text{th}i}^3} \left(\frac{\lambda}{\rho_i}\right)^{1/2} \frac{\Phi_\lambda}{\sqrt{\beta_i} \rho_i v_A}$$
$$\sim \frac{n_{0i}}{v_{\text{th}i}^3} \left(\frac{\varepsilon_{\text{KAW}}}{\varepsilon}\right)^{1/3} \frac{1}{\sqrt{\beta_i}(1+\beta_i)^{1/3}} l_0^{-1/3} \rho_i^{-5/6} \lambda^{7/6}, \quad (258)$$

where we have used Eq. (240). Comparing this with Eq. (255) and using Eq. (257), we see that $\Delta h_{i\lambda}$ in Eq. (258) is a factor of $(\lambda/\rho_i)^{1/2}$ smaller than $\Delta h_{i\lambda}$ due to the nonlinear mixing.

7.9.3. Phase-Space Cutoff

To work out the cutoff scales both in the position and velocity space, we use Eqs. (251) and (252): in Eq. (251), $\omega \sim 1/$, where is the characteristic decorrelation time of h_i given by Eq. (256); using Eq. (252), we find the cutoffs:

$$\frac{\delta v_\perp}{v_{\text{th}i}} \sim \frac{1}{k_\perp \rho_i} \sim (\nu_{ii}\tau_{\rho_i})^{3/5} = \text{Do}^{-3/5}, \qquad (259)$$

where τ_{ρ_i} is the cascade time [Eq. (256)] taken at $\lambda = \rho_i$. By a recently established convention, the dimensionless number $\text{Do} = 1/\nu_{ii}\tau_{\rho_i}$ is called the Dorland number. It plays the role of Reynolds number for kinetic turbulence, measuring the scale separation between the ion gyroscale and the collisional dissipation scale (Schekochihin et al. 2008b; Tatsuno et al. 2009a,b).

7.9.4. Parallel Phase Mixing

Another assumption, which was made implicitly, was that the parallel phase mixing due to the second term on the left-hand side of Eq. (249) could be ignored. This requires justification, especially because it is with this "ballistic" term

that one traditionally associates the emergence of small-scale structure in the velocity space (e.g., Krommes & Hu 1994; Krommes 1999; Watanabe & Sugama 2004). The effect of the parallel phase mixing is to produce small scales in velocity space $\delta v_\parallel \sim 1/k_\parallel t$. Let us assume that the KAW turbulence imparts its parallel decorrelation scale to h_i and use the scaling relation (241) to estimate $k_\parallel \sim l_{\parallel\lambda}^{-1}$. Then, after one cascade time [Eq. (256)], h_i is decorrelated on the parallel velocity scales

$$\frac{\delta v_\parallel}{v_{\text{th}i}} \sim \frac{l_{\parallel\lambda}}{v_{\text{th}i}} \sim \frac{1}{\sqrt{\beta_i(1+\beta_i)}} \sim 1. \qquad (260)$$

We conclude that the nonlinear perpendicular phase mixing [Eq. (259)] is more efficient than the linear parallel one. Note that up to a β_i-dependent factor Eq. (260) is equivalent to a critical-balance-like assumption for h_i in the sense that the propagation time is comparable to the cascade time, or $k_\parallel v_\parallel \sim$ $^{-1}$ [see Eq. (249)].

7.10. Entropy Cascade in the Absence of KAW Turbulence

It is not currently known how one might determine analytically what fraction of the turbulent power arriving from the inertial range to the ion gyroscale is channeled into the KAW cascade and what fraction is dissipated via the kinetic ion-entropy cascade introduced in § 7.9 (perhaps it can only be determined by direct numerical simulations). It is certainly a fact that in many solar-wind measurements, the relatively shallow magnetic-energy spectra associated with the KAW cascade (§ 7.5) fail to appear and much steeper spectra are detected (close to k^{-4}; see Leamon et al. 1998; Smith et al. 2006). In view of this evidence, it is interesting to ask what would be the nature of electromagnetic fluctuations below the ion gyroscale if the KAW cascade failed to be launched, i.e., if all (or most) of the turbulent power were directed into the entropy cascade (i.e., if $W \simeq W_{h_i}$ in § 7.8).

7.10.1. Equations

It is again possible to derive a closed set of equations for all fluctuating quantities.

Let us assume (and verify a posteriori; § 7.10.4) that the characteristic frequency of such fluctuations is much lower than the KAW frequency [Eq. (230)] so that the first term in Eq. (116) is small and the equation reduces to the balance of the other two terms. This gives

$$\frac{\delta n_e}{n_{0e}} = \frac{e\varphi}{T_{0e}}, \qquad (261)$$

meaning that the electrons are purely Boltzmann [$h_e = 0$ to lowest order; see Eq. (101)]. Then, from Eq. (118),

$$\frac{Ze\varphi}{T_{0i}} \equiv \frac{2\Phi}{\rho_i v_{\text{th}i}} = \left(1+\frac{\tau}{Z}\right)^{-1} \sum_{\mathbf{k}} e^{i\mathbf{k}\cdot\mathbf{r}} \frac{1}{n_{0i}} \int d^3\mathbf{v} J_0(a_i) h_{i\mathbf{k}} \quad (262)$$

Using Eq. (262), we find from Eq. (120) that the field-strength fluctuations are

$$\frac{\delta B_\parallel}{B_0} = -\frac{\beta_i}{2} \sum_{\mathbf{k}} e^{i\mathbf{k}\cdot\mathbf{r}} \frac{1}{n_{0i}} \int d^3\mathbf{v} \frac{2v_\perp^2}{v_{\text{th}i}^2} \frac{J_1(a_i)}{a_i} h_{i\mathbf{k}}, \qquad (263)$$

which is smaller than $Ze\varphi/T_{0i}$ by a factor of $\beta_i/k_\perp\rho_i$.

Therefore, we can neglect $\delta B_\parallel/B_0$ compared to $\delta n_e/n_{0e}$ in Eq. (117). Using Eq. (261), we get what is physically the

electron continuity equation:

$$\frac{\partial}{\partial t}\frac{e\varphi}{T_{0e}}+\hat{\mathbf{b}}\cdot\nabla\left(\frac{c}{4\pi en_{0e}}\nabla_{\perp}^{2}A_{\|}+u_{\|i}\right)=0, \qquad (264)$$

$$u_{\|i}=\sum_{\mathbf{k}}e^{i\mathbf{k}\cdot\mathbf{r}}\frac{1}{n_{0i}}\int d^{3}\mathbf{v}\,v_{\|}J_{0}(a_{i})h_{i\mathbf{k}}. \qquad (265)$$

Note that in terms of the stream and flux functions, Eq. (264) takes the form

$$\frac{\partial}{\partial z}\rho_{i}^{2}\nabla_{\perp}^{2}\Psi=\sqrt{\beta_{i}}\left(\frac{2\tau}{Z}\frac{1}{v_{\text{thi}}}\frac{\partial\Phi}{\partial t}+\rho_{i}\frac{\partial u_{\|i}}{\partial z}\right), \qquad (266)$$

where we have approximated $\hat{\mathbf{b}}\cdot\nabla\simeq\partial/\partial z$, which will, indeed, be shown to be correct in §7.10.4.

Together with the ion gyrokinetic equation, which determines h_i, Eqs. (261-264) form a closed set. They describe low-frequency fluctuations of the density and electromagnetic field due solely to the presence of fluctuations of h_i below the ion gyroscale.

It follows from Eq. (263) that $\delta B_{\|}/B_0$ contributes subdominantly to $\langle\chi\rangle_{\mathbf{R}_i}$ [Eq. (69) with $s=i$ and $a_i\gg 1$]. It will be verified a posteriori (§7.10.4) that the same is true for $A_{\|}$. Therefore, Eqs. (247) and (249) continue to hold, as in the case with KAW. This means that Eqs. (249) and (262) form a closed subset. Thus the kinetic ion-entropy cascade is self-regulating in the sense that h_i is no longer passive (as it was in the presence of KAW turbulence; §7.9) but is mixed by the ring-averaged "electrostatic" fluctuations of the scalar potential, which themselves are produced by h_i according to Eq. (262).

The magnetic fluctuations are passive and determined by the electrostatic and entropy fluctuations via Eqs. (263) and (264).

7.10.2. *Scalings*

From Eq. (262), we can establish a correspondence between Φ_λ and $h_{i\lambda}$ (the electrostatic fluctuations and the fluctuations of the ion-gyrocenter distribution function):

$$\Phi_\lambda\sim\rho_i v_{\text{thi}}\left(\frac{\lambda}{\rho_i}\right)^{1/2}\frac{h_{i\lambda}v_{\text{thi}}^{3}}{n_{0i}}\left(\frac{\delta v_{\perp}}{v_{\text{thi}}}\right)^{1/2}\sim\frac{v_{\text{thi}}^{4}}{n_{0i}}h_{i\lambda}\lambda, \quad (267)$$

where the factor of $(\lambda/\rho_i)^{1/2}$ comes from the Bessel function [Eq. (248)] and the factor of $(\delta v_{\perp}/v_{\text{thi}})^{1/2}$ results from the $v_{\perp}$ integration of the oscillatory factor in the Bessel function times h_i, which decorrelates on small scales in the velocity space and, therefore, its integral accumulates in a random-walk-like fashion. The velocity-space scales are related to the spatial scales via Eq. (252), which was arrived at by an argument not specific to KAW-like fluctuations and, therefore, continues to hold.

Using Eq. (267), we find that the wave–particle interaction term in the right-hand side of Eq. (249) is subdominant: comparing it with $\partial h_i/\partial t$ shows that it is smaller by a factor of $(\lambda/\rho_i)^{3/2}\ll 1$. Therefore, it is the nonlinear term in Eq. (249) that controls the scalings of $h_{i\lambda}$ and Φ_λ.

We now assume again the scale-space locality and constancy of the entropy flux, so Eq. (253) holds. The cascade (decorrelation) time is equal to the characteristic time associated with the nonlinear term in Eq. (249): $\sim(\rho_i/\lambda)^{1/2}\lambda^2/\Phi_\lambda$. Substituting this into Eq. (253) and using Eq. (267), we arrive at the desired scaling relations for the entropy cascade

(Schekochihin et al. 2008b):

$$h_{i\lambda}\sim\frac{n_{0i}}{v_{\text{thi}}^{3}}\left(\frac{\varepsilon_h}{\varepsilon}\right)^{1/3}\frac{1}{\sqrt{\beta_i}}l_{0}^{-1/3}\rho_i^{1/6}\lambda^{1/6}, \qquad (268)$$

$$\Phi_\lambda\sim\left(\frac{\varepsilon_h}{\varepsilon}\right)^{1/3}\frac{v_{\text{thi}}}{\sqrt{\beta_i}}l_{0}^{-1/3}\rho_i^{1/6}\lambda^{7/6}, \qquad (269)$$

$$\sim\left(\frac{\varepsilon}{\varepsilon_h}\right)^{1/3}\frac{\sqrt{\beta_i}}{v_{\text{thi}}}l_{0}^{1/3}\rho_i^{1/3}\lambda^{1/3}, \qquad (270)$$

where $l_0=v_A^3/\varepsilon$, as in §1.2. Note that since the existence of this cascade depends on it not being overwhelmed by the KAW fluctuations, we should have $\varepsilon_{\text{KAW}}\ll\varepsilon$ and $\varepsilon_h=\varepsilon-\varepsilon_{\text{KAW}}\approx\varepsilon$.

The scaling for the ion-gyrocenter distribution function, Eq. (268), implies a $k_{\perp}^{-4/3}$ spectrum—the same as for the KAW turbulence [Eq. (257)]. The scaling for the the cascade time, Eq. (270), is also similar to that for the KAW turbulence [Eq. (256)]. Therefore the velocity- and gyrocenter-space cutoffs are still given by Eq. (259), where τ_{ρ_i} is now given by Eq. (270) taken at $\lambda=\rho_i$.

A new feature is the scaling of the scalar potential, given by Eq. (269), which corresponds to a $k_{\perp}^{-10/3}$ spectrum (unlike the KAW spectrum, §7.5). This is a measurable prediction for the electrostatic fluctuations: the implied electric-field spectrum is $k_{\perp}^{-4/3}$. From Eq. (261), we also conclude that the density fluctuations should have the same spectrum as the scalar potential, $k_{\perp}^{-10/3}$—another measurable prediction.

The scalings derived above for the spectra of the ion distribution function and of the scalar potential have been confirmed in the numerical simulations by Tatsuno et al. (2009a,b), who studied decaying electrostatic gyrokinetic turbulence in two spatial dimensions. They also found velocity-space scalings in accord with Eq. (252) (using a spectral representation of the correlation functions in the $v_{\perp}$ space based on the Hankel transform of the distribution function; see Plunk et al. 2009).

7.10.3. *Parallel Cascade and Parallel Phase Mixing*

We have again ignored the ballistic term (the second on the left-hand side) in Eq. (249). We will estimate the efficiency of the parallel spatial cascade of the ion entropy and of the associated parallel phase mixing by making a conjecture analogous to the critical balance: assuming that any two perpendicular planes only remain correlated provided particles can stream between them in one nonlinear decorrelation time (cf. §1.2 and §7.9.4), we conclude that the parallel particle-streaming frequency $k_{\|}v_{\|}$ should be comparable at each scale to the inverse nonlinear time $^{-1}$, so

$$k_{\|}v_{\text{thi}}\sim 1. \qquad (271)$$

As we explained in §7.9.4, the parallel scales in the velocity space generated via the ballistic term are related to the parallel wavenumbers by $\delta v_{\|}\sim 1/k_{\|}t$. From Eq. (271), we find that after one cascade time , the typical parallel velocity scale is $\delta v_{\|}/v_{\text{thi}}\sim 1$, so the parallel phase mixing is again much less efficient than the perpendicular one.

Note that Eq. (271) combined with Eq. (270) means that the anisotropy is again characterized by the scaling relation $k_{\|}\sim k_{\perp}^{1/3}$, similarly to the case of KAW turbulence [see Eq. (241) and §7.9.4].

7.10.4. *Scalings for the Magnetic Fluctuations*

The scaling law for the fluctuations of the magnetic-field strength follows immediately from Eqs. (263) and (269):

$$\frac{\delta B_{\|\lambda}}{B_0} \sim \beta_i \frac{\lambda}{\rho_i} \frac{\Phi_\lambda}{\rho_i v_{\text{thi}}} \sim \sqrt{\beta_i} l_0^{-1/3} \rho_i^{-11/6} \lambda^{13/6}, \quad (272)$$

whence the spectrum of these fluctuations is $k_\perp^{-16/3}$.

The scaling of $A_\|$ (the perpendicular magnetic fluctuations) depends on the relation between $k_\|$ and $k_\perp$. Indeed, the ratio between the first and the third terms on the left-hand side of Eq. (264) [or, equivalently, between the first and second terms on the right-hand side of Eq. (266)] is $\sim (k_\| v_{\text{thi}})^{-1}$. For a critically balanced cascade, this makes the two terms comparable [Eq. (271)]. Using the first term to work out the scaling for the perpendicular magnetic fluctuations, we get, using Eq. (269),

$$\frac{\delta B_{\perp\lambda}}{B_0} \sim \frac{1}{\lambda} \frac{\Psi_\lambda}{v_A} \sim \beta_i \frac{\lambda}{\rho_i} \frac{\Phi_\lambda}{\rho_i v_{\text{thi}}} \sim \sqrt{\beta_i} l_0^{-1/3} \rho_i^{-11/6} \lambda^{13/6}, \quad (273)$$

which is the same scaling as for $\delta B_\|/B_0$ [Eq. (272)].

Using Eq. (273) together with Eqs. (269) and (270), it is now straightforward to confirm the three assumptions made in § 7.10.1 that we promised to verify a posteriori:

1. In Eq. (116), $\partial A_\|/\partial t \ll c\hat{\mathbf{b}}\cdot\nabla\varphi$, so Eq. (261) holds (the electrons remain Boltzmann). This means that no KAW can be excited by the cascade.

2. $\delta B_\perp/B_0 \ll k_\|/k_\perp$, so $\hat{\mathbf{b}}\cdot\nabla \simeq \partial/\partial z$ in Eq. (264). This means that field lines are not significantly perturbed.

3. In the expression for $\langle\chi\rangle_{\mathbf{R}_i}$ [Eq. (69)], $v_\| A_\|/c \ll \varphi$, so Eq. (249) holds. This means that the electrostatic fluctuations dominate the cascade.

7.11. *Cascades Superposed?*

The spectra of magnetic fluctuations obtained in § 7.10.4 are very steep—steeper, in fact, than those normally observed in the dissipation range of the solar wind (§ 8.2.5). One might speculate that the observed spectra may be due to a superposition of the two cascades realizable below the ion gyroscale: a high-frequency cascade of KAW (§ 7.5) and a low-frequency cascade of electrostatic fluctuations due to the ion entropy fluctuations (§ 7.10). Such a superposition could happen if the power going into the KAW cascade is relatively small, $\varepsilon_{\text{KAW}} \ll \varepsilon$. One then expects an electrostatic cascade to be set up just below the ion gyroscale with the KAW cascade superseding it deeper into the dissipation range. Comparing Eqs. (240) and (269), we can estimate the position of the spectral break:

$$k_\perp \rho_i \sim (\varepsilon/\varepsilon_{\text{KAW}})^{2/3}. \quad (274)$$

Since $\rho_i/\rho_e \sim (\tau m_i/m_e)^{1/2}/Z$ is not a very large number, the dissipation range is not very wide. It is then conceivable that the observed spectra are not true power laws but simply non-asymptotic superpositions of the electrostatic and KAW spectra with the observed range of "effective" spectral exponents due to varying values of the spectral break (274) between the two cascades.[33]

---

[33] Several alternative theories that aim to explain the dissipation-range spectra exist: see § 8.2.6.

The value of $\varepsilon_{\text{KAW}}/\varepsilon$ specific to any particular set of parameters (β_i, τ, etc.) is set by what happens at $k_\perp \rho_i \sim 1$ (§ 7.1; see § 8.2.2, § 8.2.5, and § 8.5 for further discussion).

7.12. *Below the Electron Gyroscale: The Last Cascade*

Finally, let us consider what happens when $k_\perp \rho_e \gg 1$. At these scales, we have to return to the full gyrokinetic system of equations. The quasi-neutrality [Eq. (61)], parallel [Eq. (62)] and perpendicular [Eq. (66)] Ampère's law become

$$\frac{e\varphi}{T_{0e}} = -\left(1+\frac{Z}{\tau}\right)^{-1} \sum_{\mathbf{k}} e^{i\mathbf{k}\cdot\mathbf{r}} \frac{1}{n_{0e}} \int d^3\mathbf{v} J_0(a_e) h_{e\mathbf{k}}, \quad (275)$$

$$\frac{c}{4\pi e n_{0e}} \nabla_\perp^2 A_\| = \sum_{\mathbf{k}} e^{i\mathbf{k}\cdot\mathbf{r}} \frac{1}{n_{0e}} \int d^3\mathbf{v} v_\| J_0(a_e) h_{e\mathbf{k}}, \quad (276)$$

$$\frac{\delta B_\|}{B_0} = -\frac{\beta_e}{2} \sum_{\mathbf{k}} e^{i\mathbf{k}\cdot\mathbf{r}} \frac{1}{n_{0e}} \int d^3\mathbf{v} \frac{2v_\perp^2}{v_{\text{the}}^2} \frac{J_1(a_e)}{a_e} h_{e\mathbf{k}}, \quad (277)$$

where $\beta_e = \beta_i Z/\tau$. We have discarded the velocity integrals of h_i both because the gyroaveraging makes them subdominant in powers of $(m_e/m_i)^{1/2}$ and because the fluctuations of h_i are damped by collisions [assuming the collisional cutoff given by Eq. (259) lies above the electron gyroscale]. To Eqs. (275-277), we must append the gyrokinetic equation for h_e [Eq. (57) with $s = e$], thus closing the system.

The type of turbulence described by these equations is very similar to that discussed in § 7.10. It is easy to show from Eqs. (275-277) that

$$\frac{\delta B_\perp}{B_0} \sim \frac{\delta B_\|}{B_0} \sim \frac{\beta_e}{k_\perp \rho_e} \frac{e\varphi}{T_{0e}}. \quad (278)$$

Hence the magnetic fluctuations are subdominant in the expression for $\langle\chi\rangle_{\mathbf{R}_e}$ [Eq. (69) with $s = e$ and $a_e \gg 1$], so $\langle\chi\rangle_{\mathbf{R}_e} \simeq \langle\varphi\rangle_{\mathbf{R}_e}$. The electron gyrokinetic equation then is

$$\frac{\partial h_e}{\partial t} + v_\| \frac{\partial h_e}{\partial z} + \frac{c}{B_0}\{\langle\varphi\rangle_{\mathbf{R}_e}, h_e\} = \left(\frac{\partial h_e}{\partial t}\right)_{\text{c}}, \quad (279)$$

where the wave–particle interaction term in the right-hand side has been dropped because it can be shown to be small via the same argument as in § 7.10.2.

Together with Eq. (275), Eq. (279) describes the kinetic cascade of electron entropy from the electron gyroscale down to the scale at which electron collisions can dissipate it into heat. This cascade the result of collisionless damping of KAW at $k_\perp \rho_e \sim 1$, whereby the power in the KAW cascade is converted into the electron-entropy fluctuations: indeed, in the limit $k_\perp \rho_e \gg 1$, the generalized energy is simply

$$W = \int d^3\mathbf{v} \int d^3\mathbf{R}_e \frac{T_{0e} h_e^2}{2 F_{0e}} = W_{h_e} \quad (280)$$

(see Fig. 5).

The same scaling arguments as in § 7.10.2 apply and scaling relations analogous to Eqs. (268-270), and (272) duly follow:

$$h_{e\lambda} \sim \frac{n_{0e}}{v_{\text{the}}^3} \left(\frac{\varepsilon_{\text{KAW}}}{\varepsilon}\right)^{1/3} \left(\frac{1}{\beta_e}\frac{m_e}{m_i}\right)^{1/2} l_0^{-1/3} \rho_e^{1/6} \lambda^{1/6}, \quad (281)$$

$$\Phi_\lambda \sim \left(\frac{\varepsilon_{\text{KAW}}}{\varepsilon}\right)^{1/3} \left(\frac{1}{\beta_e}\frac{m_e}{m_i}\right)^{1/2} v_{\text{the}} l_0^{-1/3} \rho_e^{1/6} \lambda^{7/6}, \quad (282)$$

$$\sim \left(\frac{\varepsilon}{\varepsilon_{\text{KAW}}}\right)^{1/3} \left(\beta_e \frac{m_i}{m_e}\right)^{1/2} \frac{l_0^{1/3} \rho_e^{1/3} \lambda^{1/3}}{v_{\text{the}}}, \quad (283)$$

$$\frac{\delta B_\lambda}{B_0} \sim \left(\frac{\varepsilon_{\text{KAW}}}{\varepsilon}\right)^{1/3} \left(\beta_e \frac{m_e}{m_i}\right)^{1/2} l_0^{-1/3} \rho_e^{-11/6} \lambda^{13/6}, \quad (284)$$

where $l_0 = v_A^3/\varepsilon$, as in § 1.2. The formula for the collisional cutoffs in the wavenumber and velocity space is analogous to Eq. (259):

$$\frac{\delta v_\perp}{v_{\text{th}i}} \sim \frac{1}{k_\perp \rho_i} \sim (\nu_{ei}\tau_{\rho_e})^{3/5}, \quad (285)$$

where τ_{ρ_e} is the cascade time (283) taken at $\lambda = \rho_e$.

7.13. *Validity of Gyrokinetics in the Dissipation Range*

As the kinetic cascade takes the (generalized) energy to ever smaller scales, the frequency ω of the fluctuations increases. In applying the gyrokinetic theory, one must be mindful of the need for this frequency to stay smaller than Ω_i. Using the scaling formulae for the characteristic times of the fluctuations derived above [Eqs. (254), (270) and (283)], we can determine the conditions for $\omega \ll \Omega_i$. Thus, for the gyrokinetic theory to be valid everywhere in the inertial range, we must have

$$k_\perp \rho_i \ll \beta_i^{3/4} \left(\frac{l_0}{\rho_i}\right)^{1/2} \quad (286)$$

at all scales down to $k_\perp \rho_i \sim 1$, i.e., $\rho_i/l_0 \ll \beta_i^{3/2}$, not a very stringent condition.

Below the ion gyroscale, the KAW cascade (§ 7.5) remains in the gyrokinetic regime as long as

$$k_\perp \rho_i \ll \left(\frac{\varepsilon}{\varepsilon_{\text{KAW}}}\right)^{1/4} \beta_i^{3/8}(1+\beta_i)^{1/4}\left(\frac{l_0}{\rho_i}\right)^{1/4} \quad (287)$$

(we are assuming $T_i/T_e \sim 1$ everywhere). The condition for this still to be true at the electron gyroscale is

$$\frac{\rho_i}{l_0} \ll \frac{\varepsilon}{\varepsilon_{\text{KAW}}} \beta_i^{3/2}(1+\beta_i)\left(\frac{m_e}{m_i}\right)^2. \quad (288)$$

The ion entropy fluctuations passively mixed by the KAW turbulence (§ 7.9) satisfy Eq. (287) at all scales down to the ion collisional cutoff [Eq. (259)] if

$$\frac{\lambda_{\text{mfp}i}}{l_0} \ll \left(\frac{\varepsilon}{\varepsilon_{\text{KAW}}}\right)^{3/4} \beta_i^{9/8}(1+\beta_i)^{3/4}\left(\frac{\rho_i}{l_0}\right)^{1/4}. \quad (289)$$

Note that the condition for the ion collisional cutoff to lie above the electron gyroscale is

$$\frac{\lambda_{\text{mfp}i}}{l_0} \ll \left(\frac{\varepsilon}{\varepsilon_{\text{KAW}}}\right)^{1/3} \sqrt{\beta_i}(1+\beta_i)^{1/3}\left(\frac{m_i}{m_e}\right)^{5/6}\left(\frac{\rho_i}{l_0}\right)^{2/3}. \quad (290)$$

In the absence of KAW turbulence, the pure ion-entropy cascade (§ 7.10) remains gyrokinetic for

$$k_\perp \rho_i \ll \beta_i^{3/2}\frac{l_0}{\rho_i}. \quad (291)$$

This is valid at all scales down to the ion collisional cutoff provided $\lambda_{\text{mfp}i}/l_0 \ll \beta_i^3(l_0/\rho_i)$, an extremely weak condition, which is always satisfied. This is because the ion-entropy fluctuations in this case have much lower frequencies than in the KAW regime. The ion collisional cutoff lies above the

electron gyroscale if, similarly to Eq. (290),

$$\frac{\lambda_{\text{mfp}i}}{l_0} \ll \sqrt{\beta_i}\left(\frac{m_i}{m_e}\right)^{5/6}\left(\frac{\rho_i}{l_0}\right)^{2/3}. \quad (292)$$

If the condition (290) is satisfied, all fluctuations of the ion distribution function are damped out above the electron gyroscale. This means that below this scale, we only need the electron gyrokinetic equation to be valid, i.e., $\omega \ll \Omega_e$. The electron-entropy cascade (§ 7.12), whose characteristic timescale is given by Eq. (283), satisfies this condition for

$$k_\perp \rho_e \ll \left(\frac{\varepsilon}{\varepsilon_{\text{KAW}}}\right) \beta_e^{3/2}\left(\frac{m_i}{m_e}\right)^{3/2}\frac{l_0}{\rho_e}. \quad (293)$$

This is valid at all scales down to the electron collisional cutoff [Eq. (285)] provided $\lambda_{\text{mfp}e}/l_0 \ll (\varepsilon/\varepsilon_{\text{KAW}})^2 \beta_e^3(m_i/m_e)^3(l_0/\rho_e)$, which is always satisfied.

Within the formal expansion we have adopted ($k_\perp \rho_i \sim 1$ and $k_\parallel \lambda_{\text{mfp}i} \sim \sqrt{\beta_i}$), it is not hard to see that $\lambda_{\text{mfp}i}/l_0 \sim \epsilon^2$ and $\rho_i/l_0 \sim \epsilon^3$. Since all other parameters (m_e/m_i, β_i, β_e etc.) are order unity with respect to ϵ, all of the above conditions for the validity of the gyrokinetics are asymptotically correct by construction. However, in application to real astrophysical plasmas, one should always check whether this construction holds. For example, substituting the relevant parameters for the solar wind shows that the gyrokinetic approximation is, in fact, likely to start breaking down somewhere between the ion and electron gyroscales (Howes et al. 2008a).[34] This releases a variety of high-frequency wave modes, which may be participating in the turbulent cascade around and below the electron gyroscale (see, e.g., the recent detailed observations of these scales in the magnetosheath by Mangeney et al. 2006; Lacombe et al. 2006 or the early measurements of high-frequency fluctuations in the solar wind by Denskat et al. 1983; Coroniti et al. 1982).

7.14. *Summary*

In this section, we have analyzed the turbulence in the dissipation range, which turned out to have many more essentially kinetic features than the inertial range.

At the ion gyroscale, $k_\perp \rho_i \sim 1$, the kinetic cascade rearranged itself into two distinct components: part of the (generalized) energy arriving from the inertial range was collisionlessly damped, giving rise to a purely kinetic cascade of ion-entropy fluctuations, the rest was converted into a cascade of Kinetic Alfvén Waves (KAW) (Fig. 5; see § 7.1 and § 7.8).

The KAW cascade is described by two fluid-like equations for two scalar functions, the magnetic flux function $\Psi = -A_\parallel/\sqrt{4\pi m_i n_{0i}}$ and the scalar potential, expressed, for continuity with the results of § 5, in terms of the function $\Phi = (c/B_0)\varphi$. The equations are (see § 7.2)

$$\frac{\partial \Psi}{\partial t} = v_A\left(1+\frac{Z}{\tau}\right)\hat{\mathbf{b}}\cdot\nabla\Phi, \quad (294)$$

$$\frac{\partial \Phi}{\partial t} = -\frac{v_A}{2+\beta_i\left(1+Z/\tau\right)}\hat{\mathbf{b}}\cdot\nabla\left(\rho_i^2\nabla_\perp^2\Psi\right), \quad (295)$$

where $\hat{\mathbf{b}}\cdot\nabla = \partial/\partial z + (1/v_A)\{\Psi, \cdots\}$. The density and

---

[34] See this paper also for a set of numerical tests of the validity of gyrokinetics in the dissipation range, a linear theory of the conversion of KAW into ion-cyclotron-damped Bernstein waves, and a discussion of the potential (un)importance of ion cyclotron damping for the dissipation of turbulence.

magnetic-field-strength fluctuations are directly related to the scalar potential:

$$\frac{\delta n_e}{n_{0e}} = -\frac{2}{\sqrt{\beta_i}}\frac{\Phi}{\rho_i v_A}, \quad \frac{\delta B_\parallel}{B_0} = \sqrt{\beta_i}\left(1+\frac{Z}{\tau}\right)\frac{\Phi}{\rho_i v_A}. \quad (296)$$

We call Eqs. (294-296) the *Electron Reduced Magnetohydrodynamics (ERMHD)*.

The ion-entropy cascade is described by the ion gyrokinetic equation:

$$\frac{\partial h_i}{\partial t} + v_\parallel \frac{\partial h_i}{\partial z} + \{\langle\Phi\rangle_{\mathbf{R}_i}, h_i\} = \langle C_{ii}[h_i]\rangle_{\mathbf{R}_i}. \quad (297)$$

The ion distribution function is mixed by the ring-averaged scalar potential and undergoes a cascade both in the velocity and gyrocenter space—this phase-space cascade is essential for the conversion of the turbulent energy into the ion heat, which can ultimately only be done by collisions (see § 7.9).

If the KAW cascade is strong (its power ε_{KAW} is an order-unity fraction of the total injected turbulent power ε), it determines Φ in Eq. (297), so the ion-entropy cascade is passive with respect to the KAW turbulence. Equations (294-295) and (297) form a closed system that determines the three functions Φ, Ψ, h_i, of which the latter is slaved to the first two. One can also compute δn_e and $\delta B_\parallel$, which are proportional to Φ [Eq. (296)]. The generalized energy conserved by these equations is given by Eq. (245).

If the KAW cascade is weak ($\varepsilon_{\text{KAW}} \ll \varepsilon$), the ion-entropy cascade dominates the turbulence in the dissipation range and drives low-frequency mostly electrostatic fluctuations, with a subdominant magnetic component. These are given by the following relations (see § 7.10)

$$\Phi = \frac{\rho_i v_{\text{th}i}}{2(1+\tau/Z)}\sum_{\mathbf{k}} e^{i\mathbf{k}\cdot\mathbf{r}}\frac{1}{n_{0i}}\int d^3\mathbf{v} J_0(a_i)h_{i\mathbf{k}}, \quad (298)$$

$$\frac{\delta n_e}{n_{0e}} = \frac{2Z}{\tau}\frac{\Phi}{\rho_i v_{\text{th}i}}, \quad (299)$$

$$\Psi = \rho_i\sqrt{\beta_i}\sum_{\mathbf{k}} e^{i\mathbf{k}\cdot\mathbf{r}} \times$$

$$\frac{1}{n_{0i}}\int d^3\mathbf{v}\left(\frac{1}{1+Z/\tau}\frac{i}{k_\parallel}\frac{\partial}{\partial t} - v_\parallel\right)\frac{J_0(a_i)}{k_\perp^2 \rho_i^2}h_{i\mathbf{k}}, \quad (300)$$

$$\frac{\delta B_\parallel}{B_0} = -\frac{\beta_i}{2}\sum_{\mathbf{k}} e^{i\mathbf{k}\cdot\mathbf{r}}\frac{1}{n_{0i}}\int d^3\mathbf{v}\frac{2v_\perp^2}{v_{\text{th}i}^2}\frac{J_1(a_i)}{a_i}h_{i\mathbf{k}}, \quad (301)$$

where $a_i = k_\perp v_\perp/\Omega_i$, Equations (297) and (298) form a closed system for Φ and h_i. The rest of the fields, namely δn_e, Ψ and $\delta B_\parallel$, are slaved to h_i via Eqs. (299-301).

The fluid and kinetic models summarized above are valid between the ion and electron gyroscales. Below the electron gyroscale, the collisionless damping of the KAW cascade converts it into a cascade of electron entropy, similar in nature to the ion-entropy cascade (§ 7.12).

The KAW cascade and the low-frequency turbulence associated with the ion-entropy cascade have distinct scaling behaviors. For the KAW cascade, the spectra of the electric, density and magnetic fluctuations are (§ 7.5)

$$E_E(k_\perp) \propto k_\perp^{-1/3}, \quad E_n(k_\perp) \propto k_\perp^{-7/3}, \quad E_B(k_\perp) \propto k_\perp^{-7/3}. \quad (302)$$

For the ion- and electron-entropy cascades (§ 7.9 and § 7.12),

$$E_E(k_\perp) \propto k_\perp^{-4/3}, \quad E_n(k_\perp) \propto k_\perp^{-10/3}, \quad E_B(k_\perp) \propto k_\perp^{-16/3}. \quad (303)$$

We argued in § 7.11 that the observed spectra in the dissipation range of the solar wind could be the result of a superposition of these two cascades, although a number of alternative theories exist (§ 8.2.6).

8. DISCUSSION OF ASTROPHYSICAL APPLICATIONS

We have so far only occasionally referred to some relevant observational evidence for space and astrophysical plasmas. We now discuss in more detail how the theoretical framework laid out above applies to real plasma turbulence in space.

Although we will discuss the interstellar medium, accretion disks and galaxy clusters towards the end of this section, the most rewarding source of observational information about plasma turbulence in astrophysical conditions is the solar wind and the magnetosheath because only there direct in situ measurements of all the interesting quantities are possible. Measurements of the fluctuating magnetic and velocity fields in the solar wind have been available since the 1960s (Coleman 1968) and a vast literature now exists on their spectra, anisotropy, Alfvénic character and many other aspects (a short recent review is Horbury et al. 2005; two long ones are Tu & Marsch 1995; Bruno & Carbone 2005). It is not our aim here to provide a comprehensive survey of what is known about plasma turbulence in the solar wind. Instead, we shall limit our discussion to a few points that we consider important in light of the theoretical framework proposed in this paper.[35] As we do this, we shall provide copious references to the main body of the paper, so this section can be read as a data-oriented guide to it, aimed both at a thorough reader who has arrived here after going through the preceding sections and an impatient one who has skipped to this one hoping to find out whether there is anything of "practical" use in the theoretical developments above.

8.1. *Inertial-Range Turbulence in the Solar Wind*

In the inertial range, i.e., for $k_\perp \rho_i \ll 1$, the solar-wind turbulence should be described by the reduced hybrid fluid-kinetic theory derived in § 5 (KRMHD). Its applicability hinges on three key assumptions: (i) the turbulence is Alfvénic, i.e., consists of small ($\delta B/B_0 \ll 1$) low-frequency ($\omega \sim k_\parallel v_A \ll \Omega_i$) perturbations of an ambient mean magnetic field and corresponding velocity fluctuations; (ii) it is strongly anisotropic, $k_\perp \gg k_\parallel$; (iii) the equilibrium distribution can be approximated or, at least, reasonably modeled by a Maxwellian without loss of essential physics (this will be discussed in § 8.3). If these assumptions are satisfied, KRMHD (summarized in § 5.7) is a rigorous set of dynamical equations for the inertial range, a set of Kolmogorov-style scaling predictions for the Alfvénic component of the turbulence can be produced (the GS theory, reviewed in § 1.2), while to the compressive fluctuations, the considerations of § 6 apply. So let us examine the observational evidence.

8.1.1. *Alfvénic Nature of the Turbulence*

The presence of Alfvén waves in the solar wind was reported already the early works of Unti & Neugebauer (1968) and Belcher & Davis (1971). Alfvén waves are detected already at very low frequencies (large scales)—and, at these

---

[35] An extended quantitative discussion of the applicability of the gyrokinetic theory to the turbulence in the slow solar wind was given by Howes et al. (2008a).

low frequencies, have a k^{-1} spectrum.[36] This spectrum corresponds to a uniform distribution of scales/frequencies of waves launched by the coronal activity of the Sun. Nonlinear interaction of these waves gives rise to an Alfvénic turbulent cascade of the type that was discussed above. The effective outer scale of this cascade can be detected as a spectral break where the k^{-1} scaling steepens to the Kolmogorov slope $k^{-5/3}$ (see Bavassano et al. 1982; Marsch & Tu 1990a; Horbury et al. 1996 for fast-wind results on the spectral break; for a discussion of the effective outer scale in the slow wind at 1 AU, see Howes et al. 2008a). The particular scale at which this happens increases with the distance from the Sun (Bavassano et al. 1982), reflecting the more developed state of the turbulence at later stages of evolution. At 1 AU, the outer scale is roughly in the range of $10^5 - 10^6$ km; the $k^{-5/3}$ range extends down to scales/frequencies that correspond to a few times the ion gyroradius ($10^2 - 10^3$ km; see Table 1).

The range between the outer scale (the spectral break) and the ion gyroscale is the inertial range. In this range, $\delta B/B_0$ decreases with scale because of the steep negative spectral slope. Therefore, the assumption of small fluctuations, $\delta B/B_0 \ll 1$, while not necessarily true at the outer scale, is increasingly better satisfied further into the inertial range (cf. § 1.3).

Are these fluctuations Alfvénic? In a plasma such as the solar wind, they ought to be because, as showed in § 5.3, for $k_\perp \rho_i \ll 1$, these fluctuations are rigorously described by the RMHD equations. The magnetic flux is frozen into the ion motions, so displacing a parcel of plasma should produce a matching (Alfvénic) perturbation of the magnetic field line and vice versa: in an Alfvén wave, $\mathbf{u}_\perp = \pm \delta \mathbf{B}_\perp / \sqrt{4\pi m_i n_{0i}}$. The strongest confirmation that this is indeed true for the inertial-range fluctuations in the solar wind was achieved by Bale et al. (2005), who compared the spectra of electric and magnetic fluctuations and found that they both scale as $k^{-5/3}$ and follow each other with remarkable precision (see Fig. 1). The electric field is a very good measure of the perpendicular velocity field because, for $k_\perp \rho_i \ll 1$, the plasma velocity is the $\mathbf{E} \times \mathbf{B}$ drift velocity, $\mathbf{u}_\perp = c\mathbf{E} \times \hat{\mathbf{z}}/B_0$ (see § 5.4).

This picture of agreement between basic theory and observations is upset in a disturbing fashion by an extraordinary recent result by Chapman & Hnat (2007); Podesta et al. (2006) and J. E. Borovsky (2008, private communication), who claim different spectral indices for velocity and magnetic fluctuations—$k^{-3/2}$ and $k^{-5/3}$, respectively. This result is puzzling because if it is asymptotically correct in the inertial range, it implies either $u_\perp \gg \delta B_\perp$ or $u_\perp \ll \delta B_\perp$ and it is not clear how perpendicular velocity fluctuations in a near-ideal plasma could fail to produce Alfvénic displacements and, therefore, perpendicular magnetic field fluctuations with matching energies. Plausible explanations may be either that the velocity field in these measurements is polluted by a non-Alfvénic component parallel to the magnetic field (although data analysis by Chapman & Hnat 2007 does not support this) or that the flattening of the velocity spectrum is due to some form of a finite-gyroradius effect or even an energy injection into the velocity fluctuations at scales approaching the ion gyroscale (e.g., from the pressure-anisotropy-driven instabili-

ties, § 8.3).

8.1.2. *Energy Spectrum*

How solid is the statement that the observed spectrum has a $k^{-5/3}$ scaling? In individual measurements of the magnetic-energy spectra, very high accuracy is claimed for this scaling: the measured spectral exponent is between 1.6 and 1.7; agreement with Kolmogorov value 1.67 is often reported to be within a few percent (see, e.g., Horbury et al. 1996; Leamon et al. 1998; Bale et al. 2005; Narita et al. 2006; Alexandrova et al. 2008a; Horbury et al. 2008)). There is a somewhat wider scatter of spectral indices if one considers large sets of measurement intervals (Smith et al. 2006), but overall, the observational evidence does not appear to be consistent with a $k_\perp^{-3/2}$ spectrum consistently found in the MHD simulations with a strong mean field (Maron & Goldreich 2001; Müller et al. 2003; Mason et al. 2007; Perez & Boldyrev 2008, 2009; Beresnyak & Lazarian 2008b) and defended on theoretical grounds in the recent modifications of the GS theory by Boldyrev (2006) and by Gogoberidze (2007) (see footnote 10). This discrepancy between observations and simulations remains an unresolved theoretical issue. It is probably best addressed by numerical modeling of the RMHD equations (§ 2.2) and by a detailed comparison of the structure of the Alfvénic fluctuations in such simulations and in the solar wind.

8.1.3. *Anisotropy*

Building up evidence for anisotropy of turbulent fluctuations has progressed from merely detecting their elongation along the magnetic field (Belcher & Davis 1971)—to fitting data to an ad hoc model mixing a 2D perpendicular and a 1D parallel ("slab") turbulent components in some proportion[37] (Matthaeus et al. 1990; Bieber et al. 1996; Dasso et al. 2005; Hamilton et al. 2008)—to formal systematic unbiased analyses showing the persistent presence of anisotropy at all scales (Bigazzi et al. 2006; Sorriso-Valvo et al. 2006)— to direct measurements of three-dimensional correlation functions (Osman & Horbury 2007)—and finally to computing spectral exponents at fixed angles between $\mathbf{k}$ and $\mathbf{B}_0$ (Horbury et al. 2008). The latter authors appear to have achieved the first direct quantitative confirmation of the GS theory by demonstrating that the magnetic-energy spectrum scales as $k_\perp^{-5/3}$ in wavenumbers perpendicular to the mean field and as $k_\parallel^{-2}$ in wavenumbers parallel to it [consistent with the first scaling relation in Eq. (4)]. This is the closest that observations have got to confirming the GS relation $k_\parallel \sim k_\perp^{2/3}$ [see Eq. (5)] in a real astrophysical turbulent plasma.

8.1.4. *Compressive Fluctuations*

According to the theory developed in § 5, the density and magnetic-field-strength fluctuations are passive, energetically decoupled from and mixed by the Alfvénic cascade (§ 5.5; these are slow and entropy modes in the collisional MHD limit—see § 2.4 and § 6.1). These fluctuations are expected to be pressure-balanced, as expressed by Eq. (22) or, more generally in gyrokinetics, by Eq. (67). There is, indeed, strong

---

[36] Inferred from the frequency spectrum f^{-1} via the Taylor (1938) hypothesis, $f \sim \mathbf{k} \cdot \mathbf{V}_{\text{sw}}$, where $\mathbf{V}_{\text{sw}}$ is the mean velocity at which the wind blows past the spacecraft. The Taylor hypothesis is a good assumption for the solar wind because V_{sw} (~ 800 km/s in the fast wind, ~ 300 km/s in the slow wind) is highly supersonic, super-Alfvénic and far exceeds the fluctuating velocities.

[37] These techniques originate from the view of MHD turbulence as a superposition of a 2D turbulence and an admixture of Alfvén waves (Fyfe et al. 1977; Montgomery & Turner 1981). As we discussed in § 1.2, we consider the Goldreich & Sridhar (1995, 1997) view of a critically balanced Alfvénic cascade to be better physically justified.

evidence that magnetic and thermal pressures in the solar wind are anticorrelated, although there are some indications of the presence of compressive, fast-wave-like fluctuations as well (Roberts 1990; Burlaga et al. 1990; Marsch & Tu 1993; Bavassano et al. 2004).

Measurements of density and field-strength fluctuations done by a variety of different methods both at 1 AU (Celnikier et al. 1983, 1987; Marsch & Tu 1990b; Bershadskii & Sreenivasan 2004; Hnat et al. 2005; Kellogg & Horbury 2005; Alexandrova et al. 2008a) and near the Sun (Lovelace et al. 1970; Woo & Armstrong 1979; Coles & Harmon 1989; Coles et al. 1991) show fluctuation levels of order 10% and spectra that appear to have a $k^{-5/3}$ scaling above scales of order $10^2 - 10^3$ km, which approximately corresponds to the ion gyroscale. The Kolmogorov value of the spectral exponent is, as in the case of Alfvénic fluctuations, measured quite accurately in individual cases (1.67 ± 0.03 in Celnikier et al. 1987). Interestingly, the higher-order structure function exponents measured for the magnetic-field strength show that it is a more intermittent quantity than the velocity or the vector magnetic field (i.e., than the Alfvénic fluctuations) and that the scaling exponents are quantitatively very close to the values found for passive scalars in neutral fluids (Bershadskii & Sreenivasan 2004; Bruno et al. 2007). One might argue that this lends some support to the theoretical expectation of passive magnetic-field-strength fluctuations.

Considering that in the collisionless regime these fluctuations are supposed to be subject to strong kinetic damping (§ 6.2.2), the presence of well-developed Kolmogorov-like and apparently undamped turbulent spectra is more surprising than has perhaps been publicly acknowledged. An extended discussion of this issue was given in § 6.3. Without the inclusion of the dissipation effects associated with the finite ion gyroscale, the passive cascade of the density and field strength is purely perpendicular to the (exact) local magnetic field and does not lead to any scale refinement along the field. This implies highly anisotropic field-aligned structures, whose length is determined by the initial conditions (i.e., conditions in the corona). The kinetic damping is inefficient for such fluctuations. While this would seem to explain the presence of fully fledged power-law spectra, it is not entirely obvious that the parallel cascade is really absent once dissipation is taken into account (Lithwick & Goldreich 2001), so the issue is not yet settled. This said, we note that there is plenty of evidence of a high degree of anisotropy and field alignment of the density microstructure in the inner solar wind and outer corona (e.g., Armstrong et al. 1990; Grall et al. 1997; Woo & Habbal 1997). There is also evidence that the local structure of the compressive fluctuations at 1 AU is correlated with the coronal activity, implying some form of memory of initial conditions (Kiyani et al. 2007; Hnat et al. 2007; Wicks et al. 2009).

We note, finally, that whether compressive fluctuations in the inertial range can develop short parallel scales should also tell us how much ion heating can result from their damping (see § 6.2.4).

8.2. Dissipation-Range Turbulence in the Solar Wind and the Magnetosheath

At scales approaching the ion gyroscale, $k_\perp \rho_i \sim 1$, effects associated with the finite extent of ion gyroorbits start to matter. Observationally, this transition manifests itself as a clear break in the spectrum of magnetic fluctuations, with the inertial-range $k^{-5/3}$ scaling replaced by a steeper slope (see Fig. 1). While the electrons at these scales can be treated as an isothermal fluid (as long as we are considering fluctuations above the electron gyroscale, $k_\perp \rho_e \ll 1$; see § 4), the fully gyrokinetic description (§ 3) has to be adopted for the ions. It is, indeed, to understand plasma dynamics at and around $k_\perp \rho_i \sim 1$ that gyrokinetics was first designed in fusion plasma theory (Frieman & Chen 1982; Brizard & Hahm 2007). In order for gyrokinetics and further dissipation-range approximations that follow from it (§ 7) to be a credible approach in the solar wind and other space plasmas, it has to be established that fluctuations at and below the ion gyroscale are still strongly anisotropic, $k_\parallel \ll k_\perp$. If that is the case, then their frequencies ($\omega \sim k_\parallel v_A k_\perp \rho_i$, see § 7.3) will still be smaller than the cyclotron frequency in at least a part of the "dissipation range"[38]—the range of scales $k_\perp \rho_i \gtrsim 1$ (see § 7.13).

Note that additional information about the dissipation-range turbulence can be extracted from the measurements in the magnetosheath—while scales above the ion gyroscale are probably non-universal there, the dissipation range appears to display universal behavior, mostly similar to the solar wind (see, e.g., Alexandrova 2008). This complements the observational picture emerging from the solar-wind data and allows us to learn more as fluctuation amplitudes in the magnetosheath are larger and much smaller scales can be probed than in the solar wind (Mangeney et al. 2006; Lacombe et al. 2006; Alexandrova et al. 2008b).

8.2.1. Anisotropy

We know with a fair degree of certainty that the fluctuations that cascade down to the ion gyroscale from the inertial range are strongly anisotropic (§ 8.1.3). While it appears likely that the anisotropy persists at $k_\perp \rho_i \sim 1$, it is extremely important to have a clear verdict on this assumption from solar wind measurements. While Leamon et al. (1998) and, more recently, Hamilton et al. (2008) did present some evidence that magnetic fluctuations in the solar wind have a degree of anisotropy below the ion gyroscale, no definitive study similar to Horbury et al. (2008) or Bigazzi et al. (2006); Sorriso-Valvo et al. (2006) exists as yet. In the magnetosheath, where the dissipation-range scales are easier to measure than in the solar wind, recent analysis by Sahraoui et al. (2006); Alexandrova et al. (2008b) does show evidence of strong anisotropy.

Besides confirming the presence of the anisotropy, it would be interesting to study its scaling characteristics: e.g., check the scaling prediction $k_\parallel \sim k_\perp^{1/3}$ [Eq. (241); see also § 7.9.4 and § 7.10.3] in a similar fashion as the GS relation $k_\parallel \sim k_\perp^{2/3}$ [Eq. (5)] was corroborated by Horbury et al. (2008).

In this paper, we have proceeded on the assumption that the anisotropy, and, therefore, low frequencies ($\omega \ll \Omega_i$) do characterize fluctuations in the dissipation range—or, at least, that the low-frequency anisotropic fluctuations are a significant energy cascade channel and can be considered decoupled from any possible high-frequency dynamics.

8.2.2. Transition at the Ion Gyroscale: Collisionless Damping and Heating

---

[38] This term, customary in the space-physics literature, is somewhat of a misnomer because, as we have seen in § 7, rich dissipationless turbulent dynamics are present in this range alongside what is normally thought of as dissipation.

If the fluctuations at the ion gyroscale have $k_\parallel \ll k_\perp$ and $\omega \ll \Omega_i$ (§ 8.2.1), they are not subject to the cyclotron resonance ($\omega - k_\parallel v_\parallel = \pm \Omega_i$), but are subject to the Landau one ($\omega = k_\parallel v_\parallel$). Alfvénic fluctuations at the ion gyroscale are no longer decoupled from the compressive fluctuations and can be Landau-damped (§ 7.1). It seems plausible that it is the inflow of energy from the Alfvénic cascade that accounts for a pronounced local flattening of the spectrum of density fluctuations in the solar wind observed just above the ion gyroscale (Woo & Armstrong 1979; Celnikier et al. 1983, 1987; Coles & Harmon 1989; Marsch & Tu 1990b; Coles et al. 1991; Kellogg & Horbury 2005).[39]

In energetic terms, Landau damping amounts to a redistribution of generalized energy from electromagnetic fluctuations to entropy fluctuations (§ 3.4, § 7.8). This gives rise to the entropy cascade, ultimately transferring the Landau-damped energy into ion heat (§ 3.5, § 7.9 and § 7.10). However, only part of the inertial-range cascade is so damped because an alternative, electron, cascade channel exists: the kinetic Alfvén waves (§§ 7.2-7.8). The energy transferred into the KAW-like fluctuations can cascade to the electron gyroscale, where it is Landau damped on electrons, converting first into the electron entropy cascade and then electron heat (§ 7.12).

Thus, the transition at the ion gyroscale ultimately decides in what proportion the turbulent energy arriving from the inertial range is distributed between the ion and electron heat. How the fraction of power going into either depends on parameters—β_i, T_i/T_e, amplitudes, . . .—is a key unanswered question both in space and astrophysical (see, e.g., § 8.5) plasmas. Gyrokinetics appears to be an ideal tool for addressing this question both analytically and numerically (Howes et al. 2008b). Within the framework outlined in this paper, the minimal model appropriate for studying the transition at the ion gyroscale is the system of equations for isothermal electrons and gyrokinetic ions derived in § 4 (it is summarized in § 4.9).

8.2.3. *Ion Gyroscale vs. Ion Inertial Scale*

It is often assumed in the space physics literature that it is at the ion inertial scale, $d_i = \rho_i/\sqrt{\beta_i}$, rather than at the ion gyroscale ρ_i that the spectral break between the inertial and dissipation range occurs. The distinction between d_i and ρ_i becomes noticeable when β_i is significantly different from unity, a relatively rare occurrence in the solar wind. While some attempts to determine at which of these two scales a spectral break between the inertial and dissipation ranges occurs have produced claims that d_i is a more likely candidate (Smith et al. 2001), more comprehensive studies of the available data sets conclude basically that it is hard to tell (Leamon et al. 2000; Markovskii et al. 2008).

In the gyrokinetic approach advocated in this paper, the ion inertial scale does not play a special role (see § 7.1). The only parameter regime in which d_i does appear as a special scale is $T_i \ll T_e$ ("cold ions"), when the Hall MHD approximation can be derived in a systematic way (see Appendix E). This, however, is not the right limit for the solar wind or most other astrophysical plasmas of interest because ions are rarely cold. Hall MHD is discussed further in § 8.2.6 and Appendix E.

8.2.4. *KAW Turbulence*

[39] Celnikier et al. (1987) proposed that the flattening might be a k^{-1} spectrum analogous to Batchelor's spectrum of passive scalar variance in the viscous-convective range. We think this analogy cannot apply because density is not passive at or below the ion gyroscale.

If gyrokinetics is valid at scales $k_\perp \rho_i \gtrsim 1$ (i.e., if $k_\parallel \ll k_\perp$, $\omega \ll \Omega_i$ and it is acceptable to at least model the equilibrium distribution as a Maxwellian; see § 8.3), the electromagnetic fluctuations below the ion gyroscale will be described by the fluid approximation that we derived in § 7.2 and referred to ERMHD. The wave solutions of this system of equations are the kinetic Alfvén waves (§§ 7.3-7.4) and it is possible to argue for a GS-style critically balanced cascade of KAW-like electromagnetic fluctuations (§ 7.5) between the ion and electron gyroscales (Landau damped on electrons at $k_\perp \rho_e \sim 1$; the expression for the KAW damping rate in the gyrokinetic limit is given in Howes et al. 2006; see also Fig. 8).

Individual KAW have, indeed, been detected in space plasmas (e.g., Grison et al. 2005). What about KAW turbulence? How does one tell whether any particular spectral slope one is measuring corresponds to the KAW cascade or fits some alternative scheme for the dissipation-range turbulence (§ 8.2.6)? It appears to be a sensible program to look for specific relationships between different fields predicted by theory (§ 7.2) and for the corresponding spectral slopes and scaling relations for the anisotropy (§ 7.5). This means that simultaneous measurements of magnetic, electric, density and magnetic-field-strength fluctuations are needed.

For the solar wind, the spectra of electric and magnetic fluctuations below the ion gyroscale reported by Bale et al. (2005) are consistent with the $k^{-1/3}$ and $k^{-7/3}$ scalings predicted for an anisotropic critically balanced KAW cascade (§ 7.5; see Fig. 1 for theoretical scaling fits superimposed on a plot taken from Bale et al. 2005; note, however, that Bale et al. 2005 themselves interpreted their data in a somewhat different way and that their resolution was in any case not sufficient to be sure of the scalings). They were also able to check that their fluctuations satisfied the KAW dispersion relation—for critically balanced fluctuations, this is, indeed, plausible. Magnetic-fluctuation spectra recently reported by Alexandrova et al. (2008a) are only slightly steeper than the theoretical $k^{-7/3}$ KAW spectrum. These authors also find a significant amount of magnetic-field-strength fluctuations in the dissipation range, with a spectrum that follows the same scaling—this is again consistent with the theoretical picture of KAW turbulence [see Eq. (223)]. Measurements reported by Czaykowska et al. (2001); Alexandrova et al. (2008b) for the magnetosheath appear to present a similar picture.

The density spectra measured by Celnikier et al. (1983, 1987) steepen below the ion gyroscale following the flattened segment around $k_\perp \rho_i \sim 1$ (discussed in § 8.2.2). For a KAW cascade, the density spectrum should be $k^{-7/3}$ (§ 7.5); without KAW, $k^{-10/3}$ (§ 7.10.2). The slope observed in the papers cited above appears to be somewhat shallower even than k^{-2} (cf. a similar result by Spangler & Gwinn 1990 for the ISM; see § 8.4.1), but, given imperfect resolution, neither seriously in contradiction with the prediction based on the KAW cascade, nor sufficient to corroborate it. Unfortunately, we have not found published simultaneous measurements of density- and magnetic- or electric-fluctuation spectra.

8.2.5. *Variability of the Spectral Slope*

While many measurements consistent with the KAW picture can be found, there are also many in which the spectra are much steeper (Denskat et al. 1983; Leamon et al. 1998). Analysis of a large set of measurements of the magnetic-fluctuation spectra in the dissipation range of the solar wind reveals a wide spread in the spectral indices: roughly between

−1 and −4 (Smith et al. 2006). There is evidence of a weak positive correlation between steeper dissipation-range spectra and higher ion temperatures (Leamon et al. 1998) or higher cascade rates calculated from the inertial range (Smith et al. 2006). This suggests that a larger amount of ion heating may correspond to a fully or partially suppressed KAW cascade, which is in line with our view of the ion heating and the KAW cascade as the two competing channels of the overall kinetic cascade (§ 7.8). With a weakened KAW cascade, all or part of the dissipation range would be dominated by the ion entropy cascade—a purely kinetic phenomenon manifested by predominantly electrostatic fluctuations and very steep magnetic-energy spectra (§ 7.10). This might account both for the steepness of the observed spectra and for the spread in their indices (§ 7.11), although many other theories exist (see § 8.2.6).

While we may thus have a plausible argument, this is not yet a satisfactory quantitative theory that would allow us to predict when the KAW cascade is present and when it is not or what dissipation-range spectrum should be expected for given values of the solar-wind parameters (β_i, T_i/T_e, etc.). Resolution of this issue again appears to hinge on the question of how much turbulent power is diverted into the ion entropy cascade (equivalently, into ion heat) at the ion gyroscale (see § 8.2.2).

8.2.6. *Alternative Theories of the Dissipation Range*

A number of alternative theories and models have been put forward to explain the observed spectral slopes (and their variability) in the dissipation range. It is not our aim to review or critique them all in detail, but perhaps it is useful to provide a few brief comments about some of them in light of the theoretical framework constructed in this paper.

This entire theoretical framework hinges on adopting gyrokinetics as a valid description or, at least, a sensible model that does not miss any significant channels of energy cascade and dissipation. While we obviously believe this to be the right approach, it is worth spelling out what effects are left out "by construction."

Parallel Alfvén-wave cascade and ion cyclotron damping. — The use of gyrokinetics assumes that fluctuations stay anisotropic at all scales, $k_\parallel \ll k_\perp$, and, therefore, $\omega \ll \Omega_i$, so the cyclotron resonances are ordered out. However, if one insists on routing the Alfvén-wave energy into a parallel cascade, e.g., by forcibly setting $k_\perp = 0$, it is possible to construct a weak turbulence theory in which it is dissipated by the ion cyclotron damping (Yoon & Fang 2008). Numerical simulations of 3D MHD turbulence do not support the possibility of a parallel Alfvén-wave cascade (Shebalin et al. 1983; Oughton et al. 1994; Cho & Vishniac 2000; Maron & Goldreich 2001; Cho et al. 2002; Müller et al. 2003). Solar-wind evidence that the perpendicular cascade dominates is quite strong for the inertial range (§ 8.1.3) and less so for the dissipation range (§ 8.2.1). While, as stated in § 8.2.1, one cannot yet definitely claim that observations tell us that $\omega \ll \Omega_i$ at $k_\perp \rho_i \sim 1$, it has been argued that observations do not appear to be consistent with cyclotron damping being the main mechanism for the dissipation of the inertial-range Alfvénic turbulence at the ion gyroscale (Leamon et al. 1998, 2000; Smith et al. 2001). Ion-cyclotron resonance could conceivably be reached somewhere in the dissipation range (see § 7.13). At this point gyrokinetics will formally break down, although, as argued by Howes et al. (2008a, see their § 3.6), this does not necessarily mean that ion cyclotron damping will become the dominant dissipation

channel for the turbulence.

Parallel whistler cascade. — A parallel magnetosonic/whistler cascade eventually damped by the electron cyclotron resonance (Stawicki et al. 2001) is also excluded in the construction of gyrokinetics. The whistler cascade has been given some consideration in the Hall MHD approximation (further discussed at the end of this section). Both weak-turbulence theory (Galtier 2006) and 3D numerical simulations (Cho & Lazarian 2004) concluded that, like in MHD, the turbulent cascade is highly anisotropic, with perpendicular energy transfer dominating over the parallel one.[40] The same conclusion appears to have been reached in recent 2D kinetic PIC simulations by Gary et al. (2008); Saito et al. (2008). Thus, the turbulence again seems to be driven into the gyrokinetically accessible regime.

While theory and numerical simulations appear to make arguing in favor of a parallel cascade and cyclotron heating difficult, there exists some observational evidence in support of them, especially for the near-Sun solar wind (e.g., Harmon & Coles 2005). Thus, the presence or relative importance of the cyclotron heating in the solar wind and, more generally, the mechanism(s) responsible for the observed perpendicular ion heating (Marsch et al. 1983) remain a largely open problem. Besides the theories mentioned above, many other ideas have been proposed, some of which attempted to reconcile the dominance of the low-frequency perpendicular cascade with the possibility of cyclotron heating (e.g., Chandran 2005b; Markovskii et al. 2006; see Hollweg 2008 for a concise recent review of the problem).

Mirror cascade. — Sahraoui et al. (2006) analyzed a set of Cluster multi-spacecraft measurements in the magnetosheath and reported a broad power-law ($\sim k^{-8/3}$) spectrum of mirror structures at and below the ion gyroscale. They claim that these are *not* KAW-like fluctuations because their frequency is zero in the plasma frame. Although these structures are highly anisotropic with $k_\parallel \ll k_\perp$, they cannot be described by the gyrokinetic theory in its present form because $\delta B_\parallel / B_0$ is very large ($\sim 40\%$, occasionally reaching unity) and because the particle trapping by fluctuations, which is likely to be important in the nonlinear physics of the mirror instability (Kivelson & Southwood 1996; Pokhotelov et al. 2008; Rincon et al. 2009), is ordered out in gyrokinetics. Thus, if a "mirror cascade" exists, it is not captured in our description. More generally, the effect of the pressure-anisotropy-driven instabilities on the turbulence in the dissipation range is a wide open area, requiring further analytical effort (see § 8.3).

If $k_\parallel \ll k_\perp$, $\omega \ll \Omega_i$, and $\delta B/B_0 \ll 1$ are accepted for the dissipation range and plasma instabilities at the ion gyroscale (§ 8.3) are ignored, the formal gyrokinetic theory and its asymptotic consequences derived above should hold. There are two essential features of the linear physics at and below the ion gyroscale that must play some role: the collisionless (Landau) damping and the dispersive nature of the wave solutions (see Fig. 8 and § 7.3; cf., e.g., Leamon et al. 1999; Stawicki et al. 2001). Both of these features have been employed to explain the spectral break at the ion gyroscale and the spectral slopes below it.

---

[40] It is possible to produce a parallel cascade artificially by running 1D simulations (Matthaeus et al. 2008b).

Landau damping and instrumental effects. — In most of our discussion, (§ 7, §§ 8.2.4-8.2.5), we effectively assumed that the Landau damping is only important at $k_\perp \rho_i \sim 1$ and $k_\perp \rho_e \sim 1$, but not in between, so we could talk about asymptotic scalings and dissipationless cascades. However, as was noted in § 7.6, a properly asymptotic scaling behavior in the dissipation range is probably impossible in nature because the scale separation between the ion and electron gyroscales is only about $(m_i/m_e)^{1/2} \simeq 43$. In particular, there is not always a wide scale interval where the kinetic damping is negligibly small (especially at low β_i; see Fig. 8; cf. Leamon et al. 1999). Howes et al. (2008a) proposed a model of how the presence of damping combined with instrumental effects (a resolution floor) could lead to measured spectra that look like power laws steeper than $k^{-7/3}$, with the effective spectral exponent depending on plasma parameters (we refer the reader to that paper for a discussion of how this compares with previous models of a similar kind, e.g., Li et al. 2001). A key physical assumption of theirs and similar models is that the amount of power drained from the Alfvén-wave and KAW cascades into the ion heat is set by the strength of the *linear* damping. Whether this is justified is not yet clear.

Hall and Electron MHD. — If Landau damping is deemed unimportant in some part of the dissipation range (which can be true in some regimes; see Fig. 8 and Howes et al. 2006, 2008a,b) and the wave dispersion is considered to be the salient feature, it might appear that a fluid, rather than kinetic, description should be sufficient. Hall MHD (Mahajan & Yoshida 1998) or its $kd_i \gg 1$ limit the Electron MHD (Kingsep et al. 1990) have been embraced by many authors as such a description, suitable both for analytical arguments (Goldreich & Reisenegger 1992; Krishan & Mahajan 2004; Gogoberidze 2005; Galtier & Bhattacharjee 2003; Galtier 2006; Alexandrova et al. 2008a) and numerical simulations (Biskamp et al. 1996, 1999; Ghosh et al. 1996; Ng et al. 2003; Cho & Lazarian 2004; Shaikh & Zank 2005; Galtier & Buchlin 2007; Matthaeus et al. 2008b).

To what extent does this constitute an approach *alternative* to (and better than?) gyrokinetics (as suggested, e.g., by Matthaeus et al. 2008b)? For fluctuations with $k_\parallel \ll k_\perp$, Hall MHD is merely a particular limit of gyrokinetics: $\beta_i \ll 1$ and $T_i/T_e \ll 1$ (cold-ion limit; see Appendix E). If $k_\parallel$ is not small compared to $k_\perp$, then the gyrokinetics is not valid, while Hall MHD continues to describe the cold-ion limit correctly (e.g., Ito et al. 2004; Hirose et al. 2004), capturing in particular the whistler branch of the dispersion relation. However, as we have already mentioned above, the dominance of the perpendicular energy transfer ($k_\parallel \ll k_\perp$) is supported both by weak-turbulence theory for Hall MHD (Galtier 2006) and by 3D numerical simulations of the Electron MHD (Cho & Lazarian 2004).

Thus, the gyrokinetic theory and its rigorous limits, such as ERMHD (§ 7.2), supersede Hall MHD for anisotropic turbulence. Since ions are generally not cold in the solar wind (or any other plasma discussed here), Hall MHD is not formally a relevant approximation. It also entirely misses the kinetic damping and the associated entropy cascade channel leading to particle heating (§ 7.1, § 7.9 and § 7.10). However, Hall MHD does capture the Alfvén waves becoming dispersive and numerical simulations of it do show a spectral break, although, technically speaking, at the wrong scale (d_i instead of ρ_i; see § 7.1). Although Hall MHD cannot be rigorously used as quantitative theory of the spectral break and the asso-

ciated change in the nature of the turbulent cascade, the Hall MHD equations in the limit $kd_i \gg 1$ are mathematically similar to our ERMHD equations (see § 7.2 and Appendix E) to within constant coefficients probably not essential for qualitative models of turbulence. Therefore, results of numerical simulations of Hall and Electron MHD cited above are directly useful for understanding the KAW cascade—and, indeed, in the limit $kd_i \gg 1$, $kd_e \ll 1$, they are mostly consistent with the scaling arguments of § 7.5.

Alfvén vortices. — Finally we mention an argument pertaining to the dissipation-range spectra that is not based on energy cascades at all. Based on the evidence of Alfvén vortices in the magnetosheath, Alexandrova (2008) speculated that steep power-law spectra observed in the dissipation range at least in some cases could reflect the geometry of the ion-gyroscale structures rather than a local energy cascade. If Alfvén vortices are a common feature, this possibility cannot be excluded. However, the resulting geometrical spectra are quite steep (k^{-4} and steeper), so they can become important only if the KAW cascade is weak or suppressed—somewhat similarly to the steep spectra associated with the entropy cascade (§ 7.11).

8.3. *Is Equilibrium Distribution Isotropic and Maxwellian?*

In rigorous theoretical terms, the weakest point of this paper is the use of a Maxwellian equilibrium. Formally, this is only justified when the collisions are weak but not too weak: we ordered the collision frequency as similar to the fluctuation frequency [Eq. (49)]. This degree of collisionality is sufficient to prove that a Maxwellian equilibrium distribution $F_{0s}(v)$ does indeed emerge in the lowest order of the gyrokinetic expansion (Howes et al. 2006). This argument works well for plasmas such as the ISM (§ 8.4), where collisions are weak ($\lambda_{\text{mfp}i} \gg \rho_i$) but non-negligible ($\lambda_{\text{mfp}i} \ll L$). In space plasmas, the mean free path is of the order of 1 AU—the distance between the Sun and the Earth (see Table 1). Strictly speaking, in so highly collisionless a plasma, the equilibrium distribution does not have to be either Maxwellian or isotropic.

The conservation of the first adiabatic invariant, $\mu = v_\perp^2/2B$, suggests that temperature anisotropy with respect to the magnetic-field direction ($T_{0\perp} \neq T_{0\parallel}$) may exist. When the relative anisotropy is larger than (roughly) $1/\beta_i$, it triggers several very fast growing plasma instabilities: most prominently the firehose ($T_{0\perp} < T_{0\parallel}$) and mirror ($T_{0\perp} > T_{0\parallel}$) modes (e.g., Gary et al. 1976). Their growth rates peak around the ion gyroscale, thus giving rise to additional energy injection at $k_\perp \rho_i \sim 1$.

No definitive analytical theory of how these fluctuations saturate, cascade and affect the equilibrium distribution has been proposed. It appears to be a reasonable expectation that the fluctuations resulting from temperature anisotropy will saturate by limiting this anisotropy. This idea has some support in solar-wind observations: while the degree of anisotropy of the core particle distribution functions varies considerably between data sets, the observed anisotropies do seem to populate the part of the parameter plane ($T_{0\perp}/T_{0\parallel}, \beta_i$) circumscribed in a rather precise way by the marginal stability boundaries for the mirror and firehose (Gary et al. 2001; Kasper et al. 2002; Marsch et al. 2004; Hellinger et al. 2006; Matteini et al. 2007).[41]

---

[41] Note that Kellogg et al. (2006) measure the electric-field fluctuations

If we want to study turbulence in data sets that do not lie too close to these stability boundaries, assuming an isotropic Maxwellian equilibrium distribution [Eq. (54)] is probably an acceptable simplification, although not an entirely rigorous one. Further theoretical work is clearly possible on this subject: thus, it is not a problem to formulate gyrokinetics with an arbitrary equilibrium distribution (Frieman & Chen 1982) and starting from that, once can generalize the results of this paper (for the KRMHD system, § 5, this has been done by Chen et al. 2009). Treating the instabilities themselves might prove more difficult, requiring the gyrokinetic ordering to be modified and the expansion carried to higher orders to incorporate features that are not captured by gyrokinetics, e.g., short parallel scales (Rosin et al. 2009), particle trapping (Pokhotelov et al. 2008; Rincon et al. 2009), or nonlinear finite-gyroradius effects (Califano et al. 2008). Note that the theory of the dissipation-range turbulence will probably need to be modified to account for the additional energy injection from the instabilities and for the (yet unclear) way in which this energy makes its way to dissipation and into heat.

Besides the anisotropies, the particle distribution functions in the solar wind (especially the electron one) exhibit non-Maxwellian suprathermal tails (see Maksimovic et al. 2005; Marsch 2006, and references therein). These contain small ($\sim 5\%$ of the total density) populations of energetic particles. Both the origin of these particles and their effect on turbulence have to be modeled kinetically. Again, it is possible to formulate gyrokinetics for general equilibrium distributions of this kind and examine the interaction between them and the turbulent fluctuations, but we leave such a theory outside the scope of this paper.

Thus, much remains to be done to incorporate realistic equilibrium distribution functions into the gyrokinetic description of the solar wind plasma. In the meanwhile, we believe that the gyrokinetic theory based on a Maxwellian equilibrium distribution as presented in this paper, while idealized and imperfect, is nevertheless a step forward in the analytical treatment of the space-plasma turbulence compared to the fluid descriptions that have prevailed thus far.

8.4. *Interstellar Medium*

While the solar wind is unmatched by other astrophysical plasmas in the level of detail with which turbulence in it can be measured, the interstellar medium (ISM) also offers an observer a number of ways of diagnosing plasma turbulence, which, in the case of the ISM, is thought to be primarily excited by supernova explosions (Norman & Ferrara 1996). The accuracy and resolution of this analysis are due to improve rapidly thanks to many new observatories, e.g., LOFAR,[42] Planck (Enßlin et al. 2006), and, in more distant future, the SKA (Lazio et al. 2004).

The ISM is a spatially inhomogeneous environment consisting of several phases that have different temperatures, densities and degrees of ionization (Ferrière 2001).[43] We will use the Warm ISM phase (see Table 1) as our fiducial interstellar plasma and discuss briefly what is known about the two main observationally accessible quantities—the electron density and magnetic fields—and how this information fits into the theoretical framework proposed here.

8.4.1. *Electron Density Fluctuations*

The electron-density fluctuations inferred from the interstellar scintillation measurements appear to have a spectrum with an exponent $\simeq -1.7$, consistent with the Kolmogorov scaling (Armstrong et al. 1981, 1995; Lazio et al. 2004; see, however, dissenting evidence by Smirnova et al. 2006, who claim a spectral exponent closer to -1.5). This holds over about 5 decades of scales: $\lambda \in (10^5, 10^{10})$ km. Other observational evidence at larger and smaller scales supports the case for this presumed inertial range to be extended over as many as 12 decades: $\lambda \in (10^2, 10^{15})$ km, a fine example of scale separation that prompted an impressed astrophysicist to dub the density scaling "The Great Power Law in the Sky." The upper cutoff here is consistent with the estimates of the supernova scale of order 100 pc—presumably the outer scale of the turbulence (Norman & Ferrara 1996) and also roughly the scale height of the galactic disk (obviously the upper bound on the validity of any homogeneous model of the ISM turbulence). The lower cutoff is an estimate for the inner scale below which the logarithmic slope of the density spectrum steepens to about -2 (Spangler & Gwinn 1990).

Higdon (1984) was the first to realize that the electron-density fluctuations in the ISM could be attributed to a cascade of a passive tracer mixed by the ambient turbulence (the MHD entropy mode; see § 2.6). This idea was brought to maturity by Lithwick & Goldreich (2001), who studied the passive cascades of the slow and entropy modes in the framework of the GS theory (see also Maron & Goldreich 2001). If the turbulence is assumed anisotropic, as in the GS theory, the passive nature of the density fluctuations with respect to the decoupled Alfvén-wave cascade becomes a rigorous result both in MHD (§ 2.4) and, as we showed above, in the more general gyrokinetic description appropriate for weakly collisional plasmas (§ 5.5). Anisotropy of the electron-density fluctuations in the ISM is, indeed, observationally supported (Wilkinson et al. 1994; Trotter et al. 1998; Rickett et al. 2002; Dennett-Thorpe & de Bruyn 2003; Heyer et al. 2008, see also Lazio et al. 2004 for a concise discussion), although detailed scale-by-scale measurements are not currently possible.

If the underlying Alfvén-wave turbulence in the ISM has a $k_\perp^{-5/3}$ spectrum, as predicted by GS, so should the electron density (see § 2.6). As we discussed in § 6.3, the physical nature of the inner scale for the density fluctuations depends on whether they have a cascade in $k_\parallel$ and are efficiently damped when $k_\parallel \lambda_{\mathrm{mfp}i} \sim 1$ or fail to develop small parallel scales and can, therefore, reach $k_\perp \rho_i \sim 1$. The observationally estimated inner scale is consistent with the ion gyroscale, $\rho_i \sim 10^3$ km (see Table 1; note that the ion inertial scale $d_i = \rho_i / \sqrt{\beta_i}$ is similar to ρ_i at the moderate values of β_i characteristic of the ISM—see further discussion of the (ir)relevance of d_i in § 7.1, § 8.2.3 and Appendix E). However, since the mean free path in the ISM is not huge (Table 1), it is not possible to distinguish this from the perpendicular cutoff $k_\perp^{-1} \sim \lambda_{\mathrm{mfp}i}^{3/2} L^{-1/2} \sim 500$ km implied by the parallel cutoff at $k_\parallel \lambda_{\mathrm{mfp}i} \sim 1$ [see Eq. (220)], as advocated by Lithwick & Goldreich (2001). Note that the relatively short mean free path means that much of the scale range spanned by the Great Power Law in the Sky is, in fact, well described by the MHD approximation either with adiabatic (§ 2) or isothermal (§ 6.1 and Appendix D) electrons.

Below the ion gyroscale, the -2 spectral exponent reported

---

in the ion-cyclotron frequency range, estimate the resulting velocity-space diffusion and argue that it is sufficient to isotropize the ion distribution

[42] http://www.lofar.org

[43] And, therefore, different degrees of importance of the neutral particles and the associated ambipolar damping effects—these will not be discussed here; see Lithwick & Goldreich 2001.

by Spangler & Gwinn (1990) is measured sufficiently imprecisely to be consistent with the $-7/3$ expected for the density fluctuations in the KAW cascade (§ 7.5). However, given the high degree of uncertainty about what happens in this "dissipation range" even in the much better resolved case of the solar wind (§ 8.2), it would probably be wise to reserve judgment until better data are available.

8.4.2. *Magnetic Fluctuations*

The second main observable type of turbulent fluctuations in the ISM are the magnetic fluctuations, accessible indirectly via the measurements of the Faraday rotation of the polarization angle of the pulsar light travelling through the ISM. The structure function of the rotation measure (RM) should have the Kolmogorov slope of $2/3$ if the magnetic fluctuations are due to Alfvénic turbulence described by the GS theory. There is a considerable uncertainty in interpreting the available data, primarily due to insufficient spatial resolution (rarely better than a few parsec). Structure function slopes consistent with $2/3$ have been reported (Minter & Spangler 1996), but, depending on where one looks, shallower structure functions that seem to steepen at scales of a few parsec are also observed (Haverkorn et al. 2004).

A recent study by Haverkorn et al. (2005) detected an interesting trend: the RM structure functions computed for regions that lie in the galactic spiral arms are nearly perfectly flat down to the resolution limit, while in the interarm regions, they have detectable slopes (although these are mostly shallower that $2/3$). Observations of magnetic fields in external galaxies also reveal a marked difference in the magnetic-field structure between arms and interarms: the spatially regular (mean) fields are stronger in the interarms, while in the arms, the stochastic fields dominate (Beck 2007). This qualitative difference between the magnetic-field structure in the arms and interarms has been attributed to smaller effective outer scale in the arms (~ 1 pc, compared to $\sim 10^2$ pc in the interarms; see Haverkorn et al. 2008) or to the turbulence in the arms and interarms belonging to the two distinct asymptotic regimes described in § 1.3: closer to the anisotropic Alfvénic turbulence with a strong mean field in the interarms and to the isotropic saturated state of small-scale dynamo in the arms (Schekochihin et al. 2007).

8.5. *Accretion Disks*

Accretion of plasma onto a central black hole or neutron star is responsible for many of the most energetic phenomena observed in astrophysics (see, e.g., Narayan & Quataert 2005 for a review). It is now believed that a linear instability of differentially rotating plasmas—the magnetorotational instability (MRI)—amplifies magnetic fields and gives rise to MHD turbulence in astrophysical disks (Balbus & Hawley 1998). Magnetic stresses due to this turbulence transport angular momentum, allowing plasma to accrete. The MRI converts the gravitational potential energy of the inflowing plasma into turbulence at the outer scale that is comparable to the scale height of the disk. This energy is then cascaded to small scales and dissipated into heat—powering the radiation that we see from accretion flows. Fluid MHD simulations show that the MRI-generated turbulence in disks is subsonic and has $\beta \sim 10-100$. Thus, on scales much smaller than the scale height of the disk, homogeneous turbulence in the parameter regimes considered in this paper is a valid idealization and the kinetic models developed above should represent a step forward compared to the purely fluid approach.

Turbulence is not yet directly observable in disks, so models of turbulence are mostly used to produce testable predictions of observable properties of disks such as their X-ray and radio emission. One of the best observed cases is the (presumed) accretion flow onto the black hole coincident with the radio source Sgr A* in the center of our Galaxy (see review by Quataert 2003).

Depending on the rate of heating and cooling in the inflowing plasma (which in turn depend on accretion rate and other properties of the system under consideration), there are different models that describe the physical properties of accretion flows onto a central object. In one class of models, a geometrically thin optically thick accretion disk (Shakura & Sunyaev 1973), the inflowing plasma is cold and dense and well described as an MHD fluid. When applied to Sgr A*, these models produce a prediction for its total luminosity that is several orders of magnitude larger than observed. Another class of models, which appears to be more consistent with the observed properties of Sgr A*, is called radiatively inefficient accretion flows (RIAFs; see Rees et al. 1982; Narayan & Yi 1995 and review by Quataert 2003 of the applications and observational constraints in Sgr A*). In these models, the inflowing plasma near the black hole is believed to adopt a two-temperature configuration, with the ions ($T_i \sim 10^{11} - 10^{12}$ K) hotter than the electrons ($T_e \sim 10^9 - 10^{11}$ K).[44] The electron and ion thermodynamics decouple because the densities are so low that the temperature equalization time $\sim \nu_{ie}^{-1}$ is longer than the time for the plasma to flow into the black hole. Thus, like the solar wind, RIAFs are macroscopically collisionless plasmas (see Table 1 for plasma parameters in the Galactic center; note that these parameters are so extreme that the gyrokinetic description, while probably better than the fluid one, cannot be expected to be rigorously valid; at the very least, it needs to be reformulated in a relativistic form). At the high temperatures appropriate to RIAFs, electrons radiate energy much more efficiently than the ions (by virtue of their much smaller mass) and are, therefore, expected to contribute dominantly to the observed emission, while the thermal energy of the ions is swallowed by the black hole. Since the plasma is collisionless, the electron heating by turbulence largely determines the thermodynamics of the electrons and thus the observable properties of RIAFs. The question of which fraction of the turbulent energy goes into ion and which into electron heating is, therefore, crucial for understanding accretion flows—and the answer to this question depends on the detailed properties of the small-scale kinetic turbulence (e.g., Quataert & Gruzinov 1999; Sharma et al. 2007), as well as on the linear properties of the collisionless MRI (Quataert et al. 2002; Sharma et al. 2003).

Since all of the turbulent power coming down the cascade must be dissipated into either ion or electron heat, it is really the amount of generalized energy diverted at the ion gyroscale into the ion entropy cascade (§§ 7.8-7.9) that decides how much energy is left to heat the electrons via the KAW cascade (§§ 7.2-7.5, § 7.12). Again, as in the case of the solar wind (§ 8.2.2 and § 8.2.5), the transition around the ion gyroscale from the Alfvénic turbulence at $k_\perp \rho_i \ll 1$ to the KAW turbulence at $k_\perp \rho_i \gg 1$ emerges as a key unsolved problem.

8.6. *Galaxy Clusters*

---

[44] It is partly with this application in mind that we carried the general temperature ratio in our calculations; see footnote 17.

Galaxy clusters are the largest plasma objects in the Universe. Like the other examples discussed above, the intracluster plasma is in the weakly collisional regime (see Table 1). Fluctuations of electron density, temperature and of magnetic fields are measured in clusters by X-ray and radio observatories, but the resolution is only just enough to claim that a fairly broad scale range of fluctuations exists (Schuecker et al. 2004; Vogt & Enßlin 2005). No power-law scalings have yet been established beyond reasonable doubt.

What fundamentally hampers quantitative modeling of turbulence and related effects in clusters is that we do not have a definite theory of the basic properties of the intracluster medium: its (effective) viscosity, magnetic diffusivity or thermal conductivity. In a weakly collisional and strongly magnetized plasma, all of these depend on the structure of the magnetic field (Braginskii 1965), which is shaped by the turbulence. If (or at scales where) a reasonable *a priori* assumption can be made about the field structure, further analytical progress is possible: thus, the theoretical models presented in this paper assume that the magnetic field is a sum of a slowly varying in space "mean field" and small low-frequency perturbations ($\delta B \ll B_0$).

In fact, since clusters do not have mean fields of any magnitude that could be considered dynamically significant, but do have stochastic fields, the outer-scale MHD turbulence in clusters falls into the weak-mean-field category (see § 1.3). The magnetic field should be highly filamentary, organized in long folded direction-reversing structures. It is not currently known what determines the reversal scale.[45] Observations, while tentatively confirming the existence of very long filaments (Clarke & Enßlin 2006), suggest that the reversal scale is much larger than the ion gyroscale: thus, the magnetic-energy spectrum for the Hydra A cluster core reported by Vogt & Enßlin (2005) peaks at around 1 kpc, compared to $\rho_i \sim 10^5$ km. Below this scale, an Alfvén-wave cascade should exist (as is, indeed, suggested by Vogt & Enßlin's spectrum being roughly consistent with $k^{-5/3}$ at scales below the peak). As these scales are collisionless ($\lambda_{\mathrm{mfp}i} \sim 100$ pc in the cores and ~ 10 kpc in the bulk of the clusters), it is to this turbulence that the theory developed in this paper should be applicable.

Another complication exists, similar to that discussed in § 8.3: pressure anisotropies could give rise to fast plasma instabilities whose growth rate peaks just above the ion gyroscale. As was pointed out by Schekochihin et al. (2005), these are, in fact, an inevitable consequence of any large-scale fluid motions that change the strength of the magnetic field. Although a number of interesting and plausible arguments can be made about the way the instabilities might determine the magnetic-field structure (Schekochihin & Cowley 2006; Schekochihin et al. 2008a; Rosin et al. 2009; Rincon et al. 2009), it is not currently understood how the small-scale fluctuations resulting from these instabilities coexist with the Alfvénic cascade.

The uncertainties that result from this imperfect understanding of the nature of the intracluster medium are exemplified by the problem of its thermal conductivity. The magnetic-field reversal scale in clusters is certainly not larger than the electron diffusion scale, $(m_i/m_e)^{1/2}\lambda_{\mathrm{mfp}i}$, which varies from a few kpc in the cores to a few hundred kpc in the bulk. Therefore, one would expect that the approximation of isothermal electron fluid (§ 4) should certainly apply at all scales below the reversal scale, where $\delta B \ll B_0$ presumably holds. Even this, however, is not absolutely clear. One could imagine the electrons being effectively adiabatic if (or in the regions where) the plasma instabilities give rise to large fluctuations of the magnetic field ($\delta B/B_0 \sim 1$) at the ion gyroscale reducing the mean free path to $\lambda_{\mathrm{mfp}i} \sim \rho_i$ (Schekochihin et al. 2008a; Rosin et al. 2009; Rincon et al. 2009). Such fluctuations cannot be described by the gyrokinetics in its current form. The current state of the observational evidence does not allow one to exclude either of these possibilities. Both isothermal (Fabian et al. 2006; Sanders & Fabian 2006) and non-isothermal (Markevitch & Vikhlinin 2007) coherent structures that appear to be shocks are observed. Disordered fluctuations of temperature can also be detected, which allows one to infer an upper limit for the scale at which the isothermal approximation can start being valid: thus, Markevitch et al. (2003) find temperature variations at all scales down to $\sim$ 100 kpc, which is the statistical limit that defines the spatial resolution of their temperature map. In none of these or similar measurements is the magnetic field data available that would make possible a pointwise comparison of the magnetic and thermal structure.

Because of this lack of information about the state of the magnetized plasma in clusters, theories of the intracluster medium are not sufficiently constrained by observations, so no one theory is in a position to prevail. This uncertain state of affairs might be improved by analyzing the observationally much better resolved case of the solar wind, which should be quite similar to the intracluster medium at very small scales (except for somewhat lower values of β_i in the solar wind).

9. CONCLUSION

In this paper, we have considered magnetized plasma turbulence in the astrophysically prevalent regime of weak collisionality. We have shown how the energy injected at the outer scale cascades in phase space, eventually to increase the entropy of the system and heat the particles. In the process, we have explained how one combines plasma physics tools—in particular, the gyrokinetic theory—with the ideas of a turbulent cascade of energy to arrive at a hierarchy of tractable models of turbulence in various physically distinct scale intervals. These models represent the branching pathways of a generalized energy cascade in phase space (the "kinetic cascade"; see Fig. 5) and make explicit the "fluid" and "kinetic" aspects of plasma turbulence.

A detailed outline of these developments was given in the Introduction. Intermediate technical summaries were provided in § 4.9, § 5.7, and § 7.14. An astrophysical summary and discussion of the observational evidence was given in § 8, with a particular emphasis on space plasmas (§§ 8.1-8.3). Our view of how the transformation of the large-scale turbulent energy into heat occurs was encapsulated in the concept of a kinetic cascade of generalized energy. It was previewed in § 1.4 and developed quantitatively in §§ 3.4-3.5, § 4.7, § 5.6, §§ 6.2.3-6.2.5, §§ 7.8-7.12, Appendices D.2 and E.2.

Following a series of analytical contributions that set up a theoretical framework for astrophysical gyrokinetics (Howes et al. 2006, 2008a; Schekochihin et al. 2007, 2008b, and this paper), an extensive program of fluid, hybrid fluid-kinetic, and fully gyrokinetic[46] numerical simulations of magnetized plasma turbulence is now underway (for the first re-

---

[45] See Schekochihin & Cowley (2006) for a detailed presentation of our views on the interplay between turbulence, magnetic field and plasma effects in cluster; for further discussions and disagreements, see Enßlin & Vogt (2006); Subramanian et al. (2006); Brunetti & Lazarian (2007).

sults of this program, see Howes et al. 2008b; Tatsuno et al. 2009a,b). Careful comparisons of the fully gyrokinetic simulations with simulations based on the more readily computable models derived in this paper (RMHD—§ 2, isothermal electron fluid—§ 4, KRMHD—§ 5, ERMHD—§ 7, HRMHD—Appendix E) as well as with the numerical studies based on various Landau fluid (Snyder et al. 1997; Goswami et al. 2005; Ramos 2005; Sharma et al. 2006, 2007; Passot & Sulem 2007) and gyrofluid (Hammett et al. 1991; Dorland & Hammett 1993; Snyder & Hammett 2001; Scott 2007) closures appear to be the way forward in developing a comprehensive numerical model of the kinetic turbulent cascade from the outer scale to the electron gyroscale. Of the many astrophysical plasmas to which these results apply, the solar wind and, perhaps, the magnetosheath, due to the high quality of turbulence measurements possible in them, appear to be the most suitable test beds for direct and detailed quantitative comparisons of the theory and simulation results with observational evidence. The objective of all this work remains a quantitative characterization of the scaling-range properties (spectra, anisotropy, nature of fluctuations and their interactions), the ion and electron heating, and the transport properties of the magnetized plasma turbulence.

[46] Using the publicly available GS2 code (developed originally for fusion applications; see http://gs2.sourceforge.net) and the purpose-built AstroGK code (see http://www.physics.uiowa.edu/~ ghowes/astrogk/).

APPENDIX

A. BRAGINSKII'S TWO-FLUID EQUATIONS AND REDUCED MHD

Here we explain how the standard one-fluid MHD equations used in § 2 and the collisional limit of the KRMHD system (§ 6.1, derived in Appendix D) both emerge as limiting cases of the two-fluid theory. For the case of anisotropic fluctuations, $k_\parallel / k_\perp \ll 1$, all of this can, of course, be derived from gyrokinetics, but it is useful to provide a connection to the more well known fluid description of collisional plasmas.

A.1. *Two-Fluid Equations*

The rigorous derivation of the fluid equations for a collisional plasma was done in the classic paper of Braginskii (1965). His equations, valid for $\omega / \nu_{ii} \ll 1$, $k_\parallel \lambda_{\mathrm{mfp}i} \ll 1$, $k_\perp \rho_i \ll 1$ (see Fig. 3), evolve the densities n_s, mean velocities $\mathbf{u}_s$ and temperatures T_s of each plasma species ($s = i, e$):

$$\left(\frac{\partial}{\partial t} + \mathbf{u}_s \cdot \nabla \right) n_s = -n_s \nabla \cdot \mathbf{u}_s, \tag{A1}$$

$$m_s n_s \left(\frac{\partial}{\partial t} + \mathbf{u}_s \cdot \nabla \right) \mathbf{u}_s = -\nabla p_s - \nabla \cdot \hat{\Pi}_s + q_s n_s \left(\mathbf{E} + \frac{\mathbf{u}_s \times \mathbf{B}}{c} \right) + \mathbf{F}_s, \tag{A2}$$

$$\frac{3}{2} n_s \left(\frac{\partial}{\partial t} + \mathbf{u}_s \cdot \nabla \right) T_s = -p_s \nabla \cdot \mathbf{u}_s - \nabla \cdot \Gamma_s - \hat{\Pi}_s : \nabla \mathbf{u}_s + Q_s, \tag{A3}$$

where $p_s = n_s T_s$ and the expressions for the viscous stress tensor $\hat{\Pi}_s$, the friction force $\mathbf{F}_s$, the heat flux Γ_s and the interspecies heat exchange Q_s are given in Braginskii (1965). Equations (A1-A3) are complemented with the quasi-neutrality condition, $n_e = Z n_i$, and the Faraday and Ampère laws, which are (in the non-relativistic limit)

$$\frac{\partial \mathbf{B}}{\partial t} = -c \nabla \times \mathbf{E}, \quad \mathbf{j} = e n_e (\mathbf{u}_i - \mathbf{u}_e) = \frac{c}{4\pi} \nabla \times \mathbf{B}. \tag{A4}$$

Because of quasi-neutrality, we only need one of the continuity equations, say the ion one. We can also use the electron momentum equation [Eq. (A2), $s = e$] to express $\mathbf{E}$, which we then substitute into the ion momentum equation and the Faraday law. The resulting system is

$$\frac{d\rho}{dt} = -\rho \nabla \cdot \mathbf{u}, \tag{A5}$$

$$\rho \frac{d\mathbf{u}}{dt} = -\nabla \left(p + \frac{B^2}{8\pi} \right) - \nabla \cdot \hat{\Pi} + \frac{\mathbf{B} \cdot \nabla \mathbf{B}}{4\pi} - \frac{Z m_e}{m_i} \rho \left(\frac{\partial}{\partial t} + \mathbf{u}_e \cdot \nabla \right) \mathbf{u}_e, \tag{A6}$$

$$\frac{\partial \mathbf{B}}{\partial t} = \nabla \times \left[\mathbf{u} \times \mathbf{B} - \frac{\mathbf{j} \times \mathbf{B}}{e n_e} + \frac{c \nabla p_e}{e n_e} + \frac{c \nabla \cdot \hat{\Pi}_e}{e n_e} - \frac{c \mathbf{F}_e}{e n_e} + \frac{c m_e}{e} \left(\frac{\partial}{\partial t} + \mathbf{u}_e \cdot \nabla \right) \mathbf{u}_e \right], \tag{A7}$$

where $\rho = m_i n_i$, $\mathbf{u} = \mathbf{u}_i$, $p = p_i + p_e$, $\hat{\Pi} = \hat{\Pi}_i + \hat{\Pi}_e$, $\mathbf{u}_e = \mathbf{u} - \mathbf{j}/en_e$, $n_e = Zn_i$, $d/dt = \partial/\partial t + \mathbf{u} \cdot \nabla$. The ion and electron temperatures continue to satisfy Eq. (A3).

A.2. *Strongly Magnetized Limit*

In this form, the two-fluid theory starts resembling the standard one-fluid MHD, which was our starting point in § 2: Eqs. (A5-A7) already look similar to the continuity, momentum and induction equations. The additional terms that appear in these equations and the temperature equations (A3) are brought under control by considering how they depend on a number of dimensionless parameters: ω/ν_{ii}, $k_\parallel \lambda_{\mathrm{mfp}i}$, $k_\perp \rho_i$, $(m_e/m_i)^{1/2}$. While all these are small in Braginskii's calculation, no assumption is made as to how they compare to each other. We now specify that

$$\frac{\omega}{\nu_{ii}} \sim \frac{k_\parallel \lambda_{\mathrm{mfp}i}}{\sqrt{\beta_i}}, \quad k_\perp \rho_i \ll k_\parallel \lambda_{\mathrm{mfp}i} \sim \sqrt{\frac{m_e}{m_i}} \ll 1 \tag{A8}$$

(see Fig. 4). Note that the first of these relations is equivalent to assuming that the fluctuation frequencies are Alfvénic—the same assumption as in gyrokinetics [Eq. (49)]. The second relation in Eq. (A8) will be referred to by us as the *strongly magnetized limit*. Under the assumptions (A8), the two-fluid equations reduce to the following closed set:[47]

$$\frac{d\rho}{dt} = -\rho \nabla \cdot \mathbf{u}, \tag{A10}$$

$$\rho \frac{d\mathbf{u}}{dt} = -\nabla \left[p + \frac{B^2}{8\pi} + \frac{1}{3} \rho \nu_{\parallel i} \left(\hat{\mathbf{b}}\hat{\mathbf{b}} : \nabla \mathbf{u} - \frac{1}{3} \nabla \cdot \mathbf{u} \right) \right] + \nabla \cdot \left[\hat{\mathbf{b}}\hat{\mathbf{b}} \rho \nu_{\parallel i} \left(\hat{\mathbf{b}}\hat{\mathbf{b}} : \nabla \mathbf{u} - \frac{1}{3} \nabla \cdot \mathbf{u} \right) \right] + \frac{\mathbf{B} \cdot \nabla \mathbf{B}}{4\pi}, \tag{A11}$$

$$\frac{d\mathbf{B}}{dt} = \mathbf{B} \cdot \nabla \mathbf{u} - \mathbf{B} \nabla \cdot \mathbf{u}, \tag{A12}$$

$$\frac{dT_i}{dt} = -\frac{2}{3} T_i \nabla \cdot \mathbf{u} + \frac{1}{\rho} \nabla \cdot \left(\hat{\mathbf{b}} \rho \kappa_{\parallel i} \hat{\mathbf{b}} \cdot \nabla T_i \right) - \nu_{ie}(T_i - T_e) + \frac{2}{3} m_i \nu_{\parallel i} \left(\hat{\mathbf{b}}\hat{\mathbf{b}} : \nabla \mathbf{u} - \frac{1}{3} \nabla \cdot \mathbf{u} \right)^2, \tag{A13}$$

$$\frac{dT_e}{dt} = -\frac{2}{3} T_e \nabla \cdot \mathbf{u} + \frac{1}{\rho} \nabla \cdot \left(\hat{\mathbf{b}} \rho \kappa_{\parallel e} \hat{\mathbf{b}} \cdot \nabla T_e \right) - \frac{1}{Z} \nu_{ie}(T_e - T_i), \tag{A14}$$

where $\nu_{\parallel i} = 0.90 v_{\mathrm{th}i} \lambda_{\mathrm{mfp}i}$ is the parallel ion viscosity, $\kappa_{\parallel i} = 2.45 v_{\mathrm{th}i} \lambda_{\mathrm{mfp}i}$ parallel ion thermal diffusivity, $\kappa_{\parallel e} = 1.40 v_{\mathrm{th}e} \lambda_{\mathrm{mfp}e} \sim \left(Z^2/\tau^{5/2} \right) (m_i/m_e)^{1/2} \kappa_{\parallel i}$ parallel electron thermal diffusivity [here $\lambda_{\mathrm{mfp}i} = v_{\mathrm{th}i}/\nu_{ii}$ with ν_{ii} defined in Eq. (52)], and ν_{ie} ion–electron collision rate [defined in Eq. (51)]. Note that the last term in Eq. (A13) represents the viscous heating of the ions.

A.3. *One-Fluid Equations (MHD)*

If we now restrict ourselves to the low-frequency regime where ion–electron collisions dominate over all other terms in the ion-temperature equation (A13),

$$\frac{\omega}{\nu_{ie}} \sim \frac{k_\parallel \lambda_{\mathrm{mfp}i}}{\sqrt{\beta_i}} \sqrt{\frac{m_i}{m_e}} \ll 1 \tag{A15}$$

[see Eqs. (A8) and (51)], we have, to lowest order in this new subsidiary expansion, $T_i = T_e = T$. We can now write $p = (n_i + n_e)T = (1 + Z)\rho T/m_i$ and, adding Eqs. (A13) and (A14), find the equation for pressure:

$$\frac{dp}{dt} + \frac{5}{3} p \nabla \cdot \mathbf{u} = \nabla \cdot \left(\hat{\mathbf{b}} n_e \kappa_{\parallel e} \hat{\mathbf{b}} \cdot \nabla T \right) + \frac{2}{3} m_i \nu_{\parallel i} \left(\hat{\mathbf{b}}\hat{\mathbf{b}} : \nabla \mathbf{u} - \frac{1}{3} \nabla \cdot \mathbf{u} \right)^2, \tag{A16}$$

where we have neglected the ion thermal diffusivity compared to the electron one, but kept the ion heating term to maintain energy conservation. Equation (A16) together with Eqs. (A10-A12) constitutes the conventional one-fluid MHD system. With the dissipative terms [which are small because of Eq. (A15)] neglected, this was the starting point for our fluid derivation of RMHD in § 2.

Note that the electrons in this regime are adiabatic because the electron thermal diffusion is small

$$\frac{\kappa_{\parallel e} k_\parallel^2}{\omega} \sim k_\parallel \lambda_{\mathrm{mfp}i} \sqrt{\beta_i} \sqrt{\frac{m_i}{m_e}} \ll 1, \tag{A17}$$

---

[47] The structure of the momentum equation (A11) is best understood by realizing that $\rho\nu_{\parallel i} \left(\hat{\mathbf{b}}\hat{\mathbf{b}} : \nabla \mathbf{u} - \nabla \cdot \mathbf{u}/3 \right) = p_\perp - p_\parallel$, the difference between the perpendicular and parallel (ion) pressures. Since the total pressure is $p = (2/3)p_\perp + (1/3)p_\parallel$, Eq. (A11) can be written

$$\rho \frac{d\mathbf{u}}{dt} = -\nabla \left(p_\perp + \frac{B^2}{8\pi} \right) + \nabla \cdot \left[\hat{\mathbf{b}}\hat{\mathbf{b}} \left(p_\perp - p_\parallel \right) \right] + \frac{\mathbf{B} \cdot \nabla \mathbf{B}}{4\pi}. \tag{A9}$$

This is the general form of the momentum equation that is also valid for collisionless plasmas, when $k_\perp \rho_i \ll 1$ but $k_\parallel \lambda_{\mathrm{mfp}i}$ is order unity or even large. Equation (A9) together with the continuity equation (A11), the induction equation (A12) and a kinetic equation for the particle distribution function (from the solution of which $p_\perp$ and $p_\parallel$ are determined) form the system known as Kinetic MHD (KMHD, see Kulsrud 1964, 1983). The collisional limit, $k_\parallel \lambda_{\mathrm{mfp}i} \ll 1$, of KMHD is again Eqs. (A10-A14).

provided Eq. (A15) holds and β_i is order unity. If we take $\beta_i \gg 1$ instead, we can still satisfy Eq. (A15), so $T_i = T_e$ follows from the ion temperature equation (A13) and the one-fluid equations emerge as an expansion in high β_i. However, these equations now describe two physical regimes: the adiabatic long-wavelength regime that satisfies Eq. (A17) and the shorter-wavelength regime in which $(m_e/m_i)^{1/2}/\sqrt{\beta_i} \ll k_\| \lambda_{\mathrm{mfp}i} \ll (m_e/m_i)^{1/2}\sqrt{\beta_i}$, so the fluid is isothermal, $T = T_0 = \mathrm{const}$, $p = [(1+Z)T_0/m_i]\rho = c_s^2 \rho$ [Eq. (9) holds with $\gamma = 1$].

A.4. *Two-Fluid Equations with Isothermal Electrons*

Let us now consider the regime in which the coupling between the ion and electron temperatures is small and the electron diffusion is large [the limit opposite to Eqs. (A15) and (A17)]:

$$\frac{\omega}{\nu_{ie}} \sim \frac{k_\| \lambda_{\mathrm{mfp}i}}{\sqrt{\beta_i}} \sqrt{\frac{m_i}{m_e}} \gg 1, \qquad \frac{\kappa_{\|e}k_\|^2}{\omega} \sim k_\| \lambda_{\mathrm{mfp}i} \sqrt{\beta_i} \sqrt{\frac{m_i}{m_e}} \gg 1, \tag{A18}$$

Then the electrons are isothermal, $T_e = T_{0e} = \mathrm{const}$ (with the usual assumption of stochastic field lines, so $\hat{\mathbf{b}} \cdot \nabla T_e = 0$ implies $\nabla T_e = 0$, as in § 4.4), while the ion temperature satisfies

$$\frac{dT_i}{dt} = -\frac{2}{3}T_i \nabla \cdot \mathbf{u} + \frac{1}{\rho}\nabla \cdot \left(\hat{\mathbf{b}}\rho\kappa_{\|i}\hat{\mathbf{b}} \cdot \nabla T_i\right) + \frac{2}{3}m_i \nu_{\|i}\left(\hat{\mathbf{b}}\hat{\mathbf{b}} : \nabla \mathbf{u} - \frac{1}{3}\nabla \cdot \mathbf{u}\right)^2. \tag{A19}$$

Equation (A19) together with Eqs. (A10-A12) and $p = \rho(T_i + ZT_{0e})/m_i$ are a closed system that describes an MHD-like fluid of adiabatic ions and isothermal electrons. Applying the ordering of § 2.1 to these equations and carrying out an expansion in $k_\|/k_\perp \ll 1$ entirely analogously to the way it was done in § 2, we arrive at the RMHD equations (17-18) for the Alfvén waves and the following system for the compressive fluctuations (slow and entropy modes):

$$\frac{d}{dt}\left(\frac{\delta\rho}{\rho_0} - \frac{\delta B_\|}{B_0}\right) + \hat{\mathbf{b}} \cdot \nabla u_\| = 0, \tag{A20}$$

$$\frac{du_\|}{dt} - v_A^2 \hat{\mathbf{b}} \cdot \nabla \frac{\delta B_\|}{B_0} = \nu_{\|i}\hat{\mathbf{b}} \cdot \nabla \left(\hat{\mathbf{b}} \cdot \nabla u_\| + \frac{1}{3}\frac{d}{dt}\frac{\delta\rho}{\rho_0}\right), \tag{A21}$$

$$\frac{d}{dt}\frac{\delta T_i}{T_{0i}} - \frac{2}{3}\frac{d}{dt}\frac{\delta\rho}{\rho_0} = \kappa_{\|i}\hat{\mathbf{b}} \cdot \nabla \left(\hat{\mathbf{b}} \cdot \nabla \frac{\delta T_i}{T_{0i}}\right), \tag{A22}$$

and the pressure balance

$$\left(1 + \frac{Z}{\tau}\right)\frac{\delta\rho}{\rho_0} = -\frac{\delta T_i}{T_{0i}} - \frac{2}{\beta_i}\left[\frac{\delta B_\|}{B_0} + \frac{1}{3v_A^2}\nu_{\|i}\left(\hat{\mathbf{b}} \cdot \nabla u_\| + \frac{1}{3}\frac{d}{dt}\frac{\delta\rho}{\rho_0}\right)\right]. \tag{A23}$$

Recall that these equations, being the consequence of Braginskii's two-fluid equations (§ A.1), are an expansion in $k_\| \lambda_{\mathrm{mfp}i} \ll 1$ correct up to first order in this small parameter. Since the dissipative terms are small, we can replace $(d/dt)\delta\rho/\rho_0$ in the viscous terms of Eqs. (A21) and (A23) by its value computed from Eqs. (A20), (A22) and (A23) in neglect of dissipation: $(d/dt)\delta\rho/\rho_0 = -\hat{\mathbf{b}} \cdot \nabla u_\|/(1+c_s^2/v_A^2)$ [cf. Eq. (25)], where the speed of sound c_s is defined by Eq. (166). Substituting this into Eqs. (A21) and (A23), we recover the collisional limit of KRMHD derived in Appendix D, see Eqs. (D18-D20) and (D22).

B. COLLISIONS IN GYROKINETICS

The general collision operator that appears in Eq. (36) is (Landau 1936)

$$\left(\frac{\partial f_s}{\partial t}\right)_c = 2\pi \ln\Lambda \sum_{s'} \frac{q_s^2 q_{s'}^2}{m_s}\frac{\partial}{\partial \mathbf{v}} \cdot \int d^3\mathbf{v}' \frac{1}{w}\left(\hat{\mathbf{I}} - \frac{\mathbf{ww}}{w^2}\right) \cdot \left[\frac{1}{m_s}f_{s'}(\mathbf{v}')\frac{\partial f_s(\mathbf{v})}{\partial \mathbf{v}} - \frac{1}{m_{s'}}f_s(\mathbf{v})\frac{\partial f_{s'}(\mathbf{v}')}{\partial \mathbf{v}'}\right], \tag{B1}$$

where $\mathbf{w} = \mathbf{v} - \mathbf{v}'$ and $\ln\Lambda$ is the Coulomb logarithm. We now take into account the expansion of the distribution function (54), use the fact that the collision operator vanishes when it acts on a Maxwellian, and retain only first-order terms in the gyrokinetic expansion. This gives us the general form of the collision term in Eq. (57): it is the ring-averaged linearized form of the Landau collision operator (B1), $(\partial h_s/\partial t)_c = \langle C_s[h]\rangle_{\mathbf{R}_s}$, where

$$C_s[h] = 2\pi \ln\Lambda \sum_{s'} \frac{q_s^2 q_{s'}^2}{m_s}\frac{\partial}{\partial \mathbf{v}} \cdot \int d^3\mathbf{v}' \frac{1}{w}\left(\hat{\mathbf{I}} - \frac{\mathbf{ww}}{w^2}\right) \cdot \left[F_{0s'}(v')\left(\frac{\mathbf{v}'}{T_{0s'}} + \frac{1}{m_s}\frac{\partial}{\partial \mathbf{v}}\right)h_s(\mathbf{v}) - F_{0s}(v)\left(\frac{\mathbf{v}}{T_{0s}} + \frac{1}{m_{s'}}\frac{\partial}{\partial \mathbf{v}'}\right)h_{s'}(\mathbf{v}')\right]. \tag{B2}$$

Note that the velocity derivatives are taken at constant $\mathbf{r}$, i.e., the gyrocenter distribution functions that appear in the integrand should be understood as $h_s(\mathbf{v}) \equiv h_s(t, \mathbf{r} + \mathbf{v}_\perp \times \hat{\mathbf{z}}/\Omega_s, v_\perp, v_\|)$. The explicit form of the gyrokinetic collision operator can be derived in k space as follows:

$$\left(\frac{\partial h_s}{\partial t}\right)_c = \left\langle C_s\left[\sum_{\mathbf{k}} e^{i\mathbf{k}\cdot\mathbf{R}}h_{\mathbf{k}}\right]\right\rangle_{\mathbf{R}_s} = \sum_{\mathbf{k}}\left\langle e^{i\mathbf{k}\cdot\mathbf{r}}C_s\left[e^{-i\mathbf{k}\cdot\rho}h_{\mathbf{k}}\right]\right\rangle_{\mathbf{R}_s} = \sum_{\mathbf{k}} e^{i\mathbf{k}\cdot\mathbf{R}_s}\left\langle e^{i\mathbf{k}\cdot\rho_s(\mathbf{v})}C_s\left[e^{-i\mathbf{k}\cdot\rho}h_{\mathbf{k}}\right]\right\rangle, \tag{B3}$$

where $\rho_s(\mathbf{v}) = -\mathbf{v}_\perp \times \hat{\mathbf{z}}/\Omega_s$ and $\mathbf{R}_s = \mathbf{r} - \rho_s(\mathbf{v})$. Angle brackets with no subscript refer to averages over the gyroangle ϑ of quantities that do not depend on spatial coordinates. Note that inside the operator $C_s[\ldots]$, h occurs both with index s and velocity $\mathbf{v}$ and with index s' and velocity $\mathbf{v}'$ (over which summation/integration is done). In the latter case, $\rho = \rho_{s'}(\mathbf{v}') = -\mathbf{v}'_\perp \times \hat{\mathbf{z}}/\Omega_{s'}$ in the exponential factor inside the operator.

Most of the properties of the collision operator that are used in the main body of this paper to order the collision terms can be established in general, already on the basis of Eq. (B3) (§§ B.1-B.2). If the explicit form of the collision operator is required, we could, in principle, perform the ring average on the linearized operator C [Eq. (B2)] and derive an explicit form of $(\partial h_s/\partial t)_c$. In practice, in gyrokinetics, as in the rest of plasma physics, the full collision operator is only used when it is absolutely unavoidable. In most problems of interest, further simplifications are possible: the same-species collisions are often modeled by simpler operators that share the full collision operator's conservation properties (§ B.3), while the interspecies collision operators are expanded in the electron–ion mass ratio (§ B.4).

B.1. *Velocity-Space Integral of the Gyrokinetic Collision Operator*

Many of our calculations involve integrating the gyrokinetic equation (57) over the velocity space while keeping $\mathbf{r}$ constant. Here we estimate the size of the integral of the collision term when $k_\perp \rho_s \ll 1$. Using Eq. (B3),

$$\int d^3\mathbf{v} \left\langle \left(\frac{\partial h_s}{\partial t}\right)_c \right\rangle_\mathbf{r} = \sum_\mathbf{k} \int d^3\mathbf{v}\, e^{i\mathbf{k}\cdot\mathbf{r} - i\mathbf{k}\cdot\rho_s(\mathbf{v})} \left\langle e^{i\mathbf{k}\cdot\rho_s(\mathbf{v})} C_s \left[e^{-i\mathbf{k}\cdot\rho}h_\mathbf{k}\right] \right\rangle$$

$$= \sum_\mathbf{k} e^{i\mathbf{k}\cdot\mathbf{r}} 2\pi \int_0^\infty dv_\perp\, v_\perp \int_{-\infty}^{+\infty} dv_\| \left\langle e^{-i\mathbf{k}\cdot\rho_s(\mathbf{v})}\right\rangle \left\langle e^{i\mathbf{k}\cdot\rho_s(\mathbf{v})} C_s \left[e^{-i\mathbf{k}\cdot\rho}h_\mathbf{k}\right]\right\rangle$$

$$= \sum_\mathbf{k} e^{i\mathbf{k}\cdot\mathbf{r}} \int d^3\mathbf{v} \left\langle e^{-i\mathbf{k}\cdot\rho_s(\mathbf{v})}\right\rangle e^{i\mathbf{k}\cdot\rho_s(\mathbf{v})} C_s \left[e^{-i\mathbf{k}\cdot\rho}h_\mathbf{k}\right] = \sum_\mathbf{k} e^{i\mathbf{k}\cdot\mathbf{r}} \int d^3\mathbf{v}\, J_0(a_s)\, e^{i\mathbf{k}\cdot\rho_s(\mathbf{v})} C_s \left[e^{-i\mathbf{k}\cdot\rho}h_\mathbf{k}\right]$$

$$= \sum_\mathbf{k} e^{i\mathbf{k}\cdot\mathbf{r}} \int d^3\mathbf{v} \left[1 - i\mathbf{k}\cdot\frac{\mathbf{v}_\perp \times \hat{\mathbf{z}}}{\Omega_s} - \frac{1}{2}\left(\mathbf{k}\cdot\frac{\mathbf{v}_\perp \times \hat{\mathbf{z}}}{\Omega_s}\right)^2 - \frac{1}{4}\left(\frac{k_\perp v_\perp}{\Omega_s}\right)^2 + \ldots\right] C_s \left[e^{-i\mathbf{k}\cdot\rho}h_\mathbf{k}\right]. \tag{B4}$$

Since the (linearized) collision operator C_s conserves particle number, the first term in the expansion vanishes. The operator $C_s = C_{ss} + C_{ss'}$ is a sum of the same-species collision operator [the $s' = s$ part of the sum in Eq. (B2)] and the interspecies collision operator (the $s' \neq s$ part). The former conserves total momentum of the particles of species s, so it gives no contribution to the second term in the expansion in Eq. (B4). Therefore,

$$\int d^3\mathbf{v} \left\langle \langle C_{ss}[h_s]\rangle_{\mathbf{R}_s}\right\rangle_\mathbf{r} \sim \nu_{ss} k_\perp^2 \rho_s^2 \delta n_s. \tag{B5}$$

The interspecies collisions do contribute to the second term in Eq. (B4) due to momentum exchange with the species s'. This contribution is readily inferred from the standard formula for the linearized friction force (see, e.g., Helander & Sigmar 2002):

$$m_s \int d^3\mathbf{v}\, \mathbf{v}\, C_{ss'}\left[e^{-i\mathbf{k}\cdot\rho}h_\mathbf{k}\right] = -\int d^3\mathbf{v}\, \mathbf{v} \left[m_s \nu_S^{ss'}(v) e^{-i\mathbf{k}\cdot\rho_s(\mathbf{v})} h_{s\mathbf{k}} + m_{s'} \nu_S^{s's}(v) e^{-i\mathbf{k}\cdot\rho_{s'}(\mathbf{v})} h_{s'\mathbf{k}}\right], \tag{B6}$$

$$\nu_S^{ss'}(v) = \frac{\sqrt{2}\pi n_{0s'} q_s^2 q_{s'}^2 \ln\Lambda}{m_s^{1/2} T_{0s}^{3/2}} \left(\frac{v_{\text{th}s}}{v}\right)^3 \left(1 + \frac{m_s}{m_{s'}}\right) \left[\text{erf}\left(\frac{v}{v_{\text{th}s'}}\right) - \frac{v}{v_{\text{th}s'}} \text{erf}'\left(\frac{v}{v_{\text{th}s'}}\right)\right], \tag{B7}$$

where $\text{erf}(x) = (2/\sqrt{\pi})\int_0^x dy\, \exp(-y^2)$ is the error function. From this, via a calculation of ring averages analogous to Eq. (B17), we get

$$\int d^3\mathbf{v} \left(-i\mathbf{k}\cdot\frac{\mathbf{v}_\perp \times \hat{\mathbf{z}}}{\Omega_s}\right) C_{ss'}\left[e^{-i\mathbf{k}\cdot\rho}h_\mathbf{k}\right] = -\int d^3\mathbf{v} \left[\nu_S^{ss'}(v)\left\langle i\mathbf{k}\cdot\rho_s(\mathbf{v}) e^{-i\mathbf{k}\cdot\rho_s(\mathbf{v})}\right\rangle h_{s\mathbf{k}} + \frac{m_{s'}}{m_s}\frac{\Omega_{s'}}{\Omega_s}\nu_S^{s's}(v)\left\langle i\mathbf{k}\cdot\rho_{s'}(\mathbf{v}) e^{-i\mathbf{k}\cdot\rho_{s'}(\mathbf{v})}\right\rangle h_{s'\mathbf{k}}\right]$$

$$= -\int d^3\mathbf{v} \left[\nu_S^{ss'}(v) a_s J_1(a_s) h_{s\mathbf{k}} + \frac{q_{s'}}{q_s}\nu_S^{s's}(v) a_{s'} J_1(a_{s'}) h_{s'\mathbf{k}}\right] \sim \nu_{ss'} k_\perp^2 \rho_s^2 \delta n_s + \nu_{s's} k_\perp^2 \rho_{s'}^2 \delta n_{s'}. \tag{B8}$$

For the ion–electron collisions ($s = i$, $s' = e$), using Eqs. (45) and (51), we find that both terms are $\sim (m_e/m_i)^{1/2} \nu_{ii} k_\perp^2 \rho_i^2 \delta n_i$. Thus, besides an extra factor of $k_\perp^2 \rho_i^2$, the ion–electron collisions are also subdominant by one order in the mass-ratio expansion compared to the ion–ion collisions. The same estimate holds for the interspecies contributions to the third and fourth terms in Eq. (B4). In a similar fashion, the integral of the electron–ion collision operator ($s = e$, $s' = i$), is $\sim \nu_{ei} k_\perp^2 \rho_e^2 \delta n_e$, which is the same order as the integral of the electron–electron collisions.

The conclusion of this section is that, both for ion and for electron collisions, the velocity-space integral (at constant $\mathbf{r}$) of the gyrokinetic collision operator is higher order than the collision operator itself by two orders of $k_\perp \rho_s$. This is the property that we relied on in neglecting collision terms in Eqs. (104) and (137).

B.2. *Ordering of Collision Terms in Eqs. (125) and (137)*

In § 5, we claimed that the contribution to the ion–ion collision term due to the $(Ze\langle\varphi\rangle_{\mathbf{R}_i}/T_{0i})F_{0i}$ part of the ion distribution function [Eq. (124)] was one order of $k_\perp \rho_i$ smaller than the contributions from the rest of h_i. This was used to order collision

terms in Eqs. (125) and (137). Indeed, from Eq. (B3),

$$
\left\langle C_{ii}\left[\frac{Ze\langle\varphi\rangle_{\mathbf{R}_i}}{T_{0i}}F_{0i}\right]\right\rangle_{\mathbf{R}_i} = \sum_{\mathbf{k}} e^{i\mathbf{k}\cdot\mathbf{R}_i}\left\langle e^{i\mathbf{k}\cdot\rho_i}C_{ii}\left[e^{-i\mathbf{k}\cdot\rho_i}J_0(a_i)F_{0i}\right]\right\rangle\frac{Ze\varphi_{\mathbf{k}}}{T_{0i}}
$$

$$
= \sum_{\mathbf{k}} e^{i\mathbf{k}\cdot\mathbf{R}_i}\left\langle e^{i\mathbf{k}\cdot\rho_i}C_{ii}\left[\left(1-i\mathbf{k}\cdot\rho_i-\frac{1}{2}(\mathbf{k}\cdot\rho_i)^2-\frac{a_i^2}{4}+\cdots\right)F_{0i}\right]\right\rangle\frac{Ze\varphi_{\mathbf{k}}}{T_{0i}} \sim \nu_{ii}k_\perp^2\rho_i^2\frac{Ze\varphi}{T_{0i}}F_{0i}. \quad (B9)
$$

This estimate holds because, as it is easy to ascertain using Eq. (B2), the operator C_{ii} annihilates the first two terms in the expansion and only acts non-trivially on an expression that is second order in $k_\perp\rho_i$. With the aid of Eq. (47), the desired ordering of the term (B9) in Eq. (125) follows. When Eq. (B9) is integrated over velocity space, the result picks up two extra orders in $k_\perp\rho_i$ [a general effect of integrating the gyroaveraged collision operator over the velocity space; see Eq. (B4)]:

$$
\frac{1}{n_{0i}}\int d^3\mathbf{v}\left\langle C_{ii}\left[\frac{Ze\langle\varphi\rangle_{\mathbf{R}_i}}{T_{0i}}F_{0i}\right]\right\rangle_{\mathbf{R}_i} \sim \nu_{ii}k_\perp^4\rho_i^4\frac{Ze\varphi}{T_{0i}}, \quad (B10)
$$

so the resulting term in Eq. (137) is third order, as stated in § 5.3.

B.3. *Model Pitch-Angle-Scattering Operator for Same-Species Collisions*

A popular model operator for same-species collisions that conserves particle number, momentum, and energy is constructed by taking the test-particle pitch-angle-scattering operator and correcting it with an additional term that ensures momentum conservation (Rosenbluth et al. 1972; see also Helander & Sigmar 2002):

$$
C_M[h_s] = \nu_D^{ss}(v)\left\{\frac{1}{2}\left[\frac{\partial}{\partial\xi}(1-\xi^2)\frac{\partial h_s}{\partial\xi}+\frac{1}{1-\xi^2}\frac{\partial^2 h_s}{\partial\vartheta^2}\right]+\frac{2\mathbf{v}\cdot\mathbf{U}[h_s]}{v_{\text{ths}}^2}F_{0s}\right\}, \quad \mathbf{U}[h_s] = \frac{3}{2}\frac{\int d^3\mathbf{v}\,\mathbf{v}\nu_D^{ss}(v)h_s}{\int d^3\mathbf{v}(v/v_{\text{ths}})^2\nu_D^{ss}(v)F_{0s}(v)}, \quad (B11)
$$

$$
\nu_D^{ss}(v) = \nu_{ss}\left(\frac{v_{\text{ths}}}{v}\right)^3\left[\left(1-\frac{1}{2}\frac{v_{\text{ths}}^2}{v^2}\right)\text{erf}\left(\frac{v}{v_{\text{ths}}}\right)+\frac{1}{2}\frac{v_{\text{ths}}}{v}\text{erf}'\left(\frac{v}{v_{\text{ths}}}\right)\right], \quad \nu_{ss} = \frac{\sqrt{2}\pi n_{0s}q_s^4\ln\Lambda}{m_s^{1/2}T_{0s}^{3/2}}, \quad (B12)
$$

where the velocity derivatives are at constant $\mathbf{r}$. The gyrokinetic version of this operator is (cf. Catto & Tsang 1977; Dimits & Cohen 1994)

$$
\langle C_M[h_s]\rangle_{\mathbf{R}_s} = \sum_{\mathbf{k}} e^{i\mathbf{k}\cdot\mathbf{R}_s}\nu_D^{ss}(v)\left\{\frac{1}{2}\frac{\partial}{\partial\xi}(1-\xi^2)\frac{\partial h_{s\mathbf{k}}}{\partial\xi}-\frac{v^2(1+\xi^2)}{4v_{\text{ths}}^2}k_\perp^2\rho_s^2h_{s\mathbf{k}}+2\frac{v_\perp J_1(a_s)U_\perp[h_{s\mathbf{k}}]+v_\parallel J_0(a_s)U_\parallel[h_{s\mathbf{k}}]}{v_{\text{ths}}^2}F_{0s}\right\}, \quad (B13)
$$

$$
U_\perp[h_{s\mathbf{k}}] = \frac{3}{2}\frac{\int d^3\mathbf{v}\,v_\perp J_1(a_s)\nu_D^{ss}(v)h_{s\mathbf{k}}(v_\perp,v_\parallel)}{\int d^3\mathbf{v}(v/v_{\text{ths}})^2\nu_D^{ss}(v)F_{0s}(v)}, \quad U_\parallel[h_{s\mathbf{k}}] = \frac{3}{2}\frac{\int d^3\mathbf{v}\,v_\parallel J_0(a_s)\nu_D^{ss}(v)h_{s\mathbf{k}}(v_\perp,v_\parallel)}{\int d^3\mathbf{v}(v/v_{\text{ths}})^2\nu_D^{ss}(v)F_{0s}(v)},
$$

where $a_s = k_\perp v_\perp/\Omega_s$. The velocity derivatives are now at constant $\mathbf{R}_s$. The spatial diffusion term appearing in the ring-averaged collision operator is physically due to the fact that a change in a particle's velocity resulting from a collision can lead to a change in the spatial position of its gyrocenter.

In order to derive Eq. (B13), we use Eq. (B3). Since, $\rho_s(\mathbf{v}) = \left(-\hat{\mathbf{x}}v\sqrt{1-\xi^2}\sin\vartheta+\hat{\mathbf{y}}v\sqrt{1-\xi^2}\cos\vartheta\right)/\Omega_s$, it is not hard to see that

$$
\frac{\partial}{\partial\xi}e^{-i\mathbf{k}\cdot\rho_s(\mathbf{v})}h_{s\mathbf{k}} = e^{-i\mathbf{k}\cdot\rho_s(\mathbf{v})}\left[\frac{\partial}{\partial\xi}-\frac{\xi}{1-\xi^2}\frac{i\mathbf{k}_\perp\cdot(\mathbf{v}_\perp\times\hat{\mathbf{z}})}{\Omega_s}\right]h_{s\mathbf{k}}, \quad \frac{\partial}{\partial\vartheta}e^{-i\mathbf{k}\cdot\rho_s(\mathbf{v})}h_{s\mathbf{k}} = e^{-i\mathbf{k}\cdot\rho(\mathbf{v})}\left(\frac{\partial}{\partial\vartheta}+\frac{i\mathbf{k}_\perp\cdot\mathbf{v}_\perp}{\Omega_s}\right)h_{s\mathbf{k}}. \quad (B14)
$$

Therefore,

$$
\left\langle e^{i\mathbf{k}\cdot\rho_s(\mathbf{v})}\frac{\partial}{\partial\xi}(1-\xi^2)\frac{\partial}{\partial\xi}e^{-i\mathbf{k}\cdot\rho_s(\mathbf{v})}h_{s\mathbf{k}}\right\rangle = \frac{\partial}{\partial\xi}(1-\xi^2)\frac{\partial h_{s\mathbf{k}}}{\partial\xi}-\frac{v^2\xi^2}{2\Omega_s^2}k_\perp^2h_{s\mathbf{k}}, \quad \left\langle e^{i\mathbf{k}\cdot\rho_s(\mathbf{v})}\frac{\partial^2}{\partial\vartheta^2}e^{-i\mathbf{k}\cdot\rho_s(\mathbf{v})}h_{s\mathbf{k}}\right\rangle = -\frac{v^2(1-\xi^2)}{2\Omega_s^2}k_\perp^2h_{s\mathbf{k}}.
$$
$$(B15)$$

Combining these formulae, we obtain the first two terms in Eq. (B13). Now let us work out the $\mathbf{U}$ term:

$$
\left\langle e^{i\mathbf{k}\cdot\rho_s(\mathbf{v})}\mathbf{v}\cdot\int d^3\mathbf{v}'\,\mathbf{v}'\nu_D^{ss}(v')e^{-i\mathbf{k}\cdot\rho_s(\mathbf{v}')}h_{s\mathbf{k}}(v'_\perp,v'_\parallel)\right\rangle = \left\langle\mathbf{v}e^{i\mathbf{k}\cdot\rho_s(\mathbf{v})}\right\rangle\cdot2\pi\int_0^\infty dv'_\perp v'_\perp\int_{-\infty}^{+\infty}dv'_\parallel\nu_D^{ss}(v')\left\langle\mathbf{v}'e^{-i\mathbf{k}\cdot\rho_s(\mathbf{v}')}\right\rangle h_{s\mathbf{k}}(v'_\perp,v'_\parallel).
$$
$$(B16)$$

Since $\left\langle\mathbf{v}e^{\pm i\mathbf{k}\cdot\rho_s(\mathbf{v})}\right\rangle = \hat{\mathbf{z}}v_\parallel\left\langle e^{\pm i\mathbf{k}\cdot\rho_s(\mathbf{v})}\right\rangle+\left\langle\mathbf{v}_\perp e^{\pm i\mathbf{k}\cdot\rho_s(\mathbf{v})}\right\rangle$, where $\left\langle e^{\pm i\mathbf{k}\cdot\rho_s(\mathbf{v})}\right\rangle = J_0(a_s)$ and

$$
\left\langle\mathbf{v}_\perp e^{\pm i\mathbf{k}\cdot\rho_s(\mathbf{v})}\right\rangle = \hat{\mathbf{z}}\times\left\langle(\mathbf{v}_\perp\times\hat{\mathbf{z}})\exp\left(\mp i\mathbf{k}_\perp\cdot\frac{\mathbf{v}_\perp\times\hat{\mathbf{z}}}{\Omega_s}\right)\right\rangle = \pm i\Omega_s\hat{\mathbf{z}}\times\frac{\partial}{\partial\mathbf{k}_\perp}\left\langle\exp\left(\mp i\mathbf{k}_\perp\cdot\frac{\mathbf{v}_\perp\times\hat{\mathbf{z}}}{\Omega_s}\right)\right\rangle = \pm i\frac{\hat{\mathbf{z}}\times\mathbf{k}_\perp}{k_\perp}v_\perp J_1(a_s), \quad (B17)
$$

we obtain the third term in Eq. (B13).

It is useful to give the lowest-order form of the operator (B13) in the limit $k_\perp \rho_s \ll 1$:

$$\langle C_M[h_s]\rangle_{\mathbf{R}_s} = \nu_D^{ss}(v)\left[\frac{1}{2}\frac{\partial}{\partial\xi}\left(1-\xi^2\right)\frac{\partial h_s}{\partial\xi} + \frac{3v_\parallel \int d^3\mathbf{v}' v'_\parallel \nu_D^{ss}(v')h_s(v'_\perp,v'_\parallel)}{\int d^3\mathbf{v}' v'^2 \nu_D^{ss}(v')F_{0s}(v')}F_{0s}\right] + O(k_\perp^2\rho_s^2). \tag{B18}$$

This is the operator that can be used in the right-hand side of Eq. (145) (as, e.g., is done in the calculation of collisional transport terms in Appendix D.3).

In practical numerical computations of gyrokinetic turbulence, the pitch-angle scattering operator is not sufficient because the distribution function develops small scales not only in ξ but also in v (M. Barnes, W. Dorland and T. Tatsuno 2006, unpublished). This is, indeed, expected because the phase-space entropy cascade produces small scales in $v_\perp$, rather than just in ξ (see § 7.9.1). In order to provide a cut off in v, an energy-diffusion operator must be added to the pitch-angle-scattering operator derived above. A numerically tractable model gyrokinetic energy-diffusion operator was proposed by Abel et al. (2008); Barnes et al. (2009).[48]

B.4. *Electron–Ion Collision Operator*

This operator can be expanded in m_e/m_i and to the lowest order is (see, e.g., Helander & Sigmar 2002)

$$C_{ei}[h] = \nu_D^{ei}(v)\left\{\frac{1}{2}\left[\frac{\partial}{\partial\xi}\left(1-\xi^2\right)\frac{\partial h_e}{\partial\xi} + \frac{1}{1-\xi^2}\frac{\partial^2 h_e}{\partial\vartheta^2}\right] + \frac{2\mathbf{v}\cdot\mathbf{u}_i}{v_{\text{the}}^2}F_{0e}\right\}, \quad \nu_D^{ei}(v) = \nu_{ei}\left(\frac{v_{\text{the}}}{v}\right)^3. \tag{B19}$$

The corrections to this form are $O(m_e/m_i)$. This is second order in the expansion of § 4 and, therefore, we need not keep these corrections. The operator (B19) is mathematically similar to the model operator for the same-species collisions [Eq. (B13)]. The gyrokinetic version of this operator is derived in the way analogous to the calculation in Appendix B.3. The result is

$$\langle C_{ei}[h]\rangle_{\mathbf{R}_e} = \sum_{\mathbf{k}} e^{i\mathbf{k}\cdot\mathbf{R}_e}\nu_D^{ei}(v)\left[\frac{1}{2}\frac{\partial}{\partial\xi}\left(1-\xi^2\right)\frac{\partial h_{e\mathbf{k}}}{\partial\xi} - \frac{v^2(1+\xi^2)}{4v_{\text{the}}^2}k_\perp^2\rho_e^2 h_{e\mathbf{k}}\right.$$
$$\left. - \frac{Zm_e}{m_i}\frac{v_\perp^2}{v_{\text{the}}^2}\frac{J_1(a_e)}{a_e}F_{0e}k_\perp^2\rho_i^2\frac{1}{n_{0i}}\int d^3\mathbf{v}'\frac{2v'^2_\perp}{v_{\text{thi}}^2}\frac{J_1(a'_i)}{a'_i}h_{i\mathbf{k}} + \frac{2v_\parallel J_0(a_e)u_{\parallel\mathbf{k}i}}{v_{\text{the}}^2}F_{0e}\right]. \tag{B20}$$

At scales not too close to the electron gyroscale, namely, such that $k_\perp\rho_e \sim (m_e/m_i)^{1/2}$, the second and third terms are manifestly second order in $(m_e/m_i)^{1/2}$, so have to be neglected along with other $O(m_e/m_i)$ contributions to the electron–ion collisions.[49] The remaining two terms are first order in the mass-ratio expansion: the first term vanishes for $h_e = h_e^{(0)}$ [Eq. (101)], so its contribution is first order; in the fourth term, we can use Eq. (87) to express $u_{\parallel i}$ in terms of quantities that are also first order. Keeping only the first-order terms, the gyrokinetic electron–ion collision operator is

$$\langle C_{ei}[h]\rangle_{\mathbf{R}_e} = \nu_D^{ei}(v)\left[\frac{1}{2}\frac{\partial}{\partial\xi}\left(1-\xi^2\right)\frac{\partial h_e^{(1)}}{\partial\xi} + \frac{2v_\parallel u_{\parallel i}}{v_{\text{the}}^2}F_{0e}\right]. \tag{B21}$$

Note that the ion drag term is essential to represent the ion–electron friction correctly and, therefore, to capture the Ohmic resistivity (which, however, is rarely more important for unfreezing flux than the electron inertia and the finiteness of the electron gyroradius; see § 7.7).

C. A HEURISTIC DERIVATION OF THE ELECTRON EQUATIONS

Here we show how the equations (116-117) of § 4 and the ERMHD equations (226-227) of § 7 can be derived heuristically from electron fluid dynamics and a number of physical assumptions, without the use of gyrokinetics (§ C.1). This derivation is *not* rigorous. Its role is to provide an intuitive route to the isothermal electron fluid and ERMHD approximations.

C.1. *Derivation of Eqs. (116-117)*

We start with the following three equations:

$$\frac{\partial\mathbf{B}}{\partial t} = -c\nabla\times\mathbf{E}, \qquad \frac{\partial n_e}{\partial t} + \nabla\cdot(n_e\mathbf{u}_e) = 0, \qquad \mathbf{E} + \frac{\mathbf{u}_e\times\mathbf{B}}{c} = -\frac{\nabla p_e}{en_e}. \tag{C1}$$

These are Faraday's law, the electron continuity equation, and the generalized Ohm's law, which is the electron momentum equation with all electron inertia terms neglected (i.e., effectively, the lowest order in the expansion in the electron mass m_e). The electron pressure is assumed to be scalar by *fiat* (this can be justified in certain limits: for example in the collisional limit, as in Appendix A, or for the isothermal electron fluid approximation derived in § 4). The electron-pressure term in the right-hand side of Ohm's law is sometimes called the thermoelectric term. We now assume the same static uniform equilibrium, $\mathbf{E}_0 = 0$, $\mathbf{B}_0 = B_0\hat{\mathbf{z}}$, that we have used throughout this paper and apply to Eqs. (C1) the fundamental ordering discussed in § 3.1.

---

[48] The collision operator now used the GS2 and AstroGK codes (see footnote 46) is their energy-diffusion operator plus the pitch-angle-scattering operator (B13).

[49] The third term in Eq. (B20) is, in fact, never important: at the electron scales, $k_\perp\rho_e \sim 1$, it is negligible because of the Bessel function in the velocity integral (Abel et al. 2008).

First consider the projection of Ohm's law onto the *total* magnetic field $\mathbf{B}$, use the definition of $\mathbf{E}$ [Eq. (37)], and keep the leading-order terms in the ϵ expansion:

$$\mathbf{E} \cdot \hat{\mathbf{b}} = -\frac{1}{en_e} \hat{\mathbf{b}} \cdot \nabla p_e \quad \Rightarrow \quad \frac{1}{c} \frac{\partial A_\parallel}{\partial t} + \hat{\mathbf{b}} \cdot \nabla \varphi = \hat{\mathbf{b}} \cdot \nabla \frac{\delta p_e}{en_{0e}}. \tag{C2}$$

This turns into Eq. (116) if we also assume isothermal electrons, $\delta p_e = T_{0e} \delta n_e$ [see Eq. (103)].

With the aid of Ohm's law, Faraday's law turns into

$$\frac{\partial \mathbf{B}}{\partial t} = \nabla \times (\mathbf{u}_e \times \mathbf{B}) = -\mathbf{u}_e \cdot \nabla \mathbf{B} + \mathbf{B} \cdot \nabla \mathbf{u}_e - \mathbf{B} \nabla \cdot \mathbf{u}_e. \tag{C3}$$

Keeping the leading-order terms, we find, for the components of Eq. (C3) perpendicular and parallel to the mean field,

$$\left(\frac{\partial}{\partial t} + \mathbf{u}_{\perp e} \cdot \nabla_\perp \right) \frac{\delta \mathbf{B}_\perp}{B_0} = \hat{\mathbf{b}} \cdot \nabla \mathbf{u}_{\perp e}, \qquad \left(\frac{\partial}{\partial t} + \mathbf{u}_{\perp e} \cdot \nabla_\perp \right) \left(\frac{\delta B_\parallel}{B_0} - \frac{\delta n_e}{n_{0e}} \right) = \hat{\mathbf{b}} \cdot \nabla u_{\parallel e}. \tag{C4}$$

In the last equation, we have used the electron continuity equation to write

$$\nabla \cdot \mathbf{u}_e = -\left(\frac{\partial}{\partial t} + \mathbf{u}_{\perp e} \cdot \nabla_\perp \right) \frac{\delta n_e}{n_{0e}}. \tag{C5}$$

From Ohm's law, we have, to lowest order,

$$\mathbf{u}_{\perp e} = -\hat{\mathbf{z}} \times \frac{c}{B_0} \left(\mathbf{E}_\perp + \nabla_\perp \frac{\delta p_e}{en_{0e}} \right) = \hat{\mathbf{z}} \times \nabla_\perp \frac{c}{B_0} \left(\varphi - \frac{\delta p_e}{en_{0e}} \right). \tag{C6}$$

Using this expression in the second of the equations (C4) gives

$$\frac{d}{dt} \left(\frac{\delta B_\parallel}{B_0} - \frac{\delta n_e}{n_{0e}} \right) - \hat{\mathbf{b}} \cdot \nabla u_{\parallel e} = \frac{c}{B_0} \left\{ \frac{\delta p_e}{en_{0e}}, \frac{\delta B_\parallel}{B_0} \right\} - \frac{c}{B_0} \left\{ \frac{\delta p_e}{en_{0e}}, \frac{\delta n_e}{n_{0e}} \right\}, \tag{C7}$$

where d/dt is defined in the usual way [Eq. (122)]. Assuming isothermal electrons ($\delta p_e = T_{0e} \delta n_e$) annihilates the second term on the right-hand side and turns the above equation into Eq. (117). As for the first of the equations (C4), the use of Eq. (C6) and substitution of $\delta \mathbf{B}_\perp = -\hat{\mathbf{z}} \times \nabla_\perp A_\parallel$ turns it into the previously derived Eq. (C2), whence follows Eq. (116).

Thus, we have shown that Eqs. (116-117) can be derived as a direct consequence of Faraday's law, electron fluid dynamics (electron continuity equation and the electron force balance, a. k. a. the generalized Ohm's law), and the assumption of isothermal electrons—all taken to the leading order in the gyrokinetic ordering given in § 3.1 (i.e., assuming strongly interacting anisotropic fluctuations with $k_\parallel \ll k_\perp$).

We have just proved that Eqs. (116) and (117) are simply the perpendicular and parallel part, respectively, of Eq. (C3). The latter equation means that the magnetic-field lines are frozen into the electron flow velocity $\mathbf{u}_e$, i.e., the flux is conserved, the result formally proven in § 4.3 [see Eq. (99)].

C.2. *Electron MHD and the Derivation of Eqs. (226-227)*

One route to Eqs. (226-227), already explained in § 7.2, is to start with Eqs. (C2) and (C7) and assume Boltzmann electrons and ions and the total pressure balance. Another approach, more standard in the literature on the Hall and Electron MHD, is to start with Eq. (C3), which states that the magnetic field is frozen into the electron flow. The electron velocity can be written in terms of the ion velocity and the current density, and the latter then related to the magnetic field via Ampère's law:

$$\mathbf{u}_e = \mathbf{u}_i - \frac{\mathbf{j}}{en_e} = \mathbf{u}_i - \frac{c}{4\pi en_e} \nabla \times \mathbf{B}. \tag{C8}$$

To the leading order in ϵ, the perpendicular and parallel parts of Eq. (C3) are Eqs. (C4), respectively, where the perpendicular and parallel electron velocities are [from Eq. (C8)]

$$\mathbf{u}_{\perp e} = \mathbf{u}_{\perp i} + \frac{c}{4\pi en_{0e}} \hat{\mathbf{z}} \times \nabla_\perp \delta B_\parallel, \quad u_{\parallel e} = u_{\parallel i} + \frac{c}{4\pi en_{0e}} \nabla_\perp^2 A_\parallel. \tag{C9}$$

The relative size of the two terms in each of these expressions is controlled by the size of $k_\perp d_i$, where $d_i = \rho_i / \sqrt{\beta_i}$ is the ion inertial scale. When $k_\perp d_i \gg 1$, we may set $\mathbf{u}_i = 0$. Note, however, that the ion motion is not totally neglected: indeed, in the second of the equations (C4), the $\delta n_e / ne$ terms comes, via Eq. (C5), from the divergence of the ion velocity [from Eq. (C8), $\nabla \cdot \mathbf{u}_i = \nabla \cdot \mathbf{u}_e$]. To complete the derivation, we relate δn_e to $\delta B_\parallel$ via the assumption of total pressure balance, as explained in § 7.2, giving us Eq. (225). Substituting this equation and Eqs. (C9) into Eqs. (C4), we obtain

$$\frac{\partial \Psi}{\partial t} = v_A^2 d_i \hat{\mathbf{b}} \cdot \nabla \frac{\delta B_\parallel}{B_0}, \qquad \frac{\partial}{\partial t} \frac{\delta B_\parallel}{B_0} = -\frac{d_i}{1 + 2/\beta_i(1 + Z/\tau)} \hat{\mathbf{b}} \cdot \nabla \nabla_\perp^2 \Psi, \tag{C10}$$

where $\Psi = -A_\parallel / \sqrt{4\pi m_i n_{0i}}$. Equations (C10) evolve the perturbed magnetic field. These equations become the ERMHD equations (226-227) if $\delta B_\parallel / B_0$ is expressed in terms of the scalar potential via Eq. (223).

Note that there are two special limits in which the assumption of immobile ions suffices to derive Eqs. (C10) from Eq. (C3) without the need for the pressure balance: $\beta_i \gg 1$ (incompressible ions) or $\tau = T_{0i}/T_{0e} \ll 1$ (cold ions) but $\beta_e = \beta_i Z/\tau \gg 1$. In both cases, Eq. (225) shows that $\delta n_e/n_{0e} \ll \delta B_\parallel/B_0$, so the density perturbation can be ignored and the coefficient of the right-hand side of the second of the equations (C10) is equal to 1. The limit of cold ions is discussed further in Appendix E.

D. FLUID LIMIT OF THE KINETIC RMHD

Taking the fluid (collisional) limit of the KRMHD system (summarized in §5.7) means carrying out another subsidiary expansion—this time in $k_\parallel \lambda_{\mathrm{mfp}i} \ll 1$. The expansion only affects the equations for the density and magnetic-field-strength fluctuations (§5.5) because the Alfvén waves are indifferent to collisional effects.

The calculation presented below follows a standard perturbation algorithm used in the kinetic theory of gases and in plasma physics to derive fluid equations with collisional transport coefficients (Chapman & Cowling 1970). For magnetized plasma, this calculation was carried out in full generality by Braginskii (1965), whose starting point was the full plasma kinetic theory [Eqs. (36-39)]. While what we do below is, strictly speaking, merely a particular case of his calculation (see Appendix A), it has the advantage of relative simplicity and also serves to show how the fluid limit is recovered from the gyrokinetic formalism—a demonstration that we believe to be of value.

It will be convenient to use the KRMHD system written in terms of the function $\delta\tilde{f}_i = g + (v_\perp^2/v_{\mathrm{th}i}^2)(\delta B_\parallel/B_0)F_{0i}$, which is the perturbation of the local Maxwellian in the frame of the Alfvén waves [Eqs. (150-152)]. We want to expand Eq. (150) in powers of $k_\parallel \lambda_{\mathrm{mfp}i}$, so we let $\delta\tilde{f}_i = \delta\tilde{f}_i^{(0)} + \delta\tilde{f}_i^{(1)} + \ldots$, $\delta B_\parallel = \delta B_\parallel^{(0)} + \delta B_\parallel^{(1)} + \ldots$, etc.

D.1. *Zeroth Order: Ideal Fluid Equations*

Since [see Eq. (49)]

$$\frac{\omega}{\nu_{ii}} \sim \frac{k_\parallel v_A}{\nu_{ii}} \sim \frac{k_\parallel \lambda_{\mathrm{mfp}i}}{\sqrt{\beta_i}}, \quad \frac{k_\parallel v_\parallel}{\nu_{ii}} \sim \frac{k_\parallel v_{\mathrm{th}i}}{\nu_{ii}} \sim k_\parallel \lambda_{\mathrm{mfp}i}, \tag{D1}$$

to zeroth order Eq. (150) becomes $\left\langle C_{ii}\left[\delta\tilde{f}_i^{(0)}\right]\right\rangle_{\mathbf{R}_i} = 0$. The zero mode of the collision operator is a Maxwellian. Therefore, we may write the full ion distribution function up to zeroth order in $k_\parallel \lambda_{\mathrm{mfp}i}$ as follows [see Eq. (144)]

$$f_i = \frac{n_i}{(2\pi T_i/m_i)^{3/2}} \exp\left\{-\frac{m_i[(\mathbf{v}_\perp - \mathbf{u}_E)^2 + (v_\parallel - u_\parallel)^2]}{2T_i}\right\}, \tag{D2}$$

where $n_i = n_{0i} + \delta n_i$ and $T_i = T_{0i} + \delta T_i$ include both the unperturbed quantities and their perturbations. The $\mathbf{E}\times\mathbf{B}$ drift velocity $\mathbf{u}_E$ comes from the Alfvén waves (see §5.4) and does not concern us here. Since the perturbations δn_i, $u_\parallel$ and δT_i are small in the original gyrokinetic expansion, Eq. (D2) is equivalent to

$$\delta\tilde{f}_i^{(0)} = \left[\frac{\delta n_e^{(0)}}{n_{0e}} + \left(\frac{v^2}{v_{\mathrm{th}i}^2} - \frac{3}{2}\right)\frac{\delta T_i^{(0)}}{T_{0i}} + \frac{2v_\parallel}{v_{\mathrm{th}i}^2}u_\parallel^{(0)}\right]F_{0i}, \tag{D3}$$

where we have used quasi-neutrality to replace $\delta n_i/n_{0i} = \delta n_e/n_{0e}$. This automatically satisfies Eq. (151), while Eq. (152) gives us an expression for the ion-temperature perturbation:

$$\frac{\delta T_i^{(0)}}{T_{0i}} = -\left(1 + \frac{Z}{\tau}\right)\frac{\delta n_e^{(0)}}{n_{0e}} - \frac{2}{\beta_i}\frac{\delta B_\parallel^{(0)}}{B_0}. \tag{D4}$$

Note that this is consistent with the interpretation of the perpendicular Ampère's law [Eq. (63), which is the progenitor of Eq. (152)] as the pressure balance [see Eq. (67)]: indeed, recalling that the electron pressure perturbation is $\delta p_e = T_{0e}\delta n_e$ [Eq. (103)], we have

$$\delta\frac{B^2}{8\pi} = \frac{B_0^2}{4\pi}\frac{\delta B_\parallel}{B_0} = -\delta p_e - \delta p_i = -\delta n_e T_{0e} - \delta n_i T_{0i} - n_{0i}\delta T_i, \tag{D5}$$

whence follows Eq. (D4) by way of quasi-neutrality ($Zn_i = n_e$) and the definitions of Z, τ, β_i [Eqs. (40-42)].

Since the collision operator conserves particle number, momentum and energy, we can obtain evolution equations for $\delta n_e^{(0)}/n_{0e}$, $u_\parallel^{(0)}$ and $\delta B_\parallel^{(0)}/B_0$ by multiplying Eq. (150) by 1, $v_\parallel$, $v^2/v_{\mathrm{th}i}^2$, respectively, and integrating over the velocity space. The three moments that emerge this way are

$$\frac{1}{n_{0i}}\int d^3\mathbf{v}\,\delta\tilde{f}_i^{(0)} = \frac{\delta n_e^{(0)}}{n_{0e}}, \quad \frac{1}{n_{0i}}\int d^3\mathbf{v}\,v_\parallel\delta\tilde{f}_i^{(0)} = u_\parallel^{(0)}, \quad \frac{1}{n_{0i}}\int d^3\mathbf{v}\,\frac{v^2}{v_{\mathrm{th}i}^2}\delta\tilde{f}_i^{(0)} = \frac{3}{2}\left(\frac{\delta n_e^{(0)}}{n_{0e}} + \frac{\delta T_i^{(0)}}{T_{0i}}\right). \tag{D6}$$

The three evolution equations for these moments are

$$\frac{d}{dt}\left(\frac{\delta n_e^{(0)}}{n_{0e}} - \frac{\delta B_\parallel^{(0)}}{B_0}\right) + \hat{\mathbf{b}}\cdot\nabla u_\parallel^{(0)} = 0, \tag{D7}$$

$$\frac{du_\parallel^{(0)}}{dt} - v_A^2\, \hat{\mathbf{b}} \cdot \nabla \frac{\delta B_\parallel^{(0)}}{B_0} = 0, \tag{D8}$$

$$\frac{d}{dt}\left[\frac{3}{2}\left(\frac{\delta n_e^{(0)}}{n_{0e}} + \frac{\delta T_i^{(0)}}{T_{0i}}\right) - \frac{5}{2}\frac{\delta B_\parallel^{(0)}}{B_0}\right] + \frac{5}{2}\,\hat{\mathbf{b}} \cdot \nabla u_\parallel^{(0)} = 0. \tag{D9}$$

These allow us to recover the fluid equations we derived in § 2.4: Eq. (D8) is the parallel component of the MHD momentum equation (27); combining Eqs. (D7), (D9) and (D4), we obtain the continuity equation and the parallel component of the induction equation—these are the same as Eqs. (25) and (26):

$$\frac{d}{dt}\frac{\delta n_e^{(0)}}{n_{0e}} = -\frac{1}{1+c_s^2/v_A^2}\,\hat{\mathbf{b}} \cdot \nabla u_\parallel^{(0)}, \quad \frac{d}{dt}\frac{\delta B_\parallel^{(0)}}{B_0} = \frac{1}{1+v_A^2/c_s^2}\,\hat{\mathbf{b}} \cdot \nabla u_\parallel^{(0)}, \tag{D10}$$

where the sound speed c_s is defined by Eq. (166). From Eqs. (D7) and (D9), we also find the analog of the entropy equation (23):

$$\frac{d}{dt}\frac{\delta T_i^{(0)}}{T_{0i}} = \frac{2}{3}\frac{d}{dt}\frac{\delta n_e^{(0)}}{n_{0e}} \quad \Leftrightarrow \quad \frac{d}{dt}\frac{\delta s^{(0)}}{s_0} = 0, \quad \frac{\delta s^{(0)}}{s_0} = \frac{\delta T_i^{(0)}}{T_{0i}} - \frac{2}{3}\frac{\delta n_e^{(0)}}{n_{0e}} = -\left(\frac{5}{3}+\frac{Z}{\tau}\right)\left(\frac{\delta n_e^{(0)}}{n_{0e}} + \frac{v_A^2}{c_s^2}\frac{\delta B_\parallel^{(0)}}{B_0}\right). \tag{D11}$$

This implies that the temperature changes due to compressional heating only.

D.2. *Generalized Energy: Five RMHD Cascades Recovered*

We now calculate the generalized energy by substituting $\delta \tilde{f}_i$ from Eq. (D3) into Eq. (153) and using Eqs. (D4) and (D11):

$$W = \int d^3\mathbf{r}\left[\frac{m_i n_{0i} u_E^2}{2} + \frac{\delta B_\perp^2}{8\pi} + \frac{m_i n_{0i} u_\parallel^2}{2} + \frac{\delta B_\parallel^2}{8\pi}\left(1+\frac{v_A^2}{c_s^2}\right) + \frac{3}{4}n_{0i}T_{0i}\frac{1+Z/\tau}{5/3+Z/\tau}\frac{\delta s^2}{s_0^2}\right]$$

$$= W_{AW}^+ + W_{AW}^- + W_{sw}^+ + W_{sw}^- + \frac{3}{2}n_{0i}T_{0i}\frac{1+Z/\tau}{5/3+Z/\tau}\,W_s. \tag{D12}$$

The first two terms are the Alfvén-wave energy [Eq. (154)]. The following two terms are the slow-wave energy, which splits into the independently cascaded energies of "+" and "−" waves (see § 2.5):

$$W_{SW} = W_{sw}^+ + W_{sw}^- = \int d^3\mathbf{r}\,\frac{m_i n_{0i}}{2}\left(|z_\parallel^+|^2 + |z_\parallel^-|^2\right). \tag{D13}$$

The last term is the total variance of the entropy mode. Thus, we have recovered the five cascades of the RMHD system (§ 2.7; Fig. 5 maps out the fate of these cascades at kinetic scales).

D.3. *First Order: Collisional Transport*

Now let us compute the collisional transport terms for the equations derived above. In order to do this, we have to determine the first-order perturbed distribution function $\delta \tilde{f}_i^{(1)}$, which satisfies [see Eq. (150)]

$$\left\langle C_{ii}\left[\delta \tilde{f}_i^{(1)}\right]\right\rangle_{\mathbf{R}_i} = \frac{d}{dt}\left(\delta \tilde{f}_i^{(0)} - \frac{v_\perp^2}{v_{thi}^2}\frac{\delta B_\parallel^{(0)}}{B_0}\right) + v_\parallel\,\hat{\mathbf{b}} \cdot \nabla\left(\delta \tilde{f}_i^{(0)} + \frac{Z}{\tau}\frac{\delta n_e^{(0)}}{n_{0e}}F_{0i}\right). \tag{D14}$$

We now use Eq. (D3) to substitute for $\delta \tilde{f}_i^{(0)}$ and Eqs. (D10-D11) and (D8) to compute the time derivatives. Equation (D14) becomes

$$\left\langle C_{ii}\left[\delta \tilde{f}_i^{(1)}\right]\right\rangle_{\mathbf{R}_i} = \left[-(1-3\xi^2)\frac{v^2}{v_{thi}^2}\frac{2/3+c_s^2/v_A^2}{1+c_s^2/v_A^2}\,\hat{\mathbf{b}} \cdot \nabla u_\parallel^{(0)} + \xi v\left(\frac{v^2}{v_{thi}^2}-\frac{5}{2}\right)\hat{\mathbf{b}} \cdot \nabla\frac{\delta T_i^{(0)}}{T_{0i}}\right]F_{0i}(v), \tag{D15}$$

where $\xi = v_\parallel/v$. Note that the right-hand side gives zero when multiplied by 1, $v_\parallel$ or v^2 and integrated over the velocity space, as it must do because the collision operator in the left-hand side conserves particle number, momentum and energy.

Solving Eq. (D15) requires inverting the collision operator. While this can be done for the general Landau collision operator (see Braginskii 1965), for our purposes, it is sufficient to use the model operator given in Appendix B.3, Eq. (B18). This simplifies calculations at the expense of an order-one inaccuracy in the numerical values of the transport coefficients. As the exact value of these coefficients will never be crucial for us, this is an acceptable loss of precision. Inverting the collision operator in Eq. (D15) then gives

$$\delta \tilde{f}_i^{(1)} = \frac{1}{\nu_D^{ii}(v)}\left[\frac{1-3\xi^2}{3}\frac{v^2}{v_{thi}^2}\frac{2/3+c_s^2/v_A^2}{1+c_s^2/v_A^2}\,\hat{\mathbf{b}} \cdot \nabla u_\parallel^{(0)} - \xi v\left(\frac{v^2}{v_{thi}^2}-\frac{5}{2}\right)\hat{\mathbf{b}} \cdot \nabla\frac{\delta T_i^{(0)}}{T_{0i}}\right]F_{0i}(v), \tag{D16}$$

where $\nu_D^{ii}(v)$ is a collision frequency defined in Eq. (B12) and we have chosen the constants of integration in such a way that the three conservation laws are respected: $\int d^3\mathbf{v}\,\delta\tilde{f}_i^{(1)} = 0$, $\int d^3\mathbf{v}\,v_\|\,\delta\tilde{f}_i^{(1)} = 0$, $\int d^3\mathbf{v}\,v^2\delta\tilde{f}_i^{(1)} = 0$. These relations mean that $\delta n_e^{(1)} = 0$, $u_\|^{(1)} = 0$, $\delta T_i^{(1)} = 0$ and that, in view of Eq. (152), we have

$$\frac{\delta B_\|^{(1)}}{B_0} = -\frac{1}{3v_A^2}\frac{2/3+c_s^2/v_A^2}{1+c_s^2/v_A^2}\,\nu_{\|i}\hat{\mathbf{b}}\cdot\nabla u_\|, \tag{D17}$$

where $\nu_{\|i}$ is defined below [Eq. (D21)]. Equations (D16-D17) are now used to calculate the first-order corrections to the moment equations (D7-D9). They become

$$\frac{d}{dt}\left(\frac{\delta n_e}{n_{0e}} - \frac{\delta B_\|}{B_0}\right) + \hat{\mathbf{b}}\cdot\nabla u_\| = 0, \tag{D18}$$

$$\frac{du_\|}{dt} - v_A^2\hat{\mathbf{b}}\cdot\nabla\frac{\delta B_\|}{B_0} = \frac{2/3+c_s^2/v_A^2}{1+c_s^2/v_A^2}\,\nu_{\|i}\hat{\mathbf{b}}\cdot\nabla\left(\hat{\mathbf{b}}\cdot\nabla u_\|\right), \tag{D19}$$

$$\frac{d}{dt}\frac{\delta T_i}{T_{0i}} - \frac{2}{3}\frac{d}{dt}\frac{\delta n_e}{n_{0e}} = \kappa_{\|i}\hat{\mathbf{b}}\cdot\nabla\left(\hat{\mathbf{b}}\cdot\nabla\frac{\delta T_i}{T_{0i}}\right), \tag{D20}$$

where we have introduced the coefficients of parallel viscosity and parallel thermal diffusivity:

$$\nu_{\|i} = \frac{2}{15}\frac{1}{n_{0i}}\int d^3\mathbf{v}\,\frac{v^4}{\nu_D^{ii}(v)v_{\mathrm{thi}}^2}F_{0i}(v), \qquad \kappa_{\|i} = \frac{2}{9}\frac{1}{n_{0i}}\int d^3\mathbf{v}\,\frac{v^4}{\nu_D^{ii}(v)v_{\mathrm{thi}}^2}\left(\frac{v^2}{v_{\mathrm{thi}}^2} - \frac{5}{2}\right)F_{0i}(v). \tag{D21}$$

All perturbed quantities are now accurate up to first order in $k_\|\lambda_{\mathrm{mfp}i}$. Note that in Eq. (D19), we used Eq. (D17) to express $\delta B_\|^{(0)} = \delta B_\| - \delta B_\|^{(1)}$. We do the same in Eq. (D4) and obtain

$$\left(1+\frac{Z}{\tau}\right)\frac{\delta n_e}{n_{0e}} = -\frac{\delta T_i}{T_{0i}} - \frac{2}{\beta_i}\left(\frac{\delta B_\|}{B_0} + \frac{1}{3v_A^2}\frac{2/3+c_s^2/v_A^2}{1+c_s^2/v_A^2}\,\nu_{\|i}\hat{\mathbf{b}}\cdot\nabla u_\|\right). \tag{D22}$$

This equation completes the system (D18-D20), which allows us to determine δn_e, $u_\|$, δT_i and $\delta B_\|$. In § 6.1, we use the equations derived above, but absorb the prefactor $(2/3+c_s^2/v_A^2)/(1+c_s^2/v_A^2)$ into the definition of $\nu_{\|i}$. The same system of equations can also be derived from Braginskii's two-fluid theory (Appendix A.4), from which we can borrow the quantitatively correct values of the viscosity and ion thermal diffusivity: $\nu_{\|i} = 0.90\,v_{\mathrm{thi}}^2/\nu_{ii}$, $\kappa_{\|i} = 2.45\,v_{\mathrm{thi}}^2/\nu_{ii}$, where ν_{ii} is defined in Eq. (52).

E. HALL REDUCED MHD

The popular Hall MHD approximation consists in assuming that the magnetic field is frozen into the electron flow velocity [Eq. (C3)]. The latter is calculated from the ion flow velocity and the current determined by Ampère's law [Eq. (C8)]:

$$\frac{\partial\mathbf{B}}{\partial t} = \nabla\times\left[\left(\mathbf{u}_i - \frac{c}{4\pi en_{0e}}\nabla\times\mathbf{B}\right)\times\mathbf{B}\right], \tag{E1}$$

where the ion flow velocity $\mathbf{u}_i$ satisfies the conventional MHD momentum equation (8). The Hall MHD is an appealing theoretical model that appears to capture both the MHD behavior at long wavelengths (when $\mathbf{u}_e \simeq \mathbf{u}_i$) and some of the kinetic effects that become important at small scales due to decoupling between the electron and ion flows (the appearance of dispersive waves) without bringing in the full complexity of the kinetic theory. However, unlike the kinetic theory, it completely ignores the collisionless damping effects and suggests that the key small-scale physical change is associated with the ion inertial scale $d_i = \rho_i/\sqrt{\beta_i}$ (or, when $\beta_e \ll 1$, the ion sound scale $\rho_s = \rho_i\sqrt{Z/2\tau}$; see § E.3), rather than the ion gyroscale ρ_i. Is this an acceptable model for plasma turbulence? Figure 8 illustrates the fact that at $\tau \sim 1$, the ion inertial scale does *not* play a special role linearly, the MHD Alfvén wave becomes dispersive at the ion gyroscale, not at d_i, and that the collisionless damping cannot in general be neglected. A detailed comparison of the Hall MHD linear dispersion relation with full hot plasma dispersion relation leads to the conclusion that Hall MHD is only a valid approximation in the limit of cold ions, namely, $\tau = T_{0i}/T_{0e} \ll 1$ (Ito et al. 2004; Hirose et al. 2004). In this Appendix, we show that a reduced (low-frequency, anisotropic) version of Hall MHD can, indeed, be derived from gyrokinetics in the limit $\tau \ll 1$.[50] This demonstrates that the Hall MHD model fits into the theoretical framework proposed in this paper as a special limit. However, the parameter regime that gives rise to this special limit is not common in space and astrophysical plasmas of interest.

E.1. *Gyrokinetic Derivation of Hall Reduced MHD*

Let us start with the equations of isothermal electron fluid, Eqs. (116-121), i.e., work within the assumptions that allowed us to carry out the mass-ratio expansion (§ 4.8). In Eq. (120) (perpendicular Ampère's law, or gyrokinetic pressure balance), taking

---

[50] Note that, strictly speaking, our ordering of the collision frequency does not allow us to take this limit (see footnote 17), but this is a minor betrayal of rigor, which does not, in fact, invalidate the results.

the limit $\tau \ll 1$ gives

$$\frac{\delta B_\parallel}{B_0} = \frac{\beta_i}{2} \frac{Z}{\tau} \left\{ \frac{Ze\varphi}{T_{0i}} - \sum_{\mathbf{k}} e^{i\mathbf{k}\cdot\mathbf{r}} \frac{1}{n_{0i}} \int d^3\mathbf{v} J_0(a_i) h_{i\mathbf{k}} \right\} = -\frac{\beta_e}{2} \frac{\delta n_e}{n_{0e}}, \tag{E2}$$

where we have used Eq. (118) to express the h_i integral and the expression for the electron beta $\beta_e = \beta_i Z/\tau$. Note that the above equation is simply the statement of a balance between the magnetic and electron thermal pressure (the ions are relatively cold, so they have fallen out of the pressure balance). Using Eq. (E2) to express δn_e in terms of $\delta B_\parallel$ in Eqs. (116) and (117) and also substituting for $u_{\parallel e}$ from Eq. (119) [or, equivalently, Eq. (87)], we get

$$\frac{\partial \Psi}{\partial t} = v_A \hat{\mathbf{b}} \cdot \nabla \left(\Phi + v_A d_i \frac{\delta B_\parallel}{B_0} \right), \qquad \frac{d}{dt} \frac{\delta B_\parallel}{B_0} = \frac{1}{1+2/\beta_e} \hat{\mathbf{b}} \cdot \nabla \left(u_{\parallel i} - d_i \nabla_\perp^2 \Psi \right), \tag{E3}$$

where we have used our usual definitions of the stream and flux functions [Eq. (135)] and of the full derivatives [Eq. (160)]. These equations determine the evolution of the magnetic field, but we still need the ion gyrokinetic equation (121) to calculate the ion motion ($\Phi = c\varphi/B_0$ and $u_{\parallel i}$) via Eqs. (118) and (88). There are two limits in which the ion kinetics can be reduced to simple fluid models.

E.1.1. *High-Ion-Beta Limit, $\beta_i \gg 1$*

In this limit, $k_\perp \rho_i = k_\perp d_i \sqrt{\beta_i} \gg 1$ as long as $k_\perp d_i$ is not small. Then the ion motion can be neglected because it is averaged out by the Bessel functions in Eqs. (118) and (88)—in the same way as in § 7.2. So we get $\Phi = (\tau/Z) v_A d_i \delta B_\parallel / B_0$ [using Eq. (E2); this is the $\tau \ll 1$ limit of Eq. (223)] and $u_{\parallel i} = 0$. Noting that $\beta_e = \beta_i Z/\tau \gg 1$ in this limit, we find that Eqs. (E3) reduce to

$$\frac{\partial \Psi}{\partial t} = v_A^2 d_i \hat{\mathbf{b}} \cdot \nabla \frac{\delta B_\parallel}{B_0}, \qquad \frac{\partial}{\partial t} \frac{\delta B_\parallel}{B_0} = -d_i \hat{\mathbf{b}} \cdot \nabla \nabla_\perp^2 \Psi, \tag{E4}$$

which is the $\tau \ll 1$ limit of our ERMHD equations (226-227) [or, equivalently, Eqs. (C10)].

E.1.2. *Low-Ion-Beta Limit, $\beta_i \sim \tau \ll 1$ (the Hall Limit)*

This limit is similar to the RMHD limit worked out in § 5: we take, for now, $k_\perp d_i \sim 1$ and $\beta_e \sim 1$ (in which subsidiary expansions can be carried out later), and expand the ion gyrokinetics in $k_\perp \rho_i = k_\perp d_i \sqrt{\beta_i} \ll 1$. Note that ordering $\beta_e \sim 1$ means that we have ordered $\beta_i \sim \tau \ll 1$. We now proceed analogously to the way we did in § 5: express the ion distribution in terms of the g function defined by Eq. (124) and, using the relation (E2) between $\delta B_\parallel/B_0$ and $\delta n_e/n_{0e}$, write Eqs. (125-127) as follows:

$$\underbrace{\frac{\partial g}{\partial t}}_{(-1)} + \underbrace{v_\parallel \frac{\partial g}{\partial z}}_{(0)} + \frac{c}{B_0} \left\{ \left\langle \underbrace{\varphi}_{(-1)} - \underbrace{\frac{v_\parallel A_\parallel}{c}}_{(0)} - \underbrace{\frac{\mathbf{v}_\perp \cdot \mathbf{A}_\perp}{c}}_{(1)} \right\rangle_{\mathbf{R}_i}, g \right\} - \underbrace{\langle C_{ii}[g] \rangle_{\mathbf{R}_i}}_{(0)}$$

$$= \frac{Ze}{T_{0i}} \left[v_\parallel \left\langle \underbrace{-\frac{1}{B_0} \{ A_\parallel, \varphi - \langle\varphi\rangle_{\mathbf{R}_i} \}}_{(1)} + \hat{\mathbf{b}} \cdot \nabla \left(\underbrace{\frac{T_{0e}}{e} \frac{2}{\beta_e} \frac{\delta B_\parallel}{B_0}}_{(-1)} + \underbrace{\left\langle \frac{\mathbf{v}_\perp \cdot \mathbf{A}_\perp}{c} \right\rangle_{\mathbf{R}_i}}_{(1)} \right) \right\rangle_{\mathbf{R}_i} F_{0i} + \left\langle C_{ii} \left[\left\langle \underbrace{\varphi}_{(1)} - \underbrace{\frac{\mathbf{v}_\perp \cdot \mathbf{A}_\perp}{c}}_{(1)} \right\rangle_{\mathbf{R}_i} F_{0i} \right] \right\rangle_{\mathbf{R}_i} \right], \tag{E5}$$

$$\underbrace{-\left[\Gamma_1(\alpha_i) + \frac{2}{\beta_e} \right] \frac{\delta B_{\parallel\mathbf{k}}}{B_0}}_{(0)} + \underbrace{\left[1 - \Gamma_0(\alpha_i) \right] \frac{Ze\varphi_{\mathbf{k}}}{T_{0i}}}_{(0)} = \underbrace{\frac{1}{n_{0i}} \int d^3\mathbf{v} J_0(a_i) g_{\mathbf{k}}}_{(-1)}, \qquad \underbrace{u_{\parallel\mathbf{k}i}}_{(-1)} = \underbrace{\frac{1}{n_{0i}} \int d^3\mathbf{v} v_\parallel J_0(a_i) g_{\mathbf{k}}}_{(-1)}. \tag{E6}$$

All terms in these equations can be ordered with respect to the small parameter $\sqrt{\beta_i}$ (an expansion subsidiary to the gyrokinetic expansion in ϵ and the Hall expansion in $\tau \ll 1$). The lowest order to which they enter is indicated underneath each term. The ordering we use is the same as in § 5.2, but now we count the powers of $\sqrt{\beta_i}$ and order formally $k_\perp d_i \sim 1$ and $\beta_e \sim 1$. It is easy to check that this ordering can be summarized as follows

$$\frac{Ze\varphi}{T_{0i}} \sim \frac{1}{\beta_i} \frac{\delta B_\parallel}{B_0}, \quad \frac{\delta B_\perp}{B_0} \sim \frac{\delta B_\parallel}{B_0}, \quad \frac{g}{F_{0i}} \sim \frac{u_\parallel}{v_{\mathrm{th}i}} \sim \frac{1}{\sqrt{\beta_i}} \frac{\delta B_\parallel}{B_0} \tag{E7}$$

and that the ion and electron terms in Eqs. (E3) are comparable under this ordering, so their competition is retained (in fact, this could be used as the underlying assumption behind the ordering). The fluctuation frequency continues to be ordered as the Alfvén frequency, $\omega \sim k_\parallel v_A$. The collision terms are ordered via $\omega/\nu_{ii} \sim k_\parallel \lambda_{\mathrm{mfp}i}/\sqrt{\beta_i}$ and $k_\parallel \lambda_{\mathrm{mfp}i} \sim 1$, although the latter assumption is not essential for what follows, because collisions turn out to be negligible and it is fine to take $k_\parallel \lambda_{\mathrm{mfp}i} \gg 1$ from the outset and neglect them completely.

In Eqs. (E6), we use Eqs. (129) and (130) to write $1 - \Gamma_0(\alpha_i) \simeq \alpha_i = k_\perp^2 \rho_i^2/2$ and $\Gamma_1(\alpha_i) \simeq 1$. These equations imply that if we expand $g = g^{(-1)} + g^{(0)} + \ldots$, we must have $\int d^3\mathbf{v} g^{(-1)} = 0$, so the contribution to the right-hand side of the first of the equations

(E6) (the quasi-neutrality equation) comes from $g^{(0)}$, while the parallel ion flow is determined by $g^{(-1)}$. Retaining only the lowest (minus first) order terms in Eq. (E5), we find the equation for $g^{(-1)}$, the $v_\parallel$ moment of which gives an equation for $u_{\parallel i}$:

$$\frac{\partial g^{(-1)}}{\partial t} + \frac{c}{B_0}\{\varphi, g^{(-1)}\} = \frac{2}{\beta_i} v_\parallel \hat{\mathbf{b}} \cdot \nabla \frac{\delta B_\parallel}{B_0} F_{0i} \quad \Rightarrow \quad \frac{du_{\parallel i}}{dt} = v_A^2 \hat{\mathbf{b}} \cdot \nabla \frac{\delta B_\parallel}{B_0}. \tag{E8}$$

Now integrating Eq. (E5) over the velocity space (at constant $\mathbf{r}$), using the first of the equations (E6) to express the integral of $g^{(0)}$, and retaining only the lowest (zeroth) order terms, we find

$$\frac{d}{dt}\left[-\frac{1}{2}\rho_i^2 \nabla_\perp^2 \frac{Ze\varphi}{T_{0i}} - \left(1 + \frac{2}{\beta_e}\right)\frac{\delta B_\parallel}{B_0}\right] + \hat{\mathbf{b}} \cdot \nabla u_{\parallel i} = 0 \quad \Rightarrow \quad \frac{d}{dt}\nabla_\perp^2 \Phi = v_A \hat{\mathbf{b}} \cdot \nabla \nabla_\perp^2 \Psi, \tag{E9}$$

where we have used the second of the equations (E3) to express the time derivative of $\delta B_\parallel/B_0$.

Together with Eqs. (E3), Eqs. (E8) and (E9) form a closed system, which it is natural to call *Hall Reduced MHD (HRMHD)* because these equations can be straightforwardly derived by applying the RMHD ordering (§ 2.1) to the MHD equations (8-10) with the induction equation (10) replaced by Eq. (E1). Indeed, Eqs. (E8) and (E9) exactly coincide with Eqs. (27) and (18), which are the parallel and perpendicular components of the MHD momentum equation (8) under the RMHD ordering; Eqs. (E3) should be compared Eqs. (17) and (26) while noticing that, in the limit $\tau \ll 1$, the sound speed is $c_s = v_A\sqrt{\beta_e/2}$ [see Eq. (166)]. The incompressible case (Mahajan & Yoshida 1998) is recovered in the subsidiary limit $\beta_e \gg 1$ (i.e., $1 \gg \beta_i \gg \tau$).

E.2. *Generalized Energy for Hall RMHD and the Passive Entropy Mode*

To work out the generalized energy (§ 3.4) for the HRMHD regime, we start with the generalized energy for the isothermal electron fluid [Eq. (109)] and use Eq. (E2) to express the density perturbation:

$$W = \int d^3\mathbf{r}\left[\int d^3\mathbf{v}\,\frac{T_{0i}\delta f_i^2}{2F_{0i}} + \frac{\delta B_\perp^2}{8\pi} + \left(1 + \frac{2}{\beta_e}\right)\frac{\delta B_\parallel^2}{8\pi}\right], \tag{E10}$$

where $\delta \mathbf{B}_\perp = \hat{\mathbf{z}} \times \nabla_\perp \Psi$. The perturbed ion distribution function can be written in the same form as it was done in § 5.4 [Eq. (143)]: to lowest order in the $\sqrt{\beta_i}$ expansion (§ E.1.2),

$$\delta f_i^{(-1)} = \frac{2\mathbf{v}_\perp \cdot \mathbf{u}_\perp}{v_{\mathrm{th}i}^2} F_{0i} + g^{(-1)} = \frac{2\mathbf{v}_\perp \cdot \mathbf{u}_\perp}{v_{\mathrm{th}i}^2} F_{0i} + \frac{2v_\parallel u_{\parallel i}}{v_{\mathrm{th}i}^2} F_{0i} + \tilde{g}, \tag{E11}$$

where $\mathbf{u}_\perp = \hat{\mathbf{z}} \times \nabla_\perp \Phi$. The last equality above is achieved by noticing that, since $g^{(-1)}$ satisfies Eq. (E8), we may split it into a perturbed Maxwellian with parallel velocity $u_{\parallel i}$ and the remainder: $g^{(-1)} = 2v_\parallel u_{\parallel i}F_{0i}/v_{\mathrm{th}i}^2 + \tilde{g}$. Then $\tilde{g}$ is the homogeneous solution of the leading-order kinetic equation [see Eq. (E8)]:

$$\frac{\partial \tilde{g}}{\partial t} + \{\Phi, \tilde{g}\} = 0, \quad \int d^3\mathbf{v}\,\tilde{g} = 0. \tag{E12}$$

Substituting Eq. (E11) into Eq. (E10) and keeping only the leading-order terms in the $\sqrt{\beta_i}$ expansion, we get

$$W = \int d^3\mathbf{r}\left[\frac{m_i n_{0i} u_\perp^2}{2} + \frac{\delta B_\perp^2}{8\pi} + \frac{m_i n_{0i} u_\parallel^2}{2} + \frac{\delta B_\parallel^2}{8\pi}\left(1 + \frac{2}{\beta_e}\right) + \int d^3\mathbf{v}\,\frac{T_{0i}\tilde{g}^2}{2F_{0i}}\right]. \tag{E13}$$

The first four terms are the energy of the Alfvénic and slow-wave-polarized fluctuations [cf. Eq. (D12)]. Unlike in RMHD, these are not decoupled in HRMHD, unless a further subsidiary long-wavelength limit is taken (see § E.4). It is easy to verify that the sum of these four terms is indeed conserved by Eqs. (E3), (E8) and (E9). The last term in Eq. (E13) is an individually conserved kinetic quantity. Its conservation reflects the fact that $\tilde{g}$ is decoupled from the wave dynamics and passively advected by the Alfvénic velocities via Eq. (E12).[51]

The passive kinetic mode $\tilde{g}$ can be thought of as a kinetic version of the MHD entropy mode and, indeed, reduces to it if the collision operator in Eq. (E5) is upgraded to the leading order by ordering $\omega/\nu_{ii} \sim 1$ (i.e., by considering long parallel wavelengths, $k_\parallel \lambda_{\mathrm{mfp}i} \sim \sqrt{\beta_i}$). In such a collisional limit, $\tilde{g}$ has to be a perturbed Maxwellian with no density or velocity perturbation [because $\int d^3\mathbf{v}\,\tilde{g} = 0$, while the velocity perturbation is explicitly separated from $\tilde{g}$ in Eq. (E11)]. Therefore,

$$\tilde{g} = \left(\frac{v^2}{v_{\mathrm{th}i}^2} - \frac{3}{2}\right)\frac{\delta T_i}{T_{0i}} F_{0i} \quad \Rightarrow \quad \frac{d}{dt}\frac{\delta T_i}{T_{0i}} = 0, \quad \int d^3\mathbf{r}\int d^3\mathbf{v}\,\frac{T_{0i}\tilde{g}^2}{2F_{0i}} = \int d^3\mathbf{r}\,\frac{3}{4}n_{0i}T_{0i}\frac{\delta T_i^2}{T_{0i}^2}. \tag{E14}$$

This is to be compared with the $\beta_i \sim \tau \ll 1$ limit of Eqs. (D11) and (D12). As we have established, in the $\sqrt{\beta_i}$ expansion, $\delta T_i = \delta T_i^{(-1)}$, $\delta n_i = \delta n_i^{(0)}$, $\delta B_\parallel = \delta B_\parallel^{(0)}$, so to lowest order $\delta s/s_0 = \delta T_i/T_{0i}$ and Eq. (E14) describes the entropy mode in the Hall limit.

---

[51] A similar splitting of the generalized energy cascade into a fluid-like cascade plus a passive cascade of a zero-density part of the distribution function occurs in the Hasegawa–Mima regime, which is the electrostatic version of the Hall limit (Plunk et al. 2009).

E.3. *Hall RMHD Dispersion Relation*

Linearizing the Hall RMHD equations (E3), (E8) and (E9) (derived in § E.1.2 assuming the ordering $\beta_i \sim \tau \ll 1$), we obtain the following dispersion relation:[52]

$$\left(\omega^2 - k_\parallel^2 v_A^2\right)\left(\omega^2 - \frac{k_\parallel^2 v_A^2}{1+2/\beta_e}\right) = \omega^2 k_\parallel^2 v_A^2 \frac{k_\perp^2 d_i^2}{1+2/\beta_e}. \tag{E15}$$

When the coupling term on the right-hand side is negligible, $k_\perp d_i/\sqrt{1+2/\beta_e} \ll 1$, we recover the MHD Alfvén wave, $\omega^2 = k_\parallel^2 v_A^2$, and the MHD slow wave, $\omega^2 = k_\parallel^2 v_A^2/(1+v_A^2/c_s^2)$ [Eq. (167)], where $c_s = v_A\sqrt{\beta_e/2}$ in the limit $\tau \ll 1$ [Eq. (166)]. In the opposite limit, we get the kinetic Alfvén wave, $\omega^2 = k_\parallel^2 v_A^2 k_\perp^2 d_i^2/(1+2/\beta_e)$ [same as Eq. (230) with $\tau \ll 1$].

The solution of the dispersion relation (E15) is

$$\omega^2 = \frac{k_\parallel^2 v_A^2}{1+2/\beta_e}\left[1 + \frac{1}{\beta_e} + \frac{k_\perp^2 d_i^2}{2} \pm \sqrt{\frac{1}{\beta_e^2} + \left(1+\frac{1}{\beta_e}\right)k_\perp^2 d_i^2 + \frac{k_\perp^4 d_i^4}{4}}\right]. \tag{E16}$$

The corresponding eigenfunctions then satisfy[53]

$$\Psi = -\frac{k_\parallel v_A}{\omega}\left(\Phi + v_A d_i \frac{\delta B_\parallel}{B_0}\right), \quad u_{\parallel i} = -\frac{k_\parallel v_A^2}{\omega}\frac{\delta B_\parallel}{B_0}, \quad \Phi = -\frac{k_\parallel v_A}{\omega}\Psi. \tag{E17}$$

Equation (E16) takes a particularly simple form in the subsidiary limits of high and low electron beta $\beta_e = \beta_i Z/\tau$:

$$\beta_e \gg 1: \ \omega^2 = k_\parallel^2 v_A^2\left[1 + \frac{k_\perp^2 d_i^2}{2} \pm \sqrt{\left(1+\frac{k_\perp^2 d_i^2}{2}\right)^2 - 1}\right], \qquad \beta_e \ll 1: \ \omega^2 = k_\parallel^2 v_A^2\left(1+k_\perp^2 \rho_s^2\right) \text{ and } \omega^2 = \frac{k_\parallel^2 c_s^2}{1+k_\perp^2 \rho_s^2}, \tag{E18}$$

where $\rho_s = d_i\sqrt{\beta_e/2} = \rho_i\sqrt{Z/2\tau} = c_s/\Omega_i$ is called the ion sound scale. The Alfvén wave and the slow wave (known as the ion acoustic wave in the limit of $\tau \ll 1$, $\beta_e \ll 1$) become dispersive at the ion inertial scale ($k_\perp d_i \sim 1$) when $\beta_e \gg 1$ and at the ion sound scale ($k_\perp \rho_s \sim 1$) when $\beta_e \ll 1$.

E.4. *Summary of Hall RMHD and the Role of the Ion Inertial and Ion Sound Scales*

We have shown that in the limit of cold ions and low ion beta ($\beta_i \sim \tau \ll 1$, "the Hall limit"), gyrokinetic turbulence can be described by five scalar functions: the stream and flux functions Φ and Ψ for the Alfvénic fluctuations, the parallel velocity and magnetic-field perturbations $u_{\parallel i}$ and $\delta B_\parallel$ for the slow-wave-polarized fluctuations, and $\tilde{g}$, the zero-density, zero-velocity part of the ion distribution function, which is the kinetic version of the MHD entropy mode. The first four of these functions satisfy a closed set of four fluid-like equations, derived in § E.1 and collected here:

$$\frac{\partial \Psi}{\partial t} = v_A \hat{\mathbf{b}} \cdot \nabla\left(\Phi + v_A d_i \frac{\delta B_\parallel}{B_0}\right), \qquad \frac{d}{dt}\frac{\delta B_\parallel}{B_0} = \frac{1}{1+2/\beta_e}\hat{\mathbf{b}} \cdot \nabla\left(u_{\parallel i} - d_i\nabla_\perp^2 \Psi\right), \tag{E19}$$

$$\frac{d}{dt}\nabla_\perp^2 \Phi = v_A \hat{\mathbf{b}} \cdot \nabla\nabla_\perp^2 \Psi, \qquad \frac{du_{\parallel i}}{dt} = v_A^2 \hat{\mathbf{b}} \cdot \nabla\frac{\delta B_\parallel}{B_0}. \tag{E20}$$

We call these equations the *Hall Reduced Magnetohydrodynamics (HRMHD)*. To fully account for the generalized energy cascade, one must append to the four HRMHD equations the fifth, kinetic equation (E12) for $\tilde{g}$, which is energetically decoupled from HRMHD and slaved to the Alfvénic velocity fluctuations (§ E.2).

The equations given above are valid above the ion gyroscale, $k_\perp \rho_i \ll 1$. They contain a special scale, $d_i/\sqrt{1+2/\beta_e}$, which is the ion inertial scale d_i for $\beta_e \gg 1$ and the ion sound scale $\rho_s = c_s/\Omega_i$ for $\beta_e \ll 1$. As becomes clear from the linear theory (§ E.3), the Alfvén and slow waves become dispersive at this scale. Nonlinearly, this scale marks the transition from the regime in which the Alfvénic and slow-wave-polarized fluctuations are decoupled to the regime in which they are mixed. Namely, when $k_\perp d_i/\sqrt{1+2/\beta_e} \ll 1$, HRMHD turns into RMHD: Eqs. (E19) become Eqs. (17) and (26), while Eqs. (E20) remain unchanged and identical to Eqs. (18) and (27); in the opposite limit, $k_\perp d_i/\sqrt{1+2/\beta_e} \gg 1$, the ion motion decouples from the magnetic-field evolution and Eqs. (E19) turn into the ERMHD equations (226-227).

Since we are considering the case $\beta_i \ll 1$, both d_i and ρ_s are much larger than the ion gyroscale ρ_i. In the opposite limit of $\beta_i \gg 1$ (§ E.1.1), while d_i is the only scale that appears explicitly in Eqs. (E4), we have $d_i \ll \rho_i$ and the equations themselves represent the dynamics at scales much smaller than the ion gyroscale, so the transition between the RMHD and ERMHD regimes occurs at $k_\perp \rho_i \sim 1$. The same is true for $\beta_i \sim 1$, when $d_i \sim \rho_i$. The ion sound scale $\rho_s \gg \rho_i$ does not play a special role when

---

[52] The full gyrokinetic dispersion relation in a similar limit was worked out in Howes et al. (2006), Appendix D.2.1.

[53] Note that wave packets with $|\mathbf{k}_\perp| = k_\perp$ and satisfying Eq. (E17) with $k_\parallel v_A/\omega$ as a function of $k_\perp$ given by Eq. (E16) are exact nonlinear solutions of the HRMHD equations (E3) and (E8-E9). This can be shown via a calculation analogous to that in § 7.3 (for the incompressible Hall MHD, this was done by Mahajan & Krishan 2005).

β_i is not small: it is not hard to see that for $k_\perp \rho_s \sim 1$, the ion motion terms in Eqs. (E19) dominate and we simply recover the inertial-range KRMHD model (§ 5) by expanding in $k_\perp \rho_i = k_\perp \rho_s \sqrt{2\tau/Z} \ll 1$.

Various theories of the dissipation-range turbulence based on Hall and Electron MHD are further discussed in § 8.2.6.

F. TWO-DIMENSIONAL INVARIANTS IN GYROKINETICS

Since gyrokinetics is in a sense a "quasi-two-dimensional" approximation, it is natural to inquire if this gives rise to additional conservation properties (besides the conservation of the generalized energy discussed in § 3.4) and how they are broken by the presence of parallel propagation terms. It is important to emphasize that, except in a few special cases, these invariants are only invariants in 2D, so gyrokinetic turbulence in 2D and 3D has fundamentally different properties, despite its seemingly "quasi-2D" nature. It is, therefore, generally not correct to think of the gyrokinetic turbulence (or its special case the MHD turbulence) as essentially a 2D turbulence with an admixture of parallel-propagating waves (Fyfe et al. 1977; Montgomery & Turner 1981).

In this Appendix, we work out the 2D invariants. Without attempting to present a complete analysis of the 2D conservation properties of gyrokinetics, we limit our discussion to showing how some more familiar fluid invariants (most notably, magnetic helicity) emerge from the general 2D invariants in the appropriate asymptotic limits.

F.1. *General 2D Invariants*

In deriving the generalized energy invariant, we used the fact that $\int d^3 \mathbf{R}_s h_s \{\langle \chi \rangle_{\mathbf{R}_s}, h_s\} = 0$, so Eq. (57) after multiplication by $T_{0s} h_s / F_{0s}$ and integration over space contains no contribution from the Poisson-bracket nonlinearity. Since we also have $\int d^3 \mathbf{R}_s \langle \chi \rangle_{\mathbf{R}_s} \{\langle \chi \rangle_{\mathbf{R}_s}, h_s\} = 0$, multiplying Eq. (57) by $q_s \langle \chi \rangle_{\mathbf{R}_s}$ and integrating over space has a similar outcome. Subtracting the latter integrated equation from the former and rearranging terms gives

$$\frac{\partial I_s}{\partial t} \equiv \frac{\partial}{\partial t} \frac{T_{0s}}{2F_{0s}} \int d^3 \mathbf{R}_s \left(h_s - \frac{q_s \langle \chi \rangle_{\mathbf{R}_s}}{T_{0s}} F_{0s} \right)^2 = q_s v_\parallel \int d^3 \mathbf{R}_s \langle \chi \rangle_{\mathbf{R}_s} \frac{\partial h_s}{\partial z} + \frac{T_{0s}}{F_{0s}} \int d^3 \mathbf{R}_s \left(h_s - \frac{q_s \langle \chi \rangle_{\mathbf{R}_s}}{T_{0s}} F_{0s} \right) \left(\frac{\partial h_s}{\partial t} \right)_{\mathrm{c}}. \quad \text{(F1)}$$

We see that in a purely 2D situation, when $\partial/\partial z = 0$, we have an infinite family of invariants $I_s = I_s(v_\perp, v_\parallel)$ whose conservation (for each species and for every value of $v_\perp$ and $v_\parallel$!) is broken only by collisions. In 3D, the parallel particle streaming (propagation) term in the gyrokinetic equation generally breaks these invariants, although special cases may arise in which the first term on the right-hand side of Eq. (F1) vanishes and a genuine 3D invariant appears.

F.2. *"$A_\parallel^2$-Stuff"*

Let apply the mass-ratio expansion (§ 4.1) to Eq. (F1) for electrons. Using the solution (101) for the electron distribution function, we find

$$\frac{\partial I_e}{\partial t} = \frac{\partial}{\partial t} \frac{T_{0e} F_{0e}}{2} \int d^3 \mathbf{r} \left(\frac{\delta n_e}{n_{0e}} - \frac{e}{T_{0e}} \frac{v_\parallel A_\parallel}{c} - \frac{v_\perp^2}{v_{\mathrm{the}}^2} \frac{\delta B_\parallel}{B_0} \right)^2 = \frac{\partial}{\partial t} \left[\frac{e^2 v_\parallel^2}{c^2} \frac{F_{0e}}{T_{0e}} \int d^3 \mathbf{r} \frac{A_\parallel^2}{2} - \frac{e v_\parallel}{c} F_{0e} \int d^3 \mathbf{r} A_\parallel \left(\frac{\delta n_e}{n_{0e}} - \frac{v_\perp^2}{v_{\mathrm{the}}^2} \frac{\delta B_\parallel}{B_0} \right) + \cdots \right]$$

$$= -e v_\parallel \int d^3 \mathbf{r} \left[\left(\varphi - \frac{v_\parallel A_\parallel}{c} - \frac{T_{0e}}{e} \frac{v_\perp^2}{v_{\mathrm{the}}^2} \frac{\delta B_\parallel}{B_0} \right) \frac{\partial}{\partial z} \left(\frac{\delta n_e}{n_{0e}} - \frac{e \varphi}{T_{0e}} \right) F_{0e} - \frac{v_\parallel A_\parallel}{c} \frac{\partial h_e^{(1)}}{\partial z} \right] - \frac{e v_\parallel}{c} \int d^3 \mathbf{r} A_\parallel \left(\frac{\partial h_e}{\partial t} \right)_{\mathrm{c}}, \quad \text{(F2)}$$

where we have kept terms to two leading orders in the expansion. To lowest order, the above equation reduces to

$$\frac{d}{dt} \int d^3 \mathbf{r} \frac{A_\parallel^2}{2} = c \int d^3 \mathbf{r} A_\parallel \frac{\partial}{\partial z} \left(\frac{T_{0e}}{e} \frac{\delta n_e}{n_{0e}} - \varphi \right). \quad \text{(F3)}$$

This equation can also be obtained directly from Eq. (116) (multiply by $A_\parallel$ and integrate). In 2D, it expresses a well known conservation law of the "$A_\parallel^2$-stuff." As this 2D invariant exists already on the level of the mass-ratio expansion of the electron kinetics, with no assumptions about the ions, it is inherited both by the RMHD equations in the limit of $k_\perp \rho_i \ll 1$ (§ 5.3) and by the ERMHD equations in the limit of $k_\perp \rho_i \gg 1$ (§ 7.2). In the former limit, $\delta n_e / n_{0e}$ on the right-hand side of Eq. (F3) is negligible (under the ordering explained in § 5.2); in the latter limit, it is expressed in terms of φ via Eq. (221). The conservation of "$A_\parallel^2$-stuff" is a uniquely 2D feature, broken by the parallel propagation term in 3D.

F.3. *Magnetic Helicity in the Electron Fluid*

If we now divide Eq. (F2) through by $e v_\parallel / c$ and integrate over velocities, we get, after some integrations by parts, another relation that becomes a conservation law in 2D and that can also easily be derived directly from the equations of the isothermal electron fluid (116-117):

$$\frac{d}{dt} \int d^3 \mathbf{r} A_\parallel \left(\frac{\delta n_e}{n_{0e}} - \frac{\delta B_\parallel}{B_0} \right) = -c \int d^3 \mathbf{r} \left[\frac{\delta n_e}{n_{0e}} \frac{\partial \varphi}{\partial z} + \frac{\delta B_\parallel}{B_0} \frac{\partial}{\partial z} \left(\frac{T_{0e}}{e} \frac{\delta n_e}{n_{0e}} - \varphi \right) + A_\parallel \frac{\partial u_{\parallel e}}{\partial z} \right]. \quad \text{(F4)}$$

In the ERMHD limit $k_\perp \rho_i \gg 1$ (§ 7.2), we use Eqs. (221-223) to simplify the above equation and find that the integral on the right-hand side vanishes and we get a genuine 3D conservation law:

$$\frac{d}{dt} \int d^3 \mathbf{r} A_\parallel \delta B_\parallel = 0. \quad \text{(F5)}$$

This can also be derived directly from the ERMHD equations (226-227) [using Eq. (223)]. The conserved quantity is readily seen to be the helicity of the perturbed magnetic field:

$$\int d^3\mathbf{r}\, \mathbf{A}\cdot\delta\mathbf{B} = \int d^3\mathbf{r}\, \left[\mathbf{A}_\perp \cdot (\nabla_\perp \times A_\|\hat{\mathbf{z}}) + A_\|\delta B_\|\right] = \int d^3\mathbf{r}\, \left[A_\|\hat{\mathbf{z}}\cdot(\nabla_\perp \times \mathbf{A}_\perp) + A_\|\delta B_\|\right] = 2\int d^3\mathbf{r}\, A_\|\delta B_\|. \tag{F6}$$

F.4. *Magnetic Helicity in the RMHD Limit*

Unlike in the case of ERMHD, the helicity of the perturbed magnetic field in RMHD is conserved only in 2D. This is because the induction equation for the perturbed field has an inhomogeneous term associated with the mean field [Eq. (10) with $\mathbf{B} = B_0\hat{\mathbf{z}} + \delta\mathbf{B}$] (this issue has been extensively discussed in the literature; see Matthaeus & Goldstein 1982; Stribling et al. 1994; Berger 1997; Montgomery & Bates 1999; Brandenburg & Matthaeus 2004). Directly from the induction equation or from its RMHD descendants Eqs. (17) and (26), we obtain [note the definitions (135)]

$$\frac{d}{dt}\int d^3\mathbf{r}\, A_\|\delta B_\| = \int d^3\mathbf{r}\, \left(c\varphi\frac{\partial\delta B_\|}{\partial z} + \frac{B_0 A_\|}{1 + v_A^2/c_s^2}\frac{\partial u_\|}{\partial z}\right), \tag{F7}$$

so helicity is conserved only if $\partial/\partial z = 0$.

For completeness, let us now show that this 2D conservation law is a particular case of Eq. (F1) for ions. Let us consider the inertial range ($k_\perp\rho_i \ll 1$). We substitute Eq. (124) into Eq. (F1) for ions and expand to two leading orders in $k_\perp\rho_i$ using the ordering explained in § 5.2:

$$\frac{\partial I_i}{\partial t} = \frac{\partial}{\partial t}\frac{T_{0i}}{2F_{0i}}\int d^3\mathbf{R}_i \left(g + \frac{Ze}{T_{0i}}\frac{v_\|\langle A_\|\rangle_{\mathbf{R}_i}}{c}F_{0i}\right)^2 = \frac{\partial}{\partial t}\left(\frac{Z^2 e^2 v_\|^2}{c^2}\frac{F_{0i}}{T_{0i}}\int d^3\mathbf{r}\frac{A_\|^2}{2} + \frac{Zev_\|}{c}\int d^3\mathbf{r}\, A_\| g + \cdots\right)$$

$$= -\frac{Z^2 e^2 v_\|^2}{c}\frac{F_{0i}}{T_{0i}}\int d^3\mathbf{r}\, A_\|\frac{\partial}{\partial z}\left(\varphi + \frac{T_{0i}}{Ze}\frac{v_\perp^2}{v_{\mathrm{thi}}^2}\frac{\delta B_\|}{B_0}\right) + Zev_\|\int d^3\mathbf{r}\left(\varphi - \frac{v_\| A_\|}{c}\right)\frac{\partial g}{\partial z} + \frac{Zev_\|}{c}\int d^3\mathbf{r}\, A_\|\left(\frac{\partial h_i}{\partial t}\right)_{\mathrm{c}}. \tag{F8}$$

The lowest-order terms in the above equations (all proportional to $v_\|^2 F_{0i}$) simply reproduce the 2D conservation of "$A_\|^2$-stuff," given by Eq. (F3). We now subtract Eq. (F3) multiplied by $(Zev_\|/c)^2 F_{0i}/T_{0i}$ from Eq. (F8). This leaves us with

$$\frac{\partial}{\partial t}\int d^3\mathbf{r}\, A_\| g = c\int d^3\mathbf{r}\left(\varphi - \frac{v_\| A_\|}{c}\right)\frac{\partial g}{\partial z} + v_\| F_{0i}\int d^3\mathbf{r}\left(\frac{Z}{\tau}\frac{\delta n_e}{n_{0e}} + \frac{v_\perp^2}{v_{\mathrm{thi}}^2}\frac{\delta B_\|}{B_0}\right)\frac{\partial A_\|}{\partial z} + \int d^3\mathbf{r}\, A_\|\left(\frac{\partial h_i}{\partial t}\right)_{\mathrm{c}}. \tag{F9}$$

This equation is a general 2D conservation law of the KRMHD equations (see § 5.7) and can also be derived directly from them. If we integrate it over velocities and use Eqs. (146) and (147), we simply recover Eq. (F4). However, since Eq. (F9) holds for every value of $v_\|$ and $v_\perp$, it carries much more information than Eq. (F4).

To make connection to MHD, let us consider the fluid (collisional) limit of KRMHD worked out in Appendix D. The distribution function to lowest order in the $k_\|\lambda_{\mathrm{mfp}i} \ll 1$ expansion is $g = -(v_\perp^2/v_{\mathrm{thi}}^2)\delta B_\|/B_0 + \delta\tilde{f}_i^{(0)}$, where $\delta\tilde{f}_i^{(0)}$ is the perturbed Maxwellian given by Eq. (D3). We can substitute this expression into Eq. (F9). Since in this expansion the collision integral is applied to $\delta\tilde{f}_i^{(1)}$ and is the same order as the rest of the terms (see § D.3), conservation laws are best derived by taking 1, $v_\|$, and v^2/v_{thi}^2 moments of Eq. (F9) so as to make the collision term vanish. In particular, multiplying Eq. (F9) by $1 + (2\tau/3Z)v^2/v_{\mathrm{thi}}^2$, integrating over velocities and using Eqs. (D4) and (D6), we obtain the evolution equation for $\int d^3\mathbf{r}\, A_\|\delta B_\|$, which coincides with Eq. (F7). Note that, either proceeding in an analogous way, one can derive similar equations for $\int d^3\mathbf{r}\, A_\|\delta n_e$ and $\int d^3\mathbf{r}\, A_\| u_\|$—these are also 2D invariants of the RMHD system, broken in 3D by the presence of the propagation terms. The same result can be derived directly from the evolution equations (D8) and (D10).

F.5. *Electrostatic Invariant*

Interestingly, the existence of the general 2D invariants introduced in § F.1 alongside the generalized energy invariant given by Eq. (73) means that one can construct a 2D invariant of gyrokinetics that does not involve any velocity-space quantities. In order to do that, one must integrate Eq. (F1) over velocities, sum over species, and subtract Eq. (73) from the resulting equation (thus removing the h_s^2 integrals). The result is not particularly edifying in the general case, but it takes a simple form if one considers electrostatic perturbations ($\delta\mathbf{B} = 0$). In this case, $\chi = \varphi$, and the manipulations described above lead to the following equation

$$\frac{dY}{dt} \equiv \frac{d}{dt}\left(\sum_s\int d^3\mathbf{v}\, I_s - W\right) = -\frac{d}{dt}\sum_s\sum_{\mathbf{k}}\frac{q_s^2 n_{0s}}{2T_{0s}}\left[1 - \Gamma_0(\alpha_s)\right]|\varphi_{\mathbf{k}}|^2 = \int d^3\mathbf{r}\, E_\| j_\| - \sum_s q_s\int d^3\mathbf{v}\int d^3\mathbf{R}_s\,\langle\varphi\rangle_{\mathbf{R}_s}\left(\frac{\partial h_s}{\partial t}\right)_{\mathrm{c}}, \tag{F10}$$

where $E_\| = -\partial\varphi/\partial z$, $\alpha_s = k_\perp^2\rho_s^2/2$ and Γ_0 is defined by Eq. (129). In 2D, $E_\| = 0$ and the above equation expresses a conservation law broken only by collisions. The complete derivation and analysis of 2D conservation properties of gyrokinetics in the electrostatic limit, including the invariant (F10), the electrostatic version of Eq. (F1), and their consequences for scalings and cascades, was given by Plunk et al. (2009). Here we briefly consider a few relevant limits.

For $k_\perp\rho_i \ll 1$, we have $\Gamma_0(\alpha) = 1 - \alpha_s + \ldots$, so the invariant given by Eq. (F10) is simply the kinetic energy of the $\mathbf{E}\times\mathbf{B}$ flows: $Y = \sum_s(m_s n_{0s}/2)\int d^3\mathbf{r}\,|\nabla_\perp\Phi|^2$, where $\Phi = c\varphi/B_0$. In the limit $k_\perp\rho_i \gg 1$, $k_\perp\rho_e \ll 1$, we have $Y = -n_{0i}\int d^3\mathbf{r}\, Z^2 e^2\varphi^2/2T_{0i}$. In

the limit $k_\perp \rho_e \gg 1$, we have $Y = -(1 + Z/\tau) n_{0e} \int d^3\mathbf{r}\, e^2 \varphi^2 / 2T_{0e}$. Whereas we are not interested in electrostatic fluctuations in the inertial range, electrostatic turbulence in the dissipation range was discussed in § 7.10 and § 7.12. The electrostatic 2D invariant in the limits $k_\perp \rho_i \gg 1$, $k_\perp \rho_e \ll 1$ and $k_\perp \rho_e \gg 1$ can also be derived directly from the equations given there [in the former limit, use Eq. (264) to express $u_{\parallel i}$ in terms of $j_\parallel$ in order to get Eq. (F10)].

Note that, taken separately and integrated over velocities, Eq. (F1) for ions (when $k_\perp \rho_i \gg 1$, $k_\perp \rho_e \ll 1$) and for electrons (when $k_\perp \rho_e \gg 1$), reduces to lowest order to the statement of 3D conservation of $\int d^3\mathbf{v} \int d^3\mathbf{R}_i\, T_{0i} h_i^2 / 2F_{0i}$ [W_{h_i} in Eq. (245)] and $\int d^3\mathbf{v} \int d^3\mathbf{R}_e\, T_{0e} h_e^2 / 2F_{0e}$ [Eq. (280)], respectively.

F.6. *Implications for Turbulent Cascades and Scalings*

Since invariants other than the generalized energy or its constituent parts are present in 2D and, in some limits, also in 3D, one might ask how their presence affects the turbulent cascades and scalings. As an example, let us consider the magnetic helicity in KAW turbulence, which is a 3D invariant of the ERMHD equations (§ F.3).

A Kolmogorov-style analysis of a local KAW cascade based on a constant flux of helicity gives (proceeding as in § 7.5):

$$\frac{\Psi_\lambda \Phi_\lambda}{\tau_{\mathrm{KAW}\lambda}} \sim \sqrt{1 + \beta_i}\, \frac{\lambda}{\rho_i}\, \frac{\Phi_\lambda^2}{\tau_{\mathrm{KAW}\lambda}} \sim \sqrt{1 + \beta_i}\, \frac{\Phi_\lambda^3}{\rho_i \lambda} \sim \varepsilon_H = \mathrm{const} \quad \Rightarrow \quad \Phi_\lambda \sim \frac{\varepsilon_H}{(1 + \beta_i)^{1/6}}\, \rho_i^{1/3} \lambda^{1/3}, \tag{F11}$$

where ε_H is the helicity flux (omitting constant dimensional factors, the helicity is now defined as $\int d^3\mathbf{r}\, \Psi\Phi$ and assumed to be non-zero). This corresponds to a $k_\perp^{-5/3}$ spectrum of magnetic energy.

In order to decide whether we expect the scalings to be determined by the constant-helicity flux or by the constant-energy flux (as assumed in § 7.5), we adapt a standard argument originally due to Fjørtoft (1953). If the helicity flux of the KAW turbulence originating at the ion gyroscale (via partial conversion from the inertial-range turbulence; see § 7) is ε_H, its energy flux is $\varepsilon_{\mathrm{KAW}} \sim \varepsilon_H$ [set $\lambda = \rho_i$ in Eq. (F11) and compare with Eq. (238)]. If the cascade between the ion and electron gyroscales is controlled by maintaining a constant flux of helicity, then the helicity flux arriving to the electron gyroscale is still ε_H, while the associated energy flux is $\varepsilon_H \rho_i / \rho_e \gg \varepsilon_{\mathrm{KAW}}$, i.e., more energy arrives to ρ_e than there was at ρ_i! This is clearly impossible in a stationary state. The way to resolve this contradiction is to conclude that the helicity cascade is, in fact, inverse (i.e., directed towards larger scales), while the energy cascade is direct (to smaller scales). A similar argument based on the constancy of the energy flux $\varepsilon_{\mathrm{KAW}}$ then leads to the conclusion that the helicity flux arriving to the electron gyroscale is $\varepsilon_{\mathrm{KAW}} \rho_e / \rho_i \ll \varepsilon_H \sim \varepsilon_{\mathrm{KAW}}$, i.e., the helicity indeed does not cascade to smaller scales. It does not, in fact, cascade to large scales either because the ERMHD equations are not valid above the ion gyroscale and the helicity of the perturbed magnetic field in the inertial range is not a 3D invariant (§ F.4). The situation would be different if an energy source existed either at the electron gyroscale or somewhere in between ρ_e and ρ_i. In such a case, one would expect an inverse helicity cascade and the consequent shallower scaling [Eq. (F11)] between the energy-injection scale and the ion gyroscale.

Other invariants introduced above can in a similar fashion be argued to give rise to inverse cascades in the hypothetical 2D situations where they are valid and provided there is energy injection at small scales (for the electrostatic case, see Plunk et al. 2009 and numerical simulations by Tatsuno et al. 2009b). The view of turbulence advanced in this paper does not generally allow for this to happen. First, the fundamentally 3D nature of the turbulence is imposed via the critical balance conjecture and supported by the argument that "two dimensionality" can only be maintained across parallel distances that do not exceed the distance a parallel-propagating wave (or parallel-streaming particles) travels over one nonlinear decorrelation time (see § 1.2, § 7.5 and § 7.10.3). Secondly, the lack of small-scale energy injection was assumed at the outset. This can, however, be violated in real astrophysical plasmas by various small-scale plasma instabilities (e.g., triggered by pressure anisotropies; see discussion in § 8.3). Treatment of such effects falls outside the scope of this paper and remains a matter for future work.

REFERENCES

Abel, I. G., Barnes, M., Cowley, S. C., Dorland, W., & Schekochihin, A. A. 2008, Phys. Plasmas, 15, 122509

Alexandrova, O. 2008, Nonlinear Process. Geophys., 15, 95

Alexandrova, O., Carbone, V., Veltri, P., & Sorriso-Valvo, L. 2008a, ApJ, 674, 1153

Alexandrova, O., Lacombe, C., & Mangeney, A. 2008b, Ann. Geophys., 26, 3585

Antonsen, T. M. & Lane, B. 1980, Phys. Fluids, 23, 1205

Armstrong, J. W., Coles, W. A., Kojima, M., & Rickett, B. J. 1990, ApJ, 358, 685

Armstrong, J. W., Cordes, J. M., & Rickett, B. J. 1981, Nature, 291, 561

Armstrong, J. W., Rickett, B. J., & Spangler, S. R. 1995, ApJ, 443, 209

Artun, M. & Tang, W. M. 1994, Phys. Plasmas, 1, 2682

Balbus, S. A. & Hawley, J. F. 1998, Rev. Mod. Phys., 70, 1

Bale, S. D., Kellogg, P. J., Mozer, F. S., Horbury, T. S., & Reme, H. 2005, Phys. Rev. Lett., 94, 215002

Barnes, A. 1966, Phys. Fluids, 9, 1483

Barnes, M. A., Abel, I. G., Dorland, W., Ernst, D. R., Hammett, G. W., Ricci, P., Rogers, B. N., Schekochihin, A. A., and Tatsuno, T. 2009, Phys. Plasmas, submitted (arXiv:0809.3945)

Bavassano, B., Dobrowolny, M., Fanfoni, G., Mariani, F., & Ness, N. F. 1982, J. Geophys. Res., 87, 3617

Bavassano, B., Pietropaolo, E., & Bruno, R. 2004, Ann. Geophys., 22, 689

Beck, R. 2007, in Polarisation 2005, ed. F. Boulanger & M. A. Miville-Deschenes, EAS Pub. Ser., 23, 19

Belcher, J. W. & Davis, L. 1971, J. Geophys. Res., 76, 3534

Beresnyak, A. & Lazarian, A. 2006, ApJ, 640, L175

Beresnyak, A. & Lazarian, A. 2008a, ApJ, 682, 1070

Beresnyak, A. & Lazarian, A. 2008b, arXiv:0812.0812

Berger, M. 1997, J. Geophys. Res., 102, 2637

Bershadskii, A. & Sreenivasan, K. R. 2004, Phys. Rev. Lett., 93, 064501

Bhattacharjee, A. & Ng, C. S. 2001, ApJ, 548, 318

Bhattacharjee, A., Ng, C. S., Spangler, S. R. 1998, ApJ, 494, 409

Bieber, J. W., Wanner, W., & Matthaeus, W. H. 1996, J. Geophys. Res., 101, 2511

Bigazzi, A., Biferale, L., Gama, S. M. A., & Velli, M. 2006, ApJ, 638, 499

Biskamp, D. & Müller, W.-C. 2000, Phys. Plasmas, 7, 4889

Biskamp, D., Schwartz, E., & Drake, J. F. 1996, Phys. Rev. Lett., 76, 1264

Biskamp, D., Schwartz, E., Zeiler, A., Celani, A., & Drake, J. F. 1999, Phys. Plasmas, 6, 751

Boldyrev, S. A. 2006, Phys. Rev. Lett., 96, 115002

Braginskii, S. I. 1965, Rev. Plasma Phys., 1, 205

Brandenburg, A. & Matthaeus, W. H. 2004, Phys. Rev. E, 69, 056407

Brizard, A. J. & Hahm, T. S. 2007, Rev. Mod. Phys., 79, 421

Brunetti, G. & Lazarian, A. 2007, MNRAS, 378, 245
Bruno, R. & Carbone, V. 2005, Living Rev. Solar Phys., 2, 4
Bruno, R., Carbone, V., Chapman, S., Hnat, B., Noullez, A., & Sorriso-Valvo, L. 2007, Phys. Plasmas, 14, 032901
Burlaga, L. F., Scudder, J. D., Klein, L. W., & Isenburg, P. A. 1990, J. Geophys. Res., 95, 2229
Califano, F., Hellinger, P., Kuznetsov, E., Passot, T., Sulem, P.-L., & Trávnícek 2008, J. Geophys. Res., 113, A08219
Candy, J. & Waltz, R. E. 2003, J. Comput. Phys., 186, 545
Carter, T. A., Brugman, B., Pribyl, P., & Lybarger, W. 2006, Phys. Rev. Lett., 96, 155001
Catto, P. J. 1978, Plasma Phys., 20, 719
Catto, P. J., Tang, W. M., & Baldwin, D. E. 1981, Plasma Phys., 23, 639
Catto, P. J. & Tsang, K. T. 1977, Phys. Fluids, 20, 396
Celnikier, L. M., Harvey, C. C., Jegou, R., Kemp, M., & Moricet, P. 1983, A&A, 126, 293
Celnikier, L. M., Muschietti, L., & Goldman, M. V. 1987, A&A, 181, 138
Chandran, B. D. G. 2005a, ApJ, 632, 809
Chandran, B. D. G. 2005b, Phys. Rev. Lett., 95, 265004
Chandran, B. D. G. 2008, ApJ, 685, 646
Chapman, S. & Cowling, T. G. 1970, The Mathematical Theory of Non-Uniform Gases (Cambridge: Cambridge Univ. Press)
Chapman, S. C. & Hnat, B. 2007, Geophys. Res. Lett., 34, L17103
Chen, Y. & Parker, S. E. 2003, J. Comput. Phys., 189, 463
Chen, C. H. K., Schekochihin, A. A., Cowley, S. C., & Horbury, T. S. 2009, ApJ, submitted
Cho, J. & Lazarian, A. 2002, Phys. Rev. Lett., 88, 245001
Cho, J. & Lazarian, A. 2003, MNRAS, 345, 325
Cho, J. & Lazarian, A. 2004, ApJ, 615, L41
Cho, J. & Vishniac, E. T. 2000, ApJ, 539, 273
Cho, J., Lazarian, A., & Vishniac, E. T. 2002, ApJ, 564, 291
Cho, J., Lazarian, A., & Vishniac, E. T. 2003, ApJ, 595, 812
Clarke, T. E. & Enßlin T. A. 2006, AJ, 131, 2900
Coleman, P. J. 1968, ApJ, 153, 371
Coles, W. A. & Harmon, J. K. 1989, ApJ, 337, 1023
Coles, W. A., Liu, W., Harmon, J. K., & Martin, C. L. 1991, J. Geophys. Res., 96, 1745
Coroniti, F. W., Kennel, C. F., Scarf, F. L., & Smith, E. J. 1982, J. Geophys. Res., 87, 6029
Corrsin, S. 1951, J. Appl. Phys., 22, 469
Cowley, S. C. 1985, Ph. D. Thesis, Princeton University
Cranmer, S. R. & van Ballegooijen, A. A. 2003, ApJ, 594, 573
Czaykowska, A., Bauer, T. M., Treumann, R. A., & Baumjohann, W. 2001, Ann. Geophys., 19, 275
Dasso, S., Milano, L. J., Matthaeus, W. H., & Smith, C. W. 2005, ApJ, 635, L181
Dennett-Thorpe, J. & de Bruyn, A. G. 2003, A&A, 404, 113
Denskat, K. U., Beinroth, H. J., & Neubauer, F. M. 1983, J. Geophys., 54, 60
Dimits, A. M. & Cohen, B. I. 1994, Phys. Rev. E, 49, 709
Dmitruk, P., Gomez, D. O., & Matthaeus, W. H. 2003, Phys. Plasmas, 10, 3584
Dobrowolny, M., Mangeney, A., & Veltri, P.-L. 1980, Phys. Rev. Lett., 45, 144
Dorland, W. & Hammett, G. W. 1993, Phys. Fluids B, 5, 812
Dubin, D. H. E., Krommes, J. A., Oberman, C., & Lee, W. W. 1983, Phys. Fluids, 26, 3524
Elsasser, W. M. 1950, Phys. Rev., 79, 183
Enßlin, T. A. & Vogt, C. 2006, A&A, 453, 447
Enßlin, T. A., Waelkens, A., Vogt, C., & Schekochihin, A. A. 2006, Astron. Nachr., 327, 626
Fabian, A. C., Sanders, J. S., Taylor, G. B., Allen, S. W., Crawford, C. S., Johnstone, R. M., & Iwasawa, K. 2006, MNRAS, 366, 417
Ferriere, K. M. 2001, Rev. Mod. Phys., 73, 1031
Fjørtoft, R. 1953, Tellus, 5, 225
Foote, E. A. & Kulsrud, R. M. 1979, ApJ, 233, 302
Fowler, T. K. 1968, Adv. Plasma Phys., 1, 201
Fried, B. D. & Conte, S. D. 1961, The Plasma Dispersion Function (San Diego, CA: Academic Press)
Frieman, E. A. & Chen, L. 1982, Phys. Fluids, 25, 502
Fyfe, D., Joyce, G., & Montgomery, D. 1977, J. Plasma Phys., 17, 317
Galtier, S. 2006, J. Plasma Phys., 72, 721
Galtier, S. & Bhattacharjee, A. 2003, Phys. Plasmas, 10, 3065
Galtier, S. & Buchlin, E. 2007, ApJ, 656, 560
Galtier, S. & Chandran, B. D. G. 2006, Phys. Plasmas, 13, 114505
Galtier, S., Nazarenko, S. V., Newell, A. C., & Pouquet, A. 2000, J. Plasma Phys., 63, 447

Galtier, S., Nazarenko, S. V., Newell, A. C., & Pouquet, A. 2002, ApJ, 564, L49
Gary, S. P., Montgomery, M. D., Feldman, W. C., & Forslund, D. W. 1976, J. Geophys. Res., 81, 1241
Gary, S. P. 1986, J. Plasma Phys., 35, 431
Gaty, S. P. & Borovsky, J. 2008, J. Geophys. Res., 113, A12104
Gary, S. P., Saito, S., & Li, H. 2008, Geophys. Res. Lett., 35, L02104
Gary, S. P., Skoug, R. M., Steinberg, J. T., & Smith, C. W. 2001, Geophys. Res. Lett., 28, 2759
Ghosh, S., Siregar, E., Roberts, D. A., & Goldstein, M. L. 1996, J. Geophys. Res., 101, 2493
Gogoberidze, G. 2005, Phys. Rev. E, 72, 046407
Gogoberidze, G. 2007, Phys. Plasmas, 14, 022304
Goldreich, P. & Reisenegger, A. 1992, ApJ, 395, 250
Goldreich, P. & Sridhar, S. 1995, ApJ, 438, 763
Goldreich, P. & Sridhar, S. 1997, ApJ, 485, 680
Goswami, P., Passot, T., & Sulem, P. L. 2005, Phys. Plasmas, 12, 102109
Grall, R. R., Coles, W. A., Spangler, S. R., Sakurai, T., & Harmon, J. K. 1997, J. Geophys. Res., 102, 263
Grison, B., Sahraoui, F., Lavraud, B., Chust, T., Cornilleau-Wehrlin, N., Rème, H., Balogh, A., & André, M. 2005, Ann. Geophys., 23, 3699
Hahm, T. S., Lee, W. W., & Brizard, A. 1988, Phys. Fluids, 31, 1940
Hallatschek, K. 2004, Phys. Rev. Lett., 93, 125001
Hamilton, K., Smith, C. W., Vasquez, B. J., & Leamon, R. J. 2008, J. Geophys. Res., 113, A01106
Hammett, G. W., Dorland, W., & Perkins, F. W. 1991, Phys. Fluids B, 4, 2052
Harmon, J. K. & Coles, W. A. 2005, J. Geophys. Res., 110, A03101
Haugen, N. E. L., Brandenburg, A., & Dobler, W. 2004, Phys. Rev. E, 70, 016308
Haverkorn, M., Gaensler, B. M., McClure-Griffiths, N. M., Dickey, J. M., & Green, A. J. 2004, ApJ, 609, 776
Haverkorn, M., Gaensler, B. M., Brown, J. C., Bizunok, N. S., McClure-Griffiths, N. M., Dickey, J. M., & Green, A. J. 2005, ApJ, 637, L33
Haverkorn, M., Brown, J. C., Gaensler, B. M., & McClure-Griffiths, N. M. 2008, ApJ, 680, 362
Hazeltine, R. D. 1983, Phys. Fluids, 26, 3242
Helander, P. & Sigmar, D. J. 2002, Collisional Transport in Magnetized Plasmas (Cambridge: Cambridge Univ. Press)
Hellinger, P., Trávnícek, P., Kasper, J. C., & Lazarus, A. J., 2006, Geophys. Res. Lett., 33, L09101
Heyer, M., Gong, H., Ostriker, E., & Brunt, C. 2008, ApJ, 680, 420
Higdon, J. C. 1984, ApJ, 285, 109
Hirose, A., Ito, A., Mahajan, S. M., & Ohsaki, S. 2004, Phys. Lett. A, 330, 474
Hnat, B., Chapman, S. C., & Rowlands, G. 2005, Phys. Rev. Lett., 94, 204502
Hnat, B., Chapman, S. C., Kiyani, K., Rowlands, G., & Watkins, N. W. 2007, Geophys. Res. Lett., 34, L15108
Hollweg, J. V. 1999, J. Geophys. Res., 104, 14811
Hollweg, J. V. 2008, J. Astrophys. Astr., 29, 217
Horbury, T. S., Balogh, A., Forsyth, R. J., & Smith E. J. 1996, A&A, 316, 333
Horbury, T. S., Forman, M. A., & Oughton, S. 2005, Plasma Phys. Control. Fusion, 47, B703
Horbury, T. S., Forman, M., & Oughton, S. 2008, Phys. Rev. Lett., 101, 175005
Howes, G. G., Cowley, S. C., Dorland, W., Hammett, G. W., Quataert, E., & Schekochihin, A. A. 2006, ApJ, 651, 590
Howes, G. G., Cowley, S. C., Dorland, W., Hammett, G. W., Quataert, E., & Schekochihin, A. A., 2008a, J. Geophys. Res., 113, A05103
Howes, G. G., Cowley, S. C., Dorland, W., Hammett, G. W., Quataert, E., Schekochihin, A. A., & Tatsuno, T. 2008b, Phys. Rev. Lett., 100, 065004
Iroshnikov, R. S. 1963, Astron. Zh., 40, 742 [English translation: 1964, Sov. Astron, 7, 566]
Ito, A., Hirose, A., Mahajan, S. M., & Ohsaki, S. 2004, Phys. Plasmas, 11, 5643
Jenko, F., Dorland, W., Kotschenreuther, M., & Rogers, B. N. 2000, Phys. Plasmas, 7, 1904
Kadomtsev, B. B. & Pogutse, O. P. 1974, Sov. Phys.—JETP, 38, 283
Kasper, J. C., Lazarus, A. J., & Gary, S. P. 2002, Geophys. Res. Lett., 29, 20
Kellogg, P. J. & Horbury, T. S. 2005, Ann. Geophys., 23, 3765
Kellogg, P. J., Bale, S. D., Mozer, F. S., Horbury, T. S., & Reme, H. 2006, ApJ, 645, 704
Kingsep, A. S., Chukbar, K. V., & Yankov, V. V. 1990, Rev. Plasma Phys., 16, 243

Kinney, R. & McWilliams, J. C., 1997, J. Plasma Phys., 57, 73

Kinney, R. M. & McWilliams, J. C. 1998, Phys. Rev. E, 57, 7111

Kivelson, M. G. & Southwood, D. J. 1996, J. Geophys. Res., 101, 17365

Kiyani, K., Chapman, S. C., Hnat, B. & Nicol, R. M. 2007, Phys. Rev. Lett., 98, 211101

Kolmogorov, A. N. 1941, Dokl. Akad. Nauk SSSR, 30, 299 [English translation: 1991, Proc. R. Soc. A, 434, 9]

Kotschenreuther, M., Rewoldt, G., & Tang, W. M. 1995, Comput. Phys. Commun., 88, 128

Kraichnan, R. H. 1965, Phys. Fluids, 8, 1385

Krishan, V. & Mahajan, S. M. 2004, J. Geophys. Res., 109, A11105

Krommes, J. A. 1999, Phys. Plasmas, 6, 1477

Krommes, J. A. 2006, in Turbulence and Coherent Structures in Fluids, Plasmas and Nonlinear Medium, eds. M. Shats & H. Punzmann (Singapore: World Scientific), 115

Krommes, J. A. & Hu, G. 1994, Phys. Plasmas, 1, 3211

Kruger, S. E., Hegna, C. C., & Callen, J. D. 1998, Phys. Plasmas, 5, 4169

Kruskal, M. D. & Oberman, C. R. 1958, Phys. Fluids, 1, 275

Kulsrud, R. 1962, Phys. Fluids, 5, 192

Kulsrud, R. M. 1964, in Teoria dei plasmi, ed. M. N. Rosenbluth (London: Academic Press), 54

Kulsrud, R. M. 1983, in Handbook of Plasma Physics, Vol. 1, ed. A. A. Galeev & R. N. Sudan (Amsterdam: North–Holland), 115

Lacombe, C., Samsonov, A. A., Mangeney, A., Maksimovic, M., Cornilleau-Wehrlin, N., Harvey, C. C., Bosqued, J.-M., & Trávnícek, P. 2006, Ann. Geophys., 24, 3523

Landau, L. 1936, Zh. Exp. Teor. Fiz., 7, 203

Landau, L. 1946, Zh. Exp. Teor. Fiz., 16, 574 [English translation: 1946, J. Phys. U.S.S.R., 10, 25]

Lazio, T. J. W., Cordes, J. M., de Bruyn, A. G., & Macquart, J.-P. 2004, New Astron. Rev., 48, 1439

Leamon, R. J., Smith, C. W., Ness, N. F., Matthaeus, W. H., & Wong, H. K. 1998, J. Geophys. Res., 103, 4775

Leamon, R. J., Smith, C. W., Ness, N. F., & Wong, H. K. 1998, J. Geophys. Res., 104, 22331

Leamon, R. J., Matthaeus, W. H., Smith, C. W., Zank, G. P., & Mullan, D. J. 2000, ApJ, 537, 1054

Li, H., Gary, P., & Stawicki, O. 2001, Geophys. Res. Lett., 28, 1347

Lithwick, Y. & Goldreich, P. 2001, ApJ, 562, 279

Lithwick, Y. & Goldreich, P. 2003, ApJ, 582, 1220

Lithwick, Y., Goldreich, P., & Sridhar, S. 2007, ApJ, 655, 269

Loeb, A. & Waxman, E. 2007, J. Cosmol. Astropart. Phys., 03, 011

Longmire, C. L. 1963, Elementary Plasma Physics (New York: Interscience)

Lovelace, R. V. E., Salpeter, E. E., Sharp, L. E., & Harris, D. E. 1970, ApJ, 159

Mahajan, S. M. & Krishan, V. 2005, MNRAS, 359, L27

Mahajan, S. M. & Yoshida, Z. 1998, Phys. Rev. Lett., 81, 4863

Maksimovic, M., Zouganelis, I., Chaufray, J.-Y., Issautier, K., Scime, E. E., Littleton, J. E., Marsch, E., McComas, D. J., Salem, C., Lin, R. P., & Elliott, H. 2005, J. Geophys. Res., 110, A09104

Mangeney, A., Lacombe, C., Maksimovic, M., Samsonov, A. A., Cornilleau-Wehrlin, N., Harvey, C. C., Bosqued, J.-M., & Trávnícek, P. 2006, Ann. Geophys., 24, 3507

Markevitch, M. & Vikhlinin, A. 2007, Phys. Rep., 443, 1

Markevitch, M., Mazzotta, P., Vikhlinin, A., Burke, D., Butt, Y., David, L., Donnelly, H., Forman, W. R., Harris, D., Kin, D.-W., Virani, S., & Vrtilek, J. 2003, ApJ, 586, L19

Markovskii, S. A., Vasquez, B. J., Smith, C. W., & Holweg, J. V. 2006, ApJ, 639, 1177

Markovskii, S. A., Vasquez, B. J., & Smith, C. W. 2008, ApJ, 675, 1576

Maron, J. & Goldreich, P. 2001, ApJ, 554, 1175

Marsch, E. 2006, Living Rev. Solar Phys., 3, 1

Marsch, E. & Tu, C.-Y. 1990a, J. Gephys. Res, 95, 8211

Marsch, E. & Tu, C.-Y. 1990b, J. Gephys. Res, 95, 11945

Marsch, E. & Tu, C.-Y. 1993, Ann. Geophys., 11, 659

Marsch, E., Ao, X.-Z., & Tu, C.-Y. 2004, J. Geophys. Res., 109, A04102

Marsch, E., Mühlhäuser, K. H., Rosenbauer, H., & Schwenn, R. 1983, J. Geophys. Res., 88, 2982

Mason, J., Cattaneo, F., & Boldyrev, S. 2006, Phys. Rev. Lett., 97, 255002

Mason, J., Cattaneo, F., & Boldyrev, S. 2007, Phys. Rev. E, 77, 036403

Matteini, L., Landi, S., Hellinger, P., Pantellini, F., Maksimovic, M., Velli, M., Goldstein, B. E., & Marsch, E. 2007, Geophys. Res. Lett., 34, L20105

Matthaeus, W. H. & Goldstein, M. L. 1982, J. Geophys. Res., 87, 6011

Matthaeus, W. H. & Brown, M. R. 1988, Phys. Fluids, 31, 3634

Matthaeus, W. H., Goldstein, M. L., & Roberts, D. A. 1990, J. Geophys. Res., 95, 20673

Matthaeus, W. H., Klein, K. W., Ghosh, S., & Brown, M. R. 1991, J. Geophys. Res., 96, 5421

Matthaeus, W. H., Pouquet, A., Mininni, P. D., Dmitruk, P., & Breech, B. 2008a, Phys. Rev. Lett., 100, 085003

Matthaeus, W. H., Servidio, S., & Dmitruk, P. 2008b, Phys. Rev. Lett., 101, 149501

Minter, A. H. & Spangler, S. R. 1996, ApJ, 458, 194

Montgomery, D. C. 1982, Phys. Scripta, T2/1, 83

Montgomery, D. C. & Bates, J. W. 1999, Phys. Plasmas, 6, 2727

Montgomery, D. & Turner, L. 1981, Phys. Fluids, 24, 825

Montgomery, D., Brown, M. R., & Matthaeus, W. H. 1987, J. Geophys. Res., 92, 282

Morales, G. J., Maggs, J. E., Burke, A. T., & Peñano, J. R. 1999, Plasma Phys. Control. Fusion, 41, A519

Müller, W.-C., Biskamp, D., & Grappin, R. 2003, Phys. Rev. E, 67, 066302

Narayan, R. & Quataert, E. 2005, Science, 307, 77

Narayan, R. & Yi, I. 1995, ApJ, 452, 710

Narita, Y., Glassmeier, K.-H., & Treumann, R. A. 2006, Phys. Rev. Lett., 97, 191101

Nazarenko, S. 2007, New J. Phys., 9, 307

Newbury, J. A., Russell, C. T., Phillips, J. L., & Gary, S. P. 1998, J. Geophys. Res., 103, 9553

Ng, C. S. & Bhattacharjee, A. 1996, ApJ, 465, 845

Ng, C. S. & Bhattacharjee, A. 1997, Phys. Plasmas, 4, 605

Ng, C. S., Bhattacharjee, A., Germaschewski, K., & Galtier, S. 2003, Phys. Plasmas, 10, 1954

Norman, C. A. & Ferrara, A. 1996, ApJ, 467, 280

Obukhov, A. M. 1941, Izv. Akad. Nauk SSSR Ser. Geogr. Geofiz., 5, 453

Obukhov, A. M. 1949, Izv. Akad. Nauk SSSR Ser. Geogr. Geofiz., 13, 58

Osman, K. T. & Horbury, T. S. 2007, 654, L103

Oughton, S., Dmitruk, P., & Matthaeus, W. H. 2004, Phys. Plasmas, 11, 2214

Oughton, S., Priest, E. R., & Matthaeus, W. H. 1994, J. Fluid Mech., 280, 95

Passot, T. & Sulem, P. L. 2007, Phys. Plasmas, 14, 082502

Perez, J. C. & Boldyrev, S. 2008, ApJ, 672, L61

Perez, J. C. & Boldyrev, S. 2009, Phys. Rev. Lett., 102, 025003

Plunk, G. G., Cowley, S. C., Schekochihin, A. A., & Tatsuno, T. 2009, J. Fluid Mech., submitted (arXiv:0904.0243)

Podesta, J. J., Roberts, D. A., & Goldstein, M. L. 2006, J. Geophys. Res., 111, A10109

Pokhotelov, O. A., Sagdeev, R. Z., Balikhin, M. A., Onishchenko, O. G., & Fedun, V. N. 2008, J. Geophys. Res., 113, A04225

Quataert, E. 2003, Astron. Nachr., 324, 435

Quataert, E. & Gruzinov, A. 1999, ApJ, 520, 248

Quataert, E., Dorland, W., & Hammett, G. W. 2002, ApJ, 577, 524

Ramos, J. J. 2005, Phys. Plasmas, 12, 052102

Rappazzo, A. F., Velli, M., Einaudi, G., & Dahlburg, R. B. 2007, ApJ, 657, L47

Rappazzo, A. F., Velli, M., Einaudi, G., & Dahlburg, R. B. 2008, ApJ, 677, 1348

Rees, M. J., Begelman, M. C., Blandford, R. D., & Phinney, E. S. 1982, Nature, 295, 17

Rickett, B. J., Kedziora-Chudczer, L., & Jauncey, D. L. 2002, ApJ, 581, 103

Rincon, F., Schekochihin, A. A., & Cowley, S. C. 2009, MNRAS, submitted

Roach, C. M., Applegate, D. J., Connor, J. W., Cowley, S. C., Dorland, W. D., Hastie, R. J., Joiner, N., Saarelma, S., Schekochihin, A. A., Akers, R. J., Brickley, C., Field, A. R., Valovic, M., & MAST Team 2005, Plasma Phys. Control. Fusion, 47, B323

Roberts, D. A. 1990, J. Geophys. Res., 95, 1087

Robinson, D. C. & Rusbridge, M. G. 1971, Phys. Fluids, 14, 2499

Rosenbluth, M. N., Hazeltine, R. D., & Hinton, F. L. 1972, Phys. Fluids, 15, 116

Rosin, M. S., Rincon, F., Schekochihin, A. A., & Cowley, S. C. 2009, MNRAS, submitted

Rutherford, P. H. & Frieman, E. A. 1968, Phys. Fluids, 11, 569

Sahraoui, F., Belmont, G., Rezeau, L., Cornilleau-Wehrlin, N., Pinçon, J. L., & Balogh, A. 2006, Phys. Rev. Lett., 96, 075002

Saito, S., Gary, S. P., Li, H., & Narita, Y. 2008, Phys. Plasmas, 15, 102305

Sanders, J. S. & Fabian, A. C. 2006, MNRAS, 371, L65

Schekochihin, A. A. & Cowley, S. C. 2006, Phys. Plasmas, 13, 056501

Schekochihin, A. A. & Cowley, S. C. 2007, in Magnetohydrodynamics: Historical Evolution and Trends, ed. S. Molokov, R. Moreau, & H. K. Moffatt, (Berlin: Springer), 85 (arXiv:astro-ph/0507686)

Schekochihin, A. A. & Cowley, S. C. 2009, Phys. Rev. Lett., submitted

Schekochihin, A. A., Cowley, S. C., Taylor, S. F., Maron, J. L., & McWilliams, J. C. 2004, ApJ, 612, 276

Schekochihin, A. A., Cowley, S. C., Kulsrud, R. M., Hammett, G. W., & Sharma, P. 2005, ApJ, 629, 139

Schekochihin, A. A., Cowley, S. C., & Dorland, W. 2007, Plasma Phys. Control. Fusion, 49, A195

Schekochihin, A. A., Cowley, S. C., Kulsrud, R. M., Rosin, M. S., & Heinemann, T. 2008a, Phys. Rev. Lett., 100, 081301

Schekochihin, A. A., Cowley, S. C., Dorland, W., Hammett, G. W., Howes, G. G., Plunk, G. G., Quataert, E., & Tatsuno, T. 2008b, Plasma Phys. Control. Fusion, 50, 124024

Schuecker, P., Finoguenov, A., Miniati, F., Böhringer, H., & Briel, U. G. 2004, A&A, 426, 387

Scott, B. D. 2007, Phys. Plasmas, submitted (arXiv:0710.4899)

Shaikh, D. & Zank, G. P. 2005, Phys. Plasmas, 12, 122310

Shakura, N. I. & Sunyaev, R. A. 1973, A&A, 24, 337

Sharma, P., Hammett, G. W., & Quataert, E. 2003, ApJ, 596, 1121

Sharma, P., Hammett, G. W., Quataert, E., & Stone, J. M. 2006, ApJ, 637, 952

Sharma, P., Quataert, E., Hammett, G. W., & Stone, J. M. 2007, ApJ, 667, 714

Shebalin, J. V., Matthaeus, W. H., & Montgomery, D. 1983, J. Plasma Phys., 29, 525

Shukurov, A. 2007, in Mathematical Aspects of Natural Dynamos, eds. E. Dormy & A. M. Soward (London: CRC Press), 313 (arXiv:astro-ph/0411739)

Smirnova, T. V., Gwinn, C. R., & Shishov, V. I. 2006, A&A, 453, 601

Smith, C. W., Mullan, D. J., Ness, N. F., Skoug, R. M., & Steinberg, J. 2001, J. Geophys. Res., 106, 18625

Smith, C. W., Hamilton, K., Vasquez, B. J., & Leamon, R. J. 2006, ApJ, 645, L85

Snyder, P. B. & Hammett, G. W. 2001, Phys. Plasmas, 8, 3199

Snyder, P. B., Hammett, G. W., & Dorland, W. 1997, Phys. Plasmas, 4, 3974

Sorriso-Valvo, L., Carbone, V., Bruno, R., & Veltri, P. 2006, Europhys. Lett., 75, 832

Spangler, S. R. & Gwinn, C. R. 1990, ApJ, 353, L29

Stawicki, O., Gary, S. P., & Li, H. 2001, J. Geophys. Res., 106, 8273

Strauss, H. R. 1976, Phys. Fluids, 19, 134

Strauss, H. R. 1977, Phys. Fluids, 20, 1354

Stribling, T., Matthaeus, W. H., & Ghosh, S. 1994, J. Geophys. Res., 99, 2567

Subramanian, K., Shukurov, A., & Haugen, N. E. L. 2006, MNRAS, 366, 1437

Sugama, H. & Horton, W. 1997, Phys. Plasmas, 4, 405

Sugama, H., Okamoto, M., Horton, W., & Wakatani, M. 1996, Phys. Plasmas, 3, 2379

Tatsuno, T., Dorland, W., Schekochihin, A. A., Plunk, G. G., Barnes, M. A., Cowley, S. C., & Howes, G. G. 2009a, Phys. Rev. Lett., submitted (arXiv:0811.2538)

Tatsuno, T., Dorland, W., Schekochihin, A. A., Plunk, G. G., Barnes, M. A., Cowley, S. C., & Howes, G. G. 2009b, Phys. Plasmas, submitted

Taylor, G. I. 1938, Proc. R. Soc. A, 164, 476

Taylor, J. B. & Hastie, R. J. 1968, Plasma Phys., 10, 479

Trotter, A. S., Moran, J. M., & Rodríguez, L. F. 1998, ApJ, 493, 666

Tu, C.-Y. & Marsch, E. 1995, Space Sci. Rev., 73, 1

Unti, T. W. J. & Neugebauer, M. 1968, Phys. Fluids, 11, 563

Vogt, C. & Enßlin, T. A. 2005, A&A, 434, 67

Voitenko, Yu. M. 1998, J. Plasma Phys., 60, 515

Watanabe, T.-H. & Sugama, H. 2004, Phys. Plasmas, 11, 1476

Wicks, R. T., Chapman, S. C., & Dendy, R. O. 2009, ApJ, 690, 734

Wilkinson, P. N., Narayan, R., & Spencer, R. E. 1994, MNRAS, 269, 67

Woo, R. & Armstrong, S. R. 1979, J. Geophys. Res., 84, 7288

Woo, R. & Habbal, S. R. 1997, ApJ, 474, L139

Yoon, P. H. & Fang, T.-M. 2008, Plasma Phys. Control. Fusion, 50, 085007

Yousef, T., Rincon, F., & Schekochihin, A. 2007, J. Fluid Mech., 575, 111

Yousef, T. A., Schekochihin, A. A., & Nazarenko, S. V. 2009, Phys. Rev. Lett., submitted

Zank, G. P. & Matthaeus, W. H., 1992, J. Plasma Phys., 48, 85

Zank, G. P. & Matthaeus, W. H., 1993, Phys. Fluids A, 5, 257

Zweben, S. J., Menyuk, C. R. & Taylor, R. J., 1979, Phys. Rev. Lett., 42, 1270